

DISSERTATION

PROCESS LINKAGES IN LARGE WATERSHEDS: CONNECTING TRIBUTARY  
EROSION TO DOWNSTREAM CHANNEL CHANGE AND FLOODPLAIN FOREST  
ESTABLISHMENT IN THE YAMPA AND GREEN RIVER BASIN

Submitted by

John Trusal Kemper

Department of Geosciences

In partial fulfillment of the requirements

For the Degree of Doctor of Philosophy

Colorado State University

Fort Collins, Colorado

Summer 2022

Doctoral Committee:

Advisor: Sara Rathburn

Jonathan Friedman

Ellen Wohl

Stephen Leisz

Miranda Redmond

Copyright by John Trusal Kemper 2022

All Rights Reserved

## ABSTRACT

### PROCESS LINKAGES IN LARGE WATERSHEDS: CONNECTING TRIBUTARY EROSION TO DOWNSTREAM CHANNEL CHANGE AND FLOODPLAIN FOREST ESTABLISHMENT IN THE YAMPA AND GREEN RIVER BASIN

It is well-understood that the physical state of a river is a combination and culmination of present processes and past trajectories. Similarly, conceptualizations of fluvial connection hold that various aspects of a given river reach – ecologic, geomorphic, hydrologic – do not operate in isolation, but rather as components within a linked system, both influencing and influenced by upstream and downstream conditions. To expand understanding of the river system as an intrinsically linked network of both process and form, here I establish connections between the processes of historical tributary erosion and distal downstream channel migration and floodplain forest establishment in the Yampa and Green River Basin. I then additionally summarize the extensive body of literature concerning the geomorphic response to sediment supply increases in low-gradient, alluvial rivers to further emphasize that the translation of sediment through the landscape can catalyze myriad responses that manifest across a continuum of scales.

Concentrating initially on the investigation of historical erosion, examination of historical documents and aerial photos suggests that three key sediment contributing tributaries of the Yampa River – Sand Creek, Muddy Creek, and Sand Wash – underwent substantial historical erosion from 1880-1940. Using field investigation to determine historical channel location and field surveys of present-day dimensions, I then calculate that historical arroyo incision within the latter two tributary watersheds injected  $30 \times 10^6$  tons of sediment into the mainstem Little Snake

and Yampa Rivers during this time. Taking present-day annual sediment loads as an approximate background for the pre-erosion sediment regime, this represented a sizable increase in the sediment load of the Yampa River during the period of historical erosion.

Moving downstream, results of dendrochronologic analysis of tree cores from three separate forest locations – Deerlodge Park on the Yampa River, Island Park and Tuxedo Bottom on the Green River – indicate that major portions of these forests established during the same time period of elevated historical erosion. Moreover, channel change analysis suggests that the channel at this time was relatively more dynamic than it has been since, and the area of forest dating to the historical period is much greater than can be explained by high flows alone. Viewed collectively, these findings suggest tributary erosion played a vital role in successful downstream forest establishment.

Additional sediment fingerprinting analysis further supports this process link between geomorphic and ecologic process. Using sediment samples taken at the rooting surface of the cottonwood forest in Deerlodge Park, geochemical analysis indicates that the majority of this sediment was sourced from those tributaries – Muddy Creek and Sand Wash – that were undergoing enhanced erosion via arroyo incision during the historical period.

Overall, the temporal overlap between the timing of historical tributary erosion and the establishment of substantial portions of downstream floodplain forest, in conjunction with the fact that floodplain sediment is dominantly sourced from watersheds that experienced enhanced historical erosion, together indicates a demonstrable link between the geomorphic process of historical erosion and the ecologic process of downstream floodplain forest establishment. From a summary of existing studies concerning the geomorphic adjustment of low-gradient, alluvial rivers to increased sediment supply, it is additionally clear that tributary erosion that injects

substantial amounts of sediment into a river system can result in the requisite channel change necessary for successful forest establishment. The fluvial system is thus best understood as not just a physically coupled network, but a collectively connected web of processes that together regulate and are regulated by one another. Such an understanding emphasizes that management of large watersheds must be holistic and undertaken at the basin scale in order to ensure that vital riverine ecosystems endure.

## ACKNOWLEDGEMENTS

It takes a village. Though you may read in the chapters that follow sentences written in the first person singular, I was dragged kicking and screaming to follow this dissertation convention. Rather, so many people were essential to this work that I have often felt the member of a great scientific collective rather than a graduate student working on his dissertation. For this, and for many other reasons, I am grateful to these people, who I will attempt to thank here, though my gratitude goes beyond that which can be expressed on paper.

First, to Sara Rathburn, my advisor and mentor, for your guidance, support, encouragement, instruction, and advice – thank you. From the very beginning, Sara believed in me as a scientist, and urged, critiqued, uplifted, and left me alone as need be. Above all else, with her trust and her tutelage, she enabled me to grow into who I am as a scientist and person today, and for that I feel blessed. Sara, thank you.

Second, to Jonathan Friedman, my unofficial co-advisor and frequent field companion whose instruction and mentorship have been so essential on this journey – my profound thanks as well. You have been an essential mentor to me throughout my time here, a constant source of thoughtful insight and hilarious anecdotes, always pushing me to observe carefully and think thoroughly. I am a better scientist and better fellow because of it – Jonathan, thank you.

Thank you also to my committee, Ellen Wohl, Steve Leisz, and Miranda Redmond, whose advice has been instrumental in improving the quality of the science contained herein. I am particularly grateful to Ellen, for lending her advice and expertise whenever I sought it out and for dependably enjoyable conversation on any occasion. And many thanks are due also to Mike Scott, who engaged with this dissertation in an unofficial capacity but has been absolutely

instrumental in both making the work here what it is and in my growth as a scientist. Thanks Mike, for your mentorship, companionship, and guidance.

Much gratitude also to those who have helped me in the field, lab, and in various other pathways of my life during the past several years. To John Nelson and Daniel Hill, thank you for your resolute assistance in the field – I am indebted to the dedication and commitment you brought to this project, and couldn't have done it without you. John, this goes ditto with your tireless lab work. To Richie Thaxton, whose dendrochronology wizardry was fundamental to the success of this research, enormous thanks. And many blessings to all the others who have helped in the field, fomented ideas, or otherwise made the science in this dissertation what it is: Erich Mueller, Kirk Vincent, Christy Leonard, Lucas Zeller, Lee and Patti Gelatt, Andrew Ruetten, Chris Lidstone, Lynn Updike, Larry Hicks, and many, many more.

Thank you to the community that surrounds me and that I have made at Colorado State, including the Fluvial Lab, especially Christoph Suhr, Celeste Wieting, Anna Marshall, Emily Iskin, and Sarah Hinshaw, who have helped with field work, given me advice, and otherwise been excellent people and companions.

Thank you to my family, to my mom and dad for their absolutely unwavering support, ceaseless encouragement, and endless capacity to listen, and to my sister, for her companionship and frank levity – you all are more than anyone could ever ask for.

And thank you finally to Juli, for oh so many things.

## DEDICATION

To my grandfather, John Kemper, who stretched out the future and told me to leap.

## TABLE OF CONTENTS

ABSTRACT.....	ii
ACKNOWLEDGEMENTS.....	v
DEDICATION.....	vii
LIST OF TABLES.....	xi
LIST OF FIGURES.....	xii
CHAPTER 1: INTRODUCTION.....	1
1.1 References.....	7
CHAPTER 2: SEDIMENT ECOLOGICAL CONNECTIVITY IN A LARGE RIVER NETWORK <sup>1</sup> .....	12
2.1. Introduction.....	12
2.2. Study Area.....	15
2.3. Methods.....	18
2.3.1. Constraining time periods of erosion in tributary watersheds.....	18
2.3.2. Estimating volumes of eroded sediment.....	20
2.3.3. Aging riparian cottonwood forest and floodplain surfaces.....	23
2.3.4. Estimations of channel change in forest areas.....	25
2.3.5. Data analysis.....	25
2.4. Results.....	27
2.4.1. Time periods and magnitude of active erosion in tributary watersheds.....	27
2.4.2. Area-age distribution of cottonwood floodplain forests and historical channel change.....	31
2.4.3. Flow-establishment correlations.....	37
2.5. Discussion.....	37
2.5.1. Tributary erosion from the late 19 <sup>th</sup> to mid-20 <sup>th</sup> century.....	37
2.5.2. The role of sediment in floodplain forest establishment.....	40
2.5.3. Sediment-ecological connectivity.....	44
2.6. Conclusions.....	47
2.7 References.....	49
CHAPTER 3: FINGERPRINTING HISTORICAL TRIBUTARY CONTRIBUTIONS TO FLOODPLAIN SEDIMENT USING BULK GEOCHEMISTRY <sup>2</sup> .....	65

3.1. Introduction.....	65
3.2. Study Area .....	68
3.3. Methods.....	72
3.3.1. Sampling contributing areas .....	72
3.3.2. Sampling Deerlodge Park floodplain sediment .....	74
3.3.3. Dating Deerlodge Park floodplain sediment.....	75
3.3.4 Grain-size and geochemical analysis of sampled sediment.....	76
3.3.5. Identifying and selecting robust geochemical sediment tracers .....	77
3.3.6. Determining sub-basin sediment sources.....	80
3.4. Results.....	81
3.4.1. Floodplain trench stratigraphic analysis and dating floodplain sediments .	81
3.4.2. Grain size analysis of sub-basin and floodplain sediment .....	85
3.4.3. Geochemical analysis and tracer selection .....	87
3.4.4. Mixing model (MixSIAR) results.....	90
3.5. Discussion .....	93
3.5.1. Optimum tracer selection.....	93
3.5.2. Provenance and age of floodplain sediment and the role of small tributaries in large watersheds.....	98
3.6. Conclusions.....	101
3.7 References.....	103
<b>CHAPTER 4: GEOMORPHIC EFFECTS OF INCREASED SEDIMENT SUPPLY IN LOW- GRADIENT, ALLUVIAL RIVERS .....</b>	<b>120</b>
4.1. Introduction.....	120
4.2. Channel adjustment and sediment load: History and state of the science .....	124
4.2.1 History.....	124
4.2.2 State of the science.....	129
4.3. Changes observed across scales of adjustment.....	138
4.3.1 Grain-size adjustments.....	138
4.3.2 Bed and bar form .....	140
4.3.3 Channel transect.....	144
4.3.4 Channel reach.....	149
4.4. Emergent knowledge: knowns and unknowns.....	156
4.4.1 Knowns: Volume-grain size interactions.....	156

4.4.2: Knowns: Antecedent conditions .....	159
4.4.3 Unknowns: Adjustment thresholds and influx effectiveness thresholds ...	162
4.5. Future work and additional considerations .....	164
4.5.1 Future work to identify influx effectiveness thresholds .....	164
4.5.2 Additional considerations .....	166
4.6. Conclusions.....	172
4.7 References.....	175
CHAPTER 5: CONCLUSIONS .....	216
5.1 References.....	220
APPENDIX A: ARROYO ASSUMPTIONS, VOLUME CALCULATIONS, AND CHANNEL MIGRATION DETERMINATION .....	222
A.1. Muddy Creek Assumptions.....	222
A.2. Sand Wash Assumptions.....	224
A.3. Volume estimations in Sand Wash and Muddy Creek .....	228
A.4. Sand Creek assumptions and volumes estimations.....	228
A.5. Conservative nature of the estimates .....	229
A.6. Estimating temporal change in channel migration rate at forest sites.....	230
APPENDIX B: TREE CORES SURROUNDING TRENCH AND PXRF ELEMENTAL DATA FOR CONSERVATIVE TRACERS .....	233

## LIST OF TABLES

<b>Table 2.1.</b> U.S. Geological Survey stream gages most proximal to the study forests and the years of the six largest recorded floods for each gage. ....	17
<b>Table 2.2.</b> Dates of General Land Office (GLO) maps and notes and aerial photographs for the tributary watersheds of Muddy Creek, Sand Creek, and Sand Wash .....	19
<b>Table 2.3.</b> Sampled trees in each forest.....	24
<b>Table 2.4.</b> Average arroyo and channel dimensions at section line crossings for the tributaries of Muddy Creek, Sand Creek, and Sand Wash .....	28
<b>Table 2.5.</b> Percent overlap of the channel through each forest reach as determined from historical maps and aerial imagery for two forests in the Green River Basin, USA. ....	33
<b>Table 2.6.</b> Coefficients of significant predictors and explanatory power (pseudo R <sup>2</sup> ) of models obtained from Poisson regressions. ....	38
<b>Table 3.1.</b> Results of the Kruskal-Wallis (KW) test on conservative tracers.....	89
<b>Table 3.2.</b> Summary statistics for mixing model results run with conservative tracers alone and with an optimized fingerprint.....	92
<b>Table 3.3.</b> Summary statistics for classification using random forest (RF) and discriminant function analysis (DFA).....	97
<b>Table 4.1.</b> Summarized papers.....	126
<b>Table B.1.</b> Center years and other metadata for cored trees in the immediate vicinity of the trench in Deerlodge Park.....	245
<b>Table B.2.</b> Standard-corrected concentrations (ppm) of conservative tracers.....	246
<b>Table B.3.</b> Standard-corrected mean concentrations and standard errors of conservative tracers for each sampled contributing area.....	258

## LIST OF FIGURES

<b>Figure 1.1.</b> a) The Green River Basin and major tributaries.....	3
<b>Figure 2.1.</b> a) The Green River Basin and major tributaries.....	16
<b>Figure 2.2.</b> Example historical maps and photos within Muddy Creek. ....	21
<b>Figure 2.3.</b> Generalized cross section of Muddy Creek terraces.. ....	22
<b>Figure 2.4.</b> Exposed arroyo wall in Sand Wash in the Yampa River Basin, USA, approximately 5 m high with cross section at nearest section line roughly 500 m downstream (inset).....	30
<b>Figure 2.5.</b> Fraction of total present-day floodplain forest by 20 year-establishment period for Fremont cottonwood at three forests locations .....	32
<b>Figure 2.6.</b> Floodplain area-age maps for three forests in the Green River Basin.....	35
<b>Figure 2.7.</b> Cumulative tree establishment as percent of total present-day forest (green points and line) plotted with peak annual discharge (gray bars) for three forests in the Green River Basin, USA. ....	36
<b>Figure 2.8.</b> Conceptual representation of the sediment-ecological connectivity framework.....	46
<b>Figure 3.1.</b> Geologic map of the Yampa River Basin with the dominant units for each subbasin indicated in the inset charts.....	69
<b>Figure 3.2.</b> Arroyos in and floodplain bank stratigraphy in Deerlodge Park.....	70
<b>Figure 3.3.</b> Floodplain stratigraphy exhumed by the trench .....	74
<b>Figure 3.4.</b> Grain size breakdowns for trench and tributary samples .....	86
<b>Figure 3.5.</b> The tracer selection process and the tracers retained by each step.....	87
<b>Figure 3.6.</b> Biplots for all tracer pairs that passed the three bracket tests for conservativeness..	88
<b>Figure 3.7.</b> Variable importance of each tracer for the classification of source samples using the random forest method. ....	90
<b>Figure 3.8.</b> Principal component analysis (PCA) plots of the sand samples from each source area and the Deerlodge trench .....	91
<b>Figure 3.9.</b> Mixing model results.....	92
<b>Figure 4.1.</b> Examples of low gradient rivers.....	123
<b>Figure 4.2.</b> The scales of adjustment at which change may occur following a sediment influx. ....	130
<b>Figure 4.3.</b> The types of adjustment that be observed at each scale, separated by thresholds of unknown magnitude.....	131
<b>Figure 4.4.</b> Burial of antecedent bed in the Ringarooma River .....	144
<b>Figure 4.5.</b> A potential adjustment at the channel transect scale to a hypothetical increase in sediment supply. ....	145
<b>Figure 4.6.</b> A depiction of a hypothetical adjustment at the channel reach scale. ....	151
<b>Figure 4.7.</b> A potential adjustment at the channel planform scale due to a hypothetical increase in sediment supply. ....	154
<b>Figure 4.8.</b> Conceptual framework of channel adjustment to a hypothetical increase in sediment supply.....	158
<b>Figure A.1</b> Arroyo field evidence.....	228

<b>Figure A.2.</b> Old channel in historical photos.....	229
<b>Figure A.3.</b> Terrace contacts.....	230
<b>Figure A.4.</b> Narrowing of the Sand Wash channel and formation of an inset floodplain from 1938-1982.....	231
<b>Figure A.5.</b> Monumented $\frac{1}{4}$ section corner between S26 and S25 in T8NR98W.....	232
<b>Figure A.6.</b> Measurement of modern cross section of Muddy Creek at Township 14 N Range 91 W subdivision line S7S6 and various identified surfaces.....	233
<b>Figure A.7.</b> Delineated channels in the Deerlodge Park forest reach.....	236
<b>Figure A.8.</b> Delineated channels in the Island Park forest reach.....	237

## CHAPTER 1: INTRODUCTION

The physical form of the fluvial system has long been appreciated as one developed by connection: a network of river channels functioning to transport sediment and water through the landscape in turn shaped – in dimension and pattern – by this flux (Schumm, 1977; Wohl et al., 2019). River ecosystems have been similarly conceived as highly interconnected, both influencing and dependent on the very same cascade of water and sediment that sets the physical watershed template (Poff et al., 1997; Wohl et al., 2015). With particular respect to sediment movement, it is now well understood that the rate and magnitude of sediment transfer through the channel network exerts a key influence on river evolution and ecosystem dynamics (Hupp and Osterkamp, 1996; Ward et al., 2002; Benda et al., 2004; Fryirs, 2013; Bracken et al., 2015; Wohl et al., 2015, 2019). A logical next step to build on this rich body of knowledge concerning the considerable influence of the sediment regime on various riverine forms and functions is to establish linkages between geomorphic processes and ecological processes separated by both space and time. To that end, this dissertation focuses on connecting historical tributary erosion to distal downstream cottonwood establishment in the Yampa and Green River Basin of Colorado, Wyoming, and Utah (Figure 1.1).

In the latter decades of the 19<sup>th</sup> century and initial years of the 20<sup>th</sup>, stream channels across the American Southwest underwent enhanced erosion via arroyo incision (Cooke and Reeves, 1977). Catalyzed by a range of possible mechanisms, including anthropogenic disturbance (e.g., overgrazing), climate change, and internal system dynamics, arroyo cutting formed characteristic deep, oversized channels with wide flat bottoms and nearly vertical walls across the region (Dodge, 1902; Bryan, 1925; Schumm and Hadley, 1957; Cooke and Reeves, 1977; Womack and Schumm, 1977; Gellis et al., 1991). Evidence of arroyo cutting abounds

throughout the Yampa River Basin, in particular the key tributaries of Sand Wash and Muddy Creek (Figure 1.1). In addition, though no prior published record of widespread arroyo development in the Yampa Basin exists, previous work has documented 4-6 m of incision along tributary Muddy Creek (Parker et al., 1985) and substantial arroyo cutting in the neighboring White River Basin (Womack and Schumm, 1977). Observable evidence of other forms of historical erosion, namely widening, are also present in the tributary of Sand Creek that has been shown to be a key player in the sediment dynamics of the Yampa (Topping et al., 2018).

Downstream of these significant sediment contributing tributaries, cottonwood gallery forests are common in the wide, alluvial areas that occur periodically between the bedrock canyons of the Yampa and Green Rivers. Riparian cottonwoods (*Populus fremontii*) are the dominant species in these alluvial parks; like many riparian trees in western North America, cottonwoods require moist, unvegetated sandy surfaces safe from future disturbance to successfully establish (Scott et al., 1996; Mahoney and Rood, 1998; Benjankar et al., 2014). It is widely accepted that these sandy surfaces are formed primarily by large floods that result in channel migration and create suitable establishment locations (Scott et al., 1996; Mahoney and Rood, 1998; Merritt and Cooper, 2000; Miller and Friedman, 2009; Schook et al., 2017), but heightened sediment loads should also catalyze migration (Constantine et al., 2014; Eke et al., 2014; Czuba and Foufoula-Georgiou, 2015; Donovan et al., 2021). Relevantly, increased sediment loads due to tributary arroyo incision have been documented in several American rivers (Graf, 1987; Gellis et al., 1991).

What follows naturally from this overview of arroyo incision and riparian tree dynamics is the intent of this dissertation: historical erosion and cottonwood establishment in the Yampa and Green River Basin are inextricably linked, and, more broadly, geomorphic process and

ecological process are intrinsically connected even when separated by ample space ( $10^5 \text{ km}^2$ ) and time ( $10^2$  years). Moreover, the work presented herein hypothesizes that tributary processes have substantial influence on the dynamics of large rivers and that management of large river basins must be holistic to ensure that vital riverine landscapes endure into the future.

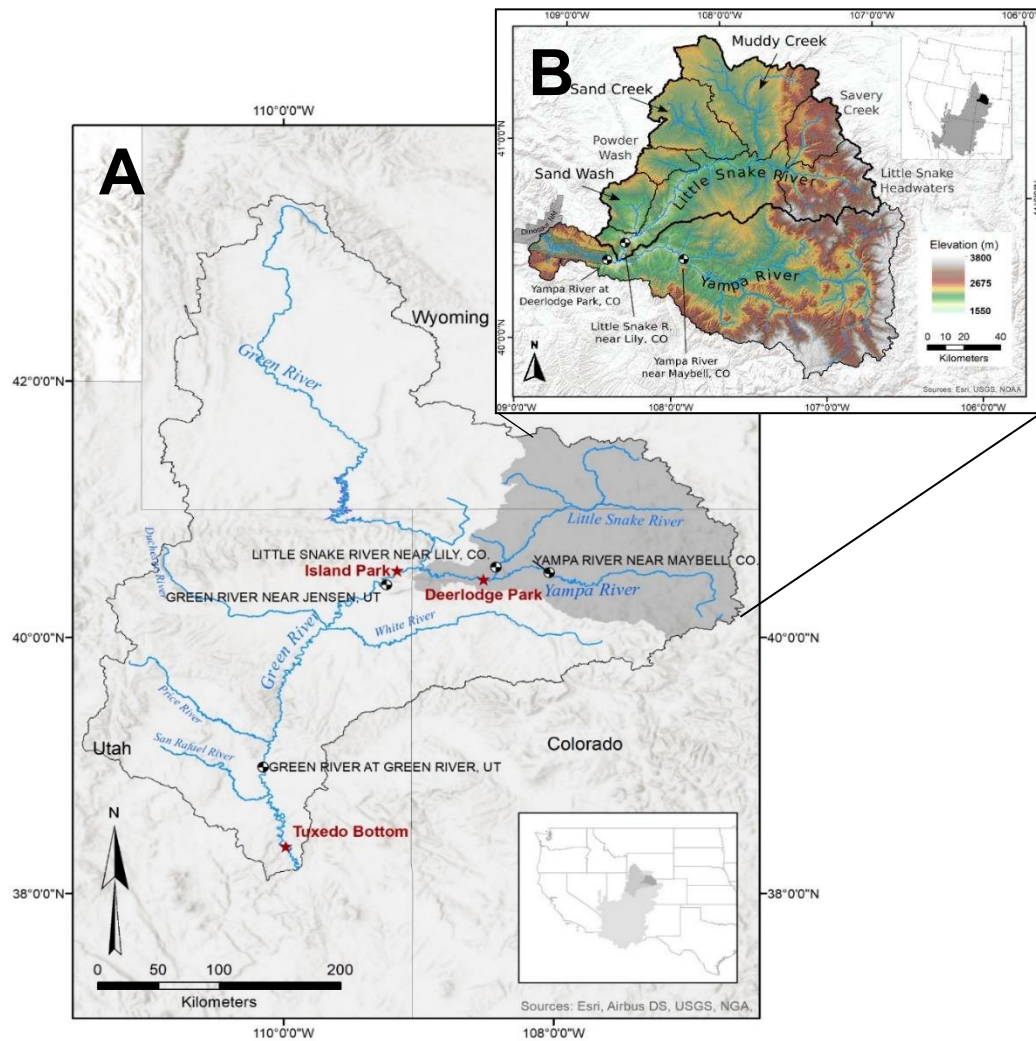


**Figure 1.1.** a) The Green River Basin and major tributaries; sampled forest locations are indicated in red. b) Detail of the Yampa River Basin including the tributaries of Sand Wash, Sand Creek, and Muddy Creek. U.S. Geological Survey gages closest to study forests are indicated by station name.

To support such hypotheses, the above outlined advantageous assemblage of attributes present in the Yampa and Green River Basin are utilized as a natural laboratory. The following chapters investigate the hypothesized process connections by constraining the timing and magnitude of historical erosion in key tributaries of the Yampa in conjunction with the timing of cottonwood establishment in downstream forests (Chapter 2), verifying the link between sediment eroded in those key tributaries and the floodplain deposits on which the cottonwood forests grow through sediment fingerprinting (Chapter 3), and finally firmly establishing via an extensive review of the extant literature that increased sediment supply can drive the requisite channel change (Chapter 4).

In Chapter 2, a sediment-ecological connectivity framework is established to relate geomorphic and ecological process across ample space and time (Kemper et al., 2022b). Historical documents, aerial photographs, and field inspection are used to determine the timing of past erosion in Sand Wash, Sand Creek, and Muddy Creek, which are key sediment contributing tributaries for the Yampa River located in the lower Little Snake Basin; calculation of total eroded volume from this historical erosion then follows. Using dendrochronology, area-age assemblage of cottonwood forest in three downstream areas on the Yampa and Green Rivers are then determined (*sensu* Schook et al., 2017) to link the timing of establishment of substantial portions of the forest in these locations to the timing of upstream arroyo incision. Results of both analyses are finally combined into a sediment-ecological connectivity framework that I contend best illustrates the intrinsic linkages between tributary morphological processes and downstream ecological processes. This framework can be applied in any basin with a similar history of human disturbance to effectively communicate the need for holistic, basin-scale management.

This construction of sediment-ecological connectivity based on temporal overlap is followed in Chapter 3 by establishment of a robust physical linkage between upstream eroded sediment and the downstream floodplain packages on which cottonwoods are rooted (Kemper et al., 2022a). In this chapter, sediment fingerprinting, in conjunction with an excavated floodplain trench, is employed to determine the provenance of the sediment package that comprises the rooting surface of cottonwoods in Deerlodge Park on the Yampa River, one of the areas of extensive cottonwood galleries investigated in Chapter 2 (Kemper et al., 2022b) (Figure 1.1). Using bulk geochemistry as a tracer (*sensu* Chapman et al., 2020) and the relatively novel machine-learning random forest method for tracer selection, elemental fingerprints capable of robustly discriminating between source areas of interest are constructed and input into a Bayesian mixing model to ascribe provenance of the floodplain sediment. Results of the fingerprinting method are then combined with additional dendrochronological analysis and the findings of Chapter 2 to further demonstrate that historical erosion exerted a key influence on the establishment of downstream floodplain cottonwoods. Together, the fingerprinting approach and subsequent results are used to additionally emphasize that responsible management of large watersheds must be built upon holistic consideration of process connections throughout the basin and extensive communication between stakeholders and managers.

Finally, in Chapter 4, a comprehensive review of the voluminous body of literature on the geomorphic impact of increased sediment supply is undertaken. Paying particular attention to low-gradient, alluvial rivers, this rich literature is summarized to a) provide a readily referenceable resource of the range of potential changes facing a river basin across a continuum of scales, b) evaluate and enhance existing conceptual models of channel adjustment (e.g., Lane, 1955; Schumm, 1969) in light of a wide array of empirical evidence, and c) identify and

emphasize areas for future work, in particular the identification of thresholds wherein a sediment influx precipitates one scale of change (e.g., channel bed fining) to transition to another (e.g., channel widening). Studies that I assessed in this endeavor span a wide range of time (a century plus) and spatial setting (northern Canada to New Zealand's North Island). I use the resulting summary to establish that increases in sediment supply can be conceived of as thresholds that, once exceeded, drive channel adjustments at additional scales, and that extensive further work is needed to broadly quantify such thresholds in order to best anticipate and predict the potential change that may result from a given sediment influx.

Chapter 5 then concludes this dissertation with a concise summary of the prior chapters and how they together illustrate the connectivity via sediment between geomorphic processes and ecologic processes in large watersheds. Following this synopsis, directions for future research are outlined and briefly discussed. Chapters 2 and 3 of this work have been published in peer-reviewed journals (Kemper et al., 2022a-b); Chapter 4 is a manuscript currently in preparation for *Earth-Science Reviews*.

## 1.1. References

- Benda, L., Poff, N.L., Miller, D., Dunne, T., Reeves, G., Pess, G., Pollock, M., 2004. The Network Dynamics Hypothesis: How Channel Networks Structure Riverine Habitats. *BioScience* 54, 413–427. [https://doi.org/10.1641/0006-3568\(2004\)054\[0413:TNDHHC\]2.0.CO;2](https://doi.org/10.1641/0006-3568(2004)054[0413:TNDHHC]2.0.CO;2)
- Benjankar, R., Burke, M., Yager, E., Tonina, D., Egger, G., Rood, S.B., Merz, N., 2014. Development of a spatially-distributed hydroecological model to simulate cottonwood seedling recruitment along rivers. *Journal of Environmental Management* 145, 277–288. <https://doi.org/10.1016/j.jenvman.2014.06.027>
- Bracken, L.J., Turnbull, L., Wainwright, J., Bogaart, P., 2015. Sediment connectivity: a framework for understanding sediment transfer at multiple scales. *Earth Surface Processes and Landforms* 40, 177–188. <https://doi.org/10.1002/esp.3635>
- Bryan, K., 1925. Date of Channel Trenching (arroyo Cutting) in the Arid Southwest. *Science* 62, 338–344. <https://doi.org/10.1126/science.62.1607.338>
- Chapman, K.A., Best, R.J., Smith, M.E., Mueller, E.R., Grams, P.E., Parnell, R.A., 2020. Estimating the contribution of tributary sand inputs to controlled flood deposits for sandbar restoration using elemental tracers, Colorado River, Grand Canyon National Park, Arizona. *GSA Bulletin* 133, 1141–1156. <https://doi.org/10.1130/B35642.1>
- Constantine, J.A., Dunne, T., Ahmed, J., Legleiter, C., Lazarus, E.D., 2014. Sediment supply as a driver of river meandering and floodplain evolution in the Amazon Basin. *Nature Geoscience* 7, 899–903. <https://doi.org/10.1038/ngeo2282>
- Cooke, R.U., Reeves, R.W., 1976. *Arroyos and Environmental Change in the American Southwest*. Oxford University Press, Oxford.

- Czuba, J.A., Foufoula-Georgiou, E., 2015. Dynamic connectivity in a fluvial network for identifying hotspots of geomorphic change. *Water Resources Research* 51, 1401–1421. <https://doi.org/10.1002/2014WR016139>
- Dodge, R.E., 1902. Arroyo Formation. *Science* 15, 746–747. <https://doi.org/10.1126/science.15.384.746>
- Donovan, M., Belmont, P., Sylvester, Z., 2021. Evaluating the relationship between meander-bend curvature, sediment supply, and migration rates. *Journal of Geophysical Research: Earth Surface*. <https://doi.org/10.1029/2020JF006058>
- Eke, E., Parker, G., Shimizu, Y., 2014. Numerical modeling of erosional and depositional bank processes in migrating river bends with self-formed width: Morphodynamics of bar push and bank pull. *Journal of Geophysical Research: Earth Surface* 119, 1455–1483. <https://doi.org/10.1002/2013JF003020>
- Fryirs, K., 2013. (Dis)Connectivity in catchment sediment cascades: a fresh look at the sediment delivery problem. *Earth Surface Processes and Landforms* 38, 30–46. <https://doi.org/10.1002/esp.3242>
- Gellis, A., Hereford, R., Schumm, S.A., Hayes, B.R., 1991. Channel evolution and hydrologic variations in the Colorado River basin: Factors influencing sediment and salt loads. *Journal of Hydrology* 124, 317–344. [https://doi.org/10.1016/0022-1694\(91\)90022-A](https://doi.org/10.1016/0022-1694(91)90022-A)
- Graf, W.L., 1987. Late Holocene sediment storage in canyons of the Colorado Plateau. *GSA Bulletin* 99, 261–271. [https://doi.org/10.1130/0016-7606\(1987\)99<261:LHSSIC>2.0.CO;2](https://doi.org/10.1130/0016-7606(1987)99<261:LHSSIC>2.0.CO;2)
- Hupp, C.R., Osterkamp, W.R., 1996. Riparian vegetation and fluvial geomorphic processes. *Geomorphology, Fluvial Geomorphology and Vegetation* 14, 277–295. [https://doi.org/10.1016/0169-555X\(95\)00042-4](https://doi.org/10.1016/0169-555X(95)00042-4)

- Kemper, J.T., Rathburn, S.L., Friedman, J.M., Nelson, J.M., Mueller, E.R., Vincent, K.R., 2022a. Fingerprinting historical tributary contributions to floodplain sediment using bulk geochemistry. *CATENA* 214, 106231. <https://doi.org/10.1016/j.catena.2022.106231>
- Kemper, J.T., Thaxton, R.D., Rathburn, S.L., Friedman, J.M., Mueller, E.R., Scott, M.L., 2022b. Sediment-ecological connectivity in a large river network. *Earth Surface Processes and Landforms* 47, 639–657. <https://doi.org/10.1002/esp.5277>
- Lane, E.W., 1955. The Importance of Fluvial Morphology in Hydraulic Engineering. *Proceedings of the American Society of Civil Engineers* 81, 1–17.
- Mahoney, J.M., Rood, S.B., 1998. Streamflow requirements for cottonwood seedling recruitment—An integrative model. *Wetlands* 18, 634–645. <https://doi.org/10.1007/BF03161678>
- Merritt, D.M., Cooper, D.J., 2000. Riparian vegetation and channel change in response to river regulation: a comparative study of regulated and unregulated streams in the Green River Basin, USA. *Regulated Rivers: Research & Management* 16, 543–564. [https://doi.org/10.1002/1099-1646\(200011/12\)16:6<543::AID-RRR590>3.0.CO;2-N](https://doi.org/10.1002/1099-1646(200011/12)16:6<543::AID-RRR590>3.0.CO;2-N)
- Miller, J.R., Friedman, J.M., 2009. Influence of flow variability on floodplain formation and destruction, Little Missouri River, North Dakota. *GSA Bulletin* 121, 752–759. <https://doi.org/10.1130/B26355.1>
- Parker, M., Wood, F.J.J., Smith, B.H., Elder, R.G., 1985. Erosional downcutting in lower order riparian ecosystems: have historical changes been caused by removal of beaver?
- Poff, N.L., Allan, J.D., Bain, M.B., Karr, J.R., Prestegard, K.L., Richter, B.D., Sparks, R.E., Stromberg, J.C., 1997. The Natural Flow Regime. *BioScience* 47, 769–784. <https://doi.org/10.2307/1313099>

- Schook, D.M., Rathburn, S.L., Friedman, J.M., Wolf, J.M., 2017. A 184-year record of river meander migration from tree rings, aerial imagery, and cross sections. *Geomorphology* 293, 227–239. <https://doi.org/10.1016/j.geomorph.2017.06.001>
- Schumm, S.A., 1977. *The Fluvial System*. Blackburn Press.
- Schumm, S.A., 1969. River Metamorphosis. *Journal of the Hydraulics Division* 95, 255–274. <https://doi.org/10.1061/JYCEAJ.0001938>
- Schumm, S.A., Hadley, R.F., 1957. Arroyos and the semiarid cycle of erosion [Wyoming and New Mexico]. *Am J Sci* 255, 161–174. <https://doi.org/10.2475/ajs.255.3.161>
- Scott, M.L., Friedman, J.M., Auble, G.T., 1996. Fluvial process and the establishment of bottomland trees. *Geomorphology, Fluvial Geomorphology and Vegetation* 14, 327–339. [https://doi.org/10.1016/0169-555X\(95\)00046-8](https://doi.org/10.1016/0169-555X(95)00046-8)
- Topping, D.J., Mueller, E.R., Schmidt, J.C., Griffiths, R.E., Dean, D.J., Grams, P.E., 2018. Long-Term Evolution of Sand Transport Through a River Network: Relative Influences of a Dam Versus Natural Changes in Grain Size From Sand Waves. *Journal of Geophysical Research: Earth Surface* 123, 1879–1909. <https://doi.org/10.1029/2017JF004534>
- Ward, J.V., Tockner, K., Arscott, D.B., Claret, C., 2002. Riverine landscape diversity. *Freshwater Biology* 47, 517–539. <https://doi.org/10.1046/j.1365-2427.2002.00893.x>
- Wohl, E., Bledsoe, B.P., Jacobson, R.B., Poff, N.L., Rathburn, S.L., Walters, D.M., Wilcox, A.C., 2015. The Natural Sediment Regime in Rivers: Broadening the Foundation for Ecosystem Management. *BioScience* 65, 358–371. <https://doi.org/10.1093/biosci/biv002>
- Wohl, E., Brierley, G., Cadol, D., Coulthard, T.J., Covino, T., Fryirs, K.A., Grant, G., Hilton, R.G., Lane, S.N., Magilligan, F.J., Meitzen, K.M., Passalacqua, P., Poepl, R.E., Rathburn,

S.L., Sklar, L.S., 2019. Connectivity as an emergent property of geomorphic systems. *Earth Surface Processes and Landforms* 44, 4–26. <https://doi.org/10.1002/esp.4434>

Womack, W.R., Schumm, S.A., 1977. Terraces of Douglas Creek, northwestern Colorado: An example of episodic erosion. *Geology* 5, 72–76. [https://doi.org/10.1130/0091-7613\(1977\)5<72:TODCNC>2.0.CO;2](https://doi.org/10.1130/0091-7613(1977)5<72:TODCNC>2.0.CO;2)

## CHAPTER 2: SEDIMENT ECOLOGICAL CONNECTIVITY IN A LARGE RIVER NETWORK<sup>1</sup>

### 2.1. Introduction

Sediment connectivity frameworks (e.g. Hooke, 2003; Bracken et al., 2015), which facilitate holistic understanding of the flux of sediment through a geomorphic system, are increasingly used to evaluate the potential for geomorphic response to disturbance events (Lisenby and Fryirs, 2017; Cossart et al., 2018; Calle et al, 2020) and to perform catchment-scale management and rehabilitation (Czuba and Foufoula-Georgiou, 2015; Lisenby and Fryirs, 2017; James et al., 2018; Keesstra et al., 2019; Lisenby et al., 2020; McMahon et al., 2020). Past studies have considered the impact of hydrologic connectivity on ecosystem response (Rincón et al., 2017; Birnie-Gauvin et al., 2020) and developed conceptual frameworks that broadly recognize that material fluxes through a river network influence ecological processes and habitat structure (e.g. Ward et al., 2002; Benda et al., 2004), setting the stage to explicitly examine the role of sediment connectivity in ecological processes (Wohl et al., 2015; Estrany et al., 2019; Turnbull and Wainwright, 2019; Gilbert and Wilcox, 2021).

Sediment connectivity describes the movement of sediment through an earth surface system, the rate and magnitude of which can have notable influence on system components (Hooke, 2003; Fryirs, 2013; Bracken et al., 2015, Wohl et al., 2019). The connectivity concept can be subdivided into twin complementary components: functional connectivity, which in a sediment context can be conceptualized as the processes governing the generation and transfer of sediment in and through the landscape, and structural connectivity, which delineates the

---

<sup>1</sup>Chapter published as Kemper, J.T., Thaxton, R.D., Rathburn, S.L., Friedman, J.M., Mueller, E.R. and Scott, M.L., 2022. Sediment-ecological connectivity in a large river network. *Earth Surface Processes and Landforms*, 47(2), 639-657. doi.org/10.1002/esp.5277

structural composition and configuration of landscape units.

These paired concepts represent the potential for sediment to be transferred from one landscape unit to another (structural) and the degree to which that transfer actually occurs (functional) (Wainwright et al., 2011; Heckmann et al., 2018; Wohl et al., 2019). Substantial progress has been made to quantify structural connectivity from the patch to landscape scale (e.g., Index of Connectivity, Borselli et al., 2008) and several studies have conceptually addressed functional sediment connectivity at a variety of scales (e.g. Jain and Tandon, 2010; Heckmann and Schwanghart, 2013; Bracken et al., 2015). However, there remains a need to expand the spatial and temporal boundaries of empirical functional sediment connectivity research to directly address the scales relevant to watershed-wide management (Wohl et al., 2018; Poepl et al., 2020; Najafi et al., 2021) and encapsulate both the full range of connectivity processes as well as their role in ecological processes such as riparian vegetation dynamics (Wainwright et al., 2011; Bracken et al., 2015; Heckmann et al., 2018; Wohl et al., 2019; Cienciala, 2021; Gilbert and Wilcox, 2021).

Many riparian trees in western North America, especially the dominant genus *Populus* (cottonwood), require wet, unvegetated sediment surfaces for successful establishment (Scott et al., 1996; Mahoney and Rood, 1998; Benjankar et al., 2014). The formation of such surfaces most often occurs as the result of channel migration due to flooding (Scott et al., 1996; Merritt and Cooper, 2000; Cooper et al., 2003; Miller and Friedman, 2009; Schook et al., 2017), leading to the development of models relating forest establishment to various flow parameters (Mahoney and Rood 1998; Benjankar et al., 2014; Scott and Friedman, 2018), but channel migration rates

are also strongly affected by sediment load (Scott et al., 1996; Naiman et al., 2010; Dean and Schmidt, 2013; Merigliano et al., 2013; Friedman et al., 2015; Dean et al., 2016; Diehl et al., 2017; Schook et al., 2017; Rathburn et al., 2018; Donovan et al., 2021). Modeling (Dunne et al. 2010, Parker et al., 2011), experimental (Wickert et al., 2013), and observational (Constantine et al., 2014, Czuba and Foufoula-Georgiou, 2015; Donovan et al., 2021) studies all show a strong influence of sediment load on channel migration rate, and models of river connectivity indicate that watershed locations of high sediment flux correspond to locations of rapid migration (Czuba and Foufoula-Georgiou, 2015). Because channel migration rates are both a function of sediment load and play a considerable role in the creation of essential cottonwood establishment surfaces, I thus posit that the area of cottonwood forest established in a given time period is strongly influenced by the rate of delivery of sediment from upstream, an influence that can be readily observed by quantifying the area-age distributions of riparian cottonwood forests, which often serve to elucidate past channel geomorphic change (Everitt, 1968; Merigliano et al., 2013; Schook et al., 2017).

Here, I investigate the connectivity between extreme tributary erosion and downstream cottonwood floodplain forest establishment in the Green and Yampa River Basin of the western United States. This research uses historical documents and sequential aerial photographs to constrain timing of headwater tributary erosion, as well as dendrochronology to calculate area-age distributions of downstream floodplain forests, to establish a framework for watershed-scale sediment-ecological connectivity. Such a framework is critical for improving understanding and management of river ecosystems by linking upstream tributary erosion and downstream forest establishment over large spatial ( $10^5$  km<sup>2</sup>) and temporal (century) scales. This research conceptualizes and expands application of a sediment-ecological connectivity framework in the

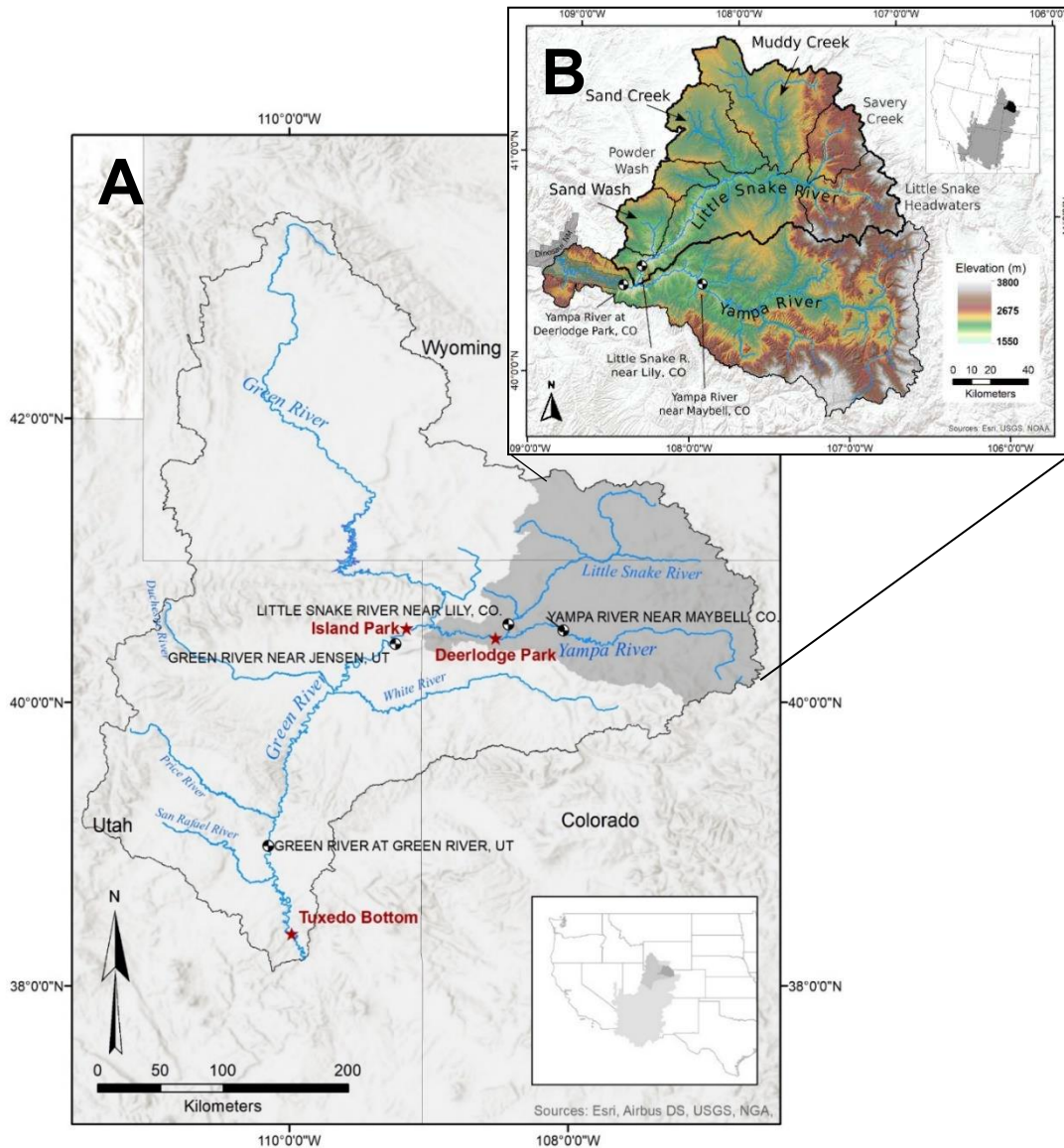
following ways: i) demonstrating the importance of sediment connectivity for maintaining riparian forest establishment processes, ii) underscoring the links between sediment load, channel change, and floodplain forest establishment and persistence, and iii) highlighting the potential to use riparian vegetation to quantify functional connectivity at large temporal and spatial scales.

## **2.2. Study Area**

The Yampa River Basin of northwestern Colorado and southwestern Wyoming is the last major tributary in the Colorado River system with minimal flow regulation (Figure 2.1). The Yampa begins in the Colorado Rocky Mountains and then flows westward across broad lowlands to a junction with the Little Snake River just upstream of Yampa Canyon, whereafter the river flows through a bedrock canyon to the confluence with the Green River (Richter and Richter, 2000; Elliott and Anders, 2004). Downstream of the confluence, the Green River course alternates between narrow canyons and wide alluvial valleys (Andrews, 1986) until it joins the Colorado River near Moab, Utah. The drainage area encompassed in this analysis spans 115,854 km<sup>2</sup>.

The primary source of sediment for the Yampa River is the Little Snake River (Andrews, 1978; Resource Consultants, 1991), and the two together are the principal source of sediment to the Green River below Flaming Gorge Dam (Andrews, 1986; Grams and Schmidt, 2005; Topping et al., 2018) (Figure 2.1). Responsible for only 27% of the total Yampa flow, the Little Snake conversely supplies roughly 70% of the annual sediment load of the Yampa as measured at Deerlodge Park (Andrews, 1980). Furthermore, nearly 60% of the Yampa annual load is derived from Muddy Creek, Sand Creek, and Sand Wash in the lower Little Snake Basin (Andrews, 1980, Topping et al., 2018), which are underlain by poorly consolidated fluvial and

lacustrine deposits (Roehler, 1973, 1985; Hansen, 1986) and have a semi-arid climate that limits both upland soil development and stabilization of upland soils by vegetation (Langbein and Schumm 1958, Andrews 1978). Sand-sized sediment supplied from these tributaries is transported downriver as elongating sand waves, with the fine fraction propagating rapidly



downstream and the coarser fractions moving comparatively slowly, often delayed by several decades (Topping et al., 2018).

**Figure 2.1.** a) The Green River Basin and major tributaries with the Colorado River Basin (inset); sampled cottonwood forest are indicated in red. b) Detail of the Yampa River Basin including the tributaries of Sand Wash, Sand Creek, and Muddy Creek. U.S. Geological Survey gages closest to study forests are indicated by station name.

Evidence of historic arroyo incision is widespread within the tributaries of Muddy Creek and Sand Wash, including characteristic wide, flat-bottomed channels with high, vertical walls. Although no published literature exists on system-wide arroyo development in the Little Snake Basin, Parker et al. (1985) documented 4-6 m of channel incision along Muddy Creek since 1905, and Womack and Schumm (1977) identified 10 m of vertical erosion in the adjacent White River Basin starting around 1900. Significant increases in the sediment loads of major rivers due to arroyo incision have been documented throughout the Colorado River Basin (Graf, 1987; Gellis et al., 1991; Webb et al., 1991; McFadden and McAuliffe, 1997; Hereford, 2002).

Large floods are known to have periodically occurred in these tributary basins in the 1950s and 60s (Topping et al., 2018), but information on earlier floods is limited by lack of flow data. United States Geological Survey (USGS) stream gages have recorded several concurrent large floods at stream gages on the Green and Yampa Rivers proximal to the cottonwood forests of interest (Andrews, 1980; Grams and Schmidt, 2002; Manners et al., 2014; Scott and Miller, 2017; Topping et al., 2018) (Figure 2.1; Table 2.1).

**Table 2.1.** U.S. Geological Survey stream gages most proximal to the study forests and the years of the six largest recorded floods for each gage. The Yampa River at Deerlodge Park gage record (09260050) can be extended to 1922 using the combined record of the Lily and Maybell gages.

Gage Number	Gage Name	Associated forest	Period of record (peak annual flow)
09260000	Little Snake River near Lily, CO	Deerlodge Park	1921-present
09251000	Yampa River near Maybell, CO	Deerlodge Park	1904-05, 1916-present
09260050	Yampa River at Deerlodge Park	Deerlodge Park	1982-present
09261000	Green River near Jensen, UT	Island Park	1904,1906,1947-present

---

Cottonwood gallery forests are common in the wide, alluvial areas that occur intermittently between the bedrock canyons of the Green and Yampa Rivers. This research focuses on the cottonwood forests of three such reaches: Deerlodge Park on the Yampa River, Island Park on the Middle Green River downstream of the Yampa-Green River confluence, and Tuxedo Bottom on the Lower Green River (Figure 2.1). Each forest is in relatively close proximity to tributary watersheds that likely underwent enhanced historical erosion; given the substantial distances between forests, however, it is unlikely that a robust connection can be established between erosion in a specific tributary and all three forest areas. At Deerlodge Park, the aforementioned tributaries of the Little Snake River are potential sources of increased sediment loads due to historical erosion; at Tuxedo Bottom, watersheds within the White River (Womack and Schumm, 1977) and Duchesne River basins (Gaeuman et al., 2005) may have contributed the most sediment (Figure 2.1).

## **2.3. Methods**

### *2.3.1. Constraining time periods of erosion in tributary watersheds*

General Land Office (GLO) survey maps and notes were obtained for the initial survey and subsequent resurvey in Muddy Creek, Sand Creek, and Sand Wash. Survey notes contain qualitative descriptions and quantitative measurements of channel dimensions where they were crossed by Public Land Survey System (PLSS) section lines, ranging from simple notation and observation to measures of channel width and depth, and have been used to constrain time periods of active arroyo incision in the American Southwest (Bryan, 1928). Because the section lines were usually not perpendicular to the channel, channel widths as delineated in the survey

notes were multiplied by the cosine of the angle between the section line and a line orthogonal to the mapped channel banks, yielding a measure of true width (Bryan, 1928).

General Land Office survey notes and maps for each township and range in the tributary watersheds date to 1881 and 1916 in Muddy Creek, 1883 and 1915 in Sand Creek, and 1882 and 1906 in Sand Wash (Table 2.2). Aerial photographs for each tributary basin were obtained from the National Archives in Washington D.C. and USGS EarthExplorer. Photographs used in this analysis are summarized in Table 2.

**Table 2.2.** Dates of General Land Office (GLO) maps and notes and aerial photographs for the tributary watersheds of Muddy Creek, Sand Creek, and Sand Wash in the Yampa River Basin, USA.

	Tributary		
	Muddy Creek	Sand Creek	Sand Wash
Initial GLO Survey	1881	1882	1881
<i>Error*</i>	<i>5 m</i>	<i>5 m</i>	<i>5 m</i>
GLO Resurvey	1915	1937	1906
<i>Error*</i>	<i>5 m</i>	<i>5 m</i>	<i>5 m</i>
Aerial Photograph Set #1	1938	1938	1938
<i>Error**</i>	<i>9.9 m</i>	<i>5 m</i>	<i>10 m</i>
Aerial Photograph Set #2	1954	1953	1953
<i>Error**</i>	<i>4.8 m</i>	<i>8.5 m</i>	<i>4.9 m</i>

\*Mapping error (horizontal root-mean square error)

\*\* Orthorectification error (horizontal and vertical root-mean square error) (e.g., Leonard et al., 2020)

Photographs were digitized and then orthorectified using Digital Elevation Models (DEM) created with Structure-from-Motion (SfM) in AgiSoft Photoscan Professional (Version 1.4) (Fonstad et al., 2013; Bakker and Lane, 2017; Leonard et al., 2020). Average horizontal and vertical orthorectification error in SfM was 4.5 and 4 m, respectively. Arroyo (where present) and channel dimensions were measured from both the orthorectified photos and the associated DEM created using SfM. Arroyo width and depth were measured relative to the pre-arroyo valley floor at locations where the channel was intersected by section lines. Channel dimensions

as measured here refer to the active channel (Hedman and Osterkamp, 1982), identified in photographs as either water or surfaces with a vegetation cover less than 10%. In this manner, time series of arroyo and channel dimensions were obtained for each tributary, beginning in 1881 and continuing until channel dimensions remained stable across multiple sequential documents/photographs (Figure 2.2). For Sand Creek in particular, the channel is an extremely wide, low-gradient sand bed channel with lack of defined bank(s) in many locations and minimal vegetation, making it difficult to know exactly whether the original surveyors' general definition of channel (which was based primarily upon observations of defined banks (White, 1991; Bryan 1928)) concurs with the present author's. I thus took the approach in Sand Creek to only compare dimensions obtained from similar sources: survey notes to survey notes and aerial photographs to aerial photographs.

Potentially stable dimensions were then compared to cross-section measurements made in the field in 2019 at each corresponding location using a Topcon GR5 real-time kinematic GPS/GNSS receiver, resulting in a nearly 140-year record of changes in channel dimensions in each tributary. The time period of active erosion in each tributary was thus identified and constrained, with the assumption that stability or decrease in channel and arroyo dimensions from a set of photographs or documents to the present indicates cessation of major erosion.

### *2.3.2. Estimating volumes of eroded sediment*

Estimates of eroded volume due to arroyo incision were calculated using field observation and measurement and interpretations aided by GLO maps, historical aerial photographs, and satellite imagery. In the field, cross sections of current channel and arroyo dimensions were measured every 1.61 km (1 mile), the same spacing as township and range



**Figure 2.2.** Muddy Creek channel in Township 13 North Range 91 West in the Yampa River Basin, USA. 1881, 1915, 1938, and 1954. Channel dimensions were measured by General Land Office surveyors in 1881 and 1915 where section lines crossed the channel. Measurements from aerial photographs were made at the same locations using 1938 and 1954 aerial photographs and in the field in 2019.

lines, which allowed comparison with GLO survey maps and notes. At Muddy Creek, cross-sections revealed flights of recurring terraces above the modern floodplain (Figure 2.3). In Sand Wash, only a single recurring terrace was generally observed. In Sand Creek, no recurring terraces exist.

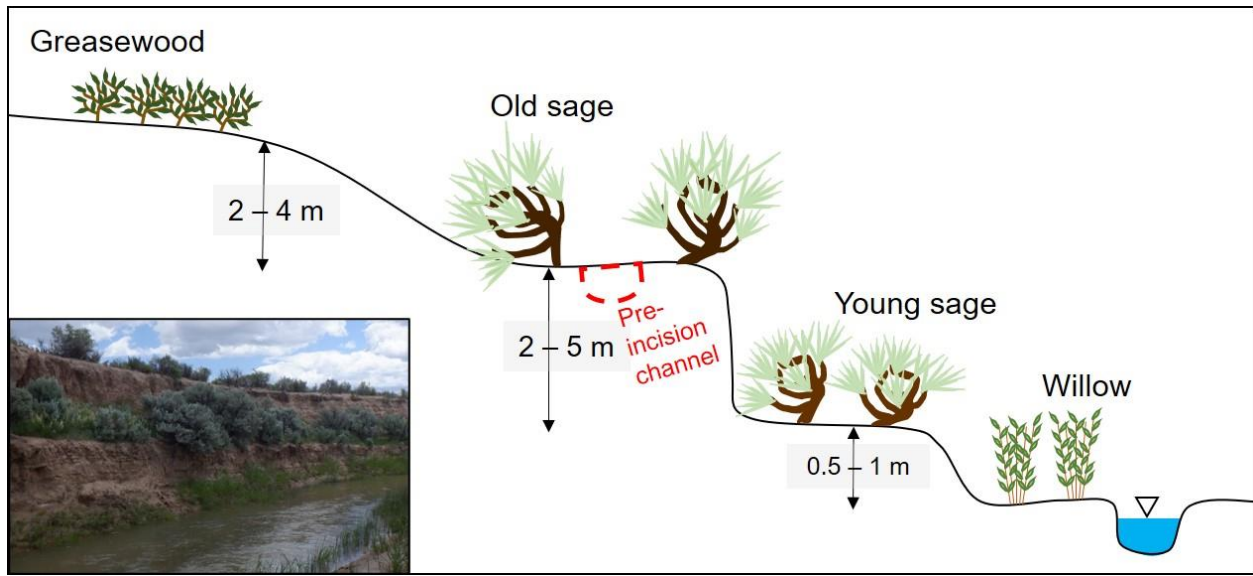


**Figure 2.3.** Generalized cross section of Muddy Creek terraces. Relict pre-arroyo channels are found on the level of the second terrace above the modern channel. This terrace was likely the floodplain of the pre-incision Muddy Creek.

Using field evidence of old channels and GLO maps that depict historical channel location, I calculated the proportion of the modern cross section representing erosion since the time of the first GLO map (Supporting Information). The volume of sediment eroded due to arroyo incision was then calculated by multiplying the area of the eroded cross section by the length of the channel between adjacent measured cross sections. In this manner, a first-order estimate of eroded volume for the Sand Wash and Muddy Creek arroyos was obtained. Because channel change in Sand Creek due to elevated historical erosion manifests solely as changes in the width of the channel, even a first-order estimation of exported sediment totals from Sand Creek is unfeasible with the current dataset. Eroded volumes for each tributary were multiplied

by the density of loose sand (1,442 kg/m<sup>3</sup>) to obtain estimated mass of sand derived from tributary erosion.

The potential error that may have resulted from incomplete capture of the full range of arroyo dimensions by measured cross-sections was estimated using a bootstrap resampling method of surveyed cross-sectional areas (Efron and Tibshirani, 1986). This generated a synthetic data set of 5,000 different volume estimates for each tributary. I then calculated the standard deviation of that synthetic data set to estimate uncertainty associated with volume calculations. Additional details, justifications, and associated assumptions of these estimation methods can be found in the Supporting Information.

### *2.3.3. Aging riparian cottonwood forest and floodplain surfaces*

Stands of Fremont cottonwood (*Populus fremontii*) in each riparian area (Figure 2.1) were sampled in September 2018 and June 2019. Forest was delineated on 2017 National Agriculture Imagery Program (NAIP) aerial imagery with 1-m spatial resolution. Fifty random points were generated within the delineated forest at each site. In the field, two cores were collected from the tree nearest each randomly generated point (Friedman and Lee, 2002) and from trees subjectively chosen based on perceived advanced age (Table 2.3). Cores were taken at ~1.2 m above the ground using either a 5.15-mm or 12-mm diameter Haglof increment borer. Cores were mounted and sanded using progressively finer grits of sandpaper and then cross-dated under a dissecting microscope using skeleton plots (Stokes and Smiley, 1968). I digitized ring widths to 0.01 mm precision using a Velmex Manual UniSlide micrometer and MeasureJ2X software (Version 5.03) and conducted quality control using the program COFECHA (Holmes, 1983). For trees where center rings were not captured by either core, the number of missing rings was approximated by dividing the radius of curvature of the innermost ring boundary by the

average width of the four innermost complete rings (Meko et al., 2015). Some trees did not yield a reliable estimation of establishment age due to rot, abundant false ring boundaries, or failure to approach the tree center (Table 2.3).

**Table 2.3.** Sampled trees in each forest.  $n_{random}$  is the number of trees cored that were associated with assigned random points,  $n_{non-random}$  is subjectively cored trees at the same site, and  $n_{dating}$  indicates the number of cores that yielded a reliable age date from the total cores sampled at each of the three forest locations in the Green River Basin, USA.

Site	Sampling Date(s)	$n_{random}$	$n_{non-random}$	$n_{dating}$
Deerlodge Park (Dinosaur National Monument)	Sep. 2018; Jun. 2019; Aug. 2020	50	9	59
Tuxedo Bottom (Canyonlands National Park)	May 2019	52	1	46
Island Park (Dinosaur National Monument)	June 2019	50	0	43

Each of  $n$  trees cored at randomly selected points within the forest represents  $1/n$  of the forest area, making it possible to plot area of floodplain as a function of estimated year of formation. This relation has annual resolution making it temporally robust and useful for comparing to time series with annual resolution, such as peak annual flow, but the spatial accuracy is limited by the small number of trees cored and the absence of forest on parts of the floodplain. To improve spatial accuracy, I combined 2016-2017 NAIP aerial imagery with 1-m resolution and a 2015 LiDAR-derived DEM with 0.5-m resolution to delineate fluvial surfaces occupied by apparently even-aged patches of trees and then used tree ages to estimate the age of each patch within 20-year bins. When applying this approach, I incorporated ages of subjectively sampled trees. In comparison to the random-point area-age distribution, this spatially robust area-age distribution has improved spatial accuracy, but degraded temporal precision (Merigliano et

al., 2013), and is most useful for examining low-frequency (decadal scale) changes in the rate of surface formation.

#### *2.3.4. Estimations of channel change in forest areas*

GLO survey maps, USGS plan and profile survey maps (U.S. Geological Survey, 1922), and historical and modern aerial imagery, were used to estimate channel change at Island Park and Deerlodge Park during the hypothesized time period of arroyo incision and thereafter (Grabowski and Gurnell, 2016). Maps and photographs were georectified in ArcGIS 10.3 using a first-order polynomial transformation (Quik and Wallinga, 2018). Channels were then digitized and the overlap between the channel in sequential documents/photos was calculated. A channel undergoing a high degree of channel change due to channel migration or other processes (e.g., growth of islands or lateral bars) has a lower degree of channel overlap between two sets of sequential photos than a relatively stable one. Channel overlap for the active arroyo incision period was compared to the overlap between the channel at the time of the cessation of arroyo incision and the channel at present to quantify the relative dynamism of the channel during and after the period of tributary erosion (Supplementary Information). Historical maps (Herron, 1917) for Tuxedo Bottom were unable to be satisfactorily referenced due to a lack of identifiable control points.

#### *2.3.5. Data analysis*

To investigate the relationship between peak flow patterns and cottonwood establishment, a nonlinear Poisson regression was applied to tree count data at each forest and annual peak discharge data from the most proximal USGS stream gage (Figure 2.1; Table 2.1). At Deerlodge Park, the flow record was extended to 1921 using a linear regression between peak annual discharge at the Deerlodge Park gage and the annual maximum of combined daily mean

flow at the Lily and Maybell gages for the years in which those gages overlap (1983-2019) (Manners et al., 2014; Schook et al., 2016) (Table 2.1). A Poisson distribution was chosen because it is the most appropriate for analysis of count data (McCullagh and Nelder, 1989; Birken and Cooper, 2006). Nonlinear models containing a three, five, and ten-year running average of peak flow magnitude prior to the calculated establishment year ( $Q_{-3}$ ,  $Q_{-5}$ ,  $Q_{-10}$ ) and three, five, and ten-year running average of peak flow magnitude after the calculated establishment year ( $Q_{+3}$ ,  $Q_{+5}$ ,  $Q_{+10}$ ) were evaluated using the Akaike information criterion corrected for small sample sizes (AICc) (Akaike, 1974). These parameters were calculated for each year in the flow record; for years where there was no corresponding tree establishment, the number of trees established that year was given a value of zero. Model strength was evaluated using a deviance-based pseudo- $R^2$  that indicates the proportion of the variance explained by the chosen model versus the null model containing only the intercept (Heinzel and Mittlböck, 2002; Birken and Cooper, 2006).

The statistical significance of observed spatial patterns in forest age between sites was investigated using a linear model containing an interaction between tree establishment frequency and year. Unadjusted p-values were calculated using the Kruskal-Wallis rank sum test. The Kruskal-Wallis H-test is a non-parametric one-way ANOVA test on ranks and is a powerful way of detecting statistically significant differences between non-parametric sample distributions (Kruskal and Wallis, 1952). Post-hoc pairwise comparisons were made using Dunn's test. A similar analysis for trends in annual peak discharge data was carried out using a linear model containing an interaction between mean-normalized peak annual discharge and flow year.

All statistical analysis was performed in R (R Core Team, 2020) using the MuMIn package (Barton, 2020), stats package (R Core Team, 2020), and the dunn.test package (Dinno,

2017). Related data processing, analysis, and figures were made using the tidyverse family of packages (Wickham et al., 2019).

## **2.4. Results**

### *2.4.1. Time periods and magnitude of active erosion in tributary watersheds*

#### 2.4.1.1. Muddy Creek

The initial GLO survey for the townships along the lower 40 km of Muddy Creek – where historical erosion appears most pervasive – was conducted from 1881-1882, with a resurvey in 1915-1916. Progressive changes in arroyo dimensions suggest that Muddy Creek eroded mostly between 1915 and 1938 but has continued to subsequently incise at a slower rate.

Survey notes indicate the Muddy Creek channel was on average ~10 m wide in 1881-1882 at locations where it was crossed by section or boundary lines (Table 2.4). Depth measurements were not reported. 1915-1916 survey notes depict a channel roughly 4 m wide and 0.5 m deep on average. Generated DEMs from the 1938 aerial photos indicate average channel and arroyo dimensions at section lines were 50 m wide and 3 m deep. At this time, the active channel filled the entire arroyo bottom, as is common for arroyos in the erosional phase (Womack and Schumm, 1977; Friedman et al., 2015). By 1953, the arroyo had average dimensions of 50 m wide and 4 m deep (Table 2.4), observably similar to 1938 dimensions. In 2019, the arroyo dimensions were 50 m wide and 5 m deep on average at measured cross sections, with an inset channel roughly 10 m wide and 1 m deep (Table 2.4).

The persistence of the pre-arroyo channel in a few areas at the locations indicated by the 1915 GLO maps (Figure 2.3) allows for calculation of the volume eroded since that time (Supporting Information). First-order estimates of the volume of sediment exported from Muddy

Creek during historical erosion suggest that arroyo incision resulted in erosion of  $14 \pm 4 \times 10^6$  metric tons of sediment.

**Table 2.4.** Average arroyo and channel dimensions at section line crossings for the tributaries of Muddy Creek, Sand Creek, and Sand Wash in the Yampa River Basin, USA. Number of section lines at which channel dimensions were measured is indicated next to each tributary name. Dimensions are in meters.

		Muddy Creek (n = 21)					
		1881	1915	1938	1953	—	2019
Channel							
Width		10	4	50	20	—	10
Depth		—	0.5	—	1	—	1
Arroyo							
Width		—	—	50	50	—	50
Depth		—	—	3	4	—	5
Error*		—	—	$\pm 5, \pm 5$	$\pm 2, \pm 3$	—	$\pm 0.1, \pm 0.1$
		Sand Creek (n = 15)					
		1881	1937	1938	1953	1968	2019
Channel							
Width		190	290	180	180	160	160
Error*		—	—	$\pm 2$	$\pm 5$	$\pm 3$	$\pm 0.1$
		Sand Wash (n = 8)					
		1881	1906	1938	1954	—	2019
Channel							
Width		—	—	60	50	—	10
Depth		—	—	2	2	—	1
Arroyo							
Width		"Gulch"	140	140	140	—	150
Depth		—	—	2	2	—	2
Error*		—	—	$\pm 5, \pm 5$	$\pm 2, \pm 4$	—	$\pm 0.1, \pm 0.1$

\*Horizontal, vertical georeferencing error

#### 2.4.1.2. Sand Creek

No immediately notable evidence of arroyo development is observable in the field in Sand Creek; instead, the channel is expansively wide, as would be expected in a system with non-cohesive banks. Already wide in 1882, Sand Creek widened further between 1882 and 1937 and then progressively narrowed from 1953 to the present.

The 1882 survey maps and notes for Sand Creek depict a wide channel with an average width of 190 m at section line crossings (Table 2.4). Subsequent resurvey notes from 1937 show that average channel width had increased to roughly 290 m. In 1938, channel dimensions measured from orthorectified aerial photographs reveal that the Sand Creek channel was on average 180 m wide – roughly 110 m narrower than the survey notes from the year prior. However, as mentioned previously, this disparity in dimensions likely results chiefly from a difference in the definition of “channel” by the author’s and the original surveyors.

Measurement of channel dimensions from aerial photographs indicate a channel that was 180 m wide, on average, in 1938, remained 180 m wide in 1953, and subsequently narrowed to an average width of 160 m by 1968 (Table 2.4). From 1968 to 2019 the channel remained dimensionally stable; the average width in 2019 was 160 m at measured cross sections.

#### 2.4.1.3. Sand Wash

The arroyo at Sand Wash eroded between 1881 and 1906 and has since only locally widened. Progressive development of an inset floodplain that was already present by 1938 further suggests that rapid erosion had largely ceased by 1938, and the channel has continued to narrow since.

The 1881 survey notes for Sand Wash lack any quantitative measurements of channel dimensions and simply note the presence and course of an unnamed “gulch” or “dry gulch,”

delineated by a single line. The lack of 1881 measurement suggests that the channel at that time was nothing more than a narrow ephemeral dryland wash, consistent with official surveyor instructions (White, 1991). In contrast, 1906 survey notes contain measurements of channel width; additionally, the 1906 resurvey map depicts a wide, stippled channel in contrast to the thin ribbon on the original 1881 map, and field observation reveals arroyo walls as much as 5 m high (Figure 2.4). The 1906 Sand Wash arroyo had an average width of 140 m at section line crossings; it is likely that the channel filled the entire arroyo bottom at this time (Table 2.4). Assuming the 1881 channel is roughly 10-m wide – determined by multiplying the width of pencil line (0.3 mm) by the map scale, consistent with survey instructions to illustrate “the distance on-line at the crossings of streams, so far as such can be noted on the paper” (White, 1991) – this indicates Sand Wash widened by 130 m, on average, from 1881 to 1906.

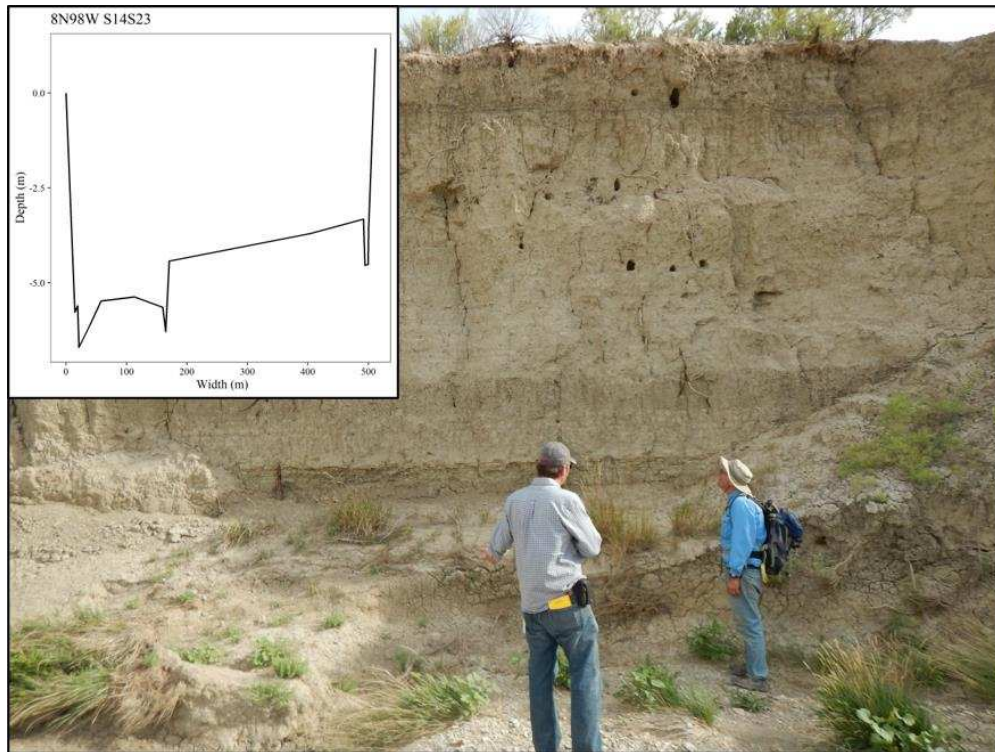


**Figure 2.4.** Exposed arroyo wall in Sand Wash in the Yampa River Basin, USA, approximately 5 m high with cross section at nearest section line roughly 500 m downstream (inset). As per official government surveyor instructions in the Manual of Surveying Instructions, it is unlikely that the surveyor’s in 1881 would have noted a channel of these dimensions as simply a “gulch.”

The 1938 arroyo dimensions measured from orthorectified aerial photographs show an arroyo channel with average dimensions of 140 m wide and 2 m deep at locations where it intersects GLO section lines, with an inset channel roughly 60 m wide and 2 m deep. Measurements from 1954 aerial photographs indicate that average arroyo dimensions were 140 m wide and 2 m deep with an inset channel 50 m and 1 m deep. Field measurements at section lines in 2019 indicated an average arroyo width of 150 m and depth of 2 m and active channel width of 10 m and depth of 1 m. There is a notable stability of arroyo dimensions from 1906 to the present (Table 2.4).

The presence of single terrace in the Sand Wash basin makes calculation of sediment volumes from historical erosion relatively straightforward (Supporting Information). Assuming the arroyo incised from roughly the level of the terrace, an estimated  $18 \pm 4 \times 10^6$  tons of sediment was exported from Sand Wash during this time period.

#### *2.4.2. Area-age distribution of cottonwood floodplain forests and historical channel change*

##### 2.4.2.1. Deerlodge Park

Establishment years of trees in Deerlodge Park ranged from 1753 to 2010. From spatially robust cottonwood maps, several broad temporal but spatially representative trends emerge. About 26% of the surviving forest in Deerlodge Park established prior to 1889 (Figure 2.5a, 2.6a). Approximately 53% of the forest was established between 1890 and 1929. Very little establishment subsequently occurred until the period between 1970-2009, when the remaining 21% of the forest established. Temporally robust data from individual trees provide additional detail and indicate substantial tree establishment occurred mostly in four pulses: 1899-1907, 1913-1930, and two smaller pulses in 1992-1998 and 2003-2010 (Figure 2.7). Establishment of the remaining forest was dispersed throughout time.

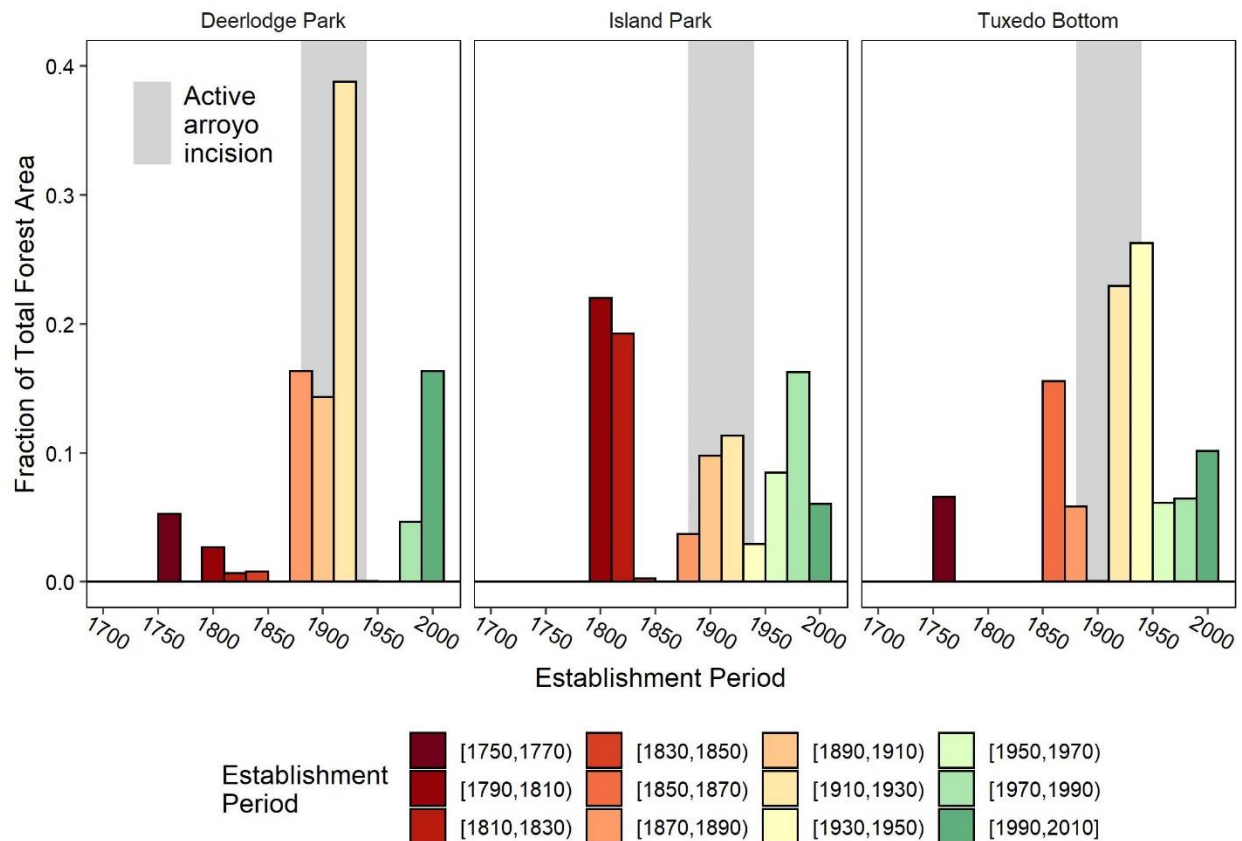


**Figure 2.5.** Fraction of total present-day floodplain forest by 20 year-establishment period for Fremont cottonwood (the spatially robust area-age distribution) at three forests in the Green River Basin, USA (a) Deerlodge Park, (b) Island Park, and (c) Tuxedo Bottom, calculated by grouping equivalent age stands based on topography and visual evidence from aerial photography. Gray shading indicates timing of active arroyo incision (1880-1940) in the upstream tributaries.

Historical channel dimensions in Deerlodge suggest a relatively dynamic channel during the period of arroyo incision. The 1922 channel overlapped merely 19% with the 1906 channel (Table 2.5, Figure A.7). The 1922 and 1938 channels and 1938 and 2019 channels have similar degrees of overlap (55% and 58%, respectively), though the latter period is roughly five times greater in length, suggesting a channel that was relatively more dynamic in the former period than the latter.

**Table 2.5.** Percent overlap of the channel through each forest reach as determined from historical maps and aerial imagery for two forests in the Green River Basin, USA. Channel overlap indicates how much of the channel in one map/image overlaps with the channel in the map/image directly preceding it. Channel overlap was calculated for each reach between years during the period of arroyo incision (indicated by the \*) and between the cessation of erosion (~1940) to the present. GLO is General Land Office, NAIP is National Agriculture Imagery Program, USGS is U.S. Geological Survey.

Deerlodge Park				
Year	1906	1922	1938	2019
Type	GLO Survey Map	USGS Plan Survey	Aerial Photograph	NAIP
Mapping error (RMSE) (m)	3	5	5	—
Active channel area (km <sup>2</sup> )	1.0	0.51	0.72	0.75
Channel Overlap (%)	—	19*	55*	58
Island Park				
Year	1906	—	1938	2019
Type	GLO Survey Map	—	Aerial Photograph	NAIP
Mapping error (RMSE) (m)	8	—	2	—
Active channel area (km <sup>2</sup> )	1.3	—	1.3	0.99
Channel Overlap (%)	—	—	62*	60

\*During period of active arroyo incision

#### 2.4.2.2. Island Park

Strikingly, in Island Park, spatially robust cottonwood maps indicate 41% of the present-day floodplain forest was established in the four decades spanning 1790 to 1829 (Figure 2.5b). An extended period of likely relative inactivity occurred from 1830-1889, followed by a period of heightened establishment from 1890-1929, when roughly 21% of the forest established. An additional burst occurred from 1950-1989 with the establishment of 25% of the forest. Overall, there is a notably greater percentage of forest dating to the late 18<sup>th</sup> and early 19<sup>th</sup> century in

Island Park (Figure 2.6b) compared to Deerlodge Park (Figure 2.6a). Temporally robust individual tree data indicate that there were three pulses of consistently frequent – no more than three years between calculated center years – substantial tree establishment: 1815-1823 (six trees), 1920-1926 (six trees), and 1989-1995 (six trees) (Figure 2.7).

Channel change in Island Park appears noticeably similar during both the historical period of arroyo incision and subsequently. The 1906 channel overlapped with the 1938 channel by 62%; the 1938 channel overlapped with the 2019 channel by 60%. It is notable, however, that the latter time period is more than twice the former in length (Table 2.5, Figure A.8), indicating the channel during historic period may have been slightly more dynamic than subsequently.

#### 2.4.2.3. Tuxedo Bottom

Spatially robust results indicate that there was observable early forest establishment in Tuxedo Bottom from 1750-1769, when 6% of the present forest became established. After a century-length gap, establishment proceeded at a slow but steady rate from 1850-1890; roughly 21% of the present-day forest dates to that time period (Figure 2.5c, 2.6c). Relatively little establishment then occurred from 1890-1909, followed immediately by a substantial burst from 1910-1949, when nearly 50% of the present-day forest established. The remaining forest was fairly steadily established in the three twenty-year periods from 1950-2010 (Figure 2.5c, 2.6c). Temporally robust data indicate a similarly pulsed pattern of frequent tree establishment, with four notable periods: 1862-1872 (six trees), 1932-1940 (seven trees), 1989-1996 (six trees), and 2004-2007 (five trees) (Figure 2.7).

Channel change in Tuxedo Bottom was unable to be quantified due to a dearth of identifiable control points for referencing historical maps.

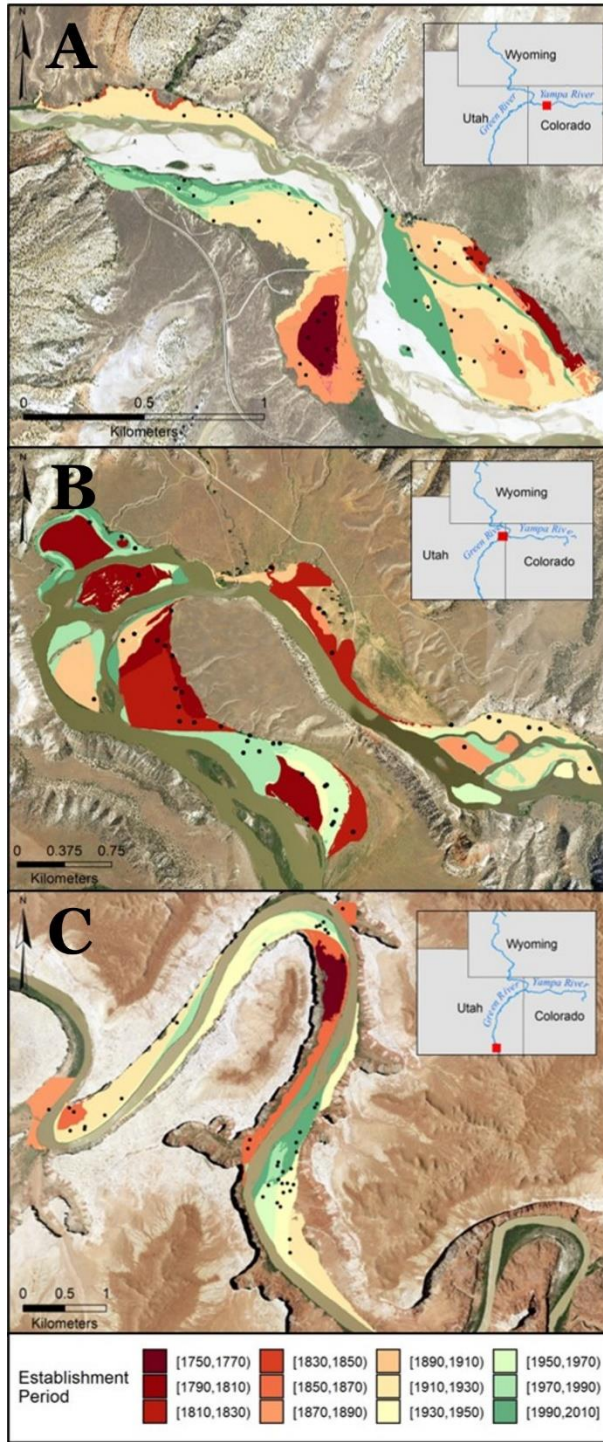


**Figure 2.6.** Floodplain area-age maps for three the forests in the Green River Basin, USA: a) Deerlodge Park, b) Island Park and c) Tuxedo Bottom. Black dots represent cored trees used in area-age calculations.

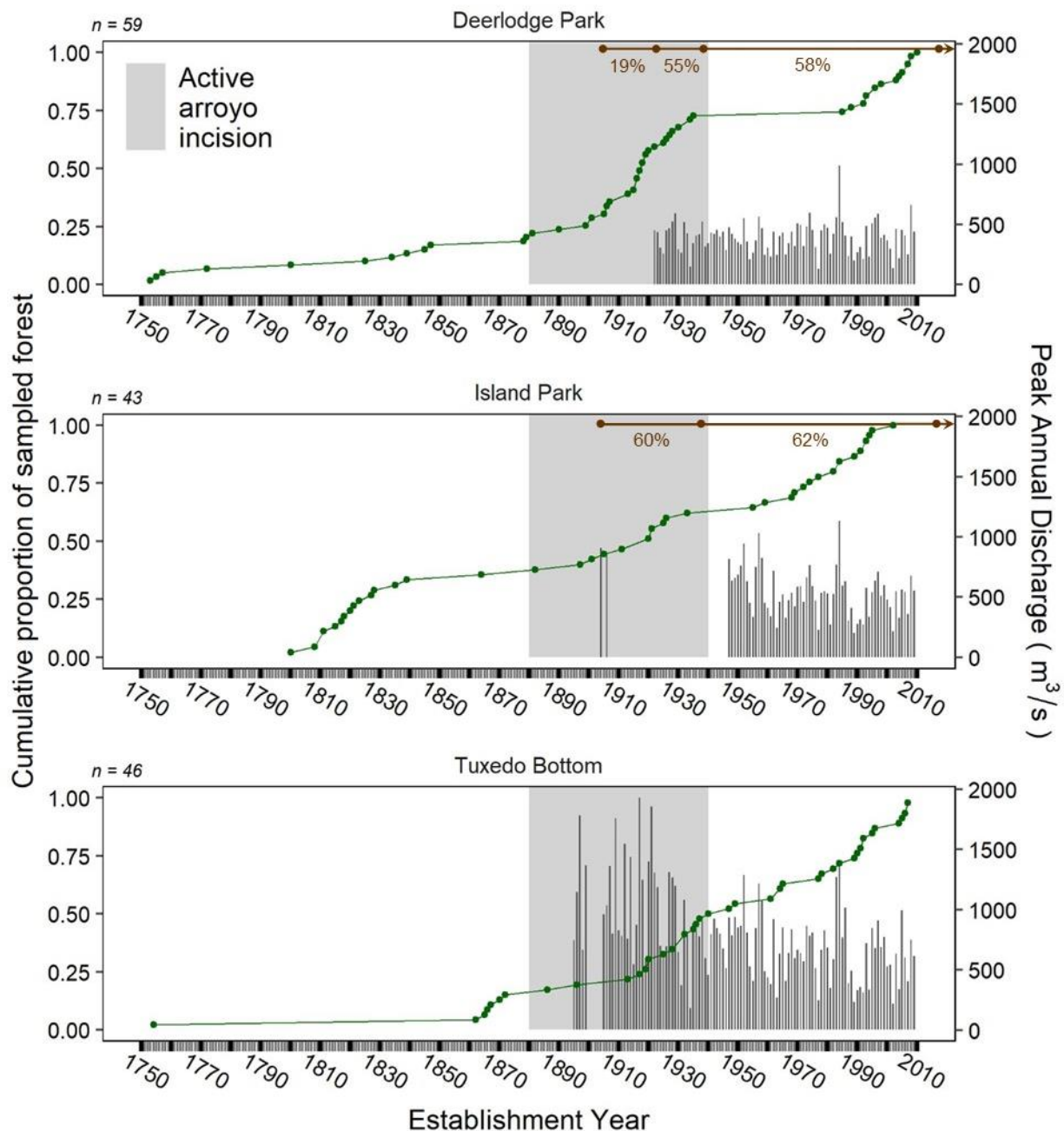


**Figure 2.7.** Cumulative tree establishment as percent of total present-day forest (green points and line) plotted with peak annual discharge (gray bars) for three forests in the Green River Basin, USA. Channel overlap for specific time periods is indicated in brown. Discharge measurements are from USGS stream gages most proximal to each forest, from top to bottom: the Deerlodge Park gage, the Green River at Jensen gage, and the Green River at Green River gage. Gray area is time span of headwater arroyo incision, 1880-1940.

### *2.4.3. Flow-establishment correlations*

Observable differences between forest age distributions are statistically significant (p-value < 0.0001 using the Kruskal-Wallis test) whereas differences in the distribution of peak flow values for each forest reach lack statistical significance (p-value = 0.98). This suggests that each forest has a unique pattern of tree establishment but experienced floods of similar relative magnitude at similar times.

Results of model fits using a nonlinear Poisson distribution indicate that the best model for the Deerlodge forest contains a five-year running average of annual peak discharge magnitude following establishment; for the Tuxedo Bottom forest, the best model contains a three-year running average of peak flow magnitude prior to the year of establishment and a five-year running average of peak flow magnitude following establishment. At Island Park, the best model is the null model. Though the modeled relationships at Deerlodge Park and Tuxedo Bottom are significant, they are of weak explanatory power; deviance based pseudo-R<sup>2</sup> do not exceed 0.12, indicating only an 12% improvement over the null model in explaining observed variability (Table 2.6).

## **2.5. Discussion**

### *2.5.1. Tributary erosion from the late 19<sup>th</sup> to mid-20<sup>th</sup> century*

Inspection of historical documents and aerial photographs suggests that Sand Wash, Sand Creek, and Muddy Creek underwent significant historical erosion in the late 19<sup>th</sup> to early 20<sup>th</sup> century. I detected a period of extreme erosion in each tributary watershed – arroyo incision in Muddy Creek between 1915 and 1938 and in Sand Wash between 1881 and 1906, and channel widening in Sand Creek between 1881 and 1937. From these results I identified a period of high sediment yield to the Little Snake River from roughly 1880 to 1940 (grey box, Figures 5 and 7).

This timing is consistent with downcutting observed by Parker et al. (1985) in the bed of Muddy Creek since 1905, and with arroyo incision in the neighboring White River and Duchesne River basins, (Figure 2.1) that began around 1900 and the early 1930s, respectively (Womack and Schumm, 1977; Gaeuman et al., 2005).

**Table 2.6.** Coefficients of significant predictors and explanatory power (pseudo  $R^2$ ) of models obtained from Poisson regressions. The response variable is the number of trees established per year in each of the three forests in the Green River Basin, USA and the potential predictors are the hydrological variables defined in the text.

Deerlodge Park ( <i>pseudo R<sup>2</sup> = 0.05</i> )		
Predictors		
	Intercept	Q <sub>+5</sub>
Coefficient	-4.01	0.006
p-value	0.004	0.05
Island Park ( <i>pseudo R<sup>2</sup> = 0</i> )		
Predictors		
	Intercept	—
Coefficient	-1.2	—
p-value	< 0.001	—
Tuxedo Bottom ( <i>pseudo R<sup>2</sup> = 0.12</i> )		
Predictors		
	Q <sub>-3</sub>	Q <sub>+5</sub>
Coefficient	-0.003	0.003
p-value	0.002	0.01

Though few other studies of arroyo incision within the Green River Basin have been published, a substantial body of work has established that the streams and rivers of the Colorado Plateau in neighboring basins were heavily eroding via arroyo development beginning in roughly 1880 (and as early as 1861 in some locations) and continuing as late as 1940 (Gregory, 1917; Duce, 1918; Bryan, 1925, 1928; Gregory and Moore, 1931; Bailey, 1935; Antevs; 1952; Cooke and Reeves, 1976; Graf, 1982, 1987; Bull, 1997; Hereford, 2002; Webb and Hereford, 2010; Harvey and Pederson, 2011; Aby, 2017). Concomitant elevated sediment loads in the major rivers were observed throughout the Colorado Basin (Gellis et al., 1991), indicating that arroyo

incision likely injected substantial quantities of sediment into the Yampa, Green, and similar rivers during this time.

In the studied tributaries, arroyo incision resulted in the export of roughly 30 million metric tons of sediment to the Little Snake River from the investigated segments of Sand Wash and Muddy Creek alone. This conservative estimate does not include sediment eroded from additional unsurveyed segments of these two creeks, their tributaries, upland areas, or from Sand Creek and other tributaries to the Little Snake and Yampa Rivers. Distributed over the 60 years between 1881 and 1940, arroyo incision would have added roughly 0.5 million metric tons of sediment per year to the background annual sediment load of the Yampa River. More recent measurements at Deerlodge Park indicate an annual sediment load between 0.83 and 1.6 million metric tons per year (Elliott et al., 1984; Elliott and Anders, 2005; Topping et al., 2018). Therefore, arroyo erosion in Muddy Creek and Sand Wash must have sizably increased the sediment loads of the Little Snake, Yampa, and Green Rivers.

Previous work has established that sand supply from the lower Little Snake watershed has declined in the last 60 years as the tail of an elongating sediment wave passed through the system after large floods in the early 1960s (Topping et al., 2018). The century-scale temporal context provided here indicates that the main pulse of sediment coming from tributaries of the lower Little Snake River occurred from roughly 1880 to 1940. This expanded context further emphasizes that the overall trajectory of sediment loads in the basin has been one of decline following past episodic sediment supply events from tributary watersheds, especially since the large sediment pulses associated with arroyo incision occurred in the late 19<sup>th</sup> and early 20<sup>th</sup> century.

### 2.5.2. *The role of sediment in floodplain forest establishment*

Current understanding of riparian *Populus* establishment states that successful seedling germination occurs on unvegetated, moist alluvium safe from future disturbance. These sites may occur on the floodplain following flood deposition or on the channel bed during extended low flows (Scott et al., 1996; Mahoney and Rood, 1998); forest establishment is thus seen largely as a function of geomorphic processes governed principally by hydrology. However, here I found a significant difference between the distribution of tree ages at each site, but a lack thereof for peak flows, as well as only modest confirmation of the positive relation between flood magnitude and tree establishment (Table 2.6). Together, this suggests an additional prominent driver beyond hydrology alone. The influence of peak flow is notably smaller than that found by other work in the area (Birken and Cooper, 2006), likely because of the much longer, more varied flow period considered by the analysis herein and because I did not excavate trees to the establishment point. On the other hand, the spatially representative sample collected in this present work allows stronger inference relating flows and sediment to establishment of the entire forest.

Cottonwood establishment for each forest showed strong decadal variation unrelated to flooding. For example, in Deerlodge Park, there is a dearth of establishment from 1950 to 1970, despite peak flows similar to those in the 1920s, when there was ample establishment (Figure 2.5-2.7). Similarly, a cohort associated with the flood of 1917 (as recorded on the Yampa River at Maybell) is larger than the cohort associated with the 1984 flood, despite the latter being the flood of record. Additionally, large floods in 1984, 1997, and 2011 did not result in larger areas of forest in Deerlodge Park than smaller floods in the 1910s and 20s (Figure 2.5-2.7). An analogous relation can be observed at Tuxedo Bottom: floods in the 1950s and mid-1980s

produced less forest than similar floods in the mid-to-late 1920s and smaller flood in the late 1930s (Figure 2.5-7). Together this suggests controlling influences on forest establishment beyond simply peak flow magnitude; I contend that one such prominent driver is sediment load.

Greater amounts of forest establishment during the historical period of heightened erosion in the tributaries of Muddy Creek, Sand Creek, and Sand Wash (grey box, Figures 5 and 7), especially at Deerlodge Park, the forest site most proximal to these tributaries, suggests that sediment loads exert a considerable control on forest establishment. Increases in tributary erosion beginning between 1881 and 1906 (Table 2.4) are consistent with enhanced forest establishment at Deerlodge Park beginning around 1900 (Figures 2.5-2.7). This sequence of events is congruent with the observation by Topping et al. (2018) that the finest sand fractions of a sediment pulse can traverse 100 km of the Yampa-Green River system in one month, while the coarsest sand fractions may take decades to cover the same distance. A more detailed investigation of transit times (*sensu* Czuba and Fofoula-Georgiou, 2015) remains an area of crucial future work.

Although the history of tributary erosion upstream of Island Park and Tuxedo Bottom is relatively less well documented, similar forest ages suggest considerable arroyo erosion may have also occurred in the watershed of the Middle and Lower Green River within a similar timeframe. Enhanced forest establishment in Tuxedo Bottom from roughly 1910-1940 appears as a more staccato version of the Deerlodge time series; a notable burst occurs in ~1910, with subsequent increases in establishment in the late 1920s and 30s (Figure 2.7). This is perhaps indicative of disparate sediment wave(s) passing through the Tuxedo Bottom reach; these bursts of establishment are roughly consistent with the time period of documented arroyo incision in the more proximal White River and Duchesne River basins (Womack and Schumm, 1977; Gaeuman et al., 2005).

Increased forest establishment in the 1980s and 1990s at Tuxedo Bottom and contemporaneous accelerated channel narrowing on the Lower Green River in the same period (Birken and Cooper, 2006; Scott and Miller, 2018; Dean et al., 2020; Walker et al., 2020) is consistent with the observation that cottonwoods may become established on low-lying bars during extended periods of reduced peak flows during channel narrowing (Scott et al. 1996); a similar pattern appears to be true of Island Park (Grams and Schmidt, 2002). Notably, forest establishment during the period of arroyo incision is equivalent to or of greater magnitude than forest establishment during the period of channel narrowing.

The less clear connection between timing of arroyo incision and large-scale forest establishment at Island Park is potentially a factor of its comparatively unique location within the river network and the dominant fluvial planform there. Island Park is downstream of two large alluvial parks (Deerlodge Park on the Yampa and Browns Park on the Green) that would likely have modulated the delivery of any upstream sediment transported downriver from eroding tributaries as sediment waves and, similarly, lacks local sediment-laden tributaries at comparatively proximal distances to those upstream of Deerlodge Park and Tuxedo Bottom (Figure 2.1). Additionally, the Island Park reach is anastomosing, and perhaps does not respond similarly to increased sediment loads as the Tuxedo and Deerlodge Park reaches. The presence of older forest of appreciably greater extent in Island Park than the other two areas suggests that Island Park may simply be less dynamic than the other two locales.

In addition to a greater degree of forest establishment during the period of arroyo incision, the channel through each study reach was likely more spatially dynamic. At Deerlodge Park, a greater degree of overlap between the 1938 channel and the 2019 channel than between the channels in the years of the arroyo incision period suggests that the increased sediment load

from arroyo incision in the tributaries resulted in enhanced channel movement in the downstream forest reach (Table 2.5). At Island Park, a similar degree of channel movement for each period despite the notably longer magnitude of the post-arroyo incision period indicates a slightly more dynamic channel during the arroyo period. Other work further suggests the Middle Green River was more dynamic in the late 19<sup>th</sup> and early 20<sup>th</sup> century, prior to the closure of Flaming Gorge Dam (Grams and Schmidt, 2002). In Tuxedo Bottom, past studies have likewise suggested that the Lower Green River in the vicinity of Tuxedo Bottom had a wider, more dynamic channel prior to the 1930s (Graf, 1978; Walker et al., 2020).

Strikingly, at all forest locations, forest areas formed a century or more ago are larger than those formed more recently (Figures 5 and 6). This pattern persists in spite of the fact that old floodplain has been subject to removal by fluvial erosion over a longer time (Merigliano et al, 2013) and reinforces the aforementioned conclusion that rates of channel migration, and the associated construction of new floodplain suitable for forest establishment, were greater during the past period of substantial tributary erosion and elevated main-stem sediment loads and have declined since.

Overall, evidence suggests that the sediment wave(s) initiated by historical erosion in the tributary watersheds of Muddy Creek, Sand Creek, and Sand Wash played a crucial role in catalyzing increased rates of downstream channel migration and forest establishment. Of course, I do not intend to diminish the importance of hydrology. High flows during the period of tributary erosion doubtless also played a role and a full separation of the relative importance of sediment and hydrology is both unfeasible and misguided; it is likely that the influence of many hydrologic parameters on forest establishment is substantial. Rather, I propose that sediment loads are an equivalently essential driver of channel migration and riparian forest establishment.

This demonstrable link between headwater erosion and distal downstream channel migration and forest establishment validates the idea that upstream watershed dynamics play a key role in governing downstream ecological processes such as riparian forest establishment. Broadly, this observable link argues for the existence and importance of network scale sediment-ecological connectivity.

### *2.5.3. Sediment-ecological connectivity*

I propose a sediment-ecological connectivity framework to link geomorphological and ecological processes across time and space at the full-watershed scale. Connectivity frameworks incorporating ecosystem processes have been developed to understand and investigate hydrological connectivity at large spatial scales (e.g., Hwang et al., 2012); here, I use similar reasoning to construct a framework capable of parsing sediment connectivity at the full basin scale.

In the sediment-ecological connectivity conceptualization, main stem channels of a given catchment are in a state of dynamic equilibrium with the discharge and sediment regime prior to a period of heightened tributary erosion (Figure 2.8, top panel). Heightened erosion in the tributaries, catalyzed by a range of possible mechanisms (including land-use and climate change), then injects substantial quantities of sediment into main-stem rivers, increasing sediment loads. Sediment is then transported downstream from tributary junctions as elongating sediment waves, resulting in increased channel migration in partially-confined and unconfined areas along the main stem (Gurnell et al., 2009). Increased establishment of pioneer riparian species (e.g., cottonwood) is concomitant with increased rates of channel migration and the greater availability of favorable establishment sites (Figure 2.8, middle panel). Heightened rates of channel migration and forest establishment are likely delayed from tributary erosion by some

period commensurate with the travel time of sediment from the tributary watershed(s) of interest to the location of the forest(s). As tributary erosion rates decline, the main stem channel begins to stabilize and eventually returns to dynamic equilibrium in which floods have lower geomorphic effectiveness than past sediment-charged floods of the same magnitude (Figure 2.8, bottom panel). This return to dynamic equilibrium may take decades from the cessation of enhanced tributary erosion, as the sediment wave moves downstream at varying rates dependent upon the grain size fraction (Gran and Czuba, 2017; Topping et al., 2018).

A sediment-ecological connectivity framework both contextualizes the use of dendrochronology as a tool for tracking sediment pulses over broad spatial and temporal scales and supports the use of a holistic approach to watershed management. Additional sediment connectivity studies relating upstream erosion to downstream channel migration rate and ecological response are a critical area of future work, especially with respect to the influence of parameters such as the network location of areas of interest (i.e., structural connectivity) and river planform on the framework. Although past work has quantified the influence of sediment load on riparian vegetation establishment (Hupp and Osterkamp, 1996) and used riparian vegetation aspects to inform estimations of sediment residence time (Pizzuto et al., 2016), this study emphasizes riparian vegetation area-age assemblages as both reflective of long-term basin-scale functional sediment connectivity and indicative of the dependence of ecological processes on distal geomorphic processes. The sediment-ecological connectivity framework can conceivably be utilized in any basin with similar assemblages of periods of past acute erosion and woody riparian pioneer species – e.g. the Murrumbidgee River in Australia (Wasson et al., 1998), various river basins of the southeastern United States (Meade and Trimble, 1974), the Garron River in southern France (Décamps et al., 1988), the Yellow River in China (Peng et al.,

2010) – to either quantify or augment existing understanding of long term, watershed-scale functional sediment connectivity and its impact on ecological processes.

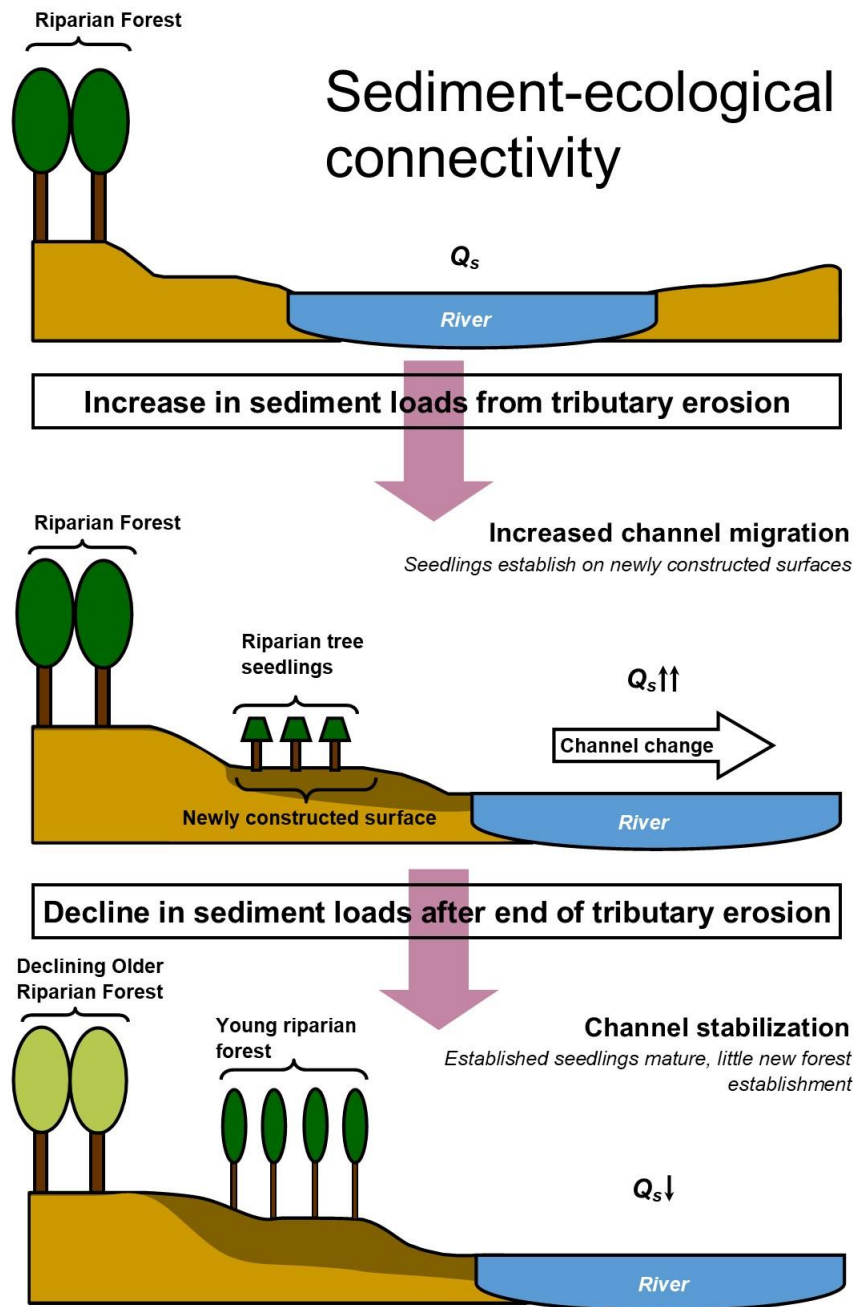


**Figure 2.8.** Conceptual representation of the sediment-ecological connectivity framework. An increase in sediment loads ( $Q_s$ ) from tributary erosion causes a previously stable river channel (top) to migrate or undergo some geomorphic change at a heightened rate, leading to increases in rates of floodplain and forest establishment (middle). Near-cessation of tributary erosion eventually leads to a river channel that is again in dynamic equilibrium and little establishment of new cottonwood forest or floodplain.

## 2.6. Conclusions

Here, I demonstrate that historical tributary erosion and downstream channel migration and floodplain forest establishment are inextricably linked processes governed by sediment connectivity. Constrained timing of each process can quantify or improve estimations of basin-scale functional sediment connectivity over century time scales. In the Yampa and Green River basin of Wyoming, Colorado, and Utah, evidence from historical documents and aerial photographic analysis indicates heightened erosion in several tributaries resulted in heightened downstream channel change and floodplain forest establishment formation in Deerlodge Park on the Yampa River. Elevated rates of cottonwood establishment and channel change also occurred in the further downstream forests of Island Park and Tuxedo Bottom during this time, a period of known extreme erosion in the region, further suggesting the considerable influence of sediment load on floodplain forest establishment.

Study findings indicate links between tributary morphological processes (e.g. elevated erosion) and distal downstream ecological processes (e.g. forest establishment) that are best understood via a sediment-ecological connectivity framework. Principally, this framework facilitates holistic, watershed-scale management by emphasizing the connectivity, even at the scale of a large river network, of what were formerly considered disparate processes or issues (tributary erosion and downstream forest establishment) and underlines the potential to use riparian vegetation assemblages to investigate functional sediment connectivity over large spatial and temporal scales. The findings of this study explicitly support and highlight the benefits of basin-scale management of sediment within the Colorado River Basin for future management of valuable resources such as cottonwood forests. The widespread occurrence of river basins facing

similar histories and possible futures emphasizes the potentially global applicability of this framework to inform basin-scale management.

## 2.7. References

- Aby SB. 2017. Date of arroyo cutting in the American Southwest and the influence of human activities. *Anthropocene* **18** : 76–88. DOI: [10.1016/j.ancene.2017.05.005](https://doi.org/10.1016/j.ancene.2017.05.005)
- Akaike H. 1974. A new look at the statistical model identification. *IEEE Transactions on Automatic Control* **19** : 716–723. DOI: [10.1109/TAC.1974.1100705](https://doi.org/10.1109/TAC.1974.1100705)
- Andrews ED. 1978. Present and potential sediment yields in the Yampa River Basin, Colorado and Wyoming . USGS Numbered Series. U.S. Geological Survey, Water Resources Division, [online]
- Andrews ED. 1980. Effective and bankfull discharges of streams in the Yampa River basin, Colorado and Wyoming. *Journal of Hydrology* **46** : 311–330. DOI: [10.1016/0022-1694\(80\)90084-0](https://doi.org/10.1016/0022-1694(80)90084-0)
- Andrews ED. 1986. Downstream effects of Flaming Gorge Reservoir on the Green River, Colorado and Utah. *GSA Bulletin* **97** : 1012–1023. DOI: [10.1130/0016-7606\(1986\)97<1012:DEOFGR>2.0.CO;2](https://doi.org/10.1130/0016-7606(1986)97<1012:DEOFGR>2.0.CO;2)
- Antevs E. 1952 . Arroyo-Cutting and Filling. *The Journal of Geology* **60**: 375-385. DOI: [10.1086/625985](https://doi.org/10.1086/625985)
- Bailey RW. 1935. Epicycles of Erosion in the Valleys of the Colorado Plateau Province. *The Journal of Geology* **43**: 337-355. DOI: [10.1086/624315](https://doi.org/10.1086/624315)
- Bakker M, Lane SN. 2017. Archival photogrammetric analysis of river–floodplain systems using Structure from Motion (SfM) methods. *Earth Surface Processes and Landforms* **42** : 1274–1286. DOI: <https://doi.org/10.1002/esp.4085>
- Barton K. 2020. MuMIn: Multi-Model Inference. R package version 1.43.17. <https://CRAN.R-project.org/package=MuMIn>

- Benda L, Poff NL, Miller D, Dunne T, Reeves G, Pess G, Pollock M. 2004. The Network Dynamics Hypothesis: How Channel Networks Structure Riverine Habitats. *BioScience* **54** : 413–427. DOI: [10.1641/0006-3568\(2004\)054\[0413:TNDHHC\]2.0.CO;2](https://doi.org/10.1641/0006-3568(2004)054[0413:TNDHHC]2.0.CO;2)
- Benjankar R, Burke M, Yager E, Tonina D, Egger G, Rood SB, Merz N. 2014. Development of a spatially-distributed hydroecological model to simulate cottonwood seedling recruitment along rivers. *Journal of Environmental Management* **145** : 277–288. DOI: [10.1016/j.jenvman.2014.06.027](https://doi.org/10.1016/j.jenvman.2014.06.027)
- Birken AS, Cooper DJ. 2006. Processes Of Tamarix Invasion And Floodplain Development Along The Lower Green River, Utah. *Ecological Applications* **16** : 1103–1120. DOI: [https://doi.org/10.1890/1051-0761\(2006\)016\[1103:POTIAF\]2.0.CO;2](https://doi.org/10.1890/1051-0761(2006)016[1103:POTIAF]2.0.CO;2)
- Birnie-Gauvin K, Nielsen J, Frandsen SB, Olsen H-M, Aarestrup K. 2020. Catchment-scale effects of river fragmentation: A case study on restoring connectivity. *Journal of Environmental Management* **264** : 110408. DOI: [10.1016/j.jenvman.2020.110408](https://doi.org/10.1016/j.jenvman.2020.110408)
- Borselli L, Cassi P, Torri D. 2008. Prolegomena to sediment and flow connectivity in the landscape: A GIS and field numerical assessment. *Catena* **75** : 268–277. DOI: [10.1016/j.catena.2008.07.006](https://doi.org/10.1016/j.catena.2008.07.006)
- Bracken LJ, Turnbull L, Wainwright J, Bogaart P. 2015. Sediment connectivity: a framework for understanding sediment transfer at multiple scales. *Earth Surface Processes and Landforms* **40** : 177–188. DOI: <https://doi.org/10.1002/esp.3635>
- Bryan K. 1925. Date of Channel Trenching (arroyo Cutting) in the Arid Southwest. *Science* **62** : 338–344. DOI: [10.1126/science.62.1607.338](https://doi.org/10.1126/science.62.1607.338)
- Bryan K. 1928. Historic Evidence on Changes in the Channel of Rio Puerco, a Tributary of the Rio Grande in New Mexico. *The Journal of Geology* **36** : 265–282. DOI: [10.1086/623512](https://doi.org/10.1086/623512)

- Bull WB. 1997. Discontinuous ephemeral streams. *Geomorphology* **19** : 227–276. DOI: [10.1016/S0169-555X\(97\)00016-0](https://doi.org/10.1016/S0169-555X(97)00016-0)
- Calle M, Calle J, Alho P, Benito G. 2020. Inferring sediment transfers and functional connectivity of rivers from repeat topographic surveys. *Earth Surface Processes and Landforms* **45** : 681–693. DOI: <https://doi.org/10.1002/esp.4765>
- Cienciala P. 2021. Vegetation and Geomorphic Connectivity in Mountain Fluvial Systems. *Water* **13**: 593. DOI: 10.3390/w13050593
- Constantine JA, Dunne T, Ahmed J, Legleiter C, Lazarus ED. 2014. Sediment supply as a driver of river meandering and floodplain evolution in the Amazon Basin. *Nature Geoscience* **7** : 899–903. DOI: [10.1038/ngeo2282](https://doi.org/10.1038/ngeo2282)
- Cooke RU, Reeves RW. 1976. *Arroyos and environmental change in the American South-West*. Clarendon Press: Oxford.
- Cooper DJ, Andersen DC, Chimner RA. 2003. Multiple pathways for woody plant establishment on floodplains at local to regional scales. *Journal of Ecology* **91** : 182–196. DOI: <https://doi.org/10.1046/j.1365-2745.2003.00766.x>
- Cossart E, Viel V, Lissak C, Reulier R, Fressard M, Delahaye D. 2018. How might sediment connectivity change in space and time? *Land Degradation & Development* **29** : 2595–2613. DOI: <https://doi.org/10.1002/ldr.3022>
- Czuba JA, Fofoula-Georgiou E. 2015. Dynamic connectivity in a fluvial network for identifying hotspots of geomorphic change. *Water Resources Research* **51** : 1401–1421. DOI: <https://doi.org/10.1002/2014WR016139>
- Dodge R.E, 1902, Arroyo Formation. *Science* **15**: 746-747. DOI: 10.1126/science.15.384.746

- Dean DJ, Schmidt JC. 2013. The geomorphic effectiveness of a large flood on the Rio Grande in the Big Bend region: Insights on geomorphic controls and post-flood geomorphic response. *Geomorphology* **201** : 183–198. DOI: [10.1016/j.geomorph.2013.06.020](https://doi.org/10.1016/j.geomorph.2013.06.020)
- Dean DJ, Topping DJ, Grams PE, Walker AE, Schmidt JC. 2020. Does Channel Narrowing by Floodplain Growth Necessarily Indicate Sediment Surplus? Lessons From Sediment Transport Analyses in the Green and Colorado Rivers, Canyonlands, Utah. *Journal of Geophysical Research: Earth Surface* **125** : e2019JF005414. DOI: <https://doi.org/10.1029/2019JF005414>
- Dean DJ, Topping DJ, Schmidt JC, Griffiths RE, Sabol TA. 2016. Sediment supply versus local hydraulic controls on sediment transport and storage in a river with large sediment loads. *Journal of Geophysical Research: Earth Surface* **121** : 82–110. DOI: <https://doi.org/10.1002/2015JF003436>
- Dunne T, Constantine JA, Singer M. 2010. The Role of Sediment Transport and Sediment Supply in the Evolution of River Channel and Floodplain Complexity. *Transactions, Japanese Geomorphological Union* **31** : 155–170.
- Décamps H, Fortuné M, Gazelle F, Pautou G. 1988. Historical influence of man on the riparian dynamics of a fluvial landscape. *Landscape Ecology* **1** : 163–173. DOI: [10.1007/BF00162742](https://doi.org/10.1007/BF00162742)
- Diehl RM, Wilcox AC, Stella JC, Kui L, Sklar LS, Lightbody A. 2017. Fluvial sediment supply and pioneer woody seedlings as a control on bar-surface topography. *Earth Surface Processes and Landforms* **42** : 724–734. DOI: <https://doi.org/10.1002/esp.4017>
- Dinno A. 2017. dunn.test: Dunn's Test of Multiple Comparisons Using Rank Sums. R package version 1.3.5. <https://CRAN.R-project.org/package=dunn.test>

- Donovan M, Belmont P, Sylvester Z. 2021. Evaluating the relationship between meander-bend curvature, sediment supply, and migration rates. *Journal of Geophysical Research: Earth Surface* **126** DOI: <https://doi.org/10.1029/2020JF006058>
- Duce JT. 1918. The Effect of Cattle on the Erosion of Canon Bottoms. *Science* **47** : 450–452. DOI: [10.1126/science.47.1219.450](https://doi.org/10.1126/science.47.1219.450)
- Efron B, Tibshirani RJ. 1994. *An Introduction to the Bootstrap*. Chapman and Hall/CRC Press: New York
- Elliott JG, Anders SP. 2004. Summary of sediment data from the Yampa river and upper Green river basins, Colorado and Utah, 1993-2002 . USGS Numbered Series. Scientific Investigations Report 2004-5242. U.S. Geological Survey
- Elliott JG, Kircher JE, Von Guerard P. 1984. Sediment Transport in the Lower Yampa River, Northwestern Colorado . USGS Numbered Series. Water-Resources Investigations Report 84-4141. U.S. Geological Survey.
- Estrany J, Ruiz M, Calsamiglia A, Carriquí M, García-Comendador J, Nadal M, Fortesa J, López-Tarazón JA, Medrano H, Gago J. 2019. Sediment connectivity linked to vegetation using UAVs: High-resolution imagery for ecosystem management. *Science of The Total Environment* **671** : 1192–1205. DOI: [10.1016/j.scitotenv.2019.03.399](https://doi.org/10.1016/j.scitotenv.2019.03.399)
- Everitt BL. 1968. Use of the cottonwood in an investigation of the recent history of a flood plain. *American Journal of Science* **266** : 417–439. DOI: [10.2475/ajs.266.6.417](https://doi.org/10.2475/ajs.266.6.417)
- Fonstad MA, Dietrich JT, Courville BC, Jensen JL, Carbonneau PE. 2013. Topographic structure from motion: a new development in photogrammetric measurement. *Earth Surface Processes and Landforms* **38** : 421–430. DOI: <https://doi.org/10.1002/esp.3366>
- Friedman JM, Griffin ER. 2017. Management of plains cottonwood at Theodore Roosevelt National Park, North Dakota . Natural Resources Report NPS/THRO/NRR—

- 2017/1395. National Park Service: Fort Collins, CO. Available from:  
<http://pubs.er.usgs.gov/publication/70187010>
- Friedman JM, Lee VJ. 2002. Extreme Floods, Channel Change, and Riparian Forests Along Ephemeral Streams. *Ecological Monographs* **72** : 409–425. DOI: [10.1890/0012-9615\(2002\)072\[0409:EFCCAR\]2.0.CO;2](https://doi.org/10.1890/0012-9615(2002)072[0409:EFCCAR]2.0.CO;2)
- Friedman JM, Vincent KR, Griffin ER, Scott ML, Shafroth PB, Auble GT. 2015. Processes of arroyo filling in northern New Mexico, USA. *GSA Bulletin* **127** : 621–640. DOI: 10.1130/B31046.1
- Fryirs K. 2013. (Dis)Connectivity in catchment sediment cascades: a fresh look at the sediment delivery problem. *Earth Surface Processes and Landforms* **38** : 30–46. DOI: <https://doi.org/10.1002/esp.3242>
- Gaeuman D, Schmidt JC, Wilcock PR. 2005. Complex channel responses to changes in stream flow and sediment supply on the lower Duchesne River, Utah. *Geomorphology* **64** : 185–206. DOI: 10.1016/j.geomorph.2004.06.007
- Gilbert JT, Wilcox AC. 2021. An ecogeomorphic framework coupling sediment modeling with invasive riparian vegetation dynamics. *Journal of Geophysical Research: Earth Surface*. DOI: 10.1029/2021JF006071
- Gellis A, Hereford R, Schumm SA, Hayes BR. 1991. Channel evolution and hydrologic variations in the Colorado River basin: Factors influencing sediment and salt loads. *Journal of Hydrology* **124** : 317–344. DOI: [10.1016/0022-1694\(91\)90022-A](https://doi.org/10.1016/0022-1694(91)90022-A)
- Grabowski RC, Gurnell AM. 2016. Using historical data in fluvial geomorphology. In *Tools in Fluvial Geomorphology*, . John Wiley & Sons, Ltd; 56–75. DOI: 10.1002/9781118648551.ch4

- Graf WL. 1978. Fluvial adjustments to the spread of tamarisk in the Colorado Plateau region. GSA Bulletin 89 : 1491–1501. DOI: 10.1130/0016-7606(1978)89<1491:FATTSO>2.0.CO;2
- Graf WL. 1982. Distance decay and arroyo development in the Henry Mountains region, Utah. American Journal of Science **282** : 1541–1554. DOI: 10.2475/ajs.282.9.1541
- Graf WL. 1987. Late Holocene sediment storage in canyons of the Colorado Plateau. GSA Bulletin **99** : 261–271. DOI: [10.1130/0016-7606\(1987\)99<261:LHSSIC>2.0.CO;2](https://doi.org/10.1130/0016-7606(1987)99<261:LHSSIC>2.0.CO;2)
- Gran KB, Czuba JA. 2017. Sediment pulse evolution and the role of network structure. Geomorphology 277 : 17–30. DOI: 10.1016/j.geomorph.2015.12.015
- Grams PE, Schmidt JC. 2002. Streamflow regulation and multi-level flood plain formation: channel narrowing on the aggrading Green River in the eastern Uinta Mountains, Colorado and Utah. Geomorphology **44** : 337–360. DOI: [10.1016/S0169-555X\(01\)00182-9](https://doi.org/10.1016/S0169-555X(01)00182-9)
- Grams PE, Schmidt JC. 2005. Equilibrium or indeterminate? Where sediment budgets fail: Sediment mass balance and adjustment of channel form, Green River downstream from Flaming Gorge Dam, Utah and Colorado. Geomorphology **71** : 156–181. DOI: [10.1016/j.geomorph.2004.10.012](https://doi.org/10.1016/j.geomorph.2004.10.012)
- Gregory HE. 1917. Geology of the Navajo Country: A Reconnaissance of Parts of Arizona, New Mexico and Utah . U.S. Government Printing Office
- Gregory HE, Moore RC. 1931. The Kaiparowits Region: A Geographic and Geologic Reconnaissance of Parts of Utah and Arizona. USGS Numbered Series Professional Paper 164 U.S. Geological Survey Available from: <https://pubs.er.usgs.gov/publication/pp164>

- Gurnell A, Surian N, Zanoni L. 2009. Multi-thread river channels: A perspective on changing European alpine river systems. *Aquatic Sciences* 71 : 253–265. DOI: [10.1007/s00027-009-9186-2](https://doi.org/10.1007/s00027-009-9186-2)
- Hansen WR. 1986. Neogene tectonics and geomorphology of the eastern Uinta Mountains in Utah, Colorado, and Wyoming . USGS Numbered Series Professional Paper 1356. U.S. Geological Survey. Available from: <http://pubs.er.usgs.gov/publication/pp1356>
- Harvey JE, Pederson JL. 2011. Reconciling arroyo cycle and paleoflood approaches to late Holocene alluvial records in dryland streams. *Quaternary Science Reviews* 30 : 855–866. DOI: [10.1016/j.quascirev.2010.12.025](https://doi.org/10.1016/j.quascirev.2010.12.025)
- Heckmann T, Schwanghart W. 2013. Geomorphic coupling and sediment connectivity in an alpine catchment — Exploring sediment cascades using graph theory. *Geomorphology* 182 : 89–103. DOI: [10.1016/j.geomorph.2012.10.033](https://doi.org/10.1016/j.geomorph.2012.10.033)
- Heckmann T, Cavalli M, Cerdan O, Foerster S, Javaux M, Lode E, Smetanová A, Vericat D, Brardinoni F. 2018. Indices of sediment connectivity: opportunities, challenges and limitations. *Earth-Science Reviews* 187 : 77–108. DOI: [10.1016/j.earscirev.2018.08.004](https://doi.org/10.1016/j.earscirev.2018.08.004)
- Hedman ER, Osterkamp WR. 1982. Streamflow characteristics related to channel geometry of streams in western United States . USGS Numbered Series Water Supply Paper 2193. U.S. G.P.O. Available from: <http://pubs.er.usgs.gov/publication/wsp2193>
- Heinzl H, Mittlböck M. 2003. Pseudo R-squared measures for Poisson regression models with over- or underdispersion. *Computational Statistics & Data Analysis* 44 : 253–271. DOI: [10.1016/S0167-9473\(03\)00062-8](https://doi.org/10.1016/S0167-9473(03)00062-8)

- Hereford R. 2002. Valley-fill alluviation during the Little Ice Age (ca. A.D. 1400–1880), Paria River basin and southern Colorado Plateau, United States. GSA Bulletin 114 : 1550–1563. DOI: 10.1130/0016-7606(2002)114<1550:VFADTL>2.0.CO;2\
- Herron WH. 1917. Profile surveys in the Colorado River basin in Wyoming, Utah, Colorado, and New Mexico . USGS Numbered Series Water Supply Paper 396. U.S. Government Printing Office: Washington, D.C. Available from:  
<http://pubs.er.usgs.gov/publication/wsp396>
- Holmes RL. 1983. Computer-Assisted Quality Control in Tree-Ring Dating and Measurement. Tree-Ring Bulletin **43** : 11.
- Hooke J. 2003. Coarse sediment connectivity in river channel systems: a conceptual framework and methodology. Geomorphology **56** : 79–94. DOI: 10.1016/S0169-555X(03)00047-3
- Hupp CR, Osterkamp WR. 1996. Riparian vegetation and fluvial geomorphic processes. Geomorphology **14** : 277–295. DOI: [10.1016/0169-555X\(95\)00042-4](https://doi.org/10.1016/0169-555X(95)00042-4)
- Hwang T, Band LE, Vose JM, Tague C. 2012. Ecosystem processes at the watershed scale: Hydrologic vegetation gradient as an indicator for lateral hydrologic connectivity of headwater catchments. Water Resources Research **48** DOI:  
<https://doi.org/10.1029/2011WR011301>
- Jain V, Tandon SK. 2010. Conceptual assessment of (dis)connectivity and its application to the Ganga River dispersal system. Geomorphology **118** : 349–358. DOI:  
10.1016/j.geomorph.2010.02.002
- James LA, Monohan C, Ertis B. 2019. Long-term hydraulic mining sediment budgets: Connectivity as a management tool. Science of The Total Environment **651** : 2024–2035. DOI: [10.1016/j.scitotenv.2018.09.358](https://doi.org/10.1016/j.scitotenv.2018.09.358)

- Keesstra SD, Davis J, Masselink RH, Casalí J, Peeters ETHM, Dijksma R. 2019. Coupling hysteresis analysis with sediment and hydrological connectivity in three agricultural catchments in Navarre, Spain. *Journal of Soils and Sediments* **19** : 1598–1612. DOI: [10.1007/s11368-018-02223-0](https://doi.org/10.1007/s11368-018-02223-0)
- Kruskal WH, Wallis WA. 1952. Use of Ranks in One-Criterion Variance Analysis. *Journal of the American Statistical Association* **47** : 583–621. DOI: 10.1080/01621459.1952.10483441
- Langbein WB, Schumm SA. 1958. Yield of sediment in relation to mean annual precipitation. *Transactions, American Geophysical Union* **39** : 1076–1084. DOI: <https://doi.org/10.1029/TR039i006p01076>
- Leonard CM, Legleiter CJ, Lea DM, Schmidt JC. 2020. Measuring channel planform change from image time series: A generalizable, spatially distributed, probabilistic method for quantifying uncertainty. *Earth Surface Processes and Landforms* **45** : 2727–2744. DOI: <https://doi.org/10.1002/esp.4926>
- Lisenby PE, Fryirs KA. 2017. Sedimentologically significant tributaries: catchment-scale controls on sediment (dis)connectivity in the Lockyer Valley, SEQ, Australia. *Earth Surface Processes and Landforms* **42** : 1493–1504. DOI: <https://doi.org/10.1002/esp.4130>
- Lisenby PE, Fryirs KA, Thompson CJ. 2020. River sensitivity and sediment connectivity as tools for assessing future geomorphic channel behavior. *International Journal of River Basin Management* **18** : 279–293. DOI: [10.1080/15715124.2019.1672705](https://doi.org/10.1080/15715124.2019.1672705)
- Mahoney JM, Rood SB. 1998. Streamflow requirements for cottonwood seedling recruitment—An integrative model. *Wetlands* **18** : 634–645. DOI: [10.1007/BF03161678](https://doi.org/10.1007/BF03161678)
- Manners RB, Schmidt JC, Scott ML. 2014. Mechanisms of vegetation-induced channel narrowing of an unregulated canyon river: Results from a natural field-scale experiment. *Geomorphology* **211** : 100–115. DOI: [10.1016/j.geomorph.2013.12.033](https://doi.org/10.1016/j.geomorph.2013.12.033)

McCullagh P, Nelder JA. 1989. *Generalized Linear Models* . 2nd edition. Chapman and Hall: New York, NY

McFadden LD, McAuliffe JR. 1997. Lithologically influenced geomorphic responses to Holocene climatic changes in the Southern Colorado Plateau, Arizona: A soil-geomorphic and ecologic perspective. *Geomorphology* **19** : 303–332. DOI: 10.1016/S0169-555X(97)00017-2

McMahon JM, Olley JM, Brooks AP, Smart JC, Stewart-Koster B, Venables WN, Curwen G, Kemp J, Stewart M, Saxton N, Haddadchi A. Vegetation and longitudinal coarse sediment connectivity affect the ability of ecosystem restoration to reduce riverbank erosion and turbidity in drinking water. *Science of The Total Environment* **707** : 135904. DOI: [10.1016/j.scitotenv.2019.135904](https://doi.org/10.1016/j.scitotenv.2019.135904)

Meade R, Trimble S. 1974. Changes in sediment loads in rivers of the Atlantic drainage of the United States since 1900. *Int. Ass. Hydrol. Sci.* **113**

Meko DM, Friedman JM, Touchan R, Edmondson JR, Griffin ER, Scott JA. 2015. Alternative standardization approaches to improving streamflow reconstructions with ring-width indices of riparian trees. *The Holocene* **25** : 1093–1101. DOI: 10.1177/0959683615580181

Merigliano MF, Friedman JM, Scott ML. 2013. 12.10 Tree-Ring Records of Variation in Flow and Channel Geometry. In *Treatise on Geomorphology* , Shroder JF (ed). Academic Press: San Diego; 145–164.

Merritt DM, Cooper DJ. 2000. Riparian vegetation and channel change in response to river regulation: a comparative study of regulated and unregulated streams in the Green River

- Basin, USA. *Regulated Rivers: Research & Management* **16** : 543–564. DOI: [https://doi.org/10.1002/1099-1646\(200011/12\)16:6<543::AID-RRR590>3.0.CO;2-N](https://doi.org/10.1002/1099-1646(200011/12)16:6<543::AID-RRR590>3.0.CO;2-N)
- Miller JR, Friedman JM. 2009. Influence of flow variability on floodplain formation and destruction, Little Missouri River, North Dakota. *GSA Bulletin* **121** : 752–759. DOI: [10.1130/B26355.1](https://doi.org/10.1130/B26355.1)
- Naiman RJ, Decamps H, McClain ME. 2010. *Riparia: Ecology, Conservation, and Management of Streamside Communities*. Elsevier.
- Najafi S, Dragovich D, Heckmann T, Sadeghi SH. 2021. Sediment connectivity concepts and approaches. *CATENA* **196** : 104880. DOI: [10.1016/j.catena.2020.104880](https://doi.org/10.1016/j.catena.2020.104880)
- Parker G, Shimizu Y, Wilkerson GV, Eke EC, Abad JD, Lauer JW, Paola C, Dietrich WE, Voller VR. 2011. A new framework for modeling the migration of meandering rivers. *Earth Surface Processes and Landforms* **36** : 70–86. DOI: <https://doi.org/10.1002/esp.2113>
- Parker M, Wood FJ, Smith BH, Elder RG. 1985. *Erosional Downcutting in Lower Order Riparian Ecosystems: Have Historical Changes Been Caused by Removal of Beaver?* presented at the First North American Riparian Conference. Tucson, AZ. 35–38 pp.
- Peng J, Chen S, Dong P. 2010. Temporal variation of sediment load in the Yellow River basin, China, and its impacts on the lower reaches and the river delta. *CATENA* **83** : 135–147. DOI: [10.1016/j.catena.2010.08.006](https://doi.org/10.1016/j.catena.2010.08.006)
- Pizzuto J, Skalak K, Pearson A, Benthem A. 2016. Active overbank deposition during the last century, South River, Virginia. *Geomorphology* **257** : 164–178. DOI: [10.1016/j.geomorph.2016.01.006](https://doi.org/10.1016/j.geomorph.2016.01.006)

- Poepl RE, Fryirs KA, Tunnicliffe J, Brierley GJ. 2020. Managing sediment (dis)connectivity in fluvial systems. *Science of The Total Environment* **736** : 139627. DOI: [10.1016/j.scitotenv.2020.139627](https://doi.org/10.1016/j.scitotenv.2020.139627)
- R Core Team (2020). *R: A language and environment for statistical computing*. R Foundation for Statistical Computing, Vienna, Austria. <https://www.R-project.org/>.
- Rathburn SL, Shahverdian SM, Ryan SE. 2018. Post-disturbance sediment recovery: Implications for watershed resilience. *Geomorphology* 305 : 61–75. DOI: 10.1016/j.geomorph.2017.08.039
- Resource Consultants. 1991. Sediment transport studies of the Little Snake, Yampa, and Green River systems . Colorado River Water Conservation District Glenwood Springs, CO and Wyoming Water Development Commission, Cheyenne, Wyoming
- Richter BD, Richter HE. 2000. Prescribing Flood Regimes to Sustain Riparian Ecosystems along Meandering Rivers. *Conservation Biology* 14 : 1467–1478. DOI: <https://doi.org/10.1046/j.1523-1739.2000.98488.x>
- Rincón G, Solana-Gutiérrez J, Alonso C, Saura S, García de Jalón D. 2017. Longitudinal connectivity loss in a riverine network: accounting for the likelihood of upstream and downstream movement across dams. *Aquatic Sciences* **79** : 573–585. DOI: [10.1007/s00027-017-0518-3](https://doi.org/10.1007/s00027-017-0518-3)
- Roehler HW. 1973. Stratigraphy of the Washakie Formation in the Washakie Basin, Wyoming. USGS Numbered Series Bulletin 1369. U.S. Govt. Print. Off., Available from: <http://pubs.er.usgs.gov/publication/b1369>
- Roehler HW. 1985. Electric-log correlations of the upper Cretaceous Rock Springs and Blair Formations on the east and west flanks of the Rock Springs Uplift, Wyoming. USGS

- Numbered Series Miscellaneous Field Studies Map 1785. U.S. Geological Survey:  
Reston, VA. Available from: <http://pubs.er.usgs.gov/publication/mf1785>
- Schook DM, Carlson, EA, Sholtes, JS, Cooper, DJ. 2016. Effects of Moderate and Extreme Flow Regulation on *Populus* Growth along the Green and Yampa Rivers, Colorado and Utah. *River Research and Applications* **32**: 1698-1708.
- Schook DM, Rathburn SL, Friedman JM, Wolf JM. 2017. A 184-year record of river meander migration from tree rings, aerial imagery, and cross sections. *Geomorphology* **293** : 227–239. DOI: [10.1016/j.geomorph.2017.06.001](https://doi.org/10.1016/j.geomorph.2017.06.001)
- Schumm SA, Hadley RF. 1957. Arroyos and the semiarid cycle of erosion [Wyoming and New Mexico]. *American Journal of Science* **255** : 161–174. DOI: [10.2475/ajs.255.3.161](https://doi.org/10.2475/ajs.255.3.161)
- Scott ML, Friedman JM. 2018. River flow and riparian vegetation dynamics - implications for management of the Yampa River through Dinosaur National Monument. Natural Resource Report NPS/NRSS/WRD/NRR—2018/1619. . 2018/1619. National Park Service : Fort Collins, CO
- Scott ML, Miller ME. 2017. Long-term cottonwood establishment along the Green River, Utah, USA. *Ecohydrology* **10** : e1818. DOI: <https://doi.org/10.1002/eco.1818>
- Scott ML, Friedman JM, Auble GT. 1996. Fluvial process and the establishment of bottomland trees. *Geomorphology* **14** : 327–339. DOI: [10.1016/0169-555X\(95\)00046-8](https://doi.org/10.1016/0169-555X(95)00046-8)
- Stokes MA, Smiley TL. 1968. *An Introduction to Tree-ring Dating* . University of Chicago Press
- Topping DJ, Mueller ER, Schmidt JC, Griffiths RE, Dean DJ, Grams PE. 2018. Long-Term Evolution of Sand Transport Through a River Network: Relative Influences of a Dam Versus Natural Changes in Grain Size From Sand Waves. *Journal of Geophysical Research: Earth Surface* **123** : 1879–1909. DOI: <https://doi.org/10.1029/2017JF004534>

- Turnbull L, Wainwright J. 2019. From structure to function: Understanding shrub encroachment in drylands using hydrological and sediment connectivity. *Ecological Indicators* **98** : 608–618. DOI: [10.1016/j.ecolind.2018.11.039](https://doi.org/10.1016/j.ecolind.2018.11.039)
- U.S. Geological Survey. 1922. Plan and profile of Yampa River from Green River to Morgan Gulch.
- Wainwright J, Turnbull L, Ibrahim TG, Lexartza-Artza I, Thornton SF, Brazier RE. 2011. Linking environmental régimes, space and time: Interpretations of structural and functional connectivity. *Geomorphology* **126** : 387–404. DOI: [10.1016/j.geomorph.2010.07.027](https://doi.org/10.1016/j.geomorph.2010.07.027)
- Walker AE, Moore JN, Grams PE, Dean DJ, Schmidt JC. 2020. Channel narrowing by inset floodplain formation of the lower Green River in the Canyonlands region, Utah. *GSA Bulletin* **132** : 2333–2352. DOI: [10.1130/B35233.1](https://doi.org/10.1130/B35233.1)
- Ward JV, Tockner K, Arscott DB, Claret C. 2002. Riverine landscape diversity. *Freshwater Biology* **47** : 517–539. DOI: <https://doi.org/10.1046/j.1365-2427.2002.00893.x>
- Wasson RJ, Mazari RK, Starr B, Clifton G. 1998. The recent history of erosion and sedimentation on the Southern Tablelands of southeastern Australia: sediment flux dominated by channel incision. *Geomorphology* **24** : 291–308. DOI: [10.1016/S0169-555X\(98\)00019-1](https://doi.org/10.1016/S0169-555X(98)00019-1)
- Webb R, Hereford R. 2010. Historical arroyo formation: documentation of magnitude and timing of historical changes using repeat photography. *Repeat Photography: Methods and Applications in the Natural Sciences* : 89–104.

- White CA. 1991. A History of the Rectangular Survey System. United States Department of the Interior Bureau of Land Management. U. S. Government Printing Office: Washington, D.C.
- Wickham H et al. 2019. Welcome to the Tidyverse. *Journal of Open Source Software* **4** : 1686. DOI: [10.21105/joss.01686](https://doi.org/10.21105/joss.01686)
- Wickert AD, Martin JM, Tal M, Kim W, Sheets B, Paola C. 2013. River channel lateral mobility: metrics, time scales, and controls. *Journal of Geophysical Research: Earth Surface* **118** : 396–412. DOI: <https://doi.org/10.1029/2012JF002386>
- Wohl E, Bledsoe BP, Jacobson RB, Poff NL, Rathburn SL, Walters DM, Wilcox AC. 2015. The Natural Sediment Regime in Rivers: Broadening the Foundation for Ecosystem Management. *BioScience* **65** : 358–371. DOI: [10.1093/biosci/biv002](https://doi.org/10.1093/biosci/biv002)
- Wohl E, Brierly G, Cadol D, Coulthard TJ, Covino T, Fryirs KA, Grant G, Hilton RG, Lane SN, Magilligan FJ, Meitzen KM, Passalacqua P, Poepfl RE, Rathburn SL, Sklar LS. Connectivity as an emergent property of geomorphic systems. *Earth Surface Processes and Landforms* **44** : 4–26. DOI: [10.1002/esp.4434](https://doi.org/10.1002/esp.4434)
- Womack WR, Schumm SA. 1977. Terraces of Douglas Creek, northwestern Colorado: An example of episodic erosion. *Geology* **5** : 72–76. DOI: [10.1130/0091-7613\(1977\)5<72:TODCNC>2.0.CO;2](https://doi.org/10.1130/0091-7613(1977)5<72:TODCNC>2.0.CO;2)

## CHAPTER 3: FINGERPRINTING HISTORICAL TRIBUTARY CONTRIBUTIONS TO FLOODPLAIN SEDIMENT USING BULK GEOCHEMISTRY<sup>2</sup>

### 3.1. Introduction

The rate and magnitude of sediment movement through a fluvial system has long been recognized as exerting important influence on the form and function of the riverine landscape (Gilbert, 1877; Mackin, 1948; Schumm and Lichty, 1965; Schumm, 1969; Walling, 1983; Fryirs et al., 2007; Bracken et al., 2015; Wohl et al., 2015, 2019). This perennial appreciation for sediment discharge as a process driver of fluvial evolution has more recently broadened in scope beyond simply geomorphic considerations, and sediment loads and fluxes are increasingly recognized as an essential component of riparian and aquatic ecosystem dynamics (Hupp and Osterkamp, 1996; Ward et al., 2002; Benda et al., 2004; Wohl et al., 2015; Vercruyssen et al., 2017; Kemper et al., 2022b). Furthermore, the cascade of sediment through the landscape – from production to transport and ultimately to deposition – has become a focus of management efforts, especially in degraded systems (Walling and Collins, 2008; Owens, 2008; Wohl et al., 2015; Mueller et al., 2018; Topping et al., 2018; Noe et al., 2020; Loire et al., 2021; Mueller and Grams, 2021).

To that end, sediment fingerprinting, which utilizes various diagnostic properties to select tracers capable of characterizing the origin of sediment within a landscape (Collins et al., 1997; Walling, 2005; Haddachi et al., 2013), has shown substantial promise as a tool for locating sediment sources, elucidating the role of various processes (anthropogenic, climatic, etc.) in the sediment dynamics of a watershed, and targeting management and restoration practices (Gellis

---

<sup>2</sup>Kemper, J.T., Rathburn, S.L., Friedman, J.M., Nelson, J.M., Mueller, E.R. and Vincent, K.R., 2022. Fingerprinting historical tributary contributions to floodplain sediment using bulk geochemistry. *Catena*, 214, p.106231. doi.org/10.1016/j.catena.2022.106231

and Walling, 2011; Mukundan et al., 2012; Walling and Collins, 2016; Collins et al., 2017, 2020). Increasingly widespread, the sediment fingerprinting approach relies on constructing a fingerprint of sediment properties (color, geochemistry, radionuclides, etc.) that meet assumptions of conservativeness (i.e., are stable across time) and representativeness (i.e., are stable across space) and are capable of adequately characterizing and discriminating between disparate source areas of interest (Haddadchi et al., 2013; Sherriff et al., 2015; Collins et al., 2017, 2020). Though prior work has used fingerprinting to establish the provenance of sediment of various grain sizes over various spatial and temporal scales, the approach is most often applied to investigate sources of fine-grained ( $< 63 \mu\text{m}$ ) sediment in intermediate-scale ( $10\text{-}10,000 \text{ km}^2$ ) watersheds over contemporary ( $\leq 50$  years) time scales (D'Haen et al., 2012). Techniques to efficiently and powerfully determine a suite of tracers that both meet conservative and representative assumptions and best fulfill diagnostic goals merit further research, especially for larger (sand to gravel) grain-size fractions and over regional ( $10,000\text{+ km}^2$ ) and historical (50-10,000 years) scales (Koiter et al., 2013; D'Haen et al., 2013; Belmont et al., 2014; Collins et al., 2017; 2020,).

Application of the traditional sediment fingerprinting approach involves building a robust fingerprint via tracer selection, wherein a suite of possible tracers is narrowed down using tests for conservativeness and discriminatory power (Collins et al., 1997). Though much attention has been paid towards the role of conservatism in the accuracy of fingerprinting results, many studies apply only the two-part test (known as the bracket test) initially developed two decades ago (Collins et al., 1997; Koiter et al., 2013). Establishing the importance of additional, more robust tests to winnow non-conservative tracers is an area of ongoing work (Collins et al., 2020). In addition to tests for conservativeness, the commonly applied fingerprinting procedure

incorporates statistical tests to develop a single optimized fingerprint capable of best categorizing potential source areas (Smith et al., 2018; Nosrati et al., 2018a). Recent work has begun to investigate the tradeoffs between optimized fingerprints and larger fingerprints incorporating more tracers (Zhang and Liu, 2016; Blake et al., 2018), as well as the use of multiple composite fingerprints constructed via a variety of statistical techniques (Zhang and Liu, 2016; Collins et al., 2017; Nosrati et al., 2018a, 2019, 2021b). Increased attention has also been paid to the application of various statistical techniques to build optimum tracer fingerprints, including relatively novel machine learning approaches (e.g., classification tree analysis, Nosrati et al., 2019).

Finally, though many studies have employed sediment fingerprinting in the context of sediment as pollutant (e.g., Gellis and Noe, 2013), recent work has used the technique to investigate sediment sources through the lens of sediment as a critical resource essential to the dynamics of a healthy river (Chapman et al., 2020); this study takes an ideologically similar approach. Here I use sediment fingerprinting to investigate the connections between upstream historical tributary erosion and downstream floodplain construction and resultant riparian forest establishment in the Yampa River Basin of Colorado and Wyoming. I utilize bulk geochemistry results from portable x-ray fluorescence analysis to construct elemental fingerprints of sand-sized sediment, which are then input into a Bayesian mixing model to determine the primary sources of floodplain deposits (Melquiades et al., 2013; Chapman et al., 2020). Prior work has established the connectivity between the upstream morphological process of historical tributary erosion and the downstream processes of channel migration and floodplain forest establishment in this basin using tree rings and historic maps and aerial imagery (Kemper et al., 2022b), but

there remains a need to verify these process linkages by determining the provenance of floodplain sediment.

I use both accepted techniques for tracer selection (D'Haen et al., 2012; Pulley et al., 2015; Collins et al., 2017, 2020; Nostrati et al., 2021), as well as the relatively novel application of a machine-learning random forest approach (Song et al., 2022), to construct multiple diagnostic geochemical fingerprints capable of linking upstream tributary incision to distal downstream forest establishment over regional (20,565 km<sup>2</sup>) and historical (100+ year) timescales. To establish these connections, I test the hypothesis that downstream floodplain surfaces deposited during a period of historical erosion in tributary watersheds are comprised of sand-sized sediment sourced primarily from those tributaries that were eroding at that time.

### **3.2. Study Area**

The Yampa River Basin of northwestern Colorado and southwestern Wyoming is the last major tributary in the Colorado River system with minimal flow regulation (Figure 3.1). The Yampa begins in the Colorado Rocky Mountains and flows westward across broad lowlands to join the Little Snake River, whereafter the river traverses an alluvial valley known as Deerlodge Park before plunging through bedrock-bound Yampa Canyon to the confluence with the Green River (Richter and Richter, 2000; Elliott and Anders, 2004).

The Little Snake River is the largest tributary and primary source of sediment for the Yampa. Responsible for only 27% of the total Yampa flow, the Little Snake conversely supplies roughly 70% of the annual sediment load of the Yampa at Deerlodge Park (Andrews, 1980). Furthermore, nearly 60% of the Yampa annual load is derived from Muddy Creek, Sand Creek, and Sand Wash in the lower Little Snake Basin (Andrews, 1980, Topping et al., 2018), which are underlain by poorly consolidated fluvial and lacustrine deposits (Roehler, 1973, 1985; Hansen,

1986) and have a semi-arid climate that limits both upland soil development and stabilization of upland soils by vegetation (Langbein and Schumm 1958, Andrews 1978).

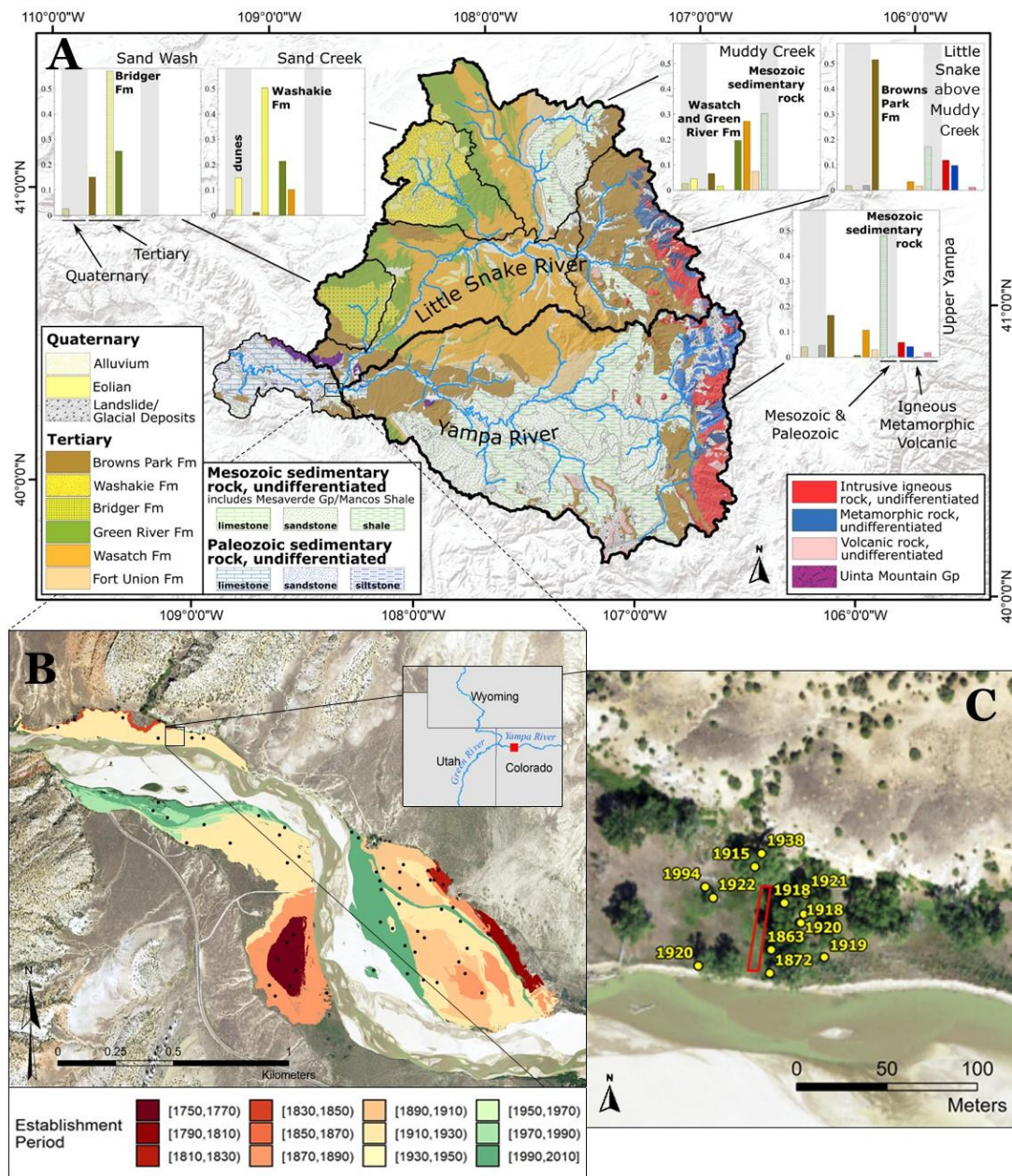


**Figure 3.1.** A) Geologic map of the Yampa River Basin with the dominant units for each subbasin indicated in the inset charts. Box indicates location of Deerlodge Park; B) Area-age distribution of Deerlodge Park forest. Note the forest in the area of the trench dates to the time period between 1910 to 1930 (from Kemper et al., 2022b). Box indicates location of the floodplain trench. C) Detail of the floodplain trench (outlined in red) within Deerlodge Park and years of the center growth ring of the surrounding cottonwoods measured 1.2 m above the ground.

Sand-sized sediment supplied from these tributaries is transported downriver as elongating sand waves, with the fine fraction propagating rapidly downstream and the coarser fractions moving comparatively slowly, often delayed by several decades (Topping et al., 2018; Dean et al., 2020).

All three of the major sediment contributing tributaries underwent heightened erosion in the late 19<sup>th</sup> and early 20<sup>th</sup> century that exported significant volumes of sediment into the Little Snake and Yampa rivers (Kemper et al., 2022b). Historical erosion took the form of arroyo incision in Muddy Creek and Sand Wash, leaving characteristic wide, flat-bottomed channels with high vertical walls throughout each drainage (Figure 3.2a-b). In Sand Creek, a wide, braided channel with large, exposed sand bars where scarcity of silt and clay limits stability of vertical banks, this episode of historical erosion occurred as widening and subsequent narrowing (Kemper et al., 2022b).

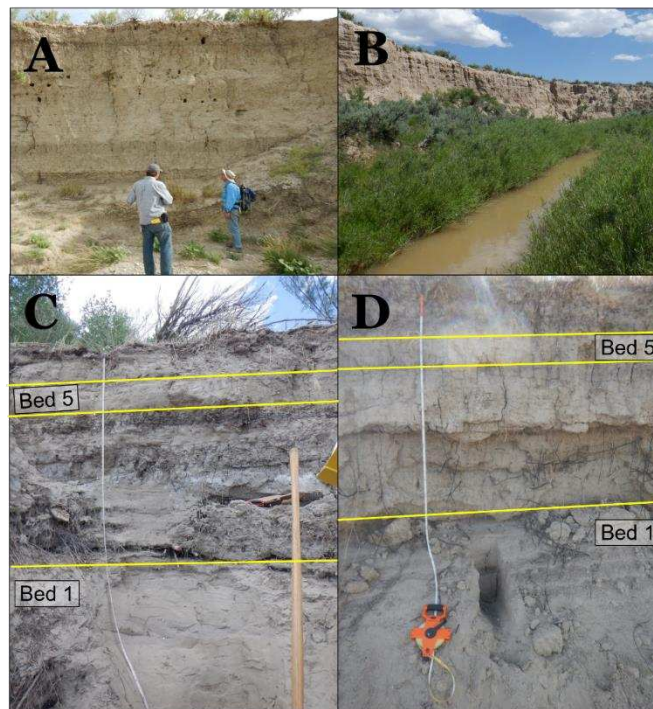


**Figure 3.2.** Arroyos in a) Sand Wash and b) Muddy Creek; Floodplain bank stratigraphy in Deerlodge Park c) on the channelward side of the floodplain trench, river right and d) 500 m upstream from the trench location on river left.

The primary sediment contributing areas for the Yampa River at Deerlodge Park can be separated into five disparate regions: 1) Muddy Creek, 2) Sand Creek, 3) Sand Wash, 4) Little Snake River above Muddy Creek, and 5) Upper Yampa River, the former three of which experienced enhanced historical erosion, while the latter two were relatively quiescent. These areas are underlain primarily by sedimentary rocks of the Wasatch, Green River, Bridger, Washakie and Browns Park Formations, as well as the Mancos Shale and Mesaverde Supergroup (Figure 3.1) (Roehler, 1985). Within the Little Snake Basin, the dominantly fluvial Wasatch, Bridger and Washakie Formations interfinger with dominantly lacustrine sediments of the Green River Formation deposited during Eocene expansion and contraction of lakes within subsiding basins (Roehler, 1992). Tuffaceous fluvial sediments of the Browns Park Formation unconformably overlie older units in the upstream and downstream-most portions of the watershed (Hansen, 1986) (Figure 3.1). Each of the four above delineated sub-basins within the Little Snake watershed are dominated by a different lithological unit: the Little Snake above Muddy Creek by the Browns Park Formation, Muddy Creek by the Wasatch and Green River Formations, Sand Creek by the Washakie Formation, and Sand Wash by the Bridger Formation. In contrast to the largely Tertiary sediments of the Little Snake basin, the Upper Yampa River basin is dominated by the older Cretaceous rocks of the Mancos Shale and Mesaverde Supergroup that gradually cede to the younger Browns Park Formation near the confluence with the Little Snake (figure 3.1). This strong variation in lithology between sub-basins enables the use of geochemical tracers to determine the provenance of downstream floodplain sediments (Klages and Hsieh, 1975; Olley and Caitcheon, 2000; Haddachi et al., 2014; Gateuielle et al., 2019; Chapman et al., 2020).

The Yampa flows through Deerlodge Park in a low gradient, slightly sinuous braided channel comprised of sand-sized and finer alluvium (Cooper et al., 1999; Elliot and Anders, 2005). Much of the Deerlodge Park valley is within the boundaries of Dinosaur National Monument and has avoided heavy logging and floodplain alteration. Channel banks reveal a floodplain stratigraphy that is largely comprised of alternating units of dominantly silt and sand (Figure 3.2c-d). The floodplain surface is dominated by forest of Fremont cottonwood (*Populus fremontii*) with smaller amounts of lanceleaf cottonwood (*P. X acuminata*). Because they are intolerant of shade and drought, establishment of cottonwood seedlings is generally limited to moist, sparsely vegetated bars near the channel (Scott et al., 1996). As a result, cottonwoods tend to occur in even aged stands whose age indicates the time since the underlying bar was deposited. A substantial portion (53%) of the forest in Deerlodge Park established from 1880-1940, a period of relatively high rates of channel migration contemporaneous with heightened erosion in tributaries of the Little Snake River (Kemper et al., 2022b). Here I investigate whether the sediment underlying the forest is primarily sourced from those Little Snake tributaries.

### **3.3. Methods**

#### *3.3.1. Sampling contributing areas*

To robustly assess the relative contributions of each of the five delineated sub-basins (Figure 3.1) to downstream floodplain sediments, sampling efforts must be spatially distributed such that collected samples are together representative of the total potential sediment source for the Yampa River floodplain in Deerlodge Park (Nosrati et al., 2019; Chapman et al., 2020). Additionally, within a given potential source area, sampling must be intensive enough to construct a comprehensive signature specific to that area (Nosrati et al., 2019). Because the end goal of this work is to determine the dominant sediment sources contributing to floodplain

construction during the time of heightened tributary erosion and downstream cottonwood establishment, samples must additionally be collected from surfaces or areas that are illustrative of the sediment being exported from a particular sub-basin during that historical period. The sampling approach in each tributary was thus tailored to the historical, morphological, and hydrologic specifics of each sub-basin, in order to result in a bulk sample that is most representative of each potential source while maintaining consistency in sampling methodology.

To that end, samples were gathered from the arroyo walls in Muddy Creek (n = 38) and Sand Wash (n = 43) (Figure 3.2a-b). Samples were taken from the wall in each tributary roughly 1 m above the active channel at longitudinal increments of 1.6 km (Muddy Creek) and between 0.4 and 0.8 km (Sand Wash). In three separate locations within each tributary, samples were also taken from a vertical profile of the arroyo wall with 0.1 m vertical spacing. This design ensured that gathered samples were together representative of the sediment exported from each tributary during the period of arroyo incision in the late 19<sup>th</sup> and early 20<sup>th</sup> century (Kemper et al., 2022b).

In Sand Creek (n = 43), where there is no arroyo but ample evidence of substantial widening during the period of historical erosion, samples were collected from the banks and the top 15 cm of the present-day dry stream bed. As in Muddy Creek and Sand Wash, samples were taken from vertical profiles of the bank in three locations (0.1 m vertical spacing) and bed samples were collected longitudinally with 0.8 km spacing.

For the Little Snake River above Muddy Creek (n = 39) and Upper Yampa River (n = 55) source areas, samples were collected from vertical profiles of the channel floodplain in areas where access proved reliable. As these are both large rivers, floodplain sediments should reflect the throughput suspended load in different historical periods and integrate all the potential source areas upstream of the sampling locations. Because layers corresponding to the late 19<sup>th</sup> and early

20<sup>th</sup> century could not be reliably identified in all locations, samples were taken from vertical profiles of the riverbanks with vertical spacing of 0.5 m, beginning 0.5 m below the surface of the present floodplain.

### 3.3.2. Sampling Deerlodge Park floodplain sediment

To collect a representative sample of the Deerlodge Park floodplain, in particular the sediment on which the dominant cottonwoods are rooted, I excavated a trench measuring 32 m by 1.5 m in the present-day floodplain of the Yampa River on a surface constructed during the period of heightened rates of both tributary historical erosion and downstream cottonwood establishment (Kemper et al., 2022b). The trench was oriented orthogonal to the riverbank and began roughly 0.5 m from the present bank of the Yampa River, extending from the edge of the floodplain and ending roughly 5 m from the valley wall (Figure 3.3).

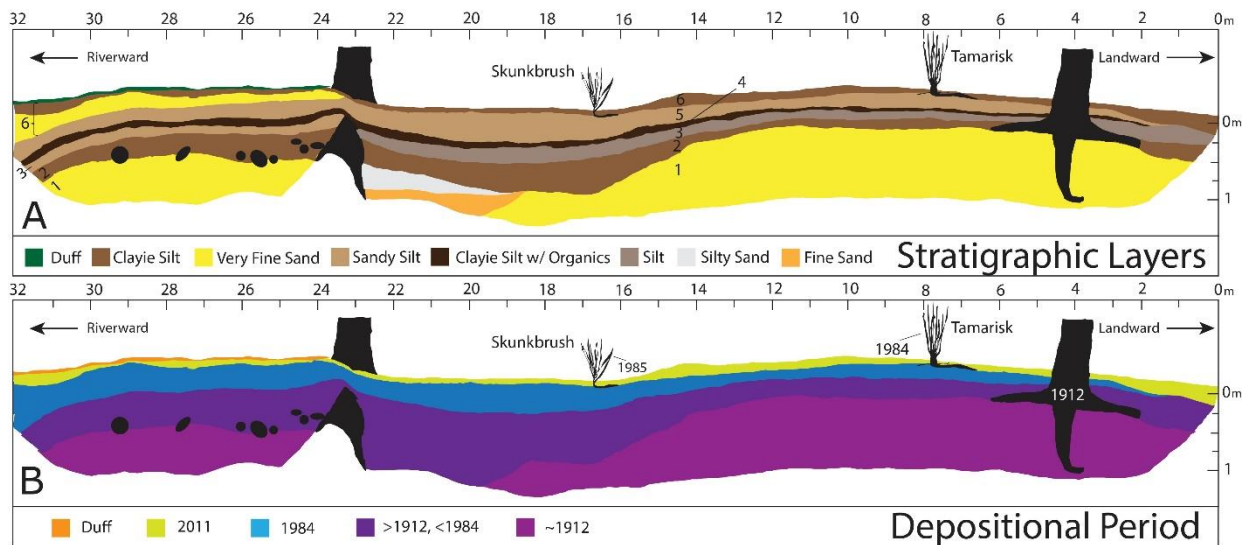


**Figure 3.3.** A) Floodplain stratigraphy exhumed by the trench, which measures 32 m long and ~1.5 m deep, ranging roughly a meter from the present-day Yampa River channel to roughly 5 meters from bedrock outcrops that mark the edge of the valley wall. Individual beds are numbered from one to six. Vegetation (stems, roots, etc.) is depicted in black. B) Depositional age ranges for floodplain stratigraphic units based on dendrochronology analysis tied to the stratigraphy. Establishment years of excavated riparian vegetation used in this analysis are noted.

Stratigraphic units exposed in the trench were analyzed and mapped in the field (Figure 3.3) (*sensu* Dean et al., 2011; Manners et al., 2014; Friedman et al., 2015; Walker et al., 2020). Thirty-eight sediment samples were collected throughout the trench; in three locations, sampling was done in intensive vertical profiles with 0.1 m vertical spacing, while other samples were targeted towards the specific stratigraphic units that represented the rooting surfaces of floodplain vegetation (Bed 1, Figure 3.3). Following this design, a bulk sediment sample ( $n = 38$ ) representative of the stratigraphic units of interest was assembled.

### 3.3.3. Dating Deerlodge Park floodplain sediment

The portion of the Deerlodge floodplain through which the trench was dug is known from ages of the floodplain cottonwoods to have been constructed between 1910 and 1930, a period of heightened tributary erosion and rapid establishment of cottonwoods in the Deerlodge Park area (Kemper et al., 2022b). I further refined this time window by counting rings in cores collected 1.2 m above ground from a spatially intensive sampling of the cottonwoods ( $n = 14$ ) immediately surrounding the trench (Schook et al., 2017). I determined the timing of deposition of several packages present in the Deerlodge Park flood using the age and microanatomy of excavated stems of cottonwood, tamarisk (*Tamarix* sp.) and skunk brush (*Rhus trilobata*) (Friedman et al., 2005, 2015; Manners et al., 2014; Metzger et al., 2020; Walker et al., 2020). I marked excavated stems in the field at stratigraphic contacts and then cut buried stems within all stratigraphic units. I sanded stem sections to make annual rings and microanatomy visible and then cross-dated stems to determine the year of formation of each ring. I determined the year and stratigraphic position of germination for each plant using two criteria: 1) this is the position along the buried stem with the oldest center ring and 2) this is the lowest point on the stem where the center ring contains pith. The year and position of germination provides a maximum date of

deposition for underlying strata and a minimum date for overlying strata. Because cottonwood and tamarisk seedlings require moist unvegetated surfaces for survival, the germination year is a good estimate of the year of formation of the underlying surface (Scott et al., 1997). To determine the year of deposition of strata above the germination point I used microanatomy within tree rings to date transitions in the wood from stem to root as indicated by narrower rings, larger vessel diameters and less distinct annual transitions (Friedman et al., 2005).

### *3.3.4 Grain-size and geochemical analysis of sampled sediment*

All collected sediment samples were initially analyzed for grain-size distribution in the lab. Samples were weighed and then wet-sieved through a 63  $\mu\text{m}$  ( $4\Phi$ ) sieve to separate out fines from the sand (and coarser) fraction; the resultant sand fraction was then dry-sieved through a stack containing the full range of sand particle sizes (2 mm to 63  $\mu\text{m}$ ,  $-1\Phi$  to  $4\Phi$ ) in single phi increments to determine the grain-size distribution within the sand fraction. Grain-size distributions for samples were then grouped by their respective location to yield representative statistics for each sub-basin and the trench. The Kruskal-Wallis H-test, a non-parametric one-way ANOVA test on ranks, was used to investigate the statistical significance of observed differences in grain size between sub-basins (Kruskal and Wallis, 1952).

Once sieved, the  $4\Phi$  (63-125  $\mu\text{m}$ ) fraction from each sample was selected for geochemical analysis with an Olympus Delta Premium handheld portable X-Ray Fluorescence (pXRF) geochemical analyzer with a 40 kV tube x-ray tube and 5mm beam (Caitcheon et al., 2006; Melquiades et al, 2013; Uber et al., 2019; Chapman et al., 2020). Fingerprinting analysis was concentrated on the  $4\Phi$  fraction because of the dominance of  $4\Phi$  sand in the floodplain sediment packages of interest (as is further discussed in Section 4.2). Sieved sand samples were packed into 26 mm ID XRF sample cups, covered with a polypropylene film window and

analyzed using the pXRF with multi-beam optimization and barometric pressure correction. The instrument was operated in a shielded stand to minimize human radiation exposure (Rouillon and Taylor, 2016). Three measurements were performed on each sample.

Elemental concentrations yielded by pXRF analysis prior to calibration are not absolute, but relative (Yalcin et al., 2008; Kenna et al., 2011; Shackley, 2011; Parsons et al., 2013). To transform results to absolute concentrations via a calculated correction factor, calibration standards were made using a laser ablation inductively coupled plasma mass spectrometry (LA-ICP-MS) analysis with a four-acid digestion (US-EPA, 1998). The latter analysis was performed on fourteen selected samples from the study area by ALS Geochemistry using an accredited near-total sample digestion technique with an LA-ICP-MS “finish” (ALS code ME-MS61) that yields robust quantitative results of sample geochemistry for 48 elements. Correction of pXRF results to fully quantitative concentrations was done using a normalization with cross-validation technique wherein pXRF results are transformed using a linear regression between pXRF-yielded concentrations and ICP-MS concentrations for the same set of samples (Parsons et al., 2013; Qu et al., 2019). Only elemental tracers with a relationship between ICP-MS and pXRF concentrations good enough to be considered quantitative by United States Environmental Protection Agency standards ( $r^2 \geq 0.7$ ) were selected to be used in the fingerprinting analysis (US-EPA, 1998).

### *3.3.5. Identifying and selecting robust geochemical sediment tracers*

#### 3.3.5.1. Identifying conservative tracers

A multi-step process was used to identify elemental tracers capable of robustly distinguishing between sediment sources of interest. First, I used the standard bracket test and mean bracket test to initially remove any elements that displayed non-conservative behavior over

the timescales and transport distances of interest (Collins et al., 1997; Collins et al., 2017, 2020; Smith et al., 2018; Nosrati et al., 2018a-b, 2019, 2021). Respectively, these procedures test for conservativeness by first removing tracers with sink (i.e., the sediment one wishes to determine provenance of) sample concentrations that fall outside the range of concentrations in source samples (Navratil et al., 2012; Haddadchi et al., 2014) and then removing any tracers whose mean sink sample concentration is outside the range of source sample mean concentrations (Wilkinson et al., 2013; Nosrati et al., 2018b). After the standard and mean bracket tests, a median mass conservation bracket (i.e., median bracket) test was used to further identify conservative behavior; this test eliminates any tracers as non-conservative where 10% of the sink samples for that particular element fall outside the range of median source concentrations (Pulley et al., 2015). Finally, bi-plots of tracers passing all three bracket tests were examined as a final test for conservativeness. Sink samples for conservative tracers should plot within source samples in graphical space (Collins et al., 2017, 2020; Nosrati et al., 2019).

#### 3.3.5.2. Identifying tracers with robust discriminatory potential

To identify which conservative tracers have significant effectiveness for discriminating source areas, the Kruskal-Wallis (KW) test was then used to further select tracers with statistically significantly different concentrations ( $p$ -value  $< 0.05$ ) between source areas, with the idea that elements with statistically similar concentrations across sub-basins lack discriminatory potential (Collins et al., 2017; Nosrati et al., 2019). In addition to the KW test, the ratio of the percent difference of the median concentration of a given tracer between a given pair of source areas to the mean coefficient of variation of that same tracer for the same pair of source areas was used to further subset tracers capable of effectively discriminating between sources (Pulley et al., 2015). Known as the variability ratio (VR), this test essentially identifies any tracers with

between-source variability less than within-source variability (i.e., a variability ratio  $< 1$ ) as having poor classification potential (Pulley et al., 2017).

### 3.3.5.3. Selecting an optimal fingerprint

Tracers identified by the KW test as having statistically significant differences in concentration between tributaries were then input into two functions designed to identify the variables most important for discrimination between sources: a stepwise discriminant function analysis (Collins et al., 1997; Gellis and Gorman, 2018; Nosrati et al., 2020) and a classification tree analysis using a random forest design. Random forest (Breiman, 2001) is a machine-learning, non-linear, non-parametric method that has rapidly grown in popularity across disciplines over the past two decades and combines classification and regression tree (CART) analysis with a type of bootstrapping aggregation known as “bagging” to perform classification analysis on datasets with a large number of predictors (Breiman, 2001; Strobl et al., 2007; Bennion et al., 2019; Gholami et al., 2020). Though a similar classification tree analysis has been used in sediment fingerprinting by prior researchers (Nosrati et al., 2019), application of the more robust random forest method has been relatively minimal (Song et al., 2022).

The random forest method was performed using the randomForest package in R (Liaw and Wiener, 2003) and run ten separate times with ten randomly selected training data subsets. Important tracers were selected by examining the aggregated variable importance from each run and determining where the largest mean decrease in accuracy occurs (Bennion et al., 2019). Mean decrease in accuracy is a variable importance metric output by the randomForest algorithm that can be understood as the difference in classification accuracy between a model containing all variables and a model with that specific variable removed (Liaw and Wiener, 2002; Archer and Kimes, 2008). In order to validate the robustness of the model comprised of tracers selected

using mean decrease in accuracy, a classification analysis was performed using the model on ten random subsets of test data corresponding to the ten random subsets of training data. Aggregated accuracy and F-statistics were used to quantify the veracity of the model.

The stepwise discriminant function analysis (DFA) is an approach for identifying variables most important for classification that is well-suited for data with unequal variances. DFA was run in R on the same ten sets of training data using the `greedy.wilks` function from the `kLAR` package (Weihs et al., 2005), a forward stepwise selection algorithm that starts with the variable that enables the greatest separation between groups and then adds variables based on the Wilk's lambda. Wilk's lambda is a test statistic that measures the significance of a given variable for the discriminant model; the closer it is to zero, the more significant the variable (Gellis and Gorman, 2018). I set the significance level above which variables should no longer be added to 0.05.

Following the above approaches, final tracer selection was made, and four composite fingerprints were constructed: one using just the KW test (henceforth referred to as KW), one using the KW test plus the VR test (KW + VR), one using the KW test and the discriminant function analysis (KW + DFA) and one using the KW test and random forest approach (KW + RF). The use of multiple composite fingerprints has been shown to provide meaningful explanatory context regarding the impact of tracer selection on sediment fingerprinting results (Collins et al., 2012; Smith and Blake, 2014; Palazón and Navas, 2017; Nosrati et al., 2018). The four tests performed here follow different statistical principles.

### *3.3.6. Determining sub-basin sediment sources*

Once the suite of geochemical tracers best suited to effectively discriminate between sediment sources was identified and selected, each of the four composite fingerprints were input

into a Bayesian mixing model to quantify the contribution of each sub-basin to Deerlodge floodplain sediment (Nosrati et al., 2019; Chapman et al., 2020; Nosrati et al., 2021a-b). The mixing model MixSIAR (Stock and Semmens, 2016), originally developed for ecological applications but increasingly used for sediment fingerprinting analysis (Liu et al., 2018; Gateuille et al., 2019; Akayezu et al., 2020; Chapman et al., 2020; Amorim et al., 2021), was used for source apportionment.

MixSIAR is an open-source model run in R using JAGS (Just Another Gibbs Sampler; Plummer, 2003) for Markov chain Monte Carlo (MCMC) simulation and easily incorporates multiple tracers (Stock and Semmens, 2016; Chapman et al., 2020). There are several model aspects and parameters that can be adjusted to best suit individual research needs, and the particulars chosen for this work are as follows: an input of each tracer's mean and standard deviation for each sub-basin was used for model runs, an uninformative prior (i.e., assuming that the contribution from each sub-basin is equal) was selected due to relatively limited previous knowledge of sediment source contributions, and a "residual-only" error structure was used. MCMC simulations were run with three separate chains and  $10^6$  iterations, the first 500,000 of which were used as burn-in and discarded. Sampled results were then thinned to 1 in every 500 to mitigate autocorrelation (Stock and Semmens, 2016; Gateuille et al., 2019). Model diagnostics indicated that adequate convergence of all chains was achieved. Once run, the model returned several descriptive statistics of the output posterior distribution of source sediment contributions; here, I present the mean and standard deviation to describe and discuss the relative contributions of each sub-basin to the Deerlodge Park floodplain.

### **3.4. Results**

#### *3.4.1. Floodplain trench stratigraphic analysis and dating floodplain sediments*

#### 3.4.1.1. Floodplain stratigraphy

Sediments exhumed in the floodplain trench revealed a sequence of distinct sedimentary packages gradually decreasing in grain size up-section (Figure 3.3a). The lower 0.5 m of the trench is composed of a massive, ~0.5 m-thick package (bed 1, Figure 3.3a) of dominantly very fine sand ( $D_{50} = 0.12$  mm), though substantial fine sand is also present (Figure 3.4). Minor, faint horizontal stratification was visible in a few locations throughout this package. Given the grain size and lack of bedding structures, this package is interpreted as an overbank floodplain sand deposit, likely emplaced during a flood of sufficient magnitude and energy to transport sand-sized sediment to the floodplain.

Moving upwards, the next package (bed 2) is silt with substantial clay inclusions throughout and is draped over the undulating surface of the lower sand package. No bedding structures are present. The contact between the underlying bed 1 is depositional on the interior (0-10 m) and grades riverward into an erosional contact (10-32 m). This package is interpreted as overbank, marginal flood deposits made during subsequent floods. This silt and clay package is topped by a thin layer of massive silt (bed 3), which grades into a sandier silt riverward of a large cottonwood (23 m horizontal distance, Figure 3.3) and other vegetation, and is interpreted to be a floodplain deposit emplaced during a flood. The contact between bed 2 and bed 3 is erosional throughout the trench. No bedding structures were observed in either bed 2 or bed 3, suggesting relatively low energy deposition.

Continuing upwards, at roughly 0.1 m, there is a laterally extensive silt layer with substantial clay and organics (bed 4), which may be a buried soil that developed as the surface was free of disturbance for many years. This potentially buried soil is then overtopped with a laterally extensive, relatively thick (0.1 to 0.2 m) sandy silt layer (bed 5), indicating deposition

from a large flood of significant magnitude. The erosional contact between beds 4 and 5 further suggests a flood with relatively greater energy, though no bedding structures are present.

Riverward of a large tree (at 23 m horizontal distance on Figure 3.3a), the next layer upwards (bed 6, at about -0.3 m on Figure 3.3a) is a very fine sand with climbing ripples; this very fine sand is not present landward of this tree, suggesting deposition by a flood flow that was blocked laterally by the tree and other riparian vegetation and flood debris. This layer grades landward into a silt package with substantial clay and no bedding structures (bed 6, Figure 3.3a), suggesting marginal deposition during the same flood that deposited the very fine sand riverward of the vegetation. The very fine sand riverward of the vegetation grades vertically into a silt, which I interpret to be a silt cap of the same flood event.

#### 3.4.1.2. Timing of deposition

Analysis of excavated vegetation enabled the dating of beds 1,5, and 6. Most of the roots of the large cottonwood exhumed within the trench (at 4 meters horizontal distance on Figure 3.3) flared out from the trunk on top of the thick, laterally extensive package of very fine sand comprising the lower 0.5 m of the trench (bed 1). The oldest of 14 wood samples collected from this tree above and below ground was found just above the top of this extensive very fine sand. The center ring of this core dated to 1912. The younger samples from lower layers all had center rings lacking pith indicating that they were root. I thus concluded that the cottonwood at 4 m (Figure 3.3) germinated on top of the extensive very fine sand in 1912 and that the sand itself was deposited in that year or one to a few years earlier (Figure 3.3b) (Scott et al. 1997). At 1.2 m above ground the center ring of this tree dated to about 1918 indicating that the tree took about 6 years to reach that height. This is consistent with results of other studies in North Dakota and

Montana finding it takes a median of 7.3 and 8.5 years for cottonwoods to grow to coring height (Friedman and Griffin, 2017; Schook et al., 2017).

To assess how representative this excavated tree was of the surrounding forest and floodplain, I cored all of the cottonwoods (n = 18) within 40 m of the trench at 1.2 m above ground (Figure 3.1C, Table B.1). Seven of these trees had center rings between 1914 and 1921, which is consistent with the hypothesis that they germinated on the same surface and at the same time as the excavated tree; two trees dated an island remnant formed much earlier (1863 and 1872); two younger trees (1938 and 1994) were apparently established on an alluvial fan deposited by a small tributary; a few more were rotten, yielding no age. At a broader scale, 53% percent of forest area at Deerlodge Park has center rings at coring height ranging from 1880 to 1940 (Kemper et al., 2022b).

Moving upwards from the very fine sand on which the cottonwoods are rooted (bed 1), the clay-rich silt, silt grading to sandier silt, and the silt with ample clay and organics that may be a buried soil O-horizon (beds 2- 4, Figure 3.3) were deposited during multiple events over substantial time subsequent to 1912 but cannot be more precisely dated. Lack of dating precision in these layers is due to lack of detected anatomical response in the xylem of the cottonwood, which is not unusual for a tree that is mature when buried by the floodplain. Several erosional contacts between beds 2-4 further suggest that vegetation that may have been present at the time was potentially removed by these flood flows, further complicating dating efforts. Eradication efforts of invasive vegetation (e.g., tamarisk) by the Monument (NPS, 2005) may have further removed vegetation that could have been potentially useful in dating these layers.

Above these layers, a tamarisk and skunkbrush excavated along the trench were established in 1984 and about 1985, respectively, on top of the extensive sandy silt that spans the

vertical range from 0.1 to -0.1m (bed 5, Figure 3.3), suggesting this sedimentary unit was deposited by the flood of record in 1984 and, furthermore, that the underlying beds 2-4 were deposited sometime between 1912 and 1984. The shallowly buried stems of these two plants within the overlying silt with clay (bed 6, Figure 3.3) both showed an increase in xylem vessel element size starting after about 2010. This anatomical change, a typical response to burial (Friedman et al., 2005, 2015; Manners et al., 2014), suggests bed 6 was deposited by the flood of 2011.

#### *3.4.2. Grain size analysis of sub-basin and floodplain sediment*

Grain-size analysis reveals observable differences between sub-basins (Figure 3.4). Sand-fine (silt and clay) splits (Figure 3.4a) indicate that sediment sourced from Sand Creek is dominantly sand with relatively little fines, whereas sediment from Muddy Creek has a more substantial fine fraction. The other contributing sub-basins of Sand Wash, the Little Snake River above Muddy Creek, and the Upper Yampa River have compositions intermediate between these two end members. Within just the sand fraction, Sand Creek is significantly coarser (p-value < 0.05) than each other sub-basin, with significantly more medium ( $2\Phi$ ) sand and significantly less very fine ( $4\Phi$ ) sand than all others (Figure 3.4b-c). The Upper Yampa River and the Little Snake River above Muddy Creek are significantly finer than Sand Creek but coarser than Sand Wash and Muddy Creek and have significantly more fine ( $3\Phi$ ) sand than each other sub-basin (Figure 3.4b-c). Sand Wash and Muddy Creek have the finest grain sand of the contributing areas, with ~50% of the sand falling within the very fine ( $4\Phi$ ) sand size classes (Figure 3.4b-c). Sediment from the large sand package exhumed by the trench (bed 1 on Figure 3.3a) and upon which the surrounding cottonwood forest is rooted is finer than each of the contributing areas – the package

contains significantly more very fine ( $4\Phi$ ) sand than any of the sub-basins, even the relatively finer areas of Sand Wash and Muddy Creek.

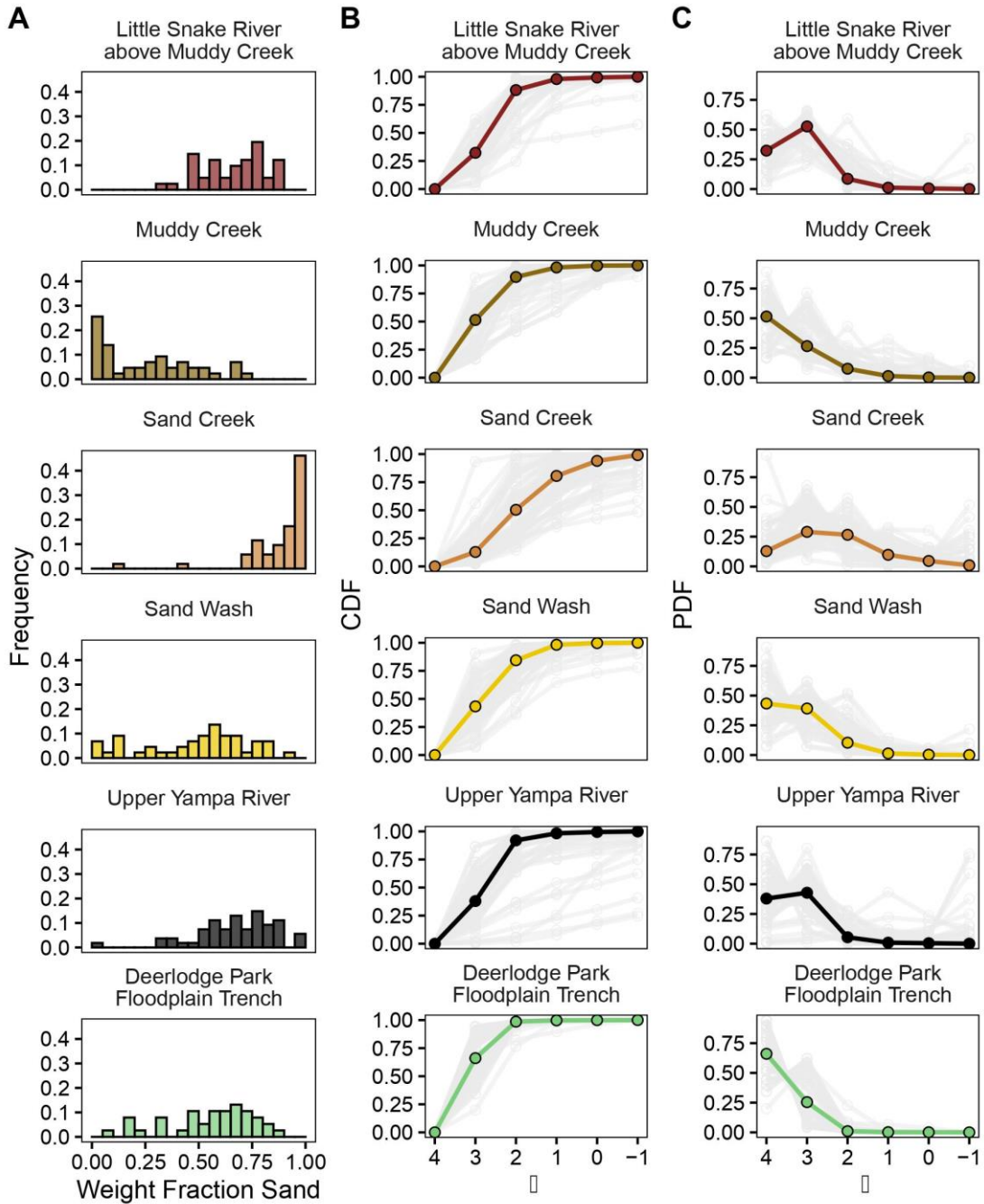


**Figure 3.4.** A) Sand-fine split by weight fraction for each sample within each source area. B) CDF of sand grain-size phi classes within the sand fraction. Color is the median for all samples, the light gray is the distribution for each individual sample. C) PDF of sand size classes. Color is the median for all samples, light gray is the distribution for each individual sample. Deerlodge Park trench samples are from the 1912 very fine sand package (Bed 1 in Figure 3.3a).

Additionally, nearly 100% of the sand contained within this layer falls within the fine (3 $\Phi$ ) and very fine (4 $\Phi$ ) sand size classes (Figure 3.4b-c).

### 3.4.3. Geochemical analysis and tracer selection

Given the dominantly very fine sand composition of the floodplain sediment package that represents the cottonwood rooting surface, geochemical and sediment fingerprinting analysis was targeted towards sand within this size class (4 $\Phi$ , or 63-125  $\mu$ m). Elements returned by the pXRF that were above detection limits in all analyzed samples and that had correlations with ICP-MS samples that fell within the quantitative range were Al, As, Ca, Fe, K, Mg, Nb, Rb, Sr, Ti, Y, and Zn (Figure 3.5).

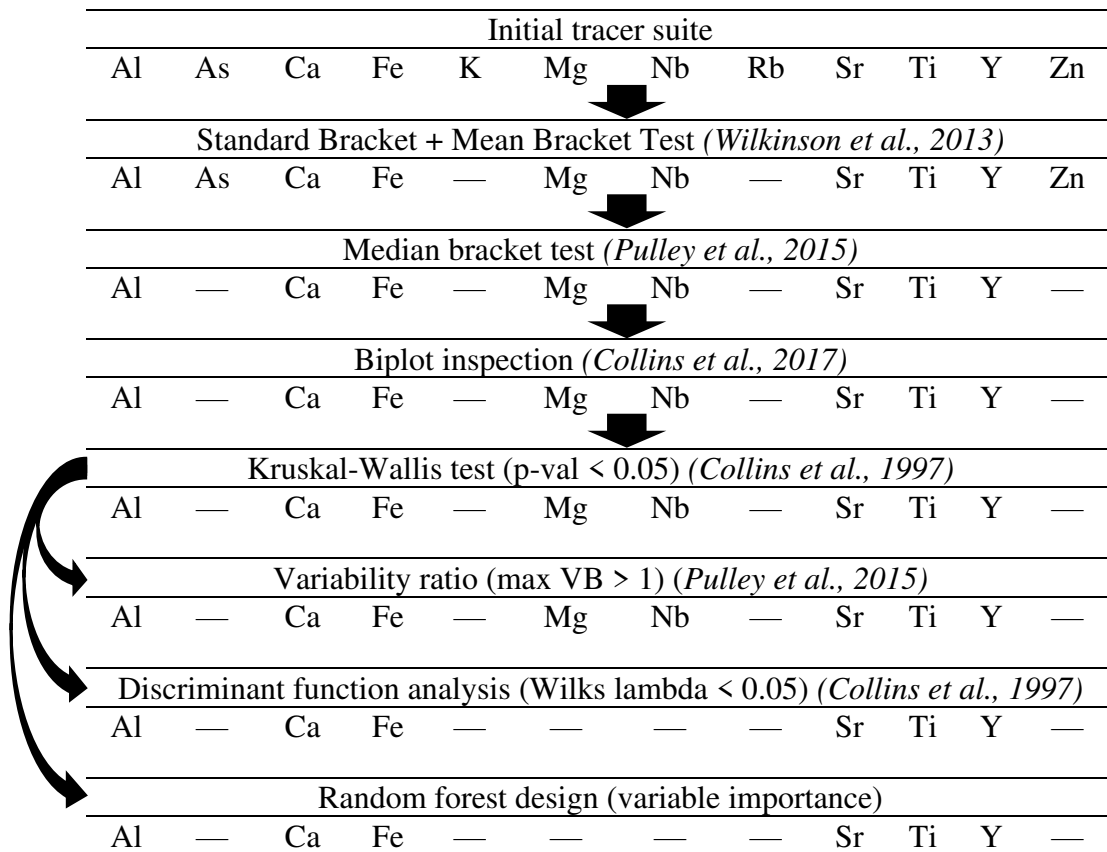


**Figure 3.5.** The tracer selection process and the tracers retained by each step. The process starts with all initial tracers then proceeds through the Kruskal-Wallis test, whereafter it branches three ways: to the variability ratio test, the DFA test, and the random forest test.

Elements that passed each of the three bracket tests for conservativeness and the inspection of biplots (Figure 3.6) were Al, Ca, Fe, Nb, Mg, Sr, Ti, and Y.

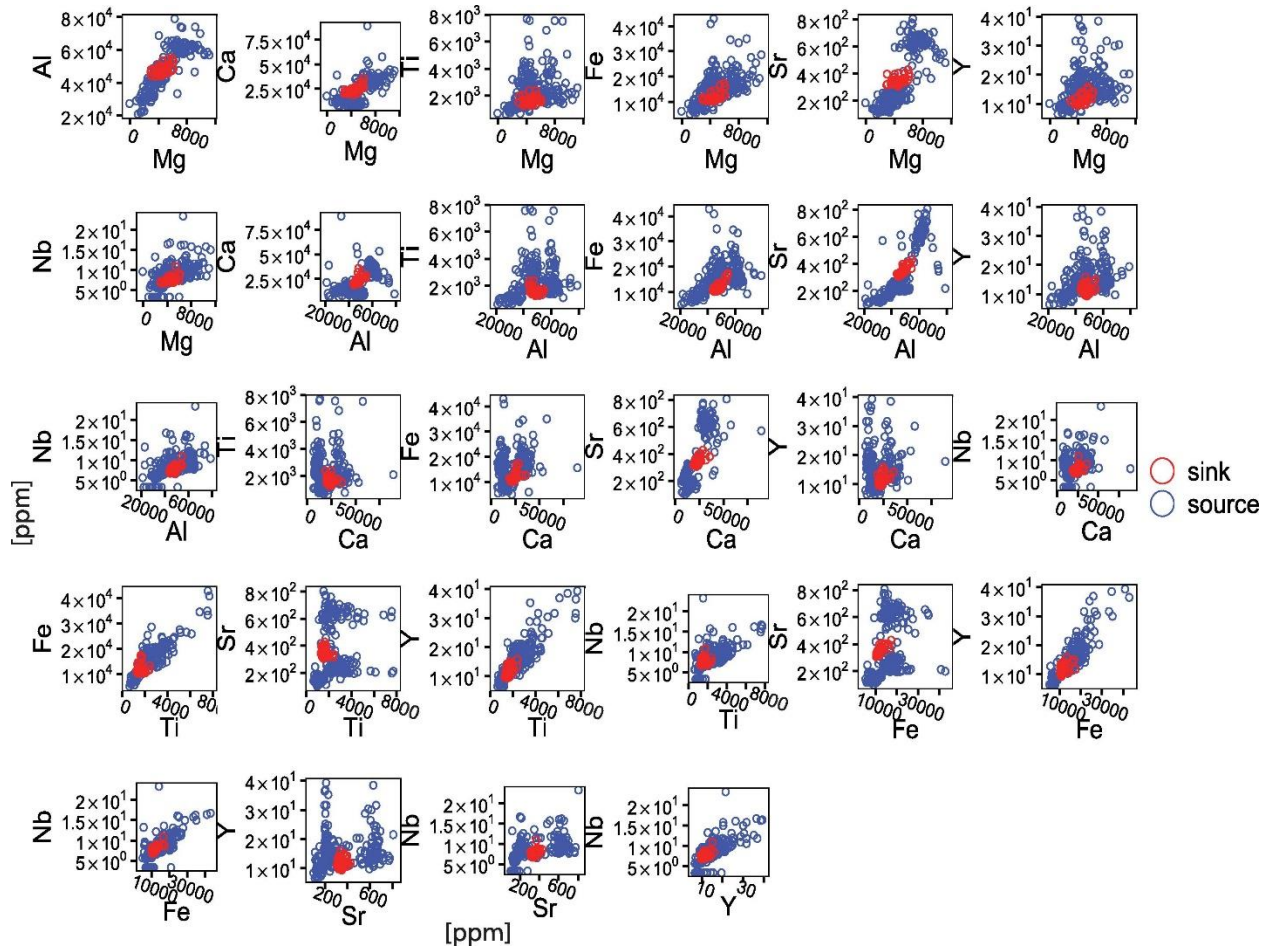


**Figure 3.6.** Biplots for all tracer pairs that passed the three bracket tests for conservativeness. Biplot inspection essentially represents a fourth test for conservativeness – if sink samples for all tracer pairs plot within source samples in graphical space, then the tracer may be deemed conservative. Sink samples shown in red, source in blue. Values reported are concentration in ppm.

Elements passing the KW test for discriminatory ability were all of the above eight elements deemed conservative, and those passing the variability ratio test were the same eight (Figure 3.5, Table 3.1). These eight elements are thus subsequently referred to the conservative-alone fingerprint. Input of these eight elements into a stepwise DFA returned six elements as having significant discriminatory potential: Al, Ca, Fe, Sr, Ti, Y. Random forest analysis of the eight elements passing the KW test revealed a clear break in the importance of each element for

classification of the source area (Figure 3.7). Disregarding jumps where the number of tracers ( $m$ ) is less than the number of sources ( $n$ ) minus one (i.e., the necessary number of tracers needed to fingerprint five potential source areas is four), the largest jump in mean decrease in accuracy occurs between Fe and Nb, indicating that the elements below Fe in a ranking of tracer importance are of relatively diminished usefulness for classification (Figure 3.7). Mg and Nb were thus discarded as tracers, and of Al, Ca, Fe, Sr, Ti, Y were selected as being most able to meaningfully distinguish between source areas by the random forest algorithm, identical to the selection from stepwise DFA. These six elements represent an optimum fingerprint for provenance analysis (Collins et al., 2017).

**Table 3.1.** Results of the Kruskal-Wallis (KW) test on conservative tracers. Notably, all conservative tracers pass the KW test.

Element	p-value	$\chi^2$
Mg	< 0.001	168.15
Al	< 0.001	172.94
Ca	< 0.001	154.68
Ti	< 0.001	111.64
Fe	< 0.001	87.67
Sr	< 0.001	189.22
Y	< 0.001	106.46
Nb	< 0.001	93.65

In all sub-basin  $4\Phi$  samples, Al was found in the highest concentrations, though significantly higher in Sand Creek and Sand Wash than in the other areas, and significantly lower in the Little Snake above Muddy Creek and the Upper Yampa River than any of the three lower Little Snake tributaries (Table B.2, B.3). Ca and Sr were also abundant in Sand Creek and Sand Wash and significantly depleted in each other sub-basin. The Upper Yampa River and Sand Creek were relatively enriched in Y; sediments coming from Muddy Creek were relatively depleted in the same. Concentrations of Fe and Ti in Muddy Creek were similarly significantly lower than in the sediments of each other area (Table B.2, B.3). For nearly all selected tracers,

concentrations were observably higher in Sand Creek than in any other sub-basin; the opposite pattern – tracers observably lower than in any other sub-basin – was seen for Muddy Creek (Table B.2, B.3).  $4\Phi$  sand from each tributary is geochemically distinct (Figure 3.8), both for the conservative-alone fingerprint (Figure 3.8a) and the optimum fingerprint (Figure 3.8b). Sediment from the trench was intermediate in composition between all five potential contributing areas (Figure 3.8).

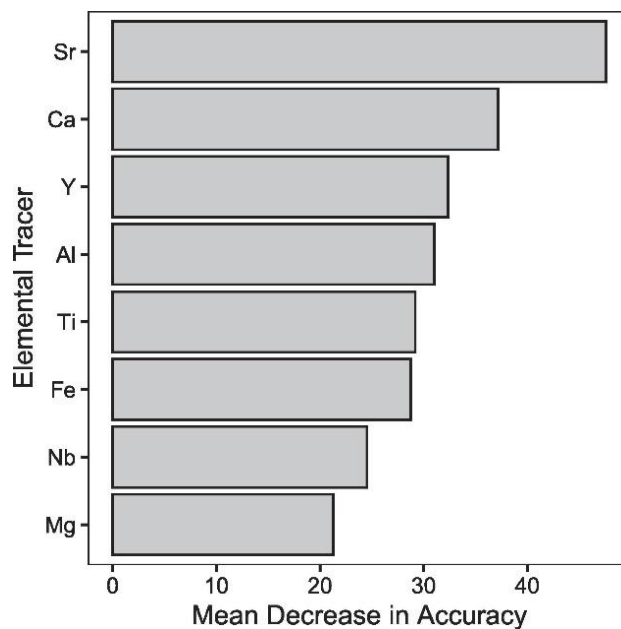


**Figure 3.7.** Variable importance of each tracer for the classification of source samples using the random forest method. Tracers are ranked by mean decrease in accuracy, which indicates how much a classification model suffers when a given tracer is removed.

#### 3.4.4. Mixing model (MixSIAR) results

Results of the Bayesian mixing model MixSIAR run with the tracers selected using the tests for conservativeness alone (and the KW test and the KW + VR test, as the results are the same) show that the large floodplain package made up of very fine sand (bed 1, Figure 3.3a) and on which cottonwoods are rooted is dominantly sourced from the Muddy Creek ( $46 \pm 4\%$ ) and Sand Wash ( $40 \pm 7\%$  tributaries) (Figure 3.9a; Table 3.2). Sand sourced from Sand Creek plays a minor role in the composition ( $8 \pm 6\%$ ) of the floodplain package, with sediment from the Little

Snake River above Muddy and the Upper Yampa River making up the small remaining fraction ( $4 \pm 3\%$  and  $3 \pm 3\%$  from each, respectively). Mixing model results using the optimum fingerprint from KW + RF selection reveal a similar composition: the floodplain package representing the cottonwood rooting surface is chiefly made up of sediment sourced from Muddy Creek ( $45 \pm 4\%$ ) and Sand Wash ( $42 \pm 6\%$ ) (Figure 3.9b; Table 3.2). As with the previously discussed model, the floodplain package contains a relatively minor portion of Sand Creek sand ( $6 \pm 5\%$ ). Similarly, there is little sediment from the Little Snake River above Muddy and the Upper Yampa River, with each contributing an equally small fraction (again,  $4\%$  and  $3\%$  from each, respectively). As tracer selection with KW + DFA yields the same optimum fingerprint as that with KW + RF, mixing model provenance results are the same. Overall, there is little observable difference between the compositions returned by the mixing model for runs with a fingerprint comprised of tracers determined solely by tests for conservativeness versus an optimum fingerprint.

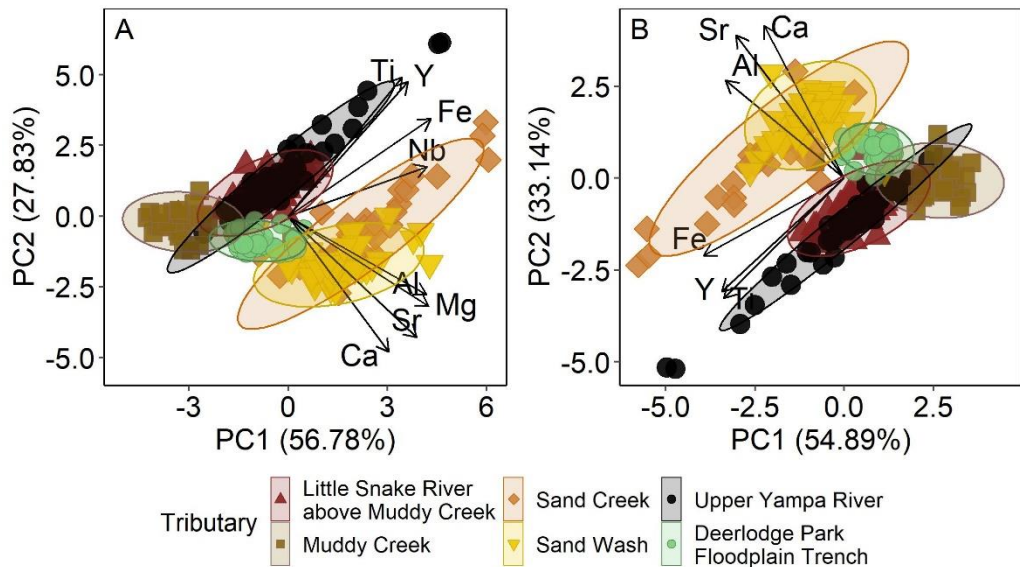


**Figure 3.8.** Principal component analysis (PCA) plots of the sand samples from each source area and the Deerlodge trench using a) just conservative tracers and b) optimum tracers for the first and second principal components (PC1 and PC2). Each source area has a geochemically distinct signature.

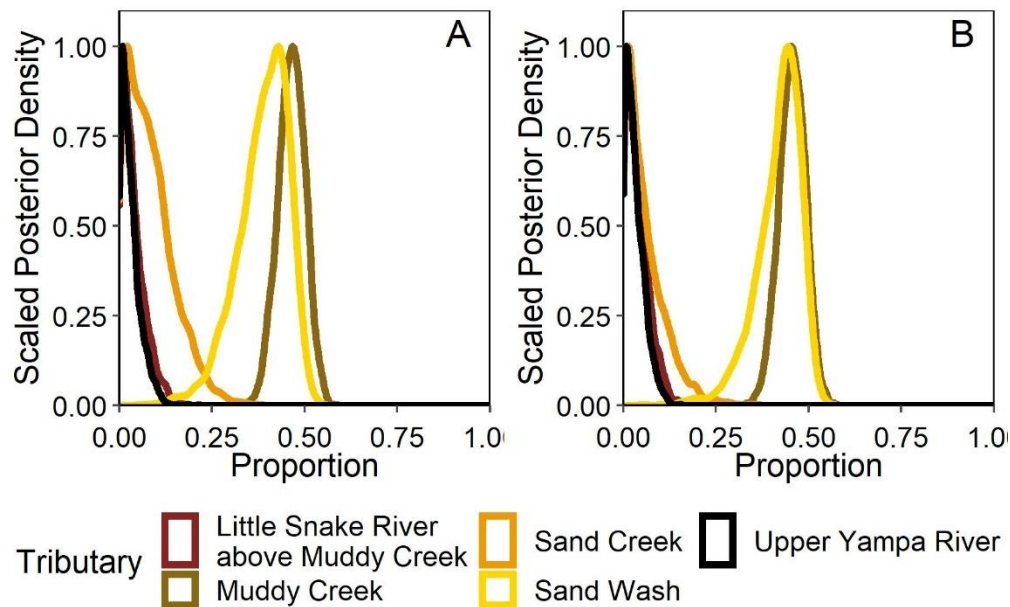


**Figure 3.9.** A) Modeled probability distributions returned for the contribution of each source area to Deerlodge Park floodplain sediments using the suite of tracers (Al, Ca, Fe, Mg, Nb, Sr, Ti, Y) that passed only the tests for conservativeness. B) Modeled probability distributions returned for the contribution of each source area to Deerlodge Park floodplain sediments using an optimized fingerprint constructed by further winnowing effective tracers (Al, Ca, Fe, Sr, Ti, Y) using a random forest (RF) analysis or a discriminant function analysis (DFA).

**Table 3.2.** Summary statistics for mixing model results run with conservative tracers alone and with an optimized fingerprint. Percentiles of the returned probability distribution are listed along with mean and standard deviation. DIC = Deviance Information Criterion.

Conservative tracers alone ( <i>DIC</i> = 92.3)									
	Mean	$\sigma$	2.5%	5%	25%	50%	75%	95%	97.5%
Little Snake above Muddy Creek	0.04	0.03	0.001	0.002	0.01	0.03	0.05	0.10	0.11
Muddy Creek	0.46	0.04	0.39	0.40	0.44	0.46	0.49	0.52	0.53
Sand Creek	0.08	0.06	0.002	0.005	0.03	0.07	0.12	0.20	0.24
Sand Wash	0.39	0.07	0.22	0.26	0.35	0.40	0.44	0.48	0.49
Upper Yampa River	0.03	0.03	0.001	0.002	0.01	0.02	0.04	0.08	0.09
Optimized fingerprint ( <i>DIC</i> = 70.9)									
	Mean	$\sigma$	2.50%	5%	25%	50%	75%	95%	97.50%
Little Snake above Muddy Creek	0.04	0.03	0.001	0.003	0.01	0.03	0.06	0.10	0.12
Muddy Creek	0.45	0.04	0.39	0.40	0.43	0.46	0.48	0.51	0.52
Sand Creek	0.06	0.05	0.001	0.003	0.02	0.04	0.08	0.17	0.20
Sand Wash	0.42	0.06	0.26	0.30	0.39	0.43	0.46	0.50	0.51
Upper Yampa River	0.03	0.02	0.001	0.00	0.01	0.03	0.04	0.08	0.09

### 3.5. Discussion

#### 3.5.1. Optimum tracer selection

From the performed statistical tracer selection techniques, only two disparate fingerprints were returned. Both the KW test alone and the KW + VR test constructed fingerprints of the same eight elements; notably, neither test discarded any of the tracers that were deemed conservative by the mean bracket, standard bracket, and median bracket tests. The fingerprint from these tests thus is identical to the one returned by tests for conservativeness alone, and in subsequent discussion I use this language to distinguish it from the optimum fingerprint returned by the DFA and random forest method (i.e., I reference a “fingerprint from conservativeness alone” and an “optimum fingerprint”). Optimum tracer selection using the KW + DFA and KW + RF reduced selected tracers to six and was thus slightly more restrictive (Figure 3.5). Tracers discarded by the latter two methods were Mg and Nb: while the latter had consistently low variability ratios and was likely discarded due to relatively poor discriminatory potential between source areas, the former was likely removed by both DFA and the random forest method due to high correlation with other tracers of substantial discriminatory power. As three of the eight tracers deemed to be conservative are alkaline earth elements – Sr, Ca, and Mg – and both Sr and Ca were of substantial importance for discrimination (Figure 3.7), removal of Mg from the optimum fingerprint is thus not surprising.

The substantial importance of Sr and Ca as tracers is likely chiefly related to the occurrence of feldspars, though may also be secondarily related to the distribution of carbonate sedimentary rocks, which have been shown to concentrate Sr (Graf, 1960; Kabata-Pendias, 2000). Feldspars are relatively abundant in the Bridger and Washakie formations of the Sand Wash and Sand Creek basins and relatively absent in the dominant formations of the three other

sub-basins, where more quartzose sandstones dominate, especially in the Little Snake above Muddy and Upper Yampa (Roehler, 1973). Carbonates are also more common in the Bridger and Washakie compared to the dominant formations of the other three sub-basins, which are primarily clastic (Roehler, 1973; Roehler, 1992; Murphey et al., 2017). The Browns Park Formation, aerially extensive in the Little Snake above Muddy Creek and the Upper Yampa River subbasins, contains sizable aeolian quartzose sandstones and conglomerate with dominantly crystalline clasts (Honey and Izett, 1988); sediments from these two areas are unsurprisingly low in Ca (Table B.2, B.3). Ca, moreover, may be additionally important in separating Sand Wash and Sand Creek sediment: the Bridger Formation of Sand Wash has abundant limestone beds, several very calcareous sand, silt, and mudstone layers, and extremely calcareous white marker beds, whereas the Washakie Formation found in Sand Creek, though similar in nature, has these in relatively diminished occurrence (Koenig, 1960; Roehler, 1973; Murphey et al., 2017). Though Ca and Sr are relatively soluble elements and may thus be susceptible to non-conservative behavior (Collins et al., 2020), here their usefulness as tracers is likely largely related to their occurrence in feldspars, where they would be expected to be fairly stable. Such occurrence in more stable silicates rather than soluble carbonates renders them suitable tracers over the spatial and temporal timescales considered.

Al as an essential tracer again likely separates the more quartzose sandstones in the Little Snake above Muddy Creek and the Upper Yampa River from the more feldspar-rich rocks of the Washakie and the Bridger in Sand Creek and Sand Wash; it also helps to discriminate between the arkose-rich Washakie of Sand Creek and the Bridger of Sand Wash (Roehler, 1973; Honey and Izett, 1988). Y as a meaningful tracer may result from titaniferous black sandstones that can occur in the Cretaceous sediments of the Mesaverde Group, which may be found in the upper

Sand Creek basin, possibly as aeolian deposits from neighboring areas where such sandstones are known to occur. Y may also be present in sediments derived from crystalline parent rocks in the Upper Yampa River Basin or the Little Snake above Muddy Creek (Sutherland et al., 2013; Smith et al., 2014). Ti serves to effectively discriminate Sand Creek possibly due to the abundance of augite in the sandstones of the Washakie (Roehler, 1973). Fe additionally may be effective in separating out Sand Creek from Sand Wash, as the abundant arkose of the Washakie is likely derived from the plutonic rocks of the Sierra Madre, while Bridger sandstones are likely comprised of clastic sediments sourced from the Paleozoic sedimentary rocks and Precambrian quartzites of the Uinta mountains (Roehler, 1973).

Sediment from Muddy Creek is likely accurately categorized by the relatively low concentrations of all selected tracers (Table B.2, B.3). Because the dominantly fine-grained rocks of the Wasatch and Green River Formations are most extensive in this sub-basin, sand-sized sediment here could be reasonably expected to be dominated by quartz more so than in all other basins, with many of the tracer elements that were detected in sand-sized sediment from other areas present primarily within clay minerals and analogous clay-sized sediments in Muddy Creek (Bradley, 1964).

The majority of elements removed by the tracer selection process failed tests for conservativeness. Of the 12 elements with concentrations above detection limits and quantitative-strength relationships, four were removed due to non-conservative behavior (i.e., concentrations in Deerlodge sediment suggest they are not stable across the spatial and temporal scales considered in this study) (Figure 3.5). Notably, the addition of the median bracket test (Pulley et al., 2015) to the common suite of the standard bracket and mean bracket test (Wilkinson et al., 2013) identified two additional tracers as non-conservative (i.e., a 100%

increase in non-conservative tracers). Inspection of bi-plots further indicated the eight tracers passing the three-fold bracket tests were conservative. As non-conservative tracers have been shown to greatly increase error in sediment fingerprinting analysis (Smith and Blake, 2014; Zhang and Liu, 2016), future studies should incorporate the initial three-pass filter of the standard, mean, and median bracket tests for conservativeness, followed by bi-plot inspection to either confirm results or remove any additional elements that display evidence of non-conservative behavior. Fingerprinting studies have increasingly concentrated tracer selection efforts towards identifying non-conservative tracers (Smith and Blake; 2014; Sherriff et al., 2015; Zhang and Liu, 2016; Collins et al., 2020); results of this work further suggest that a robust suite of conservative tracer tests should be employed as the first step in tracer selection, especially when a relatively small number of fingerprints are available.

Selection of an optimum fingerprint using both the random forest and discriminant function analysis techniques winnowed down selected elements to six (Figure 3.5). Notably, results of tracer optimization using the random forest method are identical to those using the standard KW + DFA technique (Collins et al., 1997). Moreover, summary statistics suggest that classification using a random forest algorithm is more successful and accurate than a discriminant function analysis using the same tracers (Table 3.3). Because DFA is technically bound by assumptions of normality and equality of variance and thus susceptible to error as data become increasingly non-parametric, the use of random forest – a non-linear, non-parametric method – represents an exciting alternative pathway for tracer selection. Demonstration here that tracer selection results match those of an established method emphasizes random forest as an appropriate technique; superior classification ability suggests that a random forest method may represent an enhanced approach. In studies with larger data sets (e.g., more available tracers,

more sources, etc.), it may be especially valuable, both because of the relatively more robust ability of the random forest method to incorporate a wide array of parameters in classification decisions, as well as the above-mentioned capability to handle non-normal and non-parametric data without violating statistical assumptions.

**Table 3.3.** Summary statistics for classification using random forest (RF) and discriminant function analysis (DFA). Each algorithm uses the same tracers for classification.

Random Forest (overall accuracy = 0.93)					
Tributary	Sensitivity	Specificity	Precision	Recall	F-score
Little Snake above Muddy Creek	0.94	0.99	0.92	0.94	0.93
Muddy Creek	0.96	0.99	0.96	0.96	0.96
Sand Creek	0.90	0.98	0.90	0.90	0.90
Sand Wash	0.86	0.98	0.90	0.86	0.87
Upper Yampa River	0.98	0.99	0.96	0.98	0.97
Discriminant Function Analysis (overall accuracy = 0.89)					
Tributary	Sensitivity	Specificity	Precision	Recall	F-score
Little Snake above Muddy Creek	0.91	0.98	0.90	0.91	0.90
Muddy Creek	0.96	0.97	0.90	0.96	0.93
Sand Creek	0.85	0.97	0.86	0.85	0.85
Sand Wash	0.83	0.97	0.86	0.83	0.83
Upper Yampa River	0.90	0.97	0.92	0.90	0.91

Modeling results with an optimized fingerprint additionally had greater accuracy than those run with a fingerprint constructed solely from tests for conservativeness. Standard deviations and 95% confidence intervals for the former were smaller than those for the latter (Table 3.2, Figure 3.9), as was overlap in the tail portions of the returned distributions for each tributary (Figure 3.9). In addition, model diagnostics for the MixSIAR model indicate that a relatively larger number of chains lacked adequate convergence for model runs with just the conservative tracers compared to runs with an optimized fingerprint. The deviance information criterion (DIC) for models run with an optimized fingerprint is lower than for those run with just the conservative tracers, suggesting the former is a superior model (Table 3.2).

A significant body of work within the recent sediment fingerprinting literature has given ample consideration to the question of smaller, optimized fingerprints versus larger fingerprints with potentially greater error (e.g. Haddachi et al., 2013; Smith and Blake, 2014; Sherriff et al., 2015; Zhang and Liu, 2016; Lizaga et al., 2020; Collins et al., 2020). Here I find that reducing tracers via optimization yielded the best model results. I thus contend that optimization resulting in a more restrictive tracer selection may yield better model results than a larger fingerprint when preceded by an initial robust suite of tests for conservativeness, as I have done here. I furthermore suggest that statistically optimized fingerprints should be confirmed using a knowledge-based approach to tracer selection in the context of catchment characteristics (geology, soil type, etc.) whenever possible (e.g. Koiter et al., 2013; Laceby and Olley, 2015; Collins et al., 2020). The best fingerprinting approach is thus one that initially performs four robust tests for conservativeness (standard bracket test, mean bracket test, median bracket test, bi-plot inspection), followed by optimization via a variety of statistical techniques (including random forest), and finally confirmed with a knowledge-based inquiry of returned tracers before being input into a Bayesian mixing model (e.g. MixSIAR).

### *3.5.2. Provenance and age of floodplain sediment and the role of small tributaries in large watersheds*

Mixing models indicate that Sand Wash and Muddy Creek are the dominant sources of the sand deposit that fostered a burst of cottonwood establishment on the floodplain of Deerlodge Park in the early 1900s. Sand Creek played a secondary role, and the Little Snake above Muddy and the Upper Yampa River contributed less. The outsized contributions of the three lower Little Snake tributary watersheds of Sand Wash, Sand Creek, and Muddy Creek to Deerlodge Park sediment is consistent with observations of contemporaneous accelerated erosion in these

tributaries between 1880 and 1940 (Kemper et al., 2022b) and with previous work suggesting these tributaries are important for sediment supply to the Little Snake and Yampa rivers (Andrews, 1978, 1980; Topping et al., 2018). A similarly detailed investigation of the provenance of additional floodplain packages within Deerlodge Park would provide valuable perspective on the evolution of sediment sources through the present day and is an avenue of important future research.

The calculated greater contribution from Muddy Creek and Sand Wash than from Sand Creek is notable. Given differences in grain size of sediment from each source area, this is likely both a function of the quantity of sediment exported from Muddy Creek and Sand Wash due to historical arroyo incision, as well as grain-sized constrained downstream travel times (Topping et al., 2018). Because settling velocity increases with particle size (Dietrich, 1982), finer sand travels can be deposited higher on the floodplain. The bulk of sediment from Sand Creek, notably coarser than that from any other tributary (Figure 3.4), may be disproportionately deposited in areas within the active channel, rather than on the floodplain. The influence of grain-size related dynamics on the degree to which tributary watersheds affect downstream fluvial and ecological processes remains an area of critical future work.

Dates from vegetation unearthed by floodplain trenching suggest that a large package of dominantly very fine sand was deposited in 1912. A large cottonwood exhumed by the trench (Figure 3.3) was rooted on top of this layer. Ages of additional cottonwoods suggest that establishment of most of the surrounding cottonwood forest was roughly contemporaneous, indicating that a large cohort established either on the 1912 surface exposed in the trench or on analogous surfaces directly adjacent. At a coarser scale, 53% percent of the forest at Deerlodge Park was established during the time of enhanced tributary erosion (1880-1940; Kemper et al.,

2022b), further demonstrating the connection between erosion in Sand Wash and Muddy Creek and the downstream increase in the rate of formation of surfaces necessary for cottonwood establishment.

Together with the fingerprinting analysis, results of this study indicate that floodplain sediment deposited during a time of heightened tributary erosion was primarily sourced from those tributaries (Muddy Creek and Sand Wash) experiencing increased degradation via arroyo incision. As Sand Wash is a notably smaller watershed than Muddy Creek, when contributions to Deerlodge floodplain sediment are evaluated proportional to basin area, Sand Wash has an additionally outsized role. Taken in tandem with the findings of prior work relating the timing of historical erosion and establishment of large portions of the Deerlodge forest, it is likely that increased rates of establishment of the Deerlodge forest were catalyzed by heightened construction of floodplain surfaces composed of sediments exported from Sand Wash and Muddy Creek during arroyo incision (Kemper et al., 2022b). It follows naturally that tributary morphological processes that substantially increase the sediment loads of large rivers exert significant influence on downstream sediment dynamics and related ecological processes (Dean et al., 2020). Management concerned with the long-term maintenance of vital resources such as cottonwood forests and riparian ecosystems in large river basins such as the Colorado River thus must consider both the processes operating in tributary watersheds (i.e., land-use changes and associated geomorphological adjustments) and the specific management practices undertaken in those watersheds. In short, successful management of a large river basin must be holistic and built-upon strong communication between various stakeholders present within the basin, from landowners, local conservation districts, and non-profits to federal agencies and regional water managers.

### 3.6. Conclusions

Here, I demonstrate that sediment sourced from tributary basins undergoing active arroyo incision during a period of historical erosion dominates the composition of floodplain sand deposited far downstream at this same time. Floodplain sediment revealed to be the rooting surface of extensive cottonwood forest in Deerlodge Park on the Yampa River was found to be dominantly very fine sand sourced primarily from the tributary watersheds of Muddy Creek and Sand Wash. Excavation of the floodplain and dendrochronologic analysis of unearthed riparian vegetation indicates this thick package of very fine sand was emplaced in roughly 1912, a time when Muddy Creek and Sand Wash were experiencing enhanced erosion via arroyo incision.

Floodplain sediment provenance was investigated using a geochemically-based sediment fingerprinting approach that utilized several existing and relatively novel techniques. Results of the fingerprinting analysis suggest that a robust, four-part suite of conservativeness tests should be included during tracer selection to best apply the fingerprinting approach. Additionally, the procedure detailed here demonstrates random forest as a viable technique for tracer selection, and I emphasize its potential to improve the sediment fingerprint method and advocate for its inclusion in sediment fingerprinting workflows.

Study findings further demonstrate the power of the sediment fingerprinting technique to elucidate the beneficial production and translation of sand-sized sediment across substantial space and time, as well as serve as a preliminary step in additional investigations of sediment transport through the landscape (e.g., numerical sediment modeling) by identifying dominant source areas. Moreover, this research underlines the significant role that tributary watershed dynamics play in the morphological evolution and ecological progression of large fluvial systems and emphasizes the need for a holistic, collaborative approach to the management of large

watersheds such as the Colorado River Basin. Such an approach is imperative to ensure that vital riverine landscapes endure into the future.

### 3.7. References

- Akayezu, P., Musinguzi, L., Natugonza, V., Ogutu-Ohwayo, R., Mwathe, K., Dutton, C., Manyifika, M., 2020. Using sediment fingerprinting to identify erosion hotspots in a sub-catchment of Lake Kivu, Rwanda. *Environ Monit Assess* 192, 806. <https://doi.org/10.1007/s10661-020-08774-5>
- Amorim, F., Jacques Agra Bezerra da Silva, Yuri, Cabral Nascimento, R., Jacques Agra Bezerra da Silva, Ygor, Tiecher, T., Williams Araújo do Nascimento, C., Paolo Gomes Minella, J., Zhang, Y., Ram Upadhayay, H., Pulley, S., Collins, A.L., 2021. Sediment source apportionment using optical property composite signatures in a rural catchment, Brazil. *CATENA* 202, 105208. <https://doi.org/10.1016/j.catena.2021.105208>
- Andrews, E.D., 1980. Effective and bankfull discharges of streams in the Yampa River basin, Colorado and Wyoming. *Journal of Hydrology* 46, 311–330. [https://doi.org/10.1016/0022-1694\(80\)90084-0](https://doi.org/10.1016/0022-1694(80)90084-0)
- Andrews, E.D., 1978. Present and potential sediment yields in the Yampa River Basin, Colorado and Wyoming (USGS Numbered Series No. 78–105), Present and potential sediment yields in the Yampa River Basin, Colorado and Wyoming, Water-Resources Investigations Report. U.S. Geological Survey, Water Resources Division,. <https://doi.org/10.3133/wri78105>
- Archer, K.J., Kimes, R.V., 2008. Empirical characterization of random forest variable importance measures. *Computational Statistics & Data Analysis* 52, 2249–2260. <https://doi.org/10.1016/j.csda.2007.08.015>
- Belmont, P., Willenbring, J.K., Schottler, S.P., Marquard, J., Kumarasamy, K., Hemmis, J.M., 2014. Toward generalizable sediment fingerprinting with tracers that are conservative and

- nonconservative over sediment routing timescales. *J Soils Sediments* 14, 1479–1492.  
<https://doi.org/10.1007/s11368-014-0913-5>
- Benda, L., Poff, N.L., Miller, D., Dunne, T., Reeves, G., Pess, G., Pollock, M., 2004. The Network Dynamics Hypothesis: How Channel Networks Structure Riverine Habitats. *BioScience* 54, 413–427. [https://doi.org/10.1641/0006-3568\(2004\)054\[0413:TNDHHC\]2.0.CO;2](https://doi.org/10.1641/0006-3568(2004)054[0413:TNDHHC]2.0.CO;2)
- Bennion, M., Morrison, L., Brophy, D., Carlsson, J., Abrahantes, J.C., Graham, C.T., 2019. Trace element fingerprinting of blue mussel (*Mytilus edulis*) shells and soft tissues successfully reveals harvesting locations. *Science of The Total Environment* 685, 50–58.  
<https://doi.org/10.1016/j.scitotenv.2019.05.233>
- Blake, W.H., Boeckx, P., Stock, B.C., Smith, H.G., Bodé, S., Upadhayay, H.R., Gaspar, L., Goddard, R., Lennard, A.T., Lizaga, I., Lobb, D.A., Owens, P.N., Petticrew, E.L., Kuzyk, Z.Z.A., Gari, B.D., Munishi, L., Mtei, K., Nebiyu, A., Mabit, L., Navas, A., Semmens, B.X., 2018. A deconvolutional Bayesian mixing model approach for river basin sediment source apportionment. *Sci Rep* 8, 13073. <https://doi.org/10.1038/s41598-018-30905-9>
- Bracken, L.J., Turnbull, L., Wainwright, J., Bogaart, P., 2015. Sediment connectivity: a framework for understanding sediment transfer at multiple scales. *Earth Surface Processes and Landforms* 40, 177–188. <https://doi.org/10.1002/esp.3635>
- Bradley, W.H., 1964. Geology of Green River Formation and associated Eocene rocks in southwestern Wyoming and adjacent parts of Colorado and Utah. Professional Paper. <https://doi.org/10.3133/pp496A>
- Breiman, L., 2001. Random Forests. *Machine Learning* 45, 5–32.  
<https://doi.org/10.1023/A:1010933404324>

- Caitcheon, G., Douglas, G., Palmer, M., 2006. Sediment Source Tracing in the Lake Burrangorang Catchment (CSIRO Land and Water Science Report No. 47/07). Canberra.
- Chapman, K.A., Best, R.J., Smith, M.E., Mueller, E.R., Grams, P.E., Parnell, R.A., 2020. Estimating the contribution of tributary sand inputs to controlled flood deposits for sandbar restoration using elemental tracers, Colorado River, Grand Canyon National Park, Arizona. GSA Bulletin 133, 1141–1156. <https://doi.org/10.1130/B35642.1>
- Collins, A.L., Blackwell, M., Boeckx, P., Chivers, C.-A., Emelko, M., Evrard, O., Foster, I., Gellis, A., Gholami, H., Granger, S., Harris, P., Horowitz, A.J., Laceby, J.P., Martinez-Carreras, N., Minella, J., Mol, L., Nosrati, K., Pulley, S., Silins, U., da Silva, Y.J., Stone, M., Tiecher, T., Upadhyay, H.R., Zhang, Y., 2020. Sediment source fingerprinting: benchmarking recent outputs, remaining challenges and emerging themes. J Soils Sediments 20, 4160–4193. <https://doi.org/10.1007/s11368-020-02755-4>
- Collins, A.L., Pulley, S., Foster, I.D.L., Gellis, A., Porto, P., Horowitz, A.J., 2017. Sediment source fingerprinting as an aid to catchment management: A review of the current state of knowledge and a methodological decision-tree for end-users. Journal of Environmental Management, Sediment source fingerprinting for informing catchment management: methodological approaches, problems and uncertainty 194, 86–108. <https://doi.org/10.1016/j.jenvman.2016.09.075>
- Collins, A.L., Walling, D.E., Leeks, G.J.L., 1997. Source type ascription for fluvial suspended sediment based on a quantitative composite fingerprinting technique. CATENA 29, 1–27. [https://doi.org/10.1016/S0341-8162\(96\)00064-1](https://doi.org/10.1016/S0341-8162(96)00064-1)
- Collins, A.L., Zhang, Y., McChesney, D., Walling, D.E., Haley, S.M., Smith, P., 2012. Sediment source tracing in a lowland agricultural catchment in southern England using a modified

- procedure combining statistical analysis and numerical modelling. *Science of The Total Environment* 414, 301–317. <https://doi.org/10.1016/j.scitotenv.2011.10.062>
- Cooper, D.J., Merritt, D.M., Andersen, D.C., Chimner, R.A., 1999. Factors controlling the establishment of Fremont cottonwood seedlings on the Upper Green River, USA. *Regulated Rivers: Research & Management* 15, 419–440. [https://doi.org/10.1002/\(SICI\)1099-1646\(199909/10\)15:5<419::AID-RRR555>3.0.CO;2-Y](https://doi.org/10.1002/(SICI)1099-1646(199909/10)15:5<419::AID-RRR555>3.0.CO;2-Y)
- Dean, D.J., Scott, M.L., Shafroth, P.B., Schmidt, J.C., 2011. Stratigraphic, sedimentologic, and dendrogeomorphic analyses of rapid floodplain formation along the Rio Grande in Big Bend National Park, Texas. *GSA Bulletin* 123, 1908–1925. <https://doi.org/10.1130/B30379.1>
- Dean, D.J., Topping, D.J., Grams, P.E., Walker, A.E., Schmidt, J.C., 2020. Does Channel Narrowing by Floodplain Growth Necessarily Indicate Sediment Surplus? Lessons From Sediment Transport Analyses in the Green and Colorado Rivers, Canyonlands, Utah. *Journal of Geophysical Research: Earth Surface* 125, e2019JF005414. <https://doi.org/10.1029/2019JF005414>
- D’Haen, K., Verstraeten, G., Degryse, P., 2012. Fingerprinting historical fluvial sediment fluxes. *Progress in Physical Geography: Earth and Environment* 36, 154–186. <https://doi.org/10.1177/0309133311432581>
- Dietrich, W.E., 1982. Settling velocity of natural particles. *Water Resources Research* 18, 1615–1626. <https://doi.org/10.1029/WR018i006p01615>
- Elliott, J.G., Anders, S.P., 2004. Summary of sediment data from the Yampa river and upper Green river basins, Colorado and Utah, 1993-2002 (USGS Numbered Series No. 2004–5242), Summary of sediment data from the Yampa river and upper Green river basins,

Colorado and Utah, 1993-2002, Scientific Investigations Report.

<https://doi.org/10.3133/sir20045242>

Friedman, J.M., Griffin, E.R., 2017. Management of plains cottonwood at Theodore Roosevelt National Park, North Dakota (Other Government Series No. NPS/THRO/NRR—2017/1395), Management of plains cottonwood at Theodore Roosevelt National Park, North Dakota, Natural Resource Report. National Park Service, Fort Collins, CO.

Friedman, J.M., Vincent, K.R., Griffin, E.R., Scott, M.L., Shafroth, P.B., Auble, G.T., 2015. Processes of arroyo filling in northern New Mexico, USA. GSA Bulletin 127, 621–640.

<https://doi.org/10.1130/B31046.1>

Friedman, J.M., Vincent, K.R., Shafroth, P.B., 2005. Dating floodplain sediments using tree-ring response to burial. Earth Surface Processes and Landforms 30, 1077–1091.

<https://doi.org/10.1002/esp.1263>

Fryirs, K.A., Brierley, G.J., Preston, N.J., Kasai, M., 2007. Buffers, barriers and blankets: The (dis)connectivity of catchment-scale sediment cascades. CATENA 70, 49–67.

<https://doi.org/10.1016/j.catena.2006.07.007>

Gateuille, D., Owens, P.N., Peticrew, E.L., Booth, B.P., French, T.D., Déry, S.J., 2019.

Determining contemporary and historical sediment sources in a large drainage basin impacted by cumulative effects: the regulated Nechako River, British Columbia, Canada. J Soils Sediments 19, 3357–3373. <https://doi.org/10.1007/s11368-019-02299-2>

Gellis, A.C., Gorman Sanisaca, L., 2018. Sediment Fingerprinting to Delineate Sources of Sediment in the Agricultural and Forested Smith Creek Watershed, Virginia, USA. JAWRA Journal of the American Water Resources Association 54, 1197–1221.

<https://doi.org/10.1111/1752-1688.12680>

- Gellis, A.C., Noe, G.B., 2013. Sediment source analysis in the Linganore Creek watershed, Maryland, USA, using the sediment fingerprinting approach: 2008 to 2010. *J Soils Sediments* 13, 1735–1753. <https://doi.org/10.1007/s11368-013-0771-6>
- Gellis, A.C., Walling, D.E., 2011. Sediment Source Fingerprinting (Tracing) and Sediment Budgets as Tools in Targeting River and Watershed Restoration Programs, in: *Stream Restoration in Dynamic Fluvial Systems*. American Geophysical Union (AGU), pp. 263–291. <https://doi.org/10.1029/2010GM000960>
- Gholami, H., Mohamadifar, A., Collins, A.L., 2020. Spatial mapping of the provenance of storm dust: Application of data mining and ensemble modelling. *Atmospheric Research* 233, 104716. <https://doi.org/10.1016/j.atmosres.2019.104716>
- Gilbert, G.K., 1877. Report on the geology of the Henry Mountains (USGS Unnumbered Series), Report on the geology of the Henry Mountains, Monograph. U.S. Government Printing Office, Washington, D.C. <https://doi.org/10.3133/70039916>
- Gilbert, J.T., Wilcox, A.C., 2021. An ecogeomorphic framework coupling sediment modeling with invasive riparian vegetation dynamics. *Journal of Geophysical Research: Earth Surface* n/a, e2021JF006071. <https://doi.org/10.1029/2021JF006071>
- Graf, D., 1960. Geochemistry of carbonate sediments and sedimentary carbonate rocks Part III Minor Element Distribution. Illinois State Geological Survey Circular 301.
- Hansen, W.R., 1986. Neogene tectonics and geomorphology of the eastern Uinta Mountains in Utah, Colorado, and Wyoming (USGS Numbered Series No. 1356), Professional Paper.
- Haddadchi, A., Ryder, D.S., Evrard, O., Olley, J., 2013. Sediment fingerprinting in fluvial systems: review of tracers, sediment sources and mixing models. *International Journal of Sediment Research* 28, 560–578. [https://doi.org/10.1016/S1001-6279\(14\)60013-5](https://doi.org/10.1016/S1001-6279(14)60013-5)

- Haddadchi, A., Nosrati, K., Ahmadi, F., 2014. Differences between the source contribution of bed material and suspended sediments in a mountainous agricultural catchment of western Iran. *CATENA* 116, 105–113. <https://doi.org/10.1016/j.catena.2013.12.011>
- Hupp, C.R., Osterkamp, W.R., 1996. Riparian vegetation and fluvial geomorphic processes. *Geomorphology, Fluvial Geomorphology and Vegetation* 14, 277–295. [https://doi.org/10.1016/0169-555X\(95\)00042-4](https://doi.org/10.1016/0169-555X(95)00042-4)
- Honey, J.G., Izett, G.A., 1988. Paleontology, taphonomy, and stratigraphy of the Browns Park Formation (Oligocene and Miocene) near Maybell, Moffat County, Colorado. Professional Paper. <https://doi.org/10.3133/pp1358>
- Kabata-Pendias, A., 2000. Trace Elements in Soils and Plants, 3<sup>rd</sup> ed. CRC Press, Boca Raton. <https://doi.org/10.1201/9781420039900>
- Kemper, J.T., Thaxton, R.D., Rathburn, S.L., Friedman, J.M., Mueller, E.R., Scott, M.L., n.d. Sediment-ecological connectivity in a large river network. *Earth Surface Processes and Landforms* 47, 639-657. <https://doi.org/10.1002/esp.5277>
- Kenna, T.C., Nitsche, F.O., Herron, M.M., Mailloux, B.J., Peteet, D., Sritrairat, S., Sands, E., Baumgarten, J., 2011. Evaluation and calibration of a Field Portable X-Ray Fluorescence spectrometer for quantitative analysis of siliciclastic soils and sediments. *Journal of Analytical Atomic Spectrometry* 26, 395–405. <https://doi.org/10.1039/C0JA00133C>
- Klages, M.G., Hsieh, Y.P., 1975. Suspended Solids Carried by the Gallatin River of Southwestern Montana: II. Using Mineralogy for Inferring Sources. *Journal of Environmental Quality* 4, 68–73. <https://doi.org/10.2134/jeq1975.00472425000400010016x>
- Koenig, K.J., 1960. Bridger Formation in the Bridger Basin, Wyoming 163–168.

- Koiter, A.J., Owens, P.N., Peticrew, E.L., Lobb, D.A., 2013. The behavioural characteristics of sediment properties and their implications for sediment fingerprinting as an approach for identifying sediment sources in river basins. *Earth-Science Reviews* 125, 24–42.  
<https://doi.org/10.1016/j.earscirev.2013.05.009>
- Kruskal, W.H., Wallis, W.A., 1952. Use of Ranks in One-Criterion Variance Analysis. *Null* 47, 583–621. <https://doi.org/10.1080/01621459.1952.10483441>
- Lacey, J.P., Olley, J., 2015. An examination of geochemical modelling approaches to tracing sediment sources incorporating distribution mixing and elemental correlations. *Hydrological Processes* 29, 1669–1685. <https://doi.org/10.1002/hyp.10287>
- Langbein, W.B., Schumm, S.A., 1958. Yield of sediment in relation to mean annual precipitation. *Transactions, American Geophysical Union* 39, 1076–1084.  
<https://doi.org/10.1029/TR039i006p01076>
- Liaw, A., Wiener, M., 2002. Classification and Regression by randomForest 2, 5.
- Liu, K., Lobb, D.A., Miller, J.J., Owens, P.N., Caron, M.E.G., 2018. Determining sources of fine-grained sediment for a reach of the Lower Little Bow River, Alberta, using a colour-based sediment fingerprinting approach. *Can. J. Soil. Sci.* 98, 55–69.  
<https://doi.org/10.1139/cjss-2016-0131>
- Lizaga, I., Latorre, B., Gaspar, L., Navas, A., 2020. Consensus ranking as a method to identify non-conservative and dissenting tracers in fingerprinting studies. *Science of The Total Environment* 720, 137537. <https://doi.org/10.1016/j.scitotenv.2020.137537>
- Loire, R., Piégay, H., Malavoi, J.-R., Kondolf, G.M., Bêche, L.A., 2021. From flushing flows to (eco)morphogenic releases: evolving terminology, practice, and integration into river

- management. *Earth-Science Reviews* 213, 103475.  
<https://doi.org/10.1016/j.earscirev.2020.103475>
- Mackin, J., 1948. Concept of the Graded River. *GSA Bulletin* 59, 463–512.  
[https://doi.org/10.1130/0016-7606\(1948\)59\[463:COTGR\]2.0.CO;2](https://doi.org/10.1130/0016-7606(1948)59[463:COTGR]2.0.CO;2)
- Manners, R.B., Schmidt, J.C., Scott, M.L., 2014. Mechanisms of vegetation-induced channel narrowing of an unregulated canyon river: Results from a natural field-scale experiment. *Geomorphology* 211, 100–115. <https://doi.org/10.1016/j.geomorph.2013.12.033>
- Melquiades, F.L., Andreoni, L.F.S., Thomaz, E.L., 2013. Discrimination of land-use types in a catchment by energy dispersive X-ray fluorescence and principal component analysis. *Applied Radiation and Isotopes* 77, 27–31. <https://doi.org/10.1016/j.apradiso.2013.02.015>
- Metzger, T.L., Pizzuto, J.E., Trampush, S.M., Friedman, J.M., Schook, D.M., 2020. Event-scale floodplain accretion revealed through tree-ring analysis of buried plains cottonwoods, Powder River, MT, USA. *Earth Surface Processes and Landforms* 45, 345–360.  
<https://doi.org/10.1002/esp.4734>
- Mueller, E.R., Grams, P.E., 2021. A Morphodynamic Model to Evaluate Long-Term Sandbar Rebuilding Using Controlled Floods in the Grand Canyon. *Geophysical Research Letters* 48, e2021GL093007. <https://doi.org/10.1029/2021GL093007>
- Mueller, E.R., Grams, P.E., Hazel, J.E., Schmidt, J.C., 2018. Variability in eddy sandbar dynamics during two decades of controlled flooding of the Colorado River in the Grand Canyon. *Sedimentary Geology* 363, 181–199. <https://doi.org/10.1016/j.sedgeo.2017.11.007>
- Mukundan, R., Walling, D.E., Gellis, A.C., Slattery, M.C., Radcliffe, D.E., 2012. Sediment Source Fingerprinting: Transforming From a Research Tool to a Management Tool1.

JAWRA Journal of the American Water Resources Association 48, 1241–1257.

<https://doi.org/10.1111/j.1752-1688.2012.00685.x>

Murphey, P., Townsend, K.E., Friscia, A., Westgate, J., Evanoff, E., Gunnell, G., 2017.

Paleontology and stratigraphy of Middle Eocene rock units in the southern Green River and Uinta Basins, Wyoming and Utah. *Geology of the Intermountain West* 4, 1–53.

<https://doi.org/10.31711/giw.v4.pp1-53>

National Park Service (NPS). 2005. Dinosaur National Monument: Invasive Plant Management and Environmental Assessment.

Navratil, O., Evrard, O., Esteves, M., Legout, C., Ayrault, S., Némery, J., Mate-Marin, A.,

Ahmadi, M., Lefèvre, I., Poirel, A., Bonté, P., 2012. Temporal variability of suspended sediment sources in an alpine catchment combining river/rainfall monitoring and sediment fingerprinting. *Earth Surface Processes and Landforms* 37, 828–846.

<https://doi.org/10.1002/esp.3201>

Noe, G.B., Cashman, M.J., Skalak, K., Gellis, A., Hopkins, K.G., Moyer, D., Webber, J.,

Bentham, A., Maloney, K., Brakebill, J., Sekellick, A., Langland, M., Zhang, Q., Shenk, G., Keisman, J., Hupp, C., 2020. Sediment dynamics and implications for management: State of the science from long-term research in the Chesapeake Bay watershed, USA. *WIREs Water* 7, e1454. <https://doi.org/10.1002/wat2.1454>

Nosrati, K., Akbari-Mahdiabad, M., Fiener, P., Collins, A.L., 2021a. Using different size

fractions to source fingerprint fine-grained channel bed sediment in a large drainage basin in Iran. *CATENA* 200, 105173. <https://doi.org/10.1016/j.catena.2021.105173>

Nosrati, K., Collins, A.L., Madankan, M., 2018a. Fingerprinting sub-basin spatial sediment

sources using different multivariate statistical techniques and the Modified MixSIR model. *CATENA* 164, 32–43. <https://doi.org/10.1016/j.catena.2018.01.003>

- Nosrati, K., Fathi, Z., Collins, A.L., 2019. Fingerprinting sub-basin spatial suspended sediment sources by combining geochemical tracers and weathering indices. *Environ Sci Pollut Res* 26, 28401–28414. <https://doi.org/10.1007/s11356-019-06024-x>
- Nosrati, K., Haddadchi, A., Collins, A.L., Jalali, S., Zare, M.R., 2018b. Tracing sediment sources in a mountainous forest catchment under road construction in northern Iran: comparison of Bayesian and frequentist approaches. *Environ Sci Pollut Res* 25, 30979–30997. <https://doi.org/10.1007/s11356-018-3097-5>
- Nosrati, K., Mohammadi-Raigani, Z., Haddadchi, A., Collins, A.L., 2021b. Elucidating intra-storm variations in suspended sediment sources using a Bayesian fingerprinting approach. *Journal of Hydrology* 596, 126115. <https://doi.org/10.1016/j.jhydrol.2021.126115>
- Olley, J., Caitcheon, G., 2000. Major element chemistry of sediments from the Darling–Barwon river and its tributaries: implications for sediment and phosphorus sources. *Hydrological Processes* 14, 1159–1175. [https://doi.org/10.1002/\(SICI\)1099-1085\(200005\)14:7<1159::AID-HYP6>3.0.CO;2-P](https://doi.org/10.1002/(SICI)1099-1085(200005)14:7<1159::AID-HYP6>3.0.CO;2-P)
- Owens, P.N., 2008. Sediment behaviour, functions and management in river basins, in: Owens, P.N. (Ed.), *Sustainable Management of Sediment Resources, Sediment Management at the River Basin Scale*. Elsevier, pp. 1–29. [https://doi.org/10.1016/S1872-1990\(08\)80003-7](https://doi.org/10.1016/S1872-1990(08)80003-7)
- Palazón, L., Navas, A., 2017. Variability in source sediment contributions by applying different statistic test for a Pyrenean catchment. *Journal of Environmental Management, Sediment source fingerprinting for informing catchment management: methodological approaches, problems and uncertainty* 194, 42–53. <https://doi.org/10.1016/j.jenvman.2016.07.058>
- Parsons, C., Margui Grabulosa, E., Pili, E., Floor, G.H., Roman-Ross, G., Charlet, L., 2013. Quantification of trace arsenic in soils by field-portable X-ray fluorescence spectrometry:

- Considerations for sample preparation and measurement conditions. *Journal of Hazardous Materials* 262, 1213–1222. <https://doi.org/10.1016/j.jhazmat.2012.07.001>
- Plummer, M., 2003. JAGS: A program for analysis of Bayesian graphical models using Gibbs sampling. *Proceedings of the 3<sup>rd</sup> international workshop on distributed statistical computing* 124, 1–10.
- Pulley, S., Foster, I., Antunes, P., 2015. The uncertainties associated with sediment fingerprinting suspended and recently deposited fluvial sediment in the Nene river basin. *Geomorphology* 228, 303–319. <https://doi.org/10.1016/j.geomorph.2014.09.016>
- Pulley, S., Foster, I., Collins, A.L., 2017. The impact of catchment source group classification on the accuracy of sediment fingerprinting outputs. *Journal of Environmental Management, Sediment source fingerprinting for informing catchment management: methodological approaches, problems and uncertainty* 194, 16–26.  
<https://doi.org/10.1016/j.jenvman.2016.04.048>
- Qu, M., Chen, J., Li, W., Zhang, C., Wan, M., Huang, B., Zhao, Y., 2019. Correction of in-situ portable X-ray fluorescence (PXRF) data of soil heavy metal for enhancing spatial prediction. *Environmental Pollution* 254, 112993.  
<https://doi.org/10.1016/j.envpol.2019.112993>
- Richter, B.D., Richter, H.E., 2000. Prescribing Flood Regimes to Sustain Riparian Ecosystems along Meandering Rivers. *Conservation Biology* 14, 1467–1478.  
<https://doi.org/10.1046/j.1523-1739.2000.98488.x>
- Roehler, H.W., 1992. Description and correlation of Eocene rocks in stratigraphic reference sections for the Green River and Washakie basins, Southwest Wyoming. *Professional Paper*.  
<https://doi.org/10.3133/pp1506D>

- Roehler, H.W., 1985. Electric-log correlations of the upper Cretaceous Rock Springs and Blair Formations on the east and west flanks of the Rock Springs Uplift, Wyoming (USGS Numbered Series No. 1785), Miscellaneous Field Studies Map. U.S. Geological Survey, Reston, VA.
- Roehler, H.W., 1973. Stratigraphy of the Washakie Formation in the Washakie Basin, Wyoming (No. 1369), Bulletin. U.S. Govt. Print. Off., <https://doi.org/10.3133/b1369>
- Rouillon, M., Taylor, M.P., 2016. Can field portable X-ray fluorescence (pXRF) produce high quality data for application in environmental contamination research? *Environmental Pollution* 214, 255–264. <https://doi.org/10.1016/j.envpol.2016.03.055>
- Schook, D.M., Rathburn, S.L., Friedman, J.M., Wolf, J.M., 2017. A 184-year record of river meander migration from tree rings, aerial imagery, and cross sections. *Geomorphology* 293, 227–239. <https://doi.org/10.1016/j.geomorph.2017.06.001>
- Schumm, S.A., 1969. River Metamorphosis. *Journal of the Hydraulics Division* 95, 255–274. <https://doi.org/10.1061/JYCEAJ.0001938>
- Schumm, S.A., Lichty, R.W., 1965. Time, space, and causality in geomorphology. *American Journal of Science* 263, 110–119. <https://doi.org/10.2475/ajs.263.2.110>
- Scott, M.L., Auble, G.T., Friedman, J.M., 1997. Flood Dependency of Cottonwood Establishment Along the Missouri River, Montana, Usa. *Ecological Applications* 7, 677–690. [https://doi.org/10.1890/1051-0761\(1997\)007\[0677:FDOCEA\]2.0.CO;2](https://doi.org/10.1890/1051-0761(1997)007[0677:FDOCEA]2.0.CO;2)
- Scott, M.L., Friedman, J.M., Auble, G.T., 1996. Fluvial process and the establishment of bottomland trees. *Geomorphology, Fluvial Geomorphology and Vegetation* 14, 327–339. [https://doi.org/10.1016/0169-555X\(95\)00046-8](https://doi.org/10.1016/0169-555X(95)00046-8)

- Shackley, M.S., 2011. An Introduction to X-Ray Fluorescence (XRF) Analysis in Archaeology, in: Shackley, M.S. (Ed.), X-Ray Fluorescence Spectrometry (XRF) in Geoarchaeology. Springer, New York, NY, pp. 7–44. [https://doi.org/10.1007/978-1-4419-6886-9\\_2](https://doi.org/10.1007/978-1-4419-6886-9_2)
- Sherriff, S.C., Franks, S.W., Rowan, J.S., Fenton, O., Ó'hUallacháin, D., 2015. Uncertainty-based assessment of tracer selection, tracer non-conservativeness and multiple solutions in sediment fingerprinting using synthetic and field data. *J Soils Sediments* 15, 2101–2116. <https://doi.org/10.1007/s11368-015-1123-5>
- Smith, D., Cannon, W., Woodruff, L., Solano, F., Ellefsen, K., 2014. Geochemical and mineralogical maps for soils of the conterminous United States (Open-File Report No. 1082), Open-File Report. U.S. Geological Survey.
- Smith, H.G., Blake, W.H., 2014. Sediment fingerprinting in agricultural catchments: A critical re-examination of source discrimination and data corrections. *Geomorphology* 204, 177–191. <https://doi.org/10.1016/j.geomorph.2013.08.003>
- Smith, H.G., Karam, D.S., Lennard, A.T., 2018. Evaluating tracer selection for catchment sediment fingerprinting. *J Soils Sediments* 18, 3005–3019. <https://doi.org/10.1007/s11368-018-1990-7>
- Song, Y., Chen, X., Li, Y., Fan, Y., Collins, A.L., 2022. Quantifying the provenance of dune sediments in the Taklimakan Desert using machine learning, multidimensional scaling and sediment source fingerprinting. *CATENA* 210, 105902. <https://doi.org/10.1016/j.catena.2021.105902>
- Stock, B., Semmens, B., 2016. MixSIAR User Manual Version 3.1 59. <https://doi.org/doi:10.5281/zenodo.47719>.

- Strobl, C., Boulesteix, A-L., Zeileis, A., Hothorn, T., 2007. Bias in random forest variable importance measures: Illustrations, sources and a solution. *BMC Bioinformatics* 8, 25. <https://doi.org/10.1186/1471-2105-8-25>
- Sutherland, W., Gregory, R., Carnes, J., Worman, B., 2013. Spatial variability of coalbed natural gas produced water quality, Powder River Basin, Wyoming: implications for future development (No. 65), Report of Investigations. Wyoming State Geological Survey, Laramie, Wyoming.
- Topping, D.J., Mueller, E.R., Schmidt, J.C., Griffiths, R.E., Dean, D.J., Grams, P.E., 2018. Long-Term Evolution of Sand Transport Through a River Network: Relative Influences of a Dam Versus Natural Changes in Grain Size From Sand Waves. *Journal of Geophysical Research: Earth Surface* 123, 1879–1909. <https://doi.org/10.1029/2017JF004534>
- Uber, M., Legout, C., Nord, G., Crouzet, C., Demory, F., Poulencard, J., 2019. Comparing alternative tracing measurements and mixing models to fingerprint suspended sediment sources in a mesoscale Mediterranean catchment. *J Soils Sediments* 19, 3255–3273. <https://doi.org/10.1007/s11368-019-02270-1>
- United States Environmental Protection Agency (US-EPA), 1998. Environmental Technology Verification Report, Field Portable X-ray Fluorescence Analyzer Metorex X-MET 920-P and 940. (EPA/600/R-97/146). US Environmental Protection Agency (US-EPA), Washington, D.C.
- Vercruyse, K., Grabowski, R.C., Rickson, R.J., 2017. Suspended sediment transport dynamics in rivers: Multi-scale drivers of temporal variation. *Earth-Science Reviews* 166, 38–52. <https://doi.org/10.1016/j.earscirev.2016.12.016>

- Walker, A.E., Moore, J.N., Grams, P.E., Dean, D.J., Schmidt, J.C., 2020. Channel narrowing by inset floodplain formation of the lower Green River in the Canyonlands region, Utah. *GSA Bulletin* 132, 2333–2352. <https://doi.org/10.1130/B35233.1>
- Walling, D.E., 2005. Tracing suspended sediment sources in catchments and river systems. *Science of The Total Environment, Linking Landscape Sources of Phosphorus and Sediment to Ecological Impacts in Surface Waters* 344, 159–184. <https://doi.org/10.1016/j.scitotenv.2005.02.011>
- Walling, D.E., 1983. The sediment delivery problem. *Journal of Hydrology, Scale Problems in Hydrology* 65, 209–237. [https://doi.org/10.1016/0022-1694\(83\)90217-2](https://doi.org/10.1016/0022-1694(83)90217-2)
- Walling, D.E., Collins, A.L., 2008. The catchment sediment budget as a management tool. *Environmental Science & Policy, Monitoring and modelling diffuse pollution from agriculture for policy support: UK and European experience.* 11, 136–143. <https://doi.org/10.1016/j.envsci.2007.10.004>
- Walling, D.E., Collins, A.L., 2016. Fine sediment transport and management, in: Gilvear, D., Greenwood, M.T., Thoms, M.C., Wood, P.J. (Eds.), *River Science : Research and Management for the 21<sup>st</sup> Century*, Chapter 3. Wiley-Blackwell, Chichester, Sussex, pp. 37–60.
- Ward, J.V., Tockner, K., Arscott, D.B., Claret, C., 2002. Riverine landscape diversity. *Freshwater Biology* 47, 517–539. <https://doi.org/10.1046/j.1365-2427.2002.00893.x>
- Weihs, C., Ligges, U., Luebke, K., Raabe, N., 2005. klaR Analyzing German Business Cycles, in: Baier, D., Decker, R., Schmidt-Thieme, L. (Eds.), *Data Analysis and Decision Support, Studies in Classification, Data Analysis, and Knowledge Organization.* Springer, Berlin, Heidelberg, pp. 335–343. [https://doi.org/10.1007/3-540-28397-8\\_36](https://doi.org/10.1007/3-540-28397-8_36)

- Wilkinson, S.N., Hancock, G.J., Bartley, R., Hawdon, A.A., Keen, R.J., 2013. Using sediment tracing to assess processes and spatial patterns of erosion in grazed rangelands, Burdekin River basin, Australia. *Agriculture, Ecosystems & Environment, Catchments to Reef continuum: Minimising impacts of agriculture on the Great Barrier Reef* 180, 90–102. <https://doi.org/10.1016/j.agee.2012.02.002>
- Wohl, E., Bledsoe, B.P., Jacobson, R.B., Poff, N.L., Rathburn, S.L., Walters, D.M., Wilcox, A.C., 2015. The Natural Sediment Regime in Rivers: Broadening the Foundation for Ecosystem Management. *BioScience* 65, 358–371. <https://doi.org/10.1093/biosci/biv002>
- Wohl, E., Brierley, G., Cadol, D., Coulthard, T.J., Covino, T., Fryirs, K.A., Grant, G., Hilton, R.G., Lane, S.N., Magilligan, F.J., Meitzen, K.M., Passalacqua, P., Poepl, R.E., Rathburn, S.L., Sklar, L.S., 2019. Connectivity as an emergent property of geomorphic systems. *Earth Surface Processes and Landforms* 44, 4–26. <https://doi.org/10.1002/esp.4434>
- Yalcin, M.G., Narin, I., Soylak, M., 2008. Multivariate analysis of heavy metal contents of sediments from Gumusler creek, Nigde, Turkey. *Environ Geol* 54, 1155–1163. <https://doi.org/10.1007/s00254-007-0884-6>
- Zhang, X.C. (John), Liu, B.L., 2016. Using multiple composite fingerprints to quantify fine sediment source contributions: A new direction. *Geoderma* 268, 108–118. <https://doi.org/10.1016/j.geoderma.2016.01.031>

## CHAPTER 4: GEOMORPHIC EFFECTS OF INCREASED SEDIMENT SUPPLY IN LOW-GRADIENT, ALLUVIAL RIVERS

### 4.1. Introduction

It is a long-held tenet of geomorphic theory that river channels are scaled to the water and sediment loads they carry (Mackin, 1948; Leopold and Maddock, 1953; Wolman, 1955; Leopold and Wolman, 1957; Park, 1977; Parker, 1979; Huang and Nanson, 2000; Wohl, 2004). Thus, alterations to inputs of water and sediment result in adjustments of channel morphology (Lane, 1955; Schumm, 1969; Williams and Wolman, 1984; Hey, 1988; Friend, 1993; Simon and Thorne, 1996; Brandt, 2000; Church, 2002; Gregory, 2006; Dust and Wohl, 2012; Wohl, 2015; Pfeiffer et al., 2017). Accordingly, the body of work addressing channel morphologic change under variable discharge and sediment regimes is extensive, with studies across a range of scales, from headwater channels to megarivers (Constantine et al., 2014), a multitude of settings, from Australia (e.g., Knighton, 1989) to the Arctic (Ashworth and Ferguson, 1986), and spanning at least a century (Gilbert, 1917).

Though a clean separation is realistically unlikely, many classic conceptual models treat discharge and sediment supply as independently alterable variables (Lane, 1955; Schumm, 1969). Similarly, the voluminous channel change literature can be broadly catalogued into investigations concentrated on the morphological effects of i) a change in sediment load and ii) a change in discharge. Here, I focus on the former, in particular on the channel morphologic impacts of an increased sediment supply. Sediment supply increases can result from numerous phenomena (James and Lecce, 2013; Sims and Rutherford, 2017), including direct human actions such as mining (Gilbert, 1917; Knighton, 1989; James and Lecce, 2013), urbanization (Wolman, 1967; Leopold, 1973; Chin, 2006; Leopold et al., 2005), and agriculture and

associated land clearing (Knox, 1977, 2006; Fitzpatrick and Knox, 2000; Fryirs et al., 2018), as well as more natural (or where human actions are a secondary driver) phenomena, such as floods, landslides (Nelson and Dubé, 2016; Rathburn et al., 2017) or meander cutoffs (Zinger et al., 2011).

In this chapter, I synthesize the body of work regarding the geomorphic response of a river system to increases in sediment supply in order to reevaluate existing theoretical conceptualizations using published empirical evidence – a perennially important undertaking in geomorphology and science in general (Hickin, 1983). My intent here is to distill the existing literature into an empirically supported conceptual framework of the various trajectories of river response to a sediment pulse. Development of such a framework should additionally assist evaluation and appreciation of where the present state of a given river system sits with regards to the past and how that can influence future response. A summary of empirical results from case studies relevant to the morphological evolution of river systems has substantial usefulness for providing context to aid in prediction, anticipation, and management of fluvial system response.

Moreover, as the consequences of increased sediment supply have been relatively robustly studied and summarized for mountain rivers in steeper, upland river basins – unsurprisingly so, as large periodic influxes of sediment are a common and important aspect of watershed sediment dynamics in those settings (Montgomery and Buffington, 1997) – here instead I focus on the response of low-gradient, alluvial rivers to increases in sediment load (Figure 4.1). Low-gradient is a term with many varying definitions (Flotemersch et al., 2013), often dependent upon the larger geographical context in which any given study takes place or on the conventions of the specific body of literature to which a given investigation contributes. I define low-gradient, alluvial rivers as those with a channel gradient equal to or below 0.002 –

which allows for the consideration of both coarse and finer-bed alluvial rivers in smaller drainage basins ( $< 10^3 \text{ km}^2$ , Sklar and Dietrich, 1998) and roughly encapsulates the use of the term low-gradient across both the gravel- and sand-bed stream literature, enabling both to be considered in this analysis – that flow within a self-formed floodplain and, additionally, are semi-confined or unconfined in terms of capacity for lateral adjustment (Fryirs et al., 2016). Following this definition allows me to concentrate on those rivers or reaches of rivers that are generally separated, both spatially and temporally, from immediate upland sediment sources. Such river settings, which roughly encompass everything from valley bottom streams to enormous lowland rivers, are often home to large populations; more than 2.7 billion people currently live on or along large rivers (Best, 2019), and many river valleys are locations of increasing development (Church, 2002).

As we move into the future, many of the above listed agents of sediment supply increases stand to be affected. First, climate change can broadly increase sediment yields via a variety of mechanisms, including increased occurrence of extreme rainfall and heightened wildfire risk (Meyer et al., 1992; Ashmore and Church, 2001; Goudie, 2006; Sankey et al., 2017; East and Sankey, 2020); it is now largely evident that modern climate change will have appreciable effects on geomorphic processes such as sediment production (Lane, 2013; Pelletier et al., 2015; East and Sankey, 2020). Second, population growth associated alterations (e.g., agricultural expansion [Foley et al., 2011]) as well as increasing urbanization (United Nations, 2018) will likely result in measurably enhanced sediment yields (*sensu* Hooke, 2000; Gregory, 2006; Church, 2010; James and Lecce, 2013).

Considering these projected alterations, it is evident that anticipation and prediction of geomorphic change resulting from increased sediment supply must be robust, underpinned by

well-established theory (Lane, 1955; Schumm, 1969) and informed and updated by empirical observations. Of the various factors that set river form, sediment supply may exert the most substantial influence on river morphology across scale; perturbations in sediment supply thus may have a considerable impact on river dimension, form, and function (Church, 2002). The repercussions of channel alterations may be manifold: increased flood risk (Collier et al., 1996; Czuba et al., 2010; Cashman et al., 2021), threatened infrastructure and loss of arable adjacent land (Shen et al., 1981; Simon and Rinaldi, 2000; Kondolf et al., 2002; Rinaldi, 2003; Phillips et al., 2005; Larsen et al., 2007), and various deleterious ecological impacts, including lower species abundance and diversity and reduced habitat stability (Brierley et al., 1999; Prosser et al., 2001; Rinaldi, 2003; Wohl, 2015; Wohl et al., 2015). Additionally, because an influx of a large quantity of sediment can represent a shift in the trajectory of a river system, responsible future management and restoration requires a firm grasp of the history and current state of the system (Schumm, 1977; James, 2015; Rathburn et al., 2018; Wohl, 2020; James et al., 2022).



**Figure 4.1.** Examples of low gradient rivers. (clockwise from top left) A river in central Alaska, the Amazon at flood stage, the Yellowstone River in eastern Montana, the Yampa River in

western Colorado, the Little Snake River in southern Wyoming, a river in central Alaska, a creek in southern Illinois, and a river in central Alaska.

Overall, the intent of this review is to summarize the existing studies regarding channel adjustments of low-gradient, alluvial rivers to sediment supply increase – with a particular focus on field-scale investigations – in order to 1) provide a thorough and readily accessible summary of the magnitude, direction, and character of changes observed in a variety of situations across a range of scales, 2) create a conceptual framework that can be used in concert with similar approaches (Lane, 1955; Schumm, 1969; Dust and Wohl, 2012, Huang et al., 2014) to carefully and responsibly anticipate and predict geomorphic change, and 3) highlight avenues for future examination and investigation, namely the identification of thresholds between types of change and the various characteristics that precipitate a crossing of those thresholds. To achieve these objectives, I first provide a broad synopsis of the progression of the sediment supply increase and resultant channel change literature over the last century, followed by an overview of the current state of the science. I then review the variety of adjustments observed over a continuum of scales by thoroughly summarizing the body of work wherein changes at each particular scale have been observed and documented, paying particular attention to the character and direction of change and what aspects have – and have not – been quantified. Building off this summary, I finally identify existing knowledge gaps and avenues for future work.

## **4.2. Channel adjustment and sediment load: History and state of the science**

### *4.2.1 History*

The geomorphic consequences that result from a large influx of sediment into a river system have been of keen interest to fluvial investigators for more than a century (Gilbert, 1917), though broad recognition of such impacts dates somewhat earlier (Marsh, 1864; Wohl, 2020), perhaps even to ancient times (James and Lecce, 2013). The idea of an observable geomorphic

response following an alteration in sediment supply was additionally implicit in early conceptualizations of the drivers of fluvial form, especially theories that postulated a channel is scaled just to transport the water and sediment supplied to it (Davis, 1902). Renewed recognition and further refinement of the relationship between channel dimensions and supplied discharge and sediment load in the mid-20<sup>th</sup> century (Mackin, 1948) catalyzed the development of both quantitative scaling equations for channel geometry and pattern (Leopold and Maddock, 1953; Wolman, 1955; Leopold and Wolman, 1957) and qualitative relations for the adjustment of channels to changes in either of these input variables (Lane, 1955). The latter relation, which is widely known as Lane's balance, is a conceptual model of the adjustment pathways via which a river may attempt to return to equilibrium following an alteration in inputs and was conceived explicitly to facilitate the prediction of morphological change (Eq. 4.1) (Lane, 1955).

$$Q_w S \propto Q_s D_s \quad (4.1)$$

A rather elegantly straightforward model, Lane's balance encapsulated much of the prevailing thought on channel equilibrium and adjustment at the time; it remains a widely adopted and useful model for illustrating equilibrium concepts and visualizing channel response to a change in discharge or sediment load (Dust and Wohl, 2012).

Catalyzed in part by these works as well as a continually growing recognition of the impact of human actions on various aspects of the fluvial system, studies focused explicitly on channel adjustment dynamics following perturbations to the equilibrium state began to proliferate (Knighton, 1998). The concept of river metamorphosis (Schumm, 1969) essentially extended the ideas of Lane's balance by incorporating additional measures of channel planform and cross-sectional geometry (width, depth, width-depth ratio, meander wavelength, and sinuosity) to describe and anticipate channel response, further underscoring the various pathways

and many degrees of freedom that must be considered (Wohl and Dust, 2012). Investigations of system equilibria as a function of the spatial and temporal scales under consideration (Schumm and Lichty, 1965), as well as ideas highlighting the complex response of a system to a perturbation in equilibrium (Schumm, 1973; Schumm and Parker, 1973; Womack and Schumm, 1977; Bull, 1979), served to further develop and emphasize the multifaceted nature of channel adjustment. Consideration of landscape sensitivity and the potential magnitude and rapidity of a system response to a disturbance additionally underlined the importance of lag times and buffering capacity in regulating the spatial and temporal magnitude of channel adjustment (Brunsden and Thornes, 1979).

A strong conceptual underpinning thus established (Schumm, 1977), investigations of channel adjustment began to turn more toward quantitative-focused case studies (e.g., Knox, 1977; Andrews, 1979; Trimble, 1981), likely driven by an identified need to support conceptual (and perhaps moderately speculative) assertions with field observations and studies (Hickin, 1983). Much of this work was focused on anthropogenically-caused alterations to the discharge and sediment regime of a given reach or river (e.g., Jacobson and Coleman, 1986; Knighton, 1989) and increasingly sought to answer the what, where, when, why, and how of channel adjustment to modified inputs of water and sediment (Gregory, 2006; Wohl, 2015). Notably, a substantial portion of this increasingly extensive body of work concentrated on the impacts of changes in hydrology or *reductions* in sediment load, especially downstream of dam closures (e.g., Williams and Wolman, 1984; Brandt, 2000). Additional broad conceptual models of the interplay between equilibrium, adjustment, and channel morphology continued to be developed (Carson, 1984; Schumm, 1985; Hey and Thorne, 1986). These included more site-specific channel evolution models that provided a synopsis of how certain channels exposed to certain

perturbations in certain settings evolved through time (e.g., Simon, 1989, 1995; Gellis et al., 1991). Several robustly quantitative approaches to the question of channel adjustment were also undertaken at this time (Chang, 1986), including channel pattern discriminators that sought a mechanistic explanation for the configuration of a given channel with given sediment and water inputs (Parker, 1976; Darby and Thorne, 1996) and empirically derived rational regime equations that incorporated sediment parameters into prediction of stable channel dimensions (Parker, 1979; Griffiths, 1981; Hey and Thorne, 1986).

Emphasis on quantitative field-based undertakings to investigate the impacts of changing sediment loads on channel morphology continued into the last decade of the 20<sup>th</sup> century and first decade of the 21<sup>st</sup>, remaining both focused on untangling anthropogenic influences (e.g., Brooks and Brierley, 1997) and expanding considerations of natural mechanisms, such as landslides or wildfire (e.g., Meyer et al., 1992). In the vein of classic geomorphic questions (Gilbert, 1917), numerous workers focused on interrogation of the dynamics of the mass of sediment delivered to channels during episodic events (termed sediment “waves”, “slugs”, “pulses” [Nicholas et al., 1995; James, 2010]), concentrating both on the evolution of the wave (i.e., translation vs dispersion [Lisle et al., 1997; Sutherland et al., 2002; Lisle et al., 2007]) and its geomorphic impacts (e.g., Erksine, 1994b; Madej and Ozaki, 1996; Bartley and Rutherford, 2005). Many experimental (e.g., Ashmore, 1991; Lisle et al., 1997) and modeling (e.g., Sutherland et al., 2002) studies on sediment pulse evolution impacts also arose at this time.

The first decade of the 21<sup>st</sup> century also saw great expansion of both dam removals and investigations of the geomorphic impacts and evolution that followed. Though the practice of dam removal had steadily progressed over the prior 15 years or so, post-removal studies were relatively lacking until the dawn of the new century (Bellmore et al., 2017; Major et al., 2017).

Conceptualizations of geomorphic response to removal during this time were thus largely based on the existing geomorphic theory of channel response to a sediment input (Pizzuto, 2002; Major et al., 2017); relatedly, many of the ensuing studies (e.g., Doyle et al., 2003) can be read as natural experiments of that theory. The dam removal literature, which continues to expand both in number of studies and range of dam size considered (e.g., Merritts et al., 2013; East et al., 2018), thus provides an important reference for questions of channel morphologic change following sediment supply increases.

Recent years have seen renewed attention towards developing broad scale perspectives of channel morphological change and sediment load dynamics and the various factors that link and control those dynamics (Church, 2006). These include an expanded Lane's balance with additional degrees of freedom (width/depth ratio, sinuosity, and bedform amplitude) (Dust and Wohl, 2012), various mechanistic (Candel et al. 2021) and empirical (Kleinhans and Van den Berg, 2011) channel pattern predictors, revival of the channel sensitivity concept for evaluating potential for change (Fryirs, 2017; Khan and Fryirs, 2020), and construction of several conceptual models with heavy implications for anticipating and predicting geomorphic adjustment, such as geomorphic coupling (Harvey, 2002) and sediment connectivity (Hooke, 2003; Fryirs et al., 2007; Fryirs, 2013; Bracken et al., 2015; Wohl et al., 2019; Najafi et al., 2021). In particular, the concept of connectivity – the idea that a given river reach does not operate in isolation but as a component of a system whose given state is dependent upon both upstream and downstream conditions and the strength of the linkages between them (Fryirs, 2013; Brierley et al., 2015; Hooke, 2015, Wohl et al., 2019) – has been frequently applied in the context of predicting the geomorphic change that arises from a disturbance and resulting alterations in sediment supply (Poeppl et al., 2017). Often this connectivity perspective has been

taken with regard to the role of various watershed components (e.g., network structure) in regulating the magnitude, timing, and location of geomorphic change (Czuba and Fofoula-Georgiou, 2015; Hooke, 2015; Gran and Czuba, 2017; Khan et al., 2021). Studies have also married the interrelated concepts of connectivity and sensitivity to examine channel evolutionary trajectories following alterations in input and evaluate potential for future adjustments (Reid and Brierley, 2015; Lisenby et al., 2020).

Finally, in addition to the development or revamping of broad-scale conceptual models, there continue to be a wealth of quantitative field (e.g., Dean et al., 2016; Kemper et al., 2022), experimental (Nelson et al., 2015; Morgan and Nelson 2021), and modeling studies (Parker et al., 2011; Morgan and Nelson, 2019) to investigate the relationships between channel adjustment and increased sediment load. Overall, work focusing on channel morphology and sediment transport as intrinsically linked processes is increasingly widespread, reflecting growing recognition of the “morphodynamic paradigm” that holds that sediment dynamics (i.e., supply and transport) set channel morphology and these intertwined aspects of the fluvial system should be studied as fully interactive (Church and Ferguson, 2015).

#### *4.2.2 State of the science*

It is well acknowledged and well-studied that increases in sediment supplied to a channel catalyze observable and measurable channel changes at a variety of scale(s) (Figure 4.2) of a variety of types (Figure 4.3) (Friend, 1993; Hoffman and Gabet, 2007; Buffington, 2012; Wohl, 2015); typical responses of channels to increases in sediment supply are widening, aggradation, avulsion, oftentimes fining, and potentially planform metamorphosis (Schumm, 1969; Eaton et al., 2010). However, the type, character, and direction of change is highly heterogeneous. Various studies have, for example, observed aggradation followed by incision or narrowing

(Griffiths, 1979), aggradation followed by widening (Brooks and Brierley, 1997), or narrowing followed by widening (Leopold et al., 2005). Similarly, and paradoxically, previous work has also found that sediment supply increases can drive bed fining (Knighton, 1989; Gomez et al., 2001) or bed coarsening (Kibler et al., 2011).

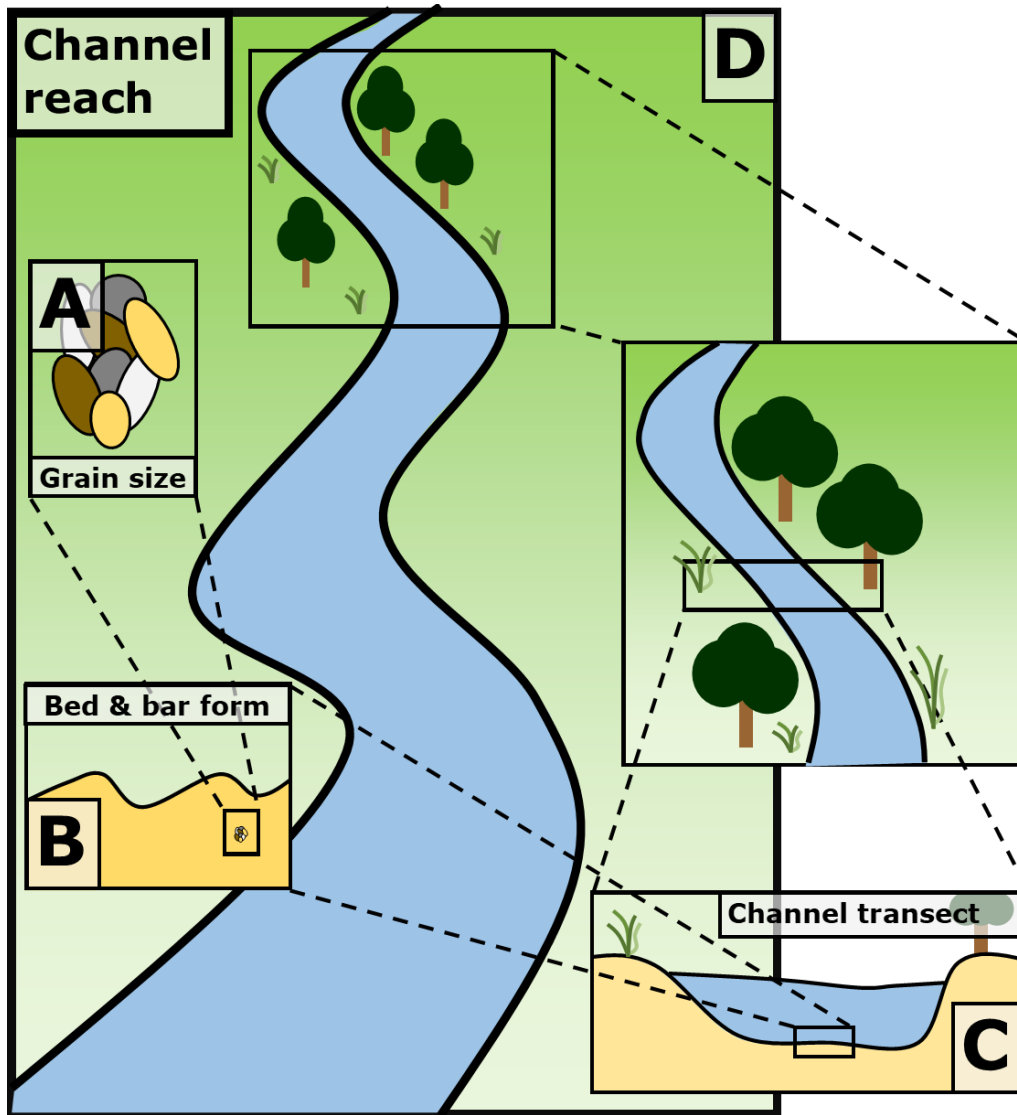


**Figure 4.2.** The scales of adjustment at which change may occur following a sediment influx.

Observed changes in low-gradient, alluvial rivers are equivalently diverse, but the body of study is comparatively smaller than that for mountain streams. Additionally, field-based and other studies of low-gradient, alluvial rivers are loosely organized and rather scattered through

the literature, a disjointedness that was once true of the general river channel change literature (Hickin, 1983) but has been seemingly largely rectified for steeper, upland streams that are well-connected (or coupled) to hillslope sediment sources (Nicholas et al., 1995; Lisle, 2007; Recking, 2012; Hassan and Zimmerman, 2012; Mueller and Pitlick, 2013, 2014). There is thus a need for a synthesis of the existing literature regarding the response of low-gradient, alluvial channels, both to distill a diffuse collection of studies spanning the better part of a century into a readily referenceable resource and coherent conceptual model and to identify existing knowledge gaps and needs for future work.

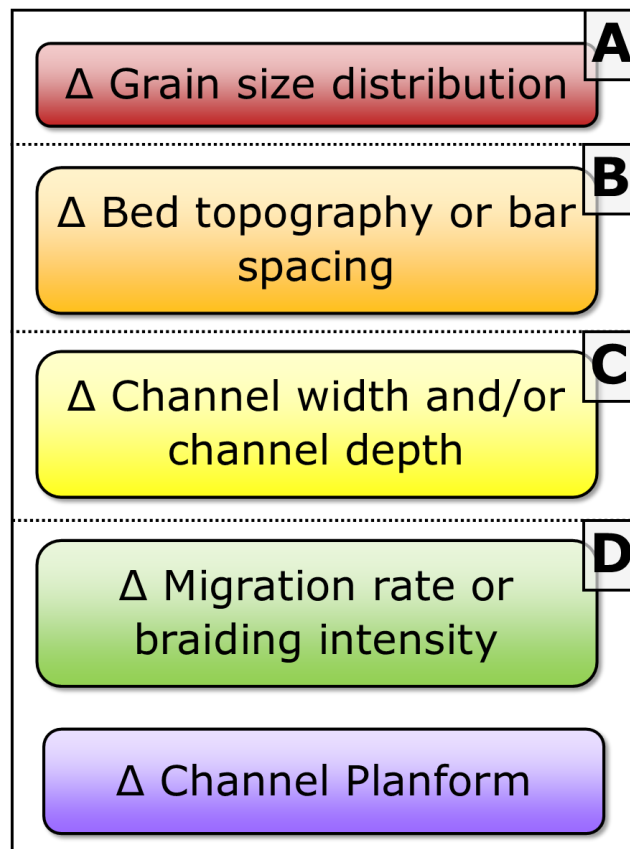


**Figure 4.3.** The types of adjustment that be observed at each scale, separated by thresholds of unknown magnitude. Letters correspond to the scales of change in Figure 4.2. Partly after Wohl et al. (2015).

At present, despite continual refinement of our understanding of channel response to increased sediment load and relative uncertainty as to the magnitude and direction of that response, what is well-established is the possible scales at which adjustment may occur (Buffington, 2012; Wohl, 2015) (Figure 4.2). Similar to the scales at which one can evaluate the fluvial system (Schumm, 1985; Montgomery and Buffington, 1998; Grabowski et al., 2014) and associated riverine habitat (Frissell et al., 1986), channel change in response to sediment load increases can occur at or across the following range of nested scales: grain-size/bed composition, bed and bar form, channel transect, and channel reach (Figure 4.2). Oftentimes, adjustments at a particular scale do not occur in isolation but rather influence or occur in concert with those at others (Buffington, 2012).

In addition to this understanding of scale, the type of potential change that may occur at each is fairly well constrained. That is, under current comprehension of channel adjustment, we have a good grasp of the range of changes that may be observed at a given scale (Figure 4.3). Thus, changes at each scale broadly correspond to, respectively: changes in grain-size distribution (Topping et al., 2018; Dean et al., 2020); changes in bed topography and/or bar spacing (Lisle, 1982; Cashman et al., 2021; Sims and Rutherford, 2021); changes in channel depth and/or channel widths (Knighton, 1989; Brooks and Brierley, 1997; Sims and Rutherford, 2017); changes in migration rate (Nanson and Hickin, 1993; Nelson and Dubé, 2016; Ahmed et al., 2019; Kemper et al., 2022); and changes in channel planform (Carson, 1984; Goswami et al., 1998; East et al., 2018). Observed adjustments may not be constrained to a single scale but occur across multiple scales (Figure 4.3). For instance, a channel may adjust at the grain size scale, bedform scale, and cross-section scale by fining, development of a plane bed, and aggradation –

a suite of changes often commonly observed in channels with substantial land-use alterations (Brooks and Brierley, 1997; Wohl, 2015).

While the scope of potential channel changes is rather well-constrained, what is comparatively less understood is the magnitude and direction of morphologic change for a given sediment influx, or, perhaps more importantly, the thresholds at which adjustments of a particular character at a particular scale segue into those of a disparate character at a different scale (e.g., when a given influx of sediment results in not simply a grain size change, but also a bedform change). Due to the significant degree of stochasticity inherent in river response and, really, fluvial system dynamics in general, part of this ambiguity in channel changes both predicted by various conceptual models (Lane, 1955; Schumm, 1969; Dust and Wohl, 2012) and observed in the field is likely unavoidable (Gaueman et al., 2005). As an additional complicating factor, potential pathways of adjustment of a river channel following a disturbance are numerous. Current theory regarding channel adjustment holds that alluvial rivers have up to ten possible adjustment mechanisms (i.e., degrees of freedom): grain size, height and wavelength of bedforms, width, depth, maximum depth, velocity, slope, meander arc length, and sinuosity (Hey, 1988; Simon and Thorne, 1996; Doyle and Harbor, 2003). In short, the range of possible responses of a river to alterations in sediment load is vast; anticipation and prediction of the specific channel response(s) to a given influx of sediment is commensurately challenging (Clark and Wilcock, 2000).

In light of this complexity, here I seek to collate the many subtleties uncovered and investigated by recent work that may lead to departures from the channel adjustments predicted by more generalized models (Table 4.1). In compiling this collection, I first look to summarize the changes observed at each scale of adjustment in order to emphasize the range of possible

responses that may follow a sediment supply increase. A firm grasp of the breadth of potential response pathways will help to improve anticipation of channel adjustment, as well as ensure that any management decisions made to mitigate those adjustments or minimize the damages that they may cause are fully informed.

**Table 4.1.** Reviewed studies of channel change in low-gradient, alluvial rivers, with categories indicating whether the work quantified influx sediment volume or grain size characteristics, the observed adjustment, and any additional notes. Bolded text indicates whether influx volumes/grain size characteristics were explicitly quantified; unbolded indicates these were mentioned or discussed, but no quantitative analysis was presented.

#	Study	Input volume	Input characteristics	Observed adjustment	Notes	Country/Region
1	Alexander and Hansen, 1986	<b>Yes</b>	<b>Yes</b>	Aggradation, widening, destroyed bed topography		USA
2	Anderson and Jaeger, 2020	No	No	Aggradation		USA
3	Andrews, 1979	Yes	No	Increases in channel cross-sectional area	Not a disturbance	USA
4	Bartley and Rutherford, 2005	<b>Yes</b>	Yes	Fining, decline in bed relief		Australia
5	Bravard, 1989	No	No	Planform change		Western Europe
6	Brooks and Brierley, 2004	No	No	Aggradation, widening.		Australia
7	Brooks and Brierly, 1997	No	Yes	Aggradation, widening		Australia
8	Burkham, 1972	No	No	Narrowing	Overfit channel	USA
9	Burroughs et al., 2009	<b>Yes</b>	<b>Yes</b>	Aggradation, widening	Dam removal	USA
10	Bushaw-Newton et al., 2002	<b>Yes</b>	<b>Yes</b>	Aggradation, bar development	Dam removal	USA
11	Cashman et al., 2021	<b>Yes</b>	<b>Yes</b>	Aggradation	Dam removal	USA
12	Cheng and Granata, 2007	<b>Yes</b>	<b>Yes</b>	Fining, aggradation.	Dam removal	USA
13	Clark and Wilcock, 2000	No	Yes	Aggradation		Caribbean

14	Coats et al., 1985	<b>Yes</b>	Yes	Widening, decreases in bed relief		USA
15	Collier et al., 1996	No	No	Aggradation	Reduction in flows but sustained sediment supply	USA
16	Collins et al., 2017	<b>Yes</b>	<b>Yes</b>	Aggradation, bed fining	Dam removal	USA
17	Collins et al., 2019	N/A	N/A	Aggradation, narrowing	Dam closure with maintained high supply	USA
18	Collins et al., 2020	<b>Yes</b>	<b>Yes</b>	Minimal change observed	Dam removal	USA
19	Czuba et al., 2012	No	<b>Yes</b>	Aggradation		USA
20	Dean et al., 2016	No	Yes	Aggradation		USA
21	Dean et al., 2020	No	Yes	Bed fining		USA
22	Doyle et al., 2003	<b>Yes</b>	<b>Yes</b>	Aggradation, bar growth	Dam removal study	USA
23	Erksine, 1994a	No	Yes	Aggradation		Australia
24	Erksine, 1994b	No	Yes	Aggradation, pool in-filling		Australia
25	Ferguson et al., 2015	Yes	Yes	Aggradation	Modeling	N/A
26	Fitzpatrick and Knox, 2000	<b>Yes</b>	Yes	Aggradation, widening.		USA
27	Florsheim and Mount, 2003	No	No	Aggradation		USA
28	Gaeuman et al., 2005	No	Yes	Grain size changes, cross section changes, avulsions, planform change		USA
29	Gilvear et al., 2000	No	No	Widening	Sediment load increase is inferred	Africa

30	Gomez et al 2001	No	No	Fining, aggradation		New Zealand
31	Goswami et al., 1999	No	No	Widening, bar growth, planform change		India
32	Grabowski and Gurnell, 2016	<b>Yes</b>	<b>Yes</b>	Narrowing		UK
33	Griffiths, 1979	<b>Yes</b>	<b>Yes</b>	Aggradation and widening		New Zealand
34	Harris and Evans, 2014	<b>Yes</b>	<b>Yes</b>	Pool infilling	Dam removal	USA
35	Heitmuller, 2014	No	No	Aggradation, Widening		USA
36	Hoffmann et al., 2009	No	No	Increased floodplain sedimentation		USA
37	Hooke et al., 1990	No	No	Aggradation		UK
38	Jacobson and Gran, 1999	No	Yes	Bar growth		USA
39	Jacobson, 1995	No	Yes	Aggradation		USA
40	James, 1991	No	No	Aggradation		USA
41	Kemper et al., 2022	<b>Yes</b>	Yes	Increased migration rates		USA
42	Kibler et al., 2011	<b>Yes</b>	<b>Yes</b>	Bed coarsening, bar growth	Dam removal	USA
43	Knighton, 1989	<b>Yes</b>	<b>Yes</b>	Fining, aggradation, widening		Australia
44	Knox, 1977	No	Yes	Narrowing		USA
45	Knox, 2006	Yes	No	Increased floodplain sedimentation		USA
46	Lecce and Pavlovsky, 2001	No	No	Increased floodplain sedimentation		USA
47	Li et al., 2007	No	No	Bar growth		China
48	Magilligan, 1985	No	Yes	Increased floodplain sedimentation, narrowing		USA

49	Miller et al., 1993	No	No	Aggradation		USA
50	Morais et al., 2016	Yes	Yes	Burial of bed topography, widening		Brazil
51	Mount et al., 2005	<b>Yes</b>	<b>Yes</b>	Widening and increased migration rates.		UK
52	Nelson and Church, 2012	<b>Yes</b>	<b>Yes</b>	Aggradation		Canada
53	Nelson and Dubé, 2016	<b>Yes</b>	<b>Yes</b>	Bar growth, aggradation and widening, increased migration rate		USA
54	Passmore et al., 1992	No	No	Aggradation		UK
55	Passmore et al., 1993	No	No	Planform change		UK
56	Pearson et al., 2011	<b>Yes</b>	<b>Yes</b>	Aggradation, widening.	Dam removal	USA
57	Pierson et al., 2011	Yes	Yes	Aggradation		USA
58	Rumsby and Macklin, 1994	No	No	Narrowing		UK
59	Rumschlag and Peck, 2007	<b>Yes</b>	<b>Yes</b>	Aggradation	Dam removal	USA
60	Salant et al., 2006	N/A	N/A	Bed infilling	Dam closure with maintained high supply	USA
61	Sarker and Thorne, 2006	<b>Yes</b>	Yes	Aggradation, widening, increase in braiding intensity		Bangladesh
62	Schumm et al., 1985	No	Yes	Planform change		USA
63	Sims and Rutherford, 2021	No	No	Bed topography buried, aggradation, widening.		Australia
64	Smith and Smith, 1984	No	<b>Yes</b>	Widening, planform change	Not a disturbance	Canada
65	Surian et al., 2009	No	Yes	Widening		Italy

66	Takagi et al., 2007	No	No	Increases in braiding intensity, widening	Bangladesh
67	Taylor et al., 2000	No	No	Increased floodplain sedimentation	UK
68	Topping et al., 2018	No	Yes	Bed fining	USA
69	Tunncliffe et al., 2018	No	Yes	Increase in migration rate	New Zealand
70	Walker et al., 2020	N/A	N/A	Narrowing	USA
71	Ward et al., 2018	Yes	Yes	Bed erasure, pool infilling, aggradation	USA

### 4.3. Changes observed across scales of adjustment

#### 4.3.1 Grain-size adjustments

Grain-size adjustments (e.g., coarsening or fining) have been suggested by many to be the component or scale at which alluvial rivers can most rapidly respond to sediment supply perturbations (Buffington, 2012; Ferguson et al., 2015) (Figure 4.3a). In the broadest sense, changes in sediment supply can drive changes in grain-size distribution as a result of the principle of conservation of mass and the interactions between sediment in transport and sediment on the bed (Topping, 2000, 2018; Cui et al., 2003; Paola and Voller, 2005; Parker, 2008; Sklar et al., 2009; Ferguson et al., 2015), as well as alterations to near-bed fluid velocities and thresholds of entrainment (Wilcock and Crowe, 2003; Venditti et al., 2010). There is also a temporal component to consider: because preferential transport of smaller grain sizes (winnowing) generally transforms (i.e., coarsens) the bed over time in the absence of inputs (Lisle et al., 1993; Rubin et al., 1998; Topping et al., 2000; Topping et al., 2018), an influx of sediment often results in an alteration of bed grain size distribution because it is essentially a resetting of the clock.

Changes to the grain-size distribution following a sediment influx have received ample attention in flume studies (e.g., Cui et al., 2003) but have also been widely observed in the field. Altered bed grain size distributions are intriguing in part because they are a potential pathway for adjustment that can leave little topographic signature; a river may accommodate a sediment influx by modifying the bed grain size distribution with very little associated obvious geomorphic change (Topping et al., 2018; Dean et al., 2020).

#### 4.3.1.1 Case studies

Adjustments in bed sediment caliber to sediment supply increases have been observed in major rivers of the Colorado Plateau. Working in the Yampa and Green River Basin of Colorado and Wyoming, USA, Topping et al. (2018) investigated the impact of an influx of sand-sized sediment from large sediment-rich floods arising in semi-arid tributaries in the late 1950's and 60's. They found that the sand was transported downstream from tributary junctions as an elongating sediment wave, resulting in bed-fining and concomitant increases in sediment transport along a 260-km long segment of the main-stem Little Snake, Yampa, and Green Rivers in the subsequent decades, with little associated morphologic change (Topping et al., 2018). Similar fining with scant observable adjustment in the macroform of the river was also found to have occurred an additional ~285 km downstream on the Green River during this time period as a result of sediment influx from several tributary watersheds (Dean et al., 2020).

Altered grain size adjustments may also occur in conjunction with larger-scale changes. Various work has identified grain size alterations in conjunction with aggradation in several diverse studies of low-gradient, alluvial streams: Alexander and Hansen (1986) and Ward et al. (2018) observed bed fining due to increased sand supply in small streams in the American Midwest, and Kibler et al. (2011) measured bed coarsening in a study of dam removal in western

Oregon, USA. Fining as one among a series of changes following a sediment influx has been similarly observed in several dam removal studies in the eastern half of the United States (Cheng and Granata, 2007; Rumschlag and Peck, 2007; Collins et al., 2017; Cashman et al., 2021).

In Australia, bed grain size alteration is often part of a suite of changes associated with drastically increased sediment supply following anthropogenic land-use alterations (land clearing, mining, etc.). Barton and Rutherford (2005) documented measurable bed fining in three southeast Australian streams exposed to land-use changes; similar bed fining has been documented elsewhere on the continent (Knighton, 1989; Sims and Rutherford, 2017), as has bed coarsening (Brooks and Brierley, 1997). Given the drastic change observed and demonstrated, it is likely that grain-size changes occurred in many of the scenarios documented in the abundant literature describing substantial channel change following the European settlement of Australia, but studies often lack details (e.g., Erksine, 1994a-b). Nearby, Gomez et al. (2001) found similar decreases in bed grain size on the Waipaoa River of New Zealand's North Island following anthropogenic land use conversion.

#### *4.3.2 Bed and bar form*

Bed and bar form adjustments (Figure 4.3b) may arise following an increase in sediment supply as a result of altered sediment transport dynamics at relatively fine scales. Pool-riffle sequences, for example, are a function of both bed grain size and the ratio of transport capacity to sediment supply (Sear, 1996; Knighton, 1998) – it follows naturally that an influx of sediment would result in alterations to this sequence. Exchange between the sediment wave formed by a discrete event and the antecedent bar morphology of the reach in question can also result in alterations to bar spacing and size via enhanced deposition and corresponding alterations to reach hydraulics (Wathen and Hoey, 1998; Wohl, 2014; Bankert and Nelson, 2018). In gravel bed

rivers, sediment supply perturbations can drive changes in mobility of the bed, which can in turn result in alterations to bed form type and organization (Venditti et al., 2017); a similar situation occurs in sand-bed streams (Allen, 1983). A sediment supply increase can also simply overwhelm the transport capacity of the river and bury antecedent bed and bar forms (Knighton, 1989). Burial of antecedent channel morphology, such as pools, riffles, and large wood can destroy the physical complexity and heterogeneous bed structure that are essential habitat for many aquatic organisms (Bond and Lake, 2005).

#### 4.3.2.1 Case studies

Similar to grain-size changes, bed and bar form adjustments in low-gradient, alluvial rivers may occur as the sole observable response or as one in a suite of changes spanning multiple spatial hierarchical scales. Changes of the former category are relatively less common but have occurred in a wide variety of settings. Li et al. (2007) found that sediment increases from heightened rates of bank failure resulted in increased growth of in-channel bars in the middle Yangtze River, China. A particularly interesting example comes from the eastern-central United States: Jacobson and Gran (1999), working in the Current River in Missouri, USA, found that the chiefly detectable response of widespread land-use alteration was an increase in gravel bar area and a change in gravel bar spacing. What makes their findings especially intriguing is the hypothesized mechanism for the locations of observed bar growth, which they believed to be primarily a function of channel network organization that resulted in accumulations of gravel in certain reaches due to variable rates of transport through the network.

Additional examples of change at the bed and bar form scale come from dam removal studies. Harris and Evans (2014) observed infilling of pools following the removal of a low-head dam on the Ottawa River in Ohio, USA, and Harrison et al. (2018) found pool filling to be the

primary response to removal in low-gradient downstream reaches of the Carmel River, California, USA. Pool infilling has also been found to be the primary response in reservoir releases that result in increased sediment supply (Rathburn and Wohl, 2003) and in reaches downstream of dams with reduced discharge but an unaltered sediment regime, a situation roughly analogous to an influx of sediment (Salant et al., 2006). Intriguingly, the direction of adjustment with regards to bed and bar form (i.e., increasing relief vs infilling), seems to be a function of preexisting conditions. Examining channel response following dam removals in Oregon, USA, Zunka et al. (2005) found that in locations with antecedent low relief (i.e., lacking bars), sediment influx increased channel relief by bar building; the converse was observed in locations with antecedent high relief (i.e., where alternate bars were present), with introduced sediments filling existing pools. Overall, this suggests that a sediment pulse can have minimally deleterious impacts on channel complexity, and may even increase morphological heterogeneity (Zunka et al., 2005).

Alterations at the bed and bar form scale can additionally occur in conjunction with larger scale adjustments or as the primary response with minor associated changes. Coats et al. (1985), for example, found pool infilling to be the major response to an influx of sediment from land sliding in the upper reaches of the San Lorenzo River, California, USA, though minor widening was also observed. Bar growth has also been found to be the more permanent change following a sediment influx, even if initially occurring in concert with aggradation (Doyle et al., 2003). Conversely, a growth in bar area has been found to be a fairly minor change accompanying major bed grain-size modification (Kibler et al., 2011) or substantial change at the cross-section scale (Goswami et al., 1999; Morais et al., 2016).

Finally, considerable change to the bed and bar forms of a river can occur as one component of a substantial alteration that spans a continuum of scales. Such change most frequently accompanies major aggradation following a large sediment influx that buries the antecedent bed and bar forms (Warner, 1984; Alexander and Hansen, 1986; Takagi et al., 2007; Cheng and Granata, 2007; Nelson and Dubé, 2016; Ward et al., 2018); often this occurs as a result of widespread land-use alteration associated with European settlement of a region (Knox, 1977; Knighton, 1989; Erksine, 1994a; Bartley and Rutherford, 2005; James and Lecce, 2013; Wohl, 2015; Sims and Rutherford, 2017, 2021). Some of the most striking examples of this combination of change again come from Australia: Bartley and Rutherford (2005), working on several streams in southeast Australia, found complete burial of antecedent bedforms by sediment slugs induced through anthropogenic land-use changes (mining, land clearing, etc.) (Figure 4.4). Additional workers determined or inferred similar smoothing of preexisting topography elsewhere in the region (Brooks et al., 2003; Hoyle et al., 2007). Overall, whether bed and bar form alterations occur as the sole observable change or in combination with others appears to be primarily a function of influx volume, especially relative to the antecedent sediment load of the river – substantial increases in sediment supply induce a series of alterations, such as those discussed in the prior sentences; relatively minor increases result in alterations to bed and bar forms alone, as reviewed in the preceding few paragraphs.



**Figure 4.4.** A) Tailings from upstream mines have buried the antecedent bed and bar forms and substantially aggraded the channel of the Ringarooma River in Tasmania, Australia. Before the sediment influx, the reach in A) was similar to the reach shown in B) which is upstream of the tributary that transports the mine tailings (Adapted with permission from Sims and Rutherford, 2017 and Bartley and Rutherford, 2005).

#### 4.3.3 Channel transect

As with changes at the prior two scales, sediment supply increases result in channel cross-section adjustments – specifically bed elevation alteration – due to the fundamental morphodynamical principle of bed sediment mass balance (Paola and Voller, 2005; Parker, 2008). Mechanistic drivers behind changes in channel width are more complex but may potentially relate to flow deflection around newly built bars increasingly directing flow towards the banks, resulting in increased fluid shear stress on the channel margins and, in turn, leading to bank erosion, destabilization, and ultimately widening (Osman and Thorne, 1988; Pizzuto, 1990; Friend, 1993; Germanowski and Schumm, 1993; Knighton, 1998; Swanson et al., 2011). Here I

use channel-cross section change to mean alterations to bed elevation and channel width (Figure 4.3c, 4.5).

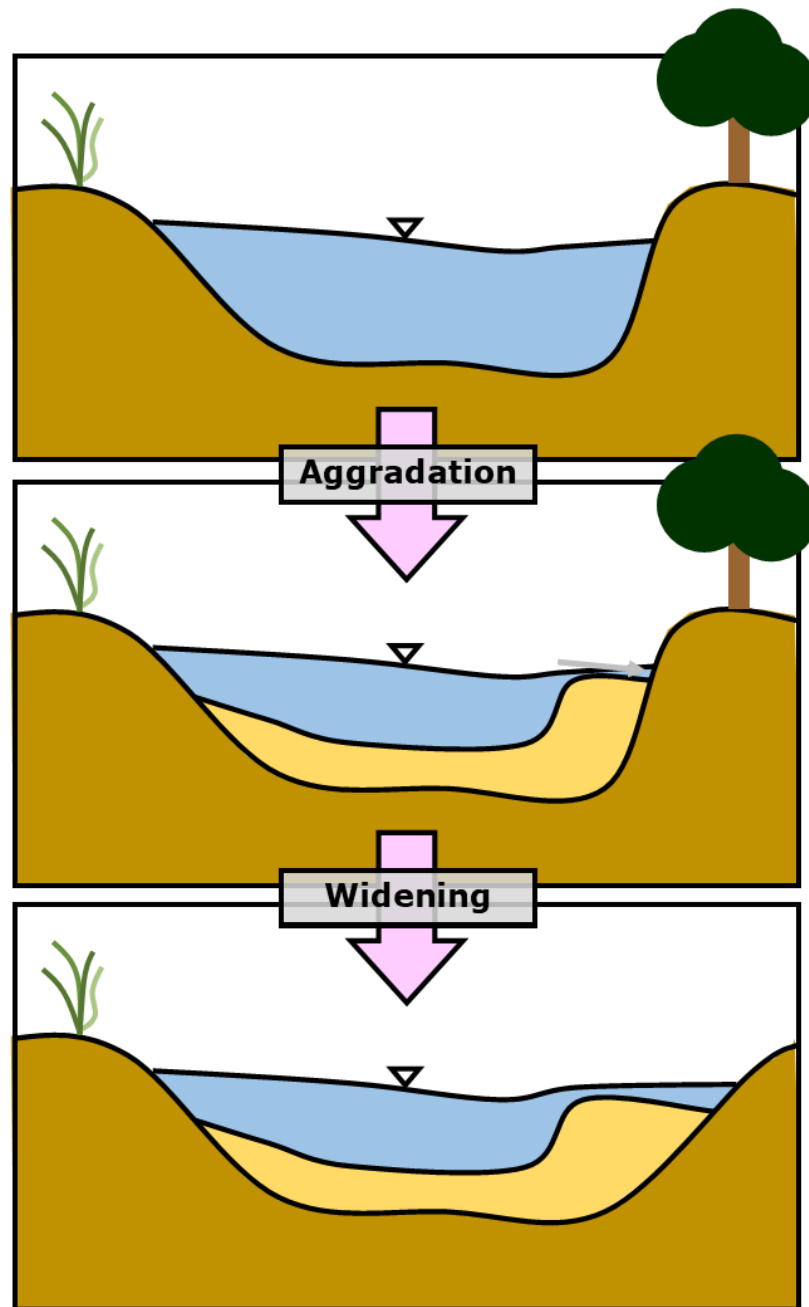


**Figure 4.5.** A potential adjustment at the channel transect scale to a hypothetical increase in sediment supply. In the situation depicted, aggradation occurs after a sediment influx that overwhelms the transport capacity of the river; flow redirection from the newly aggraded bed/formed bar directs flow (gray arrow, middle panel) into the banks, promoting widening.

#### 4.3.3.1 Case studies

Channel transect changes are potentially the most common scale of observed alteration, a condition which may partially arise as a function of their relative ease of measure. To document large-scale channel changes over a substantial spatial extent, investigation of cross-section alterations may be included in measurement approach (e.g. Griffiths, 1979); the same is true if observation of more spatially concentrated, finer-scale alterations are desired. As a result, it is often difficult to discern whether there was truly no lack of change at additionally larger or smaller scale(s) or if such change was simply not noted due to measurement ability or scope constraints. Such caveats aside, cross-section alteration in low-gradient, alluvial rivers often occurs either as the sole measured or documented change or in a suite of changes over multiple scales – the latter being the most common.

In terms of direction of change, channel aggradation is perhaps most frequently observed following a sediment influx. Examining the impact of historical mining on the morphology of Canada's Fraser River via a combination of modeling and field investigation, Nelson and Church (2012) and Ferguson et al. (2015) found that the bed of the Fraser River aggraded up to 3 m in the low-gradient lower reaches of the river. Interestingly, this aggradation was not observed further upstream in locations more proximal to the various mines, a disparity which the authors suggested was driven by several pulses effectively stalling in the low-gradient reach due a relative loss of transport capacity – a congealing of smaller pulses that alone had little observable morphological implication but together resulted in observable bed elevation change (Nelson and Church, 2012; Ferguson et al., 2015). Aggradation is a common result of many anthropogenic land-uses, with examples of increasing bed elevation in diverse low-gradient locations following logging, agricultural conversion, and urbanization (Miller et al., 1993; Erksine, 1994a-b;

Jacobson, 1995; Clark and Wilcock, 2000; Gomez et al., 2001; Heitmuller, 2014) and on streams where dam impoundment has decreased flow, but the sediment supply regime remains unaltered (Collins et al., 2019). Several interesting examples come from England (Table 4.1), where evidence for aggradation during multiple periods of land use change (i.e., the medieval period and the more recent historic period) has been found along several low-gradient, alluvial rivers, often accompanied by evidence of fining (Hooke et al., 1990; Passmore et al., 1992; Rumsby and Macklin, 1994; Taylor et al., 2000). Aggradation has additionally been observed in low-gradient reaches located downstream from mountainous tributaries that may be increasing sediment export due to climate change (Czuba et al., 2012).

Bed elevation change is additionally commonly accompanied by widening. A few particularly striking examples have been documented in Australia: Brooks and Brierley (1997) found that the lower Bega River widened by roughly 340% over a 75-year period following European settlement; widening of over 300% was similarly observed on the Ringarooma River in Tasmania (Knighton, 1989; Bartley and Rutherford, 2005). Each of these examples was accompanied by considerable (2-3 m) aggradation (Figure 4.4). Notably, channel expansion on the Bega was concentrated in the low-gradient lower reach of the river where sediment accumulated due to diminished transport capacity rather than in reaches more proximal to sediment sources, emphasizing the propensity for such reaches to respond substantially to more distal upstream influxes (Fryirs and Brierley, 2001). In an additional Australian example, Bartley and Rutherford (2005) observed relatively lesser but still substantial widening of 25% on Creighton's Creek in southeast Australia.

Substantial widening in conjunction with aggradation has also been noted following logging (Fitzpatrick and Knox, 2000) and dam removal (Doyle et al., 2003) observed in

Wisconsin, USA, as well as in other dam removal sites on various American rivers (Cheng and Granata, 2007; Rumschlag and Peck, 2007; Burroughs et al., 2009; Pearson et al., 2011; Collins et al., 2017; Cashman et al., 2021). Notably, both Burroughs et al. (2009) and Pearson et al. (2011) observed little concomitant adjustment in bed grain size; a similar lack of textural adjustment despite considerable aggradation and widening was found on the Brahmaputra–Padma–Lower Meghna river system in Bangladesh following a substantial influx of sediment from mass movements associated with the Assam earthquake (Sarker and Thorne, 2006). Together this suggests that the grain size of the sediment pulse relative to the antecedent conditions exerts a substantial control on whether larger scale adjustments are accompanied by alterations at the grain-size scale, e.g., an increased supply of sediment of similar caliber to the existing bed may result in aggradation and/or widening with little accompanying change in grain size distributions. Overall, the combination of aggradation and widening is particularly prevalent (Alexander and Hansen, 1986; Goswami et al., 1999; Takagi, et al., 2007; Surian et al., 2009; Morais et al., 2016), though it is sometimes of minor magnitude in reaches located relatively far from the source of the influx (Griffiths, 1979; Coats et al., 1985)

Conversely, channel narrowing can accompany aggradation. Knox (1977), working in the Driftless Area of Wisconsin, USA, found that bankfull dimensions of low-gradient lower reaches decreased via exorbitant overbank sedimentation in response to increased sediment supply resulting from land-use change (clearing of uplands for agriculture, etc.). He concluded that this perhaps counterintuitive response – which was directly opposite that seen in the more upstream reaches – was a result of increased suspended load material in the lower reaches, rather than bed load; the streams were unable to transport coarser-grained bed load sediment to the more distal downstream segments. Narrowing has been additionally observed in reaches where the influx

sediment is transported in the suspended fraction, leading to enhanced rates of channel margin, secondary channel, and floodplain sedimentation (Magilligan, 1985; Gaeuman et al., 2005), as well as in cases where the antecedent channel may have been overwide as a result of a prior disturbance (Burkham, 1972; Dean et al., 2016). Narrowing in this latter situation often is greatly assisted by vegetation colonization of in-channel deposits (Grabowski and Gurnell, 2016; Collins et al., 2019). Together this suggests that the grain-size of the sediment pulse, as well as the past history of the channel in question, exert a substantial influence of morphological response.

Finally, cross-section change may occur as part of a larger-scale adjustment at the channel reach or segment scale. Widening has been found to occur in conjunction with increased migration rate (Mount et al., 2005; Nelson and Dubé, 2016) or change in channel planform (Smith and Smith, 1984). Aggradation also often precludes planform change (Florsheim and Mount, 2003) or avulsion (Gaeuman et al., 2005).

#### *4.3.4 Channel reach*

Geomorphic change at the channel reach scale here refers to two related, but disparate phenomena: 1) alterations in migration rate or braiding intensity, as well as avulsion or increased overbank sedimentation (Figure 4.3d, Figure 4.6); and 2) alterations to channel planform or pattern (Figure 4.3d, 4.7).

With regards to the first phenomenon, current understanding of channel migration can be qualitatively described as a function of several hydrological and sediment supply parameters, including stream power, erosional resistance of the banks, bank height, bend geometry, and sediment supply (Nanson and Hickin, 1983; Parker et al., 2011; Eke et al., 2014). Moreover, it has been demonstrated that the mechanism by which channels migrate can be thought of in terms of two complimentary components, each with equal potential to drive migration: bank pull

(erosion of the cutbank) and bar push (deposition on the point bar). When the former dominates, erosion widens the channel, forcing deposition on the opposite bank; when the latter dominates, deposition narrows the channel, forcing erosion at the opposite bank (Parker et al., 2011).

Though it had been previously held that bar push was a more passive process, with deposition occurring in response to increased width arising from erosion at the cutbank (Nanson and Hickin, 1983), recent work has shown that both processes have equivalent capability to actively drive migration (Parker et al., 2011; Eke et al., 2014). Bar push is thus the mechanistic link between enhanced point bar deposition from a sediment influx and increased migration rates.

An increase in braiding intensity may likewise be a direct function of sediment supply: prior work has found braiding to be governed by the rate at which primary and secondary channels are infilled or “choked”, which generally results when bedforms or sediment sheets “stall” and thus occurs at an increasing rate with increased sediment supply (Germanoski and Schumm, 1993; Leddy et al., 1993; Ashworth et al., 2007; Mueller and Pitlick, 2014). Present knowledge similarly holds that avulsion frequency is a function of aggradation rate, among several other factors – enhanced aggradation can increase the relief between the channel bed and the surrounding floodplain, often resulting in a “perched” channel prone to avulsion (Everitt, 1993; Ethridge et al., 1999; Jones and Schumm, 1999; Mueller and Pitlick, 2014; Sinha et al., 2014). Increases in sediment supply, which can substantially increase aggradation, may thus potentially drive avulsion and heightened avulsion rates (Jones and Schumm, 1999; Slingerland and Smith, 1998, 2004; Phillips, 2011).

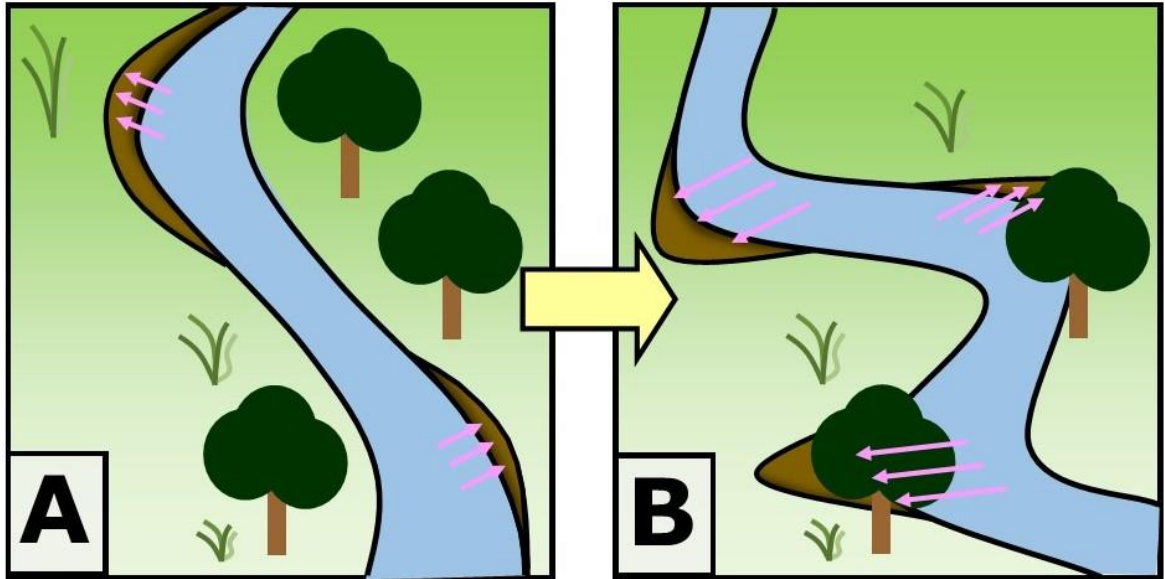


**Figure 4.6.** A depiction of a hypothetical adjustment at the channel reach scale. In the situation depicted, the river in panel A) has a migration rate defined by the pink arrows. In B) an influx of sediment has driven an increased meander rate (longer pink arrows).

With regards to the second phenomenon of channel planform change, it is generally agreed upon that channel planform is a result of a four-part interaction between the boundary conditions of flow, supplied bed material load or sediment concentration, available valley gradient, and bank material strength (Schumm, 1985; Church, 2006); braiding, for example, likely results from a high bedload supply that promotes instability and frequent channel switching (Pitlick et al., 2012). Changes in the sediment supply that alter the balance between the transporting capacity of the flow and the sediment input may result in changes to patterns of deposition, leading to a change in channel planform. Interestingly, our ability to create a working mechanistic model of planform adjustment remains limited (Candel et al., 2021).

#### 4.3.4.1 Case Studies: Changes in overbank sedimentation, migration rate, braiding intensity

Adjustments that occur at the channel reach scale, more so than those discussed prior, begin to have substantial impact on the extra-channel environment. Perhaps the adjustment with the most obvious influence on the surrounding riverine corridor is enhanced overbank

sedimentation, which often occurs following land-use alterations that increase the supply of sediment transported as suspended load. Illustrative examples of this phenomenon come from the streams of the Driftless Area in Wisconsin, USA, where Knox (1977) found that downstream channel locations, where increases in supply were finer in nature and thus capable of being transported as suspended sediment, experienced enhanced overbank sedimentation. Magilligan (1985), working in a similar area of the American Upper Midwest, found that the furthest downstream portions of the Galena River exhibited heightened rates of floodplain sedimentation due to increased fine-sediment supply from agriculture. Others working in the region observed similarly excessive sedimentation (Lecce and Pavlowski, 2001). These increased rates were still evident decades later despite nearly half a century of land conservation practices, likely due to continued erosion of stored sediment from the historical period (Knox, 2006). Comparable increases in floodplain sedimentation have been found in Europe following land-use change (Hoffman et al., 2009).

Increased sediment supply may alternately result in heightened rates of channel migration. In an investigation into channel response following a historic storm that caused widespread mass movements and an increase in sediment supply to several streams in southeastern Washington State, USA, Nelson and Dubé (2016) found enhanced lateral mobility in low-gradient depositional reaches. Similar increases in channel change rate have been observed in Wales following increased bedload sediment supply in a low-gradient stretch of the Afon Trannon River due to upstream bank erosion (Mount et al., 2005) and in the Yampa River of Colorado, USA following enhanced tributary erosion (Chapter 2; Kemper et al., 2022b). In the latter study, enhanced erosion within several tributary watersheds during the mid-19<sup>th</sup> and early 20<sup>th</sup> century led to substantially increased sediment loads on the mainstem Yampa River. This increase in

load precipitated increased channel migration rates that, in turn, resulted in concomitant construction of floodplain surfaces and establishment of cottonwood forest at a heightened clip in distal low-gradient reaches of the river. Additional results highlighting that Yampa floodplain surfaces in the low-gradient Deerlodge Park reach are comprised mainly of sediment sourced from historically eroding tributaries further emphasize the linkage between the sediment supply increase resulting from historical erosion and enhanced channel migrations rates (Chapter 3; Kemper et al., 2022a).

Additional studies that have examined migration rates of rivers with high sediment supply in relation to those with comparatively low loads – a rough analog of an increased sediment supply scenario – have found that reaches with higher sediment loads have higher rates of lateral migration (Constantine et al., 2014; Donovan et al., 2021). Modeling investigations of channel change following a diffuse, watershed-wide disturbance analogous to land-use alterations have also found that hotspots of geomorphic change in the channel network (i.e., river sections where migration rates are relatively higher than elsewhere in a similar area of the network) correspond to locations with modeled substantial sediment accumulation (Czuba and Fofoula-Georgiou, 2015).

Increased braiding intensity has also been found following sediment supply increases (Sarker and Thorne, 2006), as has avulsion – either singular or multiple. Such avulsions have been seen on the lower Duchesne River, Utah, USA, following sediment supply increases due to enhanced tributary erosion (Gaeuman et al., 2005). There, the authors determined that increases in fine sediment supply resulted in narrowing in a gravel bed reach and aggradation and avulsion in the sand bed reach. In conjunction with previously discussed studies of overbank

sedimentation, this suggests that the grain size characteristics of the sediment influx relative to antecedent conditions play a major role in determining the nature and magnitude of change.

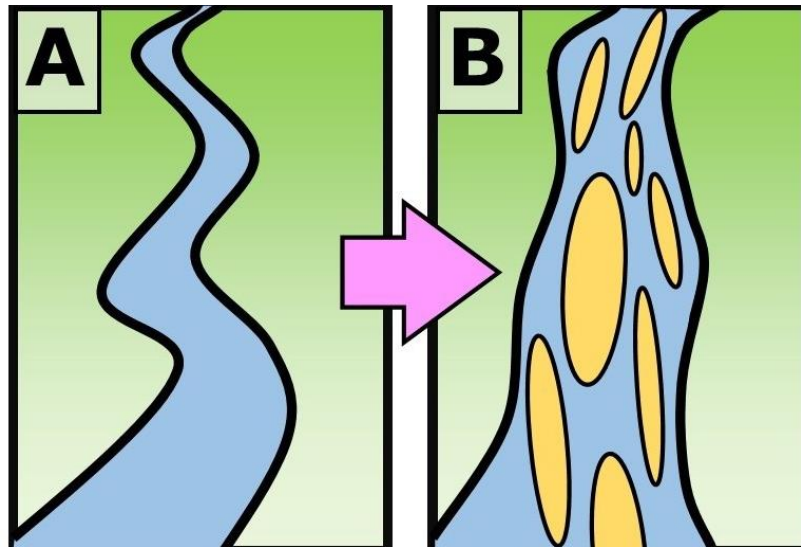


**Figure 4.7.** A potential adjustment at the channel planform scale due to a hypothetical increase in sediment supply. In the situation depicted, a substantial volume of bed-load caliber sediment has resulted in channel metamorphosis from a meandering to a braided channel.

#### 4.3.4.2 Case studies: Planform metamorphosis

Alterations to channel planform in low-gradient rivers often represent the end member scenario of a sediment influx, the classic instance of which is the metamorphosis of a meandering channel to a braided one (Schumm, 1985). Smith and Smith (1984) provide a fascinating example of the potential of a sediment supply increase to induce a planform change from meandering to braided. In a study of a reach of the Williams River that intersects the Athabasca Sand Dunes in Saskatchewan, Canada, the authors find that increases in bedload material, derived from aeolian sand deposits as the Williams River flows across a dune field, lead to a transition from single-channel planform to a thoroughly braided channel. The authors also observe substantial increases in width (5 times) and width/depth ratio (ten-fold) between the channel prior to entering the dune field and the channel in the 27 km reach that intersects the dune field. An alteration of similar nature was observed in India by Goswami et al. (1999), who

noted a change in channel planform of the Subansiri River from meandering to braided following an influx of coarse sediment as a result of increased mass movement activity during the Great Assam earthquake of 1950. A particularly interesting river planform change example comes from the same region following the same large earthquake: Sarker and Thorne (2006), working in the Brahmaputra–Padma–Lower Meghna river system of Bangladesh, found that initially anastomosing and braided channels were transformed to meandering as siltation choked secondary and tertiary channels upon the arrival of a sediment wave. Meandering persisted for some time before a secondary pulse induced braiding, followed by a return to meandering and then finally to anastomosing (Sarker and Thorne, 2006). This fairly counterintuitive response further highlights the importance of both influx characteristics (grain size) and antecedent channel conditions (in this case, planform) on observed adjustment following a sediment supply increase, as well as the complex response that may follow a sediment pulse (Sarker and Thorne, 2006).

Additional examples of channel planform metamorphosis from meandering to braided occur in historical Europe, where several studies have found evidence of reach-scale pattern adjustment following sediment supply increases resulting from a combination of anthropogenic land-use alterations (e.g., widespread land clearing) and climate (e.g., the Little Ice Age) (Bravard, 1989; Bravard et al., 1989; Passmore et al., 1993; Winterbottom, 2000). Similar alterations to channel planform have occurred in the American West following increased sediment supply due to tributary entrenchment (i.e., arroyo incision): Gaeuman et al. (2005) observed a meandering-to-braided transition on the lower Duchesne River in Utah, USA in response to arroyo entrenchment in several tributaries.

#### **4.4. Emergent knowledge: knowns and unknowns**

##### *4.4.1 Knowns: Volume-grain size interactions*

From the above summary of investigations concerning the adjustment of low-gradient, alluvial rivers to changing sediment load, several key points materialize. First, a key influence is that of the influx volume on the observed channel adjustment: influxes of substantial quantity appear to induce adjustments at larger scales. This is not in and of itself a surprising conclusion; sediment volume as a significant factor has been implicit in the earliest efforts to anticipate channel response (Lane, 1955; Schumm, 1969) and explicit in subsequent considerations (Nicholas et al., 1995; Rathburn and Wohl, 2003; Wohl and Rathburn, 2003; Buffington, 2012; Wohl, 2015; Wohl et al., 2015; Grant and Lewis, 2015; Major et al., 2017). What is clarified by this review, however, is that change can occur across a series of nested scales, and that influx volume is a partial control on how many “adjustment scale thresholds” – where one scale of change transitions into another – are crossed in response to a given influx (Figure 4.8).

Second, sediment volume alone does not strongly influence the channel adjustment response, but rather an interaction with the grain-size characteristics of the influx. The clearest examples of such an interaction are those where influxes of coarser sediment led to aggradation and widening (e.g., Knighton, 1989; Bartley and Rutherford, 2005) whereas increased supply of fine-grained sediment resulted in narrowing (e.g., Knox, 1977) despite likely similarities in influx volume due to similarities in cause (widespread land clearing). Interestingly, additional support for the controlling influence of an interaction between sediment volume and grain size comes from investigations of the roughly analogous question of tributary influence, where the impact of a given tributary on main-stem dynamics is a function of the same two variables (Knighton, 1980; Rice, 1998; Benda et al., 2004).

Thus, though recognition that grain size exerts additional control on the observed impacts of a sediment influx is not new (Wohl and Rathburn, 2003; Major et al., 2017), what is again apparent is the existence of explicit thresholds between scales of change (i.e., “adjustment thresholds”) (*sensu* Schumm, 1979; Church, 2002). More importantly, what is clear from our review is that whether adjustment threshold(s) are crossed and larger-scale adjustment(s) occur is a function of both the volume and the grain size characteristics of the pulse. Changing perspectives slightly, it is likely that there are thresholds of sediment pulse volume and grain size that precipitate adjustments to occur at more than one/additionally larger scales, which we deem “influx effectiveness thresholds” (Figure 4.8).

To that end, some insight can be provided by studies of dam removal and the associated literature, where input volumes and grain size characteristics are often expressly and carefully quantified. In a review of two decades of such investigation, Major et al. (2017) broadly concluded that if the released volume is relatively small with respect to the background sediment flux, then downstream changes may be minimal and that fine sediment, even large quantities, often results in minimal geomorphic response downstream. In contrast, they found releases of coarse-grained sediments generally cause substantial downstream geomorphic change, especially large volumes with said grain-size characteristics (i.e., those from large dams) (Grant and Lewis, 2015; Major et al., 2017). Such findings support the idea of a volume-grain size interaction exerting ample influence on observed response to a sediment influx. It is interesting to note, however, that the idea of fine-grained pulses having minimal impact is somewhat opposite to observed larger-scale channel changes following an influx of fine sediment that have been observed in more natural systems, e.g., the substantial narrowing of bankfull dimensions

observed by Knox (1977) and Magilligan (1985) due to increased floodplain sedimentation from heightened quantities of fine sediment transported in the suspended fraction.

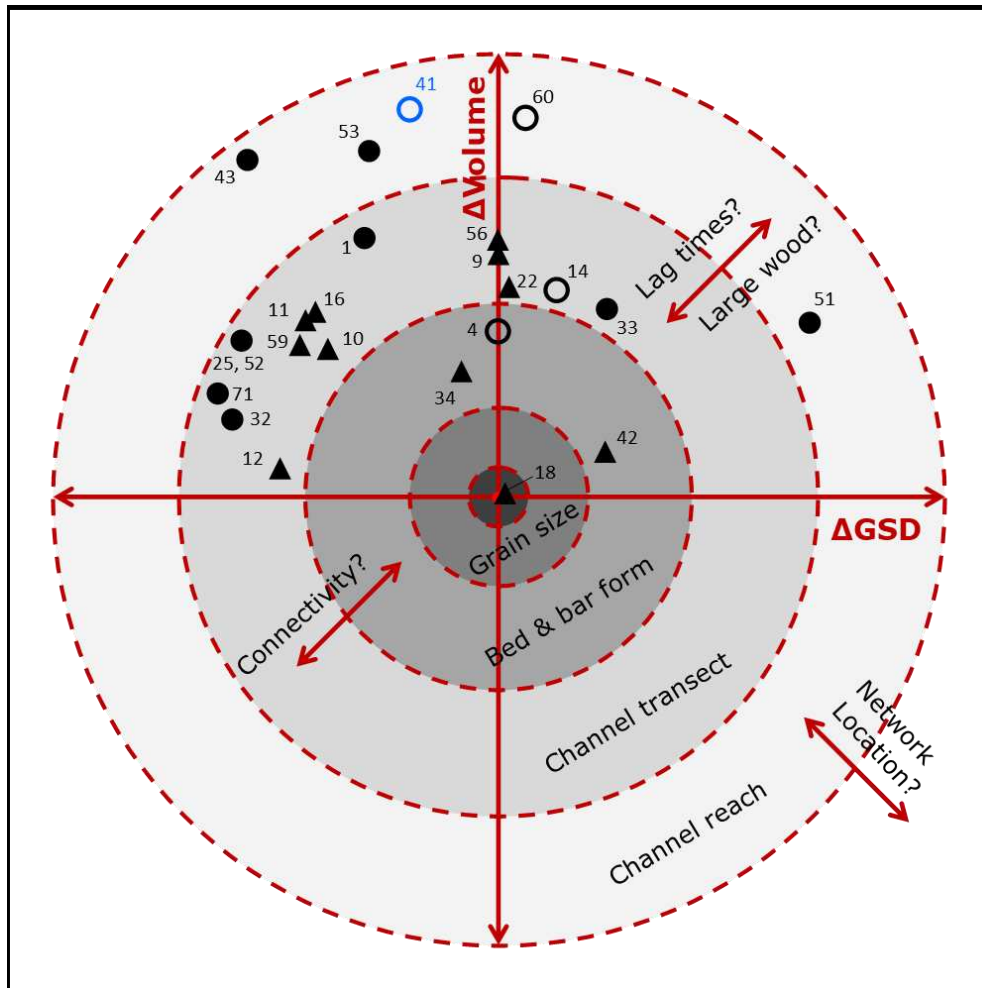


**Figure 4.8.** Conceptual framework of channel adjustment to a hypothetical increase in sediment supply. Scales of change are nested within one another (gray circles) separated by unknown adjustment thresholds (dotted lines). The influence of a given sediment influx is dependent on both influx volume relative to background sediment loads ( $\Delta$ Volume) and influx grain size distributions ( $\Delta$ GSD) relative to the antecedent bed distribution. As these parameters become (relatively) larger and larger, additional change occurs at a greater scale – the values of  $\Delta$ Volume and  $\Delta$ GSD that precipitate this increase in adjustment scale represent influx effectiveness thresholds. Location of these thresholds are altered by several additional antecedent parameters such as network location and connectivity. The extent of the role of several additional parameters in modulating the threshold location(s) is unknown (hence the question marks); they remain areas of crucial future work. Existing studies are plotted based on reported values and numbered similar to Table 4.1; triangles represent dam removal studies; filled symbols represent studies for which both parameters are expressly quantified; open symbols represent those for which one parameter is discussed. Open blue circle represents the author’s interpretation of where the historical sediment pulse from tributary arroyo incision and subsequent channel change on the Yampa River (Chapters 2 and 3) would plot.

Major et al. (2017) also found that, in addition to volume and grain-size of the freed sediment, several antecedent characteristics exerted substantial control on the observed morphological response to dam removal, including the background sediment flux, valley morphology, and geologic setting. A similar idea emerges from holistic examination of the case studies summarized above.

#### *4.4.2: Knowns: Antecedent conditions*

From my review, it is clear that antecedent conditions play a substantial role in governing channel adjustments in low-gradient rivers. By antecedent conditions here I am referring specifically to the characteristics and processes of the receiving channel prior to an increase in sediment supply (e.g., existing sediment load, dominant planform, connectivity, etc.). As is the case with volume and grain size characteristics, prior work has appreciated the importance of antecedent conditions for observed river response following sediment influx (Wohl and Rathburn, 2003; Rathburn and Wohl, 2003; Major et al., 2017). Here, however, past studies indicate that the antecedent conditions of the river exert a buffering capacity on the scale(s) of adjustment observed. In essence, the influence of the volume-grain size interaction is modulated by the antecedent conditions of the river – influxes of an equivalent volume and similar grain size characteristics will have a disparate impact on rivers with different antecedent bed grain size distributions, for example, and the number of adjustment thresholds crossed will likely be different. Here, again, the case of the Duchense River in Utah, USA, is particularly illustrative: following arroyo entrenchment in tributary watersheds, reaches of the Duchesne with antecedent gravel beds merely narrowed while sand-bedded reaches underwent meandering-to-braided transitions (Gaeuman et al., 2005). In rivers with substantial sediment supply, to use another example, the impacts of an increased sediment influx may thus be highly localized, likely

confined to a vicinity that varies proportionally to the size of the influx and potentially nearly undetectable in further downstream reaches (Major et al, 2012). The parameters of interest in the volume-grain size interaction should be quantified and considered relative to the prior conditions, as it is their relative values rather than absolute magnitudes that are most important (Figure 4.8). Influx thresholds that precipitate changes of certain scale(s) to be observed are thus heavily dependent on the preexisting state and conditions of the river.

In the same vein, it is not simply the antecedent conditions of the system at the point in time of the influx that exert control on channel response and influence influx thresholds, but also the history of past change within the system. In particular, where the system falls on an evolutionary trajectory in response to past disturbance has substantial consequence for the observed scale and character of additional change (Brewer and Lewin, 1998; Perron and Fagherazzi, 2012; Rathburn et al., 2013; Grabowski et al., 2014; James, 2015; Fryirs and Brierley, 2016; Wohl, 2018). Examples of the importance of trajectory abound – the reader is particularly referred to the aforementioned work of Burkham (1972) on the Gila River and Sarker and Thorne (2006) in Bangladesh. An additionally illustrative example comes from the American Midwest, where streams whose headwater reaches incised (and consequently increased their transport capacity and sediment delivery efficiency) early in the era of agricultural land conversion have greater overbank alluvium in their low-gradient downstream reaches than those that incised later in the period, regardless of catchment size (Faulkner, 1998).

It is further instructive to consider the importance of trajectory in terms of thresholds and proximity (*sensu* Brewer and Lewin, 1998; Hooke, 2015): a system that has responded to a previous influx of sediment by fining the bed may be near to an additional adjustment threshold, and a further influx of a relatively modest volume of fine sediment may perturb the system over

that threshold into a larger scale of change. The volume and character of sediment that precipitated such change (i.e., the influx effectiveness threshold) may be lower than would be anticipated had the history of the system not been known – influx thresholds are thus additionally a function of system trajectory.

What is particularly interesting with regards to system trajectory is evidence that many disparate sediment pulses may accumulate in low-gradient, alluvial rivers to drive change. For example, past work suggests that channel adjustment in low-gradient reaches can result from many small pulses coalescing, likely as a function of both limited transport capacity and network-scale travel time dynamics (Jacobson and Gran, 1999; Fryirs and Brierley, 2001; Nelson and Church, 2012; Czuba and Foufoula-Georgia, 2015). This suggests that disparate upstream disturbances diffuse in space and/or time (e.g., watershed-scale land use change or periodic mass movements) may have an outsized impact on low-gradient reaches that substantially outstrips their impact in more proximal channel areas.

Such importance of antecedent conditions has been illustrated by the existing concepts of river sensitivity and non-linearity, which hold that the magnitude and form of observed adjustment(s) of a given river to a disturbance are a function of several characteristics (network location, process domain, valley confinement, antecedent morphology, etc.) that control the possibility and propensity for change (Brunsdon and Thornes, 1979; Downs and Gregory, 1995; Phillips, 2006, 2009; Fryirs, 2017). Additional insight comes from the idea of geomorphic context, which emphasizes that the spatial – river geometry, as well as network and global location – and temporal – time since event, history of human alterations, etc. – setting of a given river reach has a predominant influence on the form, function, and response to disturbance of that reach (Wohl, 2018). These existing conceptualizations dovetail nicely and are congruent

with the ideas emergent from this review: that nested scales of adjustment exist separated by adjustment thresholds, that volume-grain size interactions and antecedent conditions together regulate whether (and how many) adjustment scale thresholds are crossed, and, similarly, that influx effectiveness thresholds that precipitate crossing of adjustment thresholds are dynamic functions of these parameters (Figure 4.8). Informed in part by and sharing several similarities with existing depictions of the spatial and temporal scales at which rivers adjust their components following alterations to water and sediment inputs (Knighton, 1998, fig. 5.3, p. 158, Wohl, 2014, fig 5.18, p 156, Buffington, 2012, fig 32.1), I present a conceptual model wherein influx effectiveness is presented as points that plot in the regions of observed change dependent upon the volume and grain size distribution of the influx relative to antecedent sediment loads and bed grain size, respectively. The locations of adjustment thresholds are additionally opposed (or potentially enhanced) by various additional antecedent conditions, such as network location. As relative difference in grain size distribution and influx volume increase, different adjustment thresholds are crossed, resulting in a suite of change over a continuum of scales to occur. Applying this conceptual model to the Yampa River during the period of historical channel erosion (open blue circle, Figure 4.8), it is likely that it would plot in the upper left quadrant in the region of channel reach-scale change, though  $\Delta GSD$  for this period is not quantitatively known. Notably, neither the location of the adjustment thresholds (the lines that separate adjustment scales) or the influx effectiveness thresholds are currently well constrained.

#### *4.4.3 Unknowns: Adjustment thresholds and influx effectiveness thresholds*

In similar fashion to emergent knowns, evident unknowns additionally materialize from the literature. What remains ambiguous are the thresholds at which a given sediment influx catalyzes a response at a specific scale rather than another, i.e., what thresholds of grain size and

volume with specific antecedent conditions make a given influx trigger change at an additional scale (*sensu* Métivier and Barrier, 2012; Pitlick et al., 2012). Relatedly, the locations in theoretical space of adjustment thresholds – the specific patterns by which they are related to and nested within one another – are additionally unknown. Though these unknowns have substantial codependence, the latter is of a wholly different nature than the former; a question of difficult to ascertain physical (or mechanistic) laws, its consideration is not only outside the goals of this review, but also a less useful approach for anticipating and evaluating channel change. Rather, I instead focus on the idea of influx effectiveness thresholds, which I contend to be a more practical approach to sediment influx that is conducive to management.

Determination of these thresholds requires careful quantification of several parameters: grain size distributions and volume of the sediment influx, grain size distributions of the bed, background sediment loads, and several other antecedent characteristics. As it currently stands, much of the existing literature outside of dam removal studies does not quantify these aspects in any given study (Table 4.1); of the 71 studies examined for this review, only 20 (28%) unambiguously quantified input grain size characteristics, and 11 of those were dam removal studies (Table 4.1). Additionally, only 24 studies (34%) definitively quantified influx volume, of which 11 again were dam removal studies. Future work must thus focus on explicitly determining these parameters to establish quantitative influx effectiveness thresholds. I acknowledge that such a task may be of substantial difficulty in many situations – studies may thus seek to concentrate on advantageous situations where quantification of these parameters is most straightforward (e.g., studies downstream of large construction projects or rapid response to mass movements after a storm). Undertaking to define influx effectiveness thresholds in terms of volume, grain size, and antecedent conditions is thus an area of critical future work.

## **4.5. Future work and additional considerations**

### *4.5.1 Future work to identify influx effectiveness thresholds*

To best contextualize the needs of future work with regards to defining influx effectiveness thresholds, it may be illustrative to consider a hypothetical situation in which a river manager with a local conservation district presents a series of specific questions to be answered: Will a sediment influx of two times the background sediment load cause changes at the channel transect scale? What if the sediment is finer than the bed, does that mean only fining and pool infilling will be seen? If the reach is still recovering from a flood that occurred a few years ago, will that impact the adjustments observed?

Answers to these questions are highly unlikely to be straightforward, and it is eminently probable that a complex combination of characteristics and processes together control the location of influx effectiveness thresholds. However, such complexity does not preclude working to identify the aspects of sediment influx that control whether resultant change crosses a threshold from one scale to the next. To do so, future investigations should seek to quantify both characteristics of the sediment influx – chiefly volume and grain size distributions as well as network location – and antecedent conditions – bed grain size, suspended load grain size, dominant bar forms, cross-sectional geometry, channel planform, connectivity. In addition, studies should explicitly link the influx of sediment to observed downstream change, taking care to minimize or account for the impact of other alterations as much as possible. In this manner, quantitative effectiveness thresholds of influx traits that result in changes of specific scale and nature can begin to be drawn.

Concepts and measures developed for inexpensive and relatively rapid prediction of response to dam removal may have applicability across more diverse sediment influx scenarios

and be instrumental in this regard. In particular, the  $V^*$ ,  $E^*$ , and  $S^*$  ratios may have conceptual relevance for downstream response to sediment supply increases. Importantly,  $V^*$  in this context is a measure of the ratio of total sediment volume stored in the formerly impounded reservoir (or, in a non-removal scenario, to the total influx volume) to the background average annual sediment load (Major et al., 2017), rather than a measure of pool filling (Lisle and Hilton, 1992).  $E^*$  is the ratio of the volume of sediment mobilized in the first year following removal (or, again, influx) to the background sediment load. Essentially,  $E^*$  is the ratio of the mobilized annual load to the background annual load (Grant and Lewis, 2015).  $S^*$  is the ratio of sediment supply below a dam to that above the dam (Grant et al., 2003) Each measure has been shown to have substantial utility for predicting the magnitude and duration of downstream response and distances of coarse sediment transport, respectively. Application of these straightforward, relatively simple empirically derived measures may have broad appeal in sediment influx scenarios, especially because utilization of sophisticated numerical and physical models for predicting the impacts of a given influx of sediment may be outside the scope or budget of many projects (as is the case with dam removal [Grant and Lewis, 2015]). Usage of metrics developed for stream restoration applications, such as the Capacity-Supply Ratio (CSR) – the bed material load transported through a given reach over a specific time period divided by the bed material load supplied (or transported *into*) a given reach over that same time period (Soar and Thorne, 2001) – may be additionally useful.

Of course, development of a set quantitative thresholds is unlikely – quantifying specific thresholds for even a single system, let alone widely applicable ones, remains universally acknowledged as a perennial geomorphic challenge (Hooke, 2015). For that reason, exact ones may not be found. Rather, quantification of broadly identifiable thresholds, as well as an

emphasis of the threshold approach to influx effectiveness, will enable better approximations of adjustment than what might potentially be concluded from more general conceptual models (e.g., Lane, 1955). Moreover, broadly generalizable influx effectiveness thresholds can harmonize with similar approaches such as sensitivity and connectivity (Fryirs, 2017; Khan and Fryirs, 2020; Lisenby et al., 2020) to best anticipate and predict geomorphic adjustments following a sediment supply increase. In total, I contend that influx effectiveness thresholds are a worthwhile step towards coherent incorporation of the three C's of rivers – connectivity, complexity, and context, that together govern river form and function (Wohl, 2016, 2017, 2018) – into management of low-gradient, alluvial river response to increases in sediment supply.

Finally, there are similarities here in my recommendations for future work to calls for careful documentation and quantification of inputs, alterations, and responses in order to identify causes of river degradation and best evaluate potential for restoration (e.g., Grabowski et al., 2014). I see this not as an indicator of redundancy, but rather view it as validation of identified needs; questions of similar geomorphic nature require similar knowledge to address. Along those lines, several additional considerations that could be broadly incorporated into the influx effectiveness framework.

#### *4.5.2 Additional considerations*

##### 4.5.2.1 Lag times and persistence

As is the case with many questions concerning the downstream translation and impact of sediment, lag times are likely to exert a substantial control on both the extent and timing of channel adjustment in low-gradient, alluvial channels, especially considering that such rivers or reaches of rivers are decoupled from more spatially immediate sediment sources. Multiple levels of lag time exist that are specific to and dependent on the process under consideration; together

these interact to result in a system-scale lag time that modulates the downstream delivery of sediment and occurrence of associated impacts. Lag time controls on this downstream translation can be considerable (Benda and Dunne, 1997; Wohl et al., 2019; East and Sankey, 2020), even in homogenized landscapes (Kemper et al., 2019); prior work has moreover suggested that lag times in low-gradient reaches may be additionally substantial (Czuba et al., 2012; Macklin et al., 2014; Anderson and Konrad, 2019). While temporal considerations are implicit in the influx effectiveness framework as currently conceived (e.g., the influence of network location) (Figure 4.8), lag times – in particular, non-stationarity in time and space – remain rather loosely addressed in existing investigations of channel adjustment to increased sediment supply. Future work that seeks to further unravel the influence of various levels of lag time on channel adjustment will provide expanded temporal context to the framework that is essential for expanding its capability and applicability.

The first of these facets of lag time that should ideally be considered is the lag time associated with the type of disturbance that results in a sediment supply increase, which may be more effectively considered to be a question of persistence or duration. Upstream alterations to sediment supply can occur at a variety of timescales, from short – landslides or hillslope failure during an intense rainfall event – to moderate – sediment waves from upstream logjam breakage – to long-term or persistent – changes in land-use or construction of relatively permanent structures such as dams (Hooke, 2015). It is important when anticipating future system trajectory to have a firm grasp on the timescales over which a given perturbation in upstream sediment supply may operate (Hooke, 2015). In other words, if a sediment supply increase is catalyzed by an individual event (e.g., mass movement during an intense storm), then both the timing and persistence of increased loads and the associated morphological effects will be markedly

different than if the upstream increase was driven by a longer-term process (e.g., land-use change). Future studies should seek to explicitly link considerations and measures of disturbance duration to observed downstream adjustments.

Moreover, the persistence and duration of elevated sediment yields following disturbance may be dynamic in time, often as a function of relative location in the river network. Temporally dynamic sediment delivery goes beyond questions of static connectivity presently incorporated into the framework. Olley and Wasson (2003), working in the Upper Murrumbidgee catchment of southeastern Australia, found that elevated sediment yields catalyzed by anthropogenic land-use declined at different rates in different parts of the watershed. After gullying reached maximum extension, sediment yields from headwater catchments declined by roughly a factor of 40, whereas yields for the entire watershed diminished only by a factor of two. The authors conclude that such spatial disparity suggests that geomorphic changes wrought by increased sediment loads – mainly channel widening – have resulted in increased sediment delivery efficiency through the stream network. The large volumes of sediment that entered the stream network from gullying in headwater areas during the disturbance period are thus continuing to move efficiently through the system, resulting in persistently elevated sediment loads at the whole watershed scale. A roughly analogous situation has been observed in watersheds responding to agricultural development in the Midwestern United States (Knox, 1977; Trimble 1981, 1983, 1999, 2009).

Similar results, of increasing sediment delivery ratios through time following a disturbance, have been found in several disturbed basins (Lecce, 1997). The implication of these findings is substantial: temporally elongated impacts of sediment supply increases may extend beyond simply downstream transit and storage-remobilization-associated lag times to alterations

in the connectivity of the network. Responsible prediction and management of downstream impacts may need to account for a system of substantially different character than prior to disturbance; mitigation of undesirable impacts at downstream locations may thus require a holistic approach, including treatment or restoration of (perhaps distal) upstream reaches and a firm grasp of the evolutionary trajectory of the system (James, 2015). To best incorporate and expand understanding of how dynamic connectivity impacts influx effectiveness and scales of adjustment observed, subsequent studies should seek to monitor such changes in connectivity through time and explicitly relate them to the character and the magnitude of the disturbance.

Hydrology furthermore can regulate the temporal disparity in timing of the sediment influx and timing of downstream effects. Prior work has found that aggradation following a sediment supply increase was disparate rather than constant in time; sedimentation rates were relatively high during wet years but interspersed with time periods of relatively little deposition during dry stretches (Miller et al., 1993). The degree to which the downstream impact of influxes of various size and character can be influenced by hydrological factors such as flood sequencing (Magilligan et al., 1998) remains an area of critical study; to that end, future work should look to carefully monitor the interactions between discharge and downstream adjustments with respect to the various parameters of sediment influx, e.g., whether the impacts of a large influx are largely independent of hydrology whereas the consequences of a smaller one are heavily dependent.

Further complicating anticipation or prediction of lag times is the existence of self-organized criticality (Van De Wiel and Coulthard, 2010). Broadly, self-organized criticality is a system state wherein vastly different bedload sediment yields can occur for floods of similar magnitude and character. Among various other implications, this chiefly means that fluvial

system behavior with regards to sediment load may be unpredictable (Van De Wiel and Coulthard, 2010). Such additional uncertainty in turn emphasizes the need for geomorphic impacts of heightened sediment load to be well-understood and quantified, as mitigation or prevention efforts may need to be quickly undertaken in response to a relatively unexpected sediment influx. Additional studies that quantify sediment loads and channel adjustments over longer post-disturbance time periods (>5 years) will lend insight into how rapidly a system may approach the self-organized state following disturbances of certain magnitude and character. In turn, such investigations will expand understanding of the timescales over which downstream adjustments may evolve in a broadly anticipatable vs entirely stochastic manner.

Finally, network scale modeling may present one additional path forward for examining lag times of channel adjustment (Czuba and Fofoula-Georgiou, 2015). Modelling exercises of steeper, upland watersheds have quantified grain-size associated lag times that regulate the linkages between downstream sediment loads and upstream debris flows (Murphy et al., 2019) and predicted discharges required to mobilize large volumes of flood sediment (Eidmann et al., 2022). Similar undertakings in a variety of low-gradient settings can help to expand understanding of lag time influence on influx effectiveness thresholds.

#### 4.5.2.2 Vegetation and large wood

The presence of large wood can additionally impact the downstream translation of a sediment pulse, often via attenuation of the wave due to increased in-channel storage behind logjams (Miller and Benda, 2000; Short et al., 2015; Grabowski and Wohl, 2021; Wohl et al., 2022). Though it is well-established that large wood is a notable component of sediment storage dynamics in forested watersheds (e.g., Wohl and Scott, 2017; Hinshaw et al., 2020), such a focus merits explicit future work because of the comparative paucity of studies that investigate the role

of large wood in influencing the nature and timing of downstream response to a sediment influx (Grabowski and Wohl, 2021). Future studies that seek to examine how large wood interacts with various influx parameters (volume, grain size, etc.) to influence observed adjustment will serve to expand prediction capabilities of the influx effectiveness threshold framework.

Similarly, vegetation presence on the floodplain and the resultant influence on channel stability via alterations to either physical (e.g., increases in tensile strength) or hydrological (e.g., roughness) characteristics can have an observable impact on the observed geomorphological response to a sediment supply increase (Gurnell, 1997; Diel et al., 2017); vegetation can both encourage sediment deposition, thereby altering the translation of a sediment wave through the channel network, as well as decrease (or occasionally increase) the erosive susceptibility of various surfaces, thus modifying the potential for channel change to occur in response to a sediment influx (Corenblit et al., 2007; Gurnell, 2013). Work that quantifies influx parameters and evaluates their influence on downstream adjustment in the context of carefully documented vegetation can serve to expand understanding of its influence in regulating change.

#### 4.5.2.3 Compound impacts

Determining drivers of fluvial adjustment and channel morphological changes in environments exposed to a variety of impacts – that may be either compounding or dissonant – is challenging (Morais et al., 2016); many studies have shown that such multiple alterations can complicate anticipation of change (e.g., Florsheim and Mount, 2003; Downs et al., 2013). As low-gradient, alluvial rivers often have complex and intertwined histories of land-use change and other anthropogenic alterations (e.g., wood removal, Brooks and Brierley, 2004), elucidating the impact of any single driver (such as a sediment load) on observed morphologic changes may be more difficult than in locations with a relatively straightforward or more easily deciphered

disturbance history (e.g., mountain rivers). For example, low-gradient rivers, even when exposed to increases in sediment supply, may be responding to a greater degree to different drivers, such as construction of artificial levees. Such complexity increases the difficulty in both predicting change or ascribing observed change to a particular driver. To begin to address such complexities, future studies should carefully contextualize a sediment influx of interest within the disturbance history of the catchment and suite of present stressors on channel form and function. Though this may be challenging for low gradient channels, where human settlement and other alterations (e.g., grazing) has often concentrated, investigations that explicitly account for and address these complexities will help to continue to improve the practice of anticipating and predicating channel adjustment.

#### **4.6. Conclusions**

In the above review, I summarize the extensive body of literature concerning channel adjustments to sediment supply increases in low-gradient, alluvial rivers. A collection of impressive breadth and depth, studies concerning this vital aspect of the fluvial system date back more than a century and span the globe. From early conceptualizations (Gilbert, 1917), appreciation for the dynamics that govern the translation, dissemination, and evolution of a sediment influx has grown to network-scale perspectives capable of parsing geomorphic change across extensive space and time (e.g., Fryirs, 2013; Bracken et al., 2015; Fryirs, 2017; Lisenby et al., 2018; Wohl et al., 2019). However, the anticipation and prediction of adjustments observed in response to a sediment supply increase remains challenging, despite existence of many relevant conceptual frameworks (e.g., Lane, 1955; Schumm, 1969; Dust and Wohl, 2012). The course of this review and discussion reveals emergent knowledge from an array of field,

experimental, and modeling studies that can serve to improve prediction and understanding of channel adjustments in low gradient, alluvial rivers. They are as follows:

- Channel change can occur at a series of nested scales separated by adjustment thresholds, the crossing of which results in observed adjustments at additional scale(s).
- Whether such adjustment thresholds are crossed is a function of the volume and grain size characteristics of the sediment influx, as buffered (or enhanced) by antecedent channel conditions.
- Broadly generalizable influx effectiveness thresholds exist – when such a threshold is crossed, there is a resultant change in the scales of adjustment that are likely to be observed in response.
- Future work concentrated on careful quantification of influx characteristics, antecedent conditions, and the particulars of observed change must be undertaken to establish and further quantify influx effectiveness thresholds.
- Additional considerations of the influence of lag times, compound impacts, and vegetation and large wood should be included in subsequent studies to establish a framework most capable of anticipating and predicting change in low-gradient, alluvial rivers.

What is additionally important to emphasize is that the summary here of low-gradient alluvial river response reframes consideration of potential geomorphic response as a function primarily of sediment pulse parameters that are then modulated by antecedent channel conditions. The upshot of this is a call for ample future work that seeks to explicitly link the volume and grain-size characteristics of supplied influx to the scale and extent of observed change, with careful consideration paid to antecedent conditions as a buffering influence. Such

studies will allow for the better identification of firmer thresholds of influx attributes that result in channel adjustment to occur at a certain scale rather than another. Put another way, if we begin to compile knowledge that enables us to say, for example, that a sediment pulse of sand-sized sediment with roughly a volume of 3x the annual load will likely cause no larger-scale change than minor aggradation on a preexisting meandering, sandy-bedded river reach, this will go a long way in helping managers – especially those without considerable budgets – to best anticipate and respond to coming adjustments. Research focused in this manner should additionally help to unpack the currently acknowledged exceptional complexity of channel adjustment prediction.

Finally, findings and concepts summarized in this review are not necessarily different from those that may occur in steeper, upland watersheds; indeed, the ideas I outline and present here may apply to such streams. However, given that geomorphic principles are especially beholden to setting-specific idiosyncrasies, a synthesis of past work regarding channel adjustment in explicitly low-gradient, alluvial settings is necessary to ensure that management of low-gradient rivers is based upon the most relevant science. In that sense, the generalizable framework developed here can be responsibly applied to comparable settings, though the additional peculiarities of a given site or situation can exert a complicating influence and must be considered.

#### 4.7. References

- Ahmed, J., Constantine, J.A., Dunne, T., 2019a. The role of sediment supply in the adjustment of channel sinuosity across the Amazon Basin. *Geology* 47, 807–810.  
<https://doi.org/10.1130/G46319.1>
- Ahmed, J., Constantine, J.A., Dunne, T., 2019b. The role of sediment supply in the adjustment of channel sinuosity across the Amazon Basin. *Geology* 47, 807–810.  
<https://doi.org/10.1130/G46319.1>
- Alexander, G.R., Hansen, E.A., 1986. Sand Bed Load in a Brook Trout Stream. *North American Journal of Fisheries Management* 6, 9–23. [https://doi.org/10.1577/1548-8659\(1986\)6<9:SBLIAB>2.0.CO;2](https://doi.org/10.1577/1548-8659(1986)6<9:SBLIAB>2.0.CO;2)
- Allen, J.R.L., 1983. River Bedforms: Progress and Problems, in: *Modern and Ancient Fluvial Systems*. John Wiley & Sons, Ltd, pp. 19–33.  
<https://doi.org/10.1002/9781444303773.ch2>
- Anderson, S.W., Jaeger, K.L., 2020. Coarse sediment dynamics in a large glaciated river system: Holocene history and storage dynamics dictate contemporary climate sensitivity. *GSA Bulletin* 133, 899–922. <https://doi.org/10.1130/B35530.1>
- Anderson, S.W., Konrad, C.P., 2019. Downstream-Propagating Channel Responses to Decadal-Scale Climate Variability in a Glaciated River Basin. *Journal of Geophysical Research: Earth Surface* 124, 902–919. <https://doi.org/10.1029/2018JF004734>
- Andrews, E.D., 1979. Hydraulic Adjustment of the East Fork River, Wyoming to the Supply of Sediment, in: *Adjustments of the Fluvial System*. Routledge.

- Ashmore, P., 1991. Channel Morphology and Bed Load Pulses in Braided, Gravel-Bed Streams. *Geografiska Annaler: Series A, Physical Geography* 73, 37–52. <https://doi.org/10.1080/04353676.1991.11880331>
- Ashmore, P., Church, M., 2001. The impact of climate change on rivers and river processes in Canada (No. 555), Geological Survey of Canada Bulletin.
- Ashworth, P.J., Best, J.L., Jones, M.A., 2007. The relationship between channel avulsion, flow occupancy and aggradation in braided rivers: insights from an experimental model. *Sedimentology* 54, 497–513. <https://doi.org/10.1111/j.1365-3091.2006.00845.x>
- Ashworth, P.J., Ferguson, R.I., 1986. Interrelationships of Channel Processes, Changes and Sediments in a Proglacial Braided River. *Geografiska Annaler: Series A, Physical Geography* 68, 361–371. <https://doi.org/10.1080/04353676.1986.11880186>
- Bankert, A.R., Nelson, P.A., 2018. Alternate bar dynamics in response to increases and decreases of sediment supply. *Sedimentology* 65, 702–720. <https://doi.org/10.1111/sed.12399>
- Bartley, R., Rutherford, I., 2005. Re-evaluation of the wave model as a tool for quantifying the geomorphic recovery potential of streams disturbed by sediment slugs. *Geomorphology* 64, 221–242. <https://doi.org/10.1016/j.geomorph.2004.07.005>
- Bellmore, J.R., Duda, J.J., Craig, L.S., Greene, S.L., Torgersen, C.E., Collins, M.J., Vittum, K., 2017. Status and trends of dam removal research in the United States. *WIREs Water* 4, e1164. <https://doi.org/10.1002/wat2.1164>
- Benda, L., Andras, K., Miller, D., Bigelow, P., 2004. Confluence effects in rivers: Interactions of basin scale, network geometry, and disturbance regimes. *Water Resources Research* 40. <https://doi.org/10.1029/2003WR002583>

- Benda, L., Dunne, T., 1997. Stochastic forcing of sediment routing and storage in channel networks. *Water Resources Research* 33, 2865–2880.  
<https://doi.org/10.1029/97WR02387>
- Benda, L., Veldhuisen, C., Black, J., 2003. Debris flows as agents of morphological heterogeneity at low-order confluences, Olympic Mountains, Washington. *GSA Bulletin* 115, 1110–1121. <https://doi.org/10.1130/B25265.1>
- Bertrand, M., Liébault, F., 2019. Active channel width as a proxy of sediment supply from mining sites in New Caledonia. *Earth Surface Processes and Landforms* 44, 67–76.  
<https://doi.org/10.1002/esp.4478>
- Best, J., 2019. Anthropogenic stresses on the world’s big rivers. *Nature Geosci* 12, 7–21.  
<https://doi.org/10.1038/s41561-018-0262-x>
- Bond, N.R., Lake, P.S., 2005. Ecological Restoration and Large-Scale Ecological Disturbance: The Effects of Drought on the Response by Fish to a Habitat Restoration Experiment. *Restoration Ecology* 13, 39–48. <https://doi.org/10.1111/j.1526-100X.2005.00006.x>
- Bracken, L.J., Turnbull, L., Wainwright, J., Bogaart, P., 2015. Sediment connectivity: a framework for understanding sediment transfer at multiple scales. *Earth Surface Processes and Landforms* 40, 177–188. <https://doi.org/10.1002/esp.3635>
- Brandt, S.A., 2000. Classification of geomorphological effects downstream of dams. *CATENA* 40, 375–401. [https://doi.org/10.1016/S0341-8162\(00\)00093-X](https://doi.org/10.1016/S0341-8162(00)00093-X)
- Bravard, J.-P., 1989. La tectamorphose des rivières des Alpes françaises à la fin du Moyen-Âge et à l’époque contemporaine. *BSGLg* 145–157.

- Brewer, P.A., Lewin, J., 1998. Planform cyclicality in an unstable reach: complex fluvial response to environmental change. *Earth Surface Processes and Landforms* 23, 989–1008.  
[https://doi.org/10.1002/\(SICI\)1096-9837\(1998110\)23:11<989::AID-ESP917>3.0.CO;2-4](https://doi.org/10.1002/(SICI)1096-9837(1998110)23:11<989::AID-ESP917>3.0.CO;2-4)
- Brierley, G.J., Cohen, T., Fryirs, K., Brooks, A., 1999. Post-European changes to the fluvial geomorphology of Bega catchment, Australia: implications for river ecology. *Freshwater Biology* 41, 839–848. <https://doi.org/10.1046/j.1365-2427.1999.00397.x>
- Brooks, A.P., Brierley, G.J., 2004. Framing realistic river rehabilitation targets in light of altered sediment supply and transport relationships: lessons from East Gippsland, Australia. *Geomorphology* 58, 107–123. [https://doi.org/10.1016/S0169-555X\(03\)00227-7](https://doi.org/10.1016/S0169-555X(03)00227-7)
- Brooks, A.P., Brierley, G.J., 1997. Geomorphic responses of lower Bega River to catchment disturbance, 1851–1926. *Geomorphology* 18, 291–304. [https://doi.org/10.1016/S0169-555X\(96\)00033-5](https://doi.org/10.1016/S0169-555X(96)00033-5)
- Brooks, A.P., Brierley, G.J., Millar, R.G., 2003. The long-term control of vegetation and woody debris on channel and flood-plain evolution: insights from a paired catchment study in southeastern Australia. *Geomorphology, Interactions between Wood and Channel Forms and Processes* 51, 7–29. [https://doi.org/10.1016/S0169-555X\(02\)00323-9](https://doi.org/10.1016/S0169-555X(02)00323-9)
- Brunsdon, D., Thornes, J.B., 1979. Landscape Sensitivity and Change. *Transactions of the Institute of British Geographers* 4, 463–484. <https://doi.org/10.2307/622210>
- Buffington, J.M., 2012. Changes in Channel Morphology Over Human Time Scales, in: *Gravel-Bed Rivers*. John Wiley & Sons, Ltd, pp. 433–463.  
<https://doi.org/10.1002/9781119952497.ch32>
- Bull, W.B., 1979. Threshold of critical power in streams. *GSA Bulletin* 90, 453–464.  
[https://doi.org/10.1130/0016-7606\(1979\)90<453:TOCPIS>2.0.CO;2](https://doi.org/10.1130/0016-7606(1979)90<453:TOCPIS>2.0.CO;2)

- Buraas, E.M., Renshaw, C.E., Magilligan, F.J., Dade, W.B., 2014. Impact of reach geometry on stream channel sensitivity to extreme floods. *Earth Surface Processes and Landforms* 39, 1778–1789. <https://doi.org/10.1002/esp.3562>
- Burkham, D.E., 1972. Channel changes of the Gila River in Safford Valley, Arizona, 1846-1970 (No. 655- G), Professional Paper. U.S. Govt. Print. Off.,. <https://doi.org/10.3133/pp655G>
- Burroughs, B.A., Hayes, D.B., Klomp, K.D., Hansen, J.F., Mistak, J., 2009. Effects of Stronach Dam removal on fluvial geomorphology in the Pine River, Michigan, United States. *Geomorphology* 110, 96–107. <https://doi.org/10.1016/j.geomorph.2009.03.019>
- Bushaw-Newton, K.L., Hart, D.D., Pizzuto, J.E., Thomson, J.R., Egan, J., Ashley, J.T., Johnson, T.E., Horwitz, R.J., Keeley, M., Lawrence, J., Charles, D., Gatenby, C., Kreeger, D.A., Nightengale, T., Thomas, R.L., Velinsky, D.J., 2002. An Integrative Approach Towards Understanding Ecological Responses to Dam Removal: The Manatawny Creek Study. *JAWRA Journal of the American Water Resources Association* 38, 1581–1599. <https://doi.org/10.1111/j.1752-1688.2002.tb04366.x>
- Candel, J., Kleinhans, M., Makaske, B., Wallinga, J., 2021. Predicting river channel pattern based on stream power, bed material and bank strength. *Progress in Physical Geography: Earth and Environment* 45, 253–278. <https://doi.org/10.1177/0309133320948831>
- Carson, M.A., 1984. The meandering-braided river threshold: A reappraisal. *Journal of Hydrology* 73, 315–334. [https://doi.org/10.1016/0022-1694\(84\)90006-4](https://doi.org/10.1016/0022-1694(84)90006-4)
- Cashman, M.J., Gellis, A.C., Boyd, E., Collins, M.J., Anderson, S.W., McFarland, B.D., Ryan, A.M., 2021. Channel response to a dam-removal sediment pulse captured at high-temporal resolution using routine gage data. *Earth Surface Processes and Landforms* 46, 1145–1159. <https://doi.org/10.1002/esp.5083>

- Chang, H.H., 1986. River Channel Changes: Adjustments of Equilibrium. *Journal of Hydraulic Engineering* 112, 43–55. [https://doi.org/10.1061/\(ASCE\)0733-9429\(1986\)112:1\(43\)](https://doi.org/10.1061/(ASCE)0733-9429(1986)112:1(43))
- Cheng, F., Granata, T., 2007. Sediment transport and channel adjustments associated with dam removal: Field observations. *Water Resources Research* 43. <https://doi.org/10.1029/2005WR004271>
- Chin, A., 2006. Urban transformation of river landscapes in a global context. *Geomorphology, 37<sup>th</sup> Binghamton Geomorphology Symposium* 79, 460–487. <https://doi.org/10.1016/j.geomorph.2006.06.033>
- Church, M., 2010. The trajectory of geomorphology. *Progress in Physical Geography: Earth and Environment* 34, 265–286. <https://doi.org/10.1177/0309133310363992>
- Church, M., 2002. Geomorphic thresholds in riverine landscapes. *Freshwater Biology* 47, 541–557. <https://doi.org/10.1046/j.1365-2427.2002.00919.x>
- Church, M., Ferguson, R.I., 2015. Morphodynamics: Rivers beyond steady state. *Water Resources Research* 51, 1883–1897. <https://doi.org/10.1002/2014WR016862>
- Clark, J.J., Wilcock, P.R., 2000. Effects of land-use change on channel morphology in northeastern Puerto Rico. *GSA Bulletin* 112, 1763–1777. [https://doi.org/10.1130/0016-7606\(2000\)112<1763:EOLUCO>2.0.CO;2](https://doi.org/10.1130/0016-7606(2000)112<1763:EOLUCO>2.0.CO;2)
- Coats, R., Collins, L., Florsheim, J., Kaufman, D., 1985. Channel change, sediment transport, and fish habitat in a coastal stream: Effects of an extreme event. *Environmental Management* 9, 35–48. <https://doi.org/10.1007/BF01871443>
- Collier, M., Webb, R.H., Schmidt, J.C., 1996. Dams and Rivers: A Primer on the Downstream Effects of Dams (No. 1126), Circular. U.S. Geological Survey. <https://doi.org/10.3133/cir1126>

- Collins, B.D., Dickerson-Lange, S.E., Schanz, S., Harrington, S., 2019. Differentiating the effects of logging, river engineering, and hydropower dams on flooding in the Skokomish River, Washington, USA. *Geomorphology* 332, 138–156. <https://doi.org/10.1016/j.geomorph.2019.01.021>
- Collins, M.J., Kelley, A.R., Lombard, P.J., 2020. River channel response to dam removals on the lower Penobscot River, Maine, United States. *River Research and Applications* 36, 1778–1789. <https://doi.org/10.1002/rra.3700>
- Collins, M.J., Snyder, N.P., Boardman, G., Banks, W.S.L., Andrews, M., Baker, M.E., Conlon, M., Gellis, A., McClain, S., Miller, A., Wilcock, P., 2017. Channel response to sediment release: insights from a paired analysis of dam removal. *Earth Surface Processes and Landforms* 42, 1636–1651. <https://doi.org/10.1002/esp.4108>
- Constantine, J.A., Dunne, T., Ahmed, J., Legleiter, C., Lazarus, E.D., 2014. Sediment supply as a driver of river meandering and floodplain evolution in the Amazon Basin. *Nature Geoscience* 7, 899–903. <https://doi.org/10.1038/ngeo2282>
- Cui, Y., Parker, G., Lisle, T.E., Gott, J., Hansler-Ball, M.E., Pizzuto, J.E., Allmendinger, N.E., Reed, J.M., 2003. Sediment pulses in mountain rivers: 1. Experiments. *Water Resources Research* 39. <https://doi.org/10.1029/2002WR001803>
- Czuba, J.A., Czuba, C.R., Magirl, C.S., Voss, F.D., 2010. Channel-conveyance capacity, channel change, and sediment transport in the lower Puyallup, White, and Carbon Rivers, western Washington (No. 2010–5240), Scientific Investigations Report. U.S. Geological Survey. <https://doi.org/10.3133/sir20105240>

- Czuba, J.A., Foufoula-Georgiou, E., 2015. Dynamic connectivity in a fluvial network for identifying hotspots of geomorphic change. *Water Resources Research* 51, 1401–1421.  
<https://doi.org/10.1002/2014WR016139>
- Czuba, J.A., Magirl, C.S., Czuba, C.R., Curran, C.A., Johnson, K.H., Olsen, T.D., Kimball, H.K., Gish, C.C., 2012. Geomorphic analysis of the river response to sedimentation downstream of Mount Rainier, Washington (No. 2012–1242), Open-File Report. U.S. Department of the Interior, U.S. Geological Survey.
- Darby, S.E., Thorne, C.R., 1996a. Modelling the Sensitivity of Channel Adjustments in Destabilized Sand-Bed Rivers. *Earth Surface Processes and Landforms* 21, 1109–1125.  
[https://doi.org/10.1002/\(SICI\)1096-9837\(199612\)21:12<1109::AID-ESP655>3.0.CO;2-F](https://doi.org/10.1002/(SICI)1096-9837(199612)21:12<1109::AID-ESP655>3.0.CO;2-F)
- Darby, S.E., Thorne, C.R., 1996b. Modelling the Sensitivity of Channel Adjustments in Destabilized Sand-Bed Rivers. *Earth Surface Processes and Landforms* 21, 1109–1125.  
[https://doi.org/10.1002/\(SICI\)1096-9837\(199612\)21:12<1109::AID-ESP655>3.0.CO;2-F](https://doi.org/10.1002/(SICI)1096-9837(199612)21:12<1109::AID-ESP655>3.0.CO;2-F)
- Davis, W.M., 1902. Baselevel, Grade and Peneplain. *The Journal of Geology* 10, 77–111.  
<https://doi.org/10.1086/620982>
- Dean, D.J., Topping, D.J., Grams, P.E., Walker, A.E., Schmidt, J.C., 2020. Does Channel Narrowing by Floodplain Growth Necessarily Indicate Sediment Surplus? Lessons From Sediment Transport Analyses in the Green and Colorado Rivers, Canyonlands, Utah. *Journal of Geophysical Research: Earth Surface* 125, e2019JF005414.  
<https://doi.org/10.1029/2019JF005414>
- Dean, D.J., Topping, D.J., Schmidt, J.C., Griffiths, R.E., Sabol, T.A., 2016. Sediment supply versus local hydraulic controls on sediment transport and storage in a river with large

- sediment loads. *Journal of Geophysical Research: Earth Surface* 121, 82–110.  
<https://doi.org/10.1002/2015JF003436>
- Diehl, R.M., Wilcox, A.C., Stella, J.C., Kui, L., Sklar, L.S., Lightbody, A., 2017. Fluvial sediment supply and pioneer woody seedlings as a control on bar-surface topography. *Earth Surface Processes and Landforms* 42, 724–734. <https://doi.org/10.1002/esp.4017>
- Downs, P.W., Dusterhoff, S.R., Sears, W.A., 2013. Reach-scale channel sensitivity to multiple human activities and natural events: Lower Santa Clara River, California, USA. *Geomorphology* 189, 121–134. <https://doi.org/10.1016/j.geomorph.2013.01.023>
- Downs, P.W., Gregory, K.J., 1995. Approaches to River Channel Sensitivity\*. *The Professional Geographer* 47, 168–175. <https://doi.org/10.1111/j.0033-0124.1995.00168.x>
- Doyle, M.W., Harbor, J.M., 2003. Modelling the effect of form and profile adjustments on channel equilibrium timescales. *Earth Surface Processes and Landforms* 28, 1271–1287.  
<https://doi.org/10.1002/esp.516>
- Doyle, M.W., Stanley, E.H., Harbor, J.M., 2003. Channel adjustments following two dam removals in Wisconsin. *Water Resources Research* 39.  
<https://doi.org/10.1029/2002WR001714>
- Dust, D., Wohl, E., 2012. Conceptual model for complex river responses using an expanded Lane’s relation. *Geomorphology* 139–140, 109–121.  
<https://doi.org/10.1016/j.geomorph.2011.10.008>
- East, A.E., Logan, J.B., Mastin, M.C., Ritchie, A.C., Bountry, J.A., Magirl, C.S., Sankey, J.B., 2018. Geomorphic Evolution of a Gravel-Bed River Under Sediment-Starved Versus Sediment-Rich Conditions: River Response to the World’s Largest Dam Removal.

Journal of Geophysical Research: Earth Surface 123, 3338–3369.

<https://doi.org/10.1029/2018JF004703>

East, A.E., Sankey, J.B., 2020. Geomorphic and Sedimentary Effects of Modern Climate Change: Current and Anticipated Future Conditions in the Western United States.

Reviews of Geophysics 58, e2019RG000692. <https://doi.org/10.1029/2019RG000692>

Eaton, B.C., Andrews, C.A.E., Giles, T.R., Phillips, J.C., 2010. Wildfire, morphologic change and bed material transport at Fishtrap Creek, British Columbia. *Geomorphology* 118, 409–424. <https://doi.org/10.1016/j.geomorph.2010.02.008>

Eidmann, J.S., Rathburn, S.L., White, D., Huson, K., 2022. Channel Response and Reservoir Delta Evolution From Source to Sink Following an Extreme Flood. *Journal of Geophysical Research: Earth Surface* 127, e2020JF006013.

<https://doi.org/10.1029/2020JF006013>

Eke, E., Parker, G., Shimizu, Y., 2014. Numerical modeling of erosional and depositional bank processes in migrating river bends with self-formed width: Morphodynamics of bar push and bank pull. *Journal of Geophysical Research: Earth Surface* 119, 1455–1483.

<https://doi.org/10.1002/2013JF003020>

Erskine, W., 1994. River responses to accelerated soil erosion in the Glenelg River Catchment, Victoria. *Australian Journal of Soil and Water Conservation* 7, 39–47.

Erskine, W.D., 1994. Sand slugs generated by catastrophic floods on the Goulburn River, New South Wales (Variability in Stream Erosion and Sediment Transport), Proceedings of the Canberra Symposium. IAHS Publications.

Ethridge, F.G., Skelly, R.L., Bristow, C.S., 1999. Avulsion and Crevassing in the Sandy, Braided Niobrara River: Complex Response to Base-Level Rise and Aggradation, in: *Fluvial*

Sedimentology VI. John Wiley & Sons, Ltd, pp. 179–191.

<https://doi.org/10.1002/9781444304213.ch14>

Faulkner, D.J., 1998. Spatially Variable Historical Alluviation and Channel Incision in West-Central Wisconsin. *Annals of the Association of American Geographers* 88, 666–685.

<https://doi.org/10.1111/0004-5608.00117>

Ferguson, R.I., Church, M., Rennie, C.D., Venditti, J.G., 2015. Reconstructing a sediment pulse: Modeling the effect of placer mining on Fraser River, Canada. *Journal of Geophysical Research: Earth Surface* 120, 1436–1454. <https://doi.org/10.1002/2015JF003491>

Fitzpatrick, F.A., Knox, J.C., 2000. Spatial and Temporal Sensitivity of Hydrogeomorphic Response and Recovery to Deforestation, Agriculture, and Floods. *Physical Geography* 21, 89–108. <https://doi.org/10.1080/02723646.2000.10642701>

Florsheim, J.L., Mount, J.F., 2003a. Changes in lowland floodplain sedimentation processes: pre-disturbance to post-rehabilitation, Cosumnes River, CA. *Geomorphology, Floodplains: environment and process* 56, 305–323. [https://doi.org/10.1016/S0169-555X\(03\)00158-2](https://doi.org/10.1016/S0169-555X(03)00158-2)

Florsheim, J.L., Mount, J.F., 2003b. Changes in lowland floodplain sedimentation processes: pre-disturbance to post-rehabilitation, Cosumnes River, CA. *Geomorphology, Floodplains: environment and process* 56, 305–323. [https://doi.org/10.1016/S0169-555X\(03\)00158-2](https://doi.org/10.1016/S0169-555X(03)00158-2)

Foley, J.A., Ramankutty, N., Brauman, K.A., Cassidy, E.S., Gerber, J.S., Johnston, M., Mueller, N.D., O’Connell, C., Ray, D.K., West, P.C., Balzer, C., Bennett, E.M., Carpenter, S.R., Hill, J., Monfreda, C., Polasky, S., Rockström, J., Sheehan, J., Siebert, S., Tilman, D., Zaks, D.P.M., 2011. Solutions for a cultivated planet. *Nature* 478, 337–342.

<https://doi.org/10.1038/nature10452>

- Friend, P.F., 1993. Control of river morphology by the grain-size of sediment supplied. *Sedimentary Geology* 85, 171–177. [https://doi.org/10.1016/0037-0738\(93\)90081-F](https://doi.org/10.1016/0037-0738(93)90081-F)
- Frissell, C.A., Liss, W.J., Warren, C.E., Hurley, M.D., 1986. A hierarchical framework for stream habitat classification: Viewing streams in a watershed context. *Environmental Management* 10, 199–214. <https://doi.org/10.1007/BF01867358>
- Fryirs, K., 2013. (Dis)Connectivity in catchment sediment cascades: a fresh look at the sediment delivery problem. *Earth Surface Processes and Landforms* 38, 30–46. <https://doi.org/10.1002/esp.3242>
- Fryirs, K., Brierley, G.J., 2001. Variability in sediment delivery and storage along river courses in Bega catchment, NSW, Australia: implications for geomorphic river recovery. *Geomorphology* 38, 237–265. [https://doi.org/10.1016/S0169-555X\(00\)00093-3](https://doi.org/10.1016/S0169-555X(00)00093-3)
- Fryirs, K.A., 2017. River sensitivity: a lost foundation concept in fluvial geomorphology. *Earth Surface Processes and Landforms* 42, 55–70. <https://doi.org/10.1002/esp.3940>
- Fryirs, K.A., Brierley, G.J., 2016. Assessing the geomorphic recovery potential of rivers: forecasting future trajectories of adjustment for use in management. *WIREs Water* 3, 727–748. <https://doi.org/10.1002/wat2.1158>
- Fryirs, K.A., Brierley, G.J., Hancock, F., Cohen, T.J., Brooks, A.P., Reinfelds, I., Cook, N., Raine, A., 2018. Tracking geomorphic recovery in process-based river management. *Land Degradation & Development* 29, 3221–3244. <https://doi.org/10.1002/ldr.2984>
- Fryirs, K.A., Brierley, G.J., Preston, N.J., Kasai, M., 2007. Buffers, barriers and blankets: The (dis)connectivity of catchment-scale sediment cascades. *CATENA* 70, 49–67. <https://doi.org/10.1016/j.catena.2006.07.007>

- Fryirs, K.A., Wheaton, J.M., Brierley, G.J., 2016. An approach for measuring confinement and assessing the influence of valley setting on river forms and processes. *Earth Surface Processes and Landforms* 41, 701–710. <https://doi.org/10.1002/esp.3893>
- Gaeuman, D., Schmidt, J.C., Wilcock, P.R., 2005. Complex channel responses to changes in stream flow and sediment supply on the lower Duchesne River, Utah. *Geomorphology* 64, 185–206. <https://doi.org/10.1016/j.geomorph.2004.06.007>
- Gellis, A., Hereford, R., Schumm, S.A., Hayes, B.R., 1991. Channel evolution and hydrologic variations in the Colorado River basin: Factors influencing sediment and salt loads. *Journal of Hydrology* 124, 317–344. [https://doi.org/10.1016/0022-1694\(91\)90022-A](https://doi.org/10.1016/0022-1694(91)90022-A)
- Germanoski, D., Schumm, S.A., 1993. Changes in Braided River Morphology Resulting from Aggradation and Degradation. *The Journal of Geology* 101, 451–466. <https://doi.org/10.1086/648239>
- Gilbert, G.K., 1917. Hydraulic-mining debris in the Sierra Nevada. Professional Paper. <https://doi.org/10.3133/pp105>
- Gilvear, D., Winterbottom, S., Sickingabula, H., 2000. Character of channel planform change and meander development: Luangwa River, Zambia. *Earth Surface Processes and Landforms* 25, 421–436. [https://doi.org/10.1002/\(SICI\)1096-9837\(200004\)25:4<421::AID-ESP65>3.0.CO;2-Q](https://doi.org/10.1002/(SICI)1096-9837(200004)25:4<421::AID-ESP65>3.0.CO;2-Q)
- Gomez, B., Rosser, B.J., Peacock, D.H., Hicks, D.M., Palmer, J.A., 2001. Downstream fining in a rapidly aggrading gravel bed river. *Water Resources Research* 37, 1813–1823. <https://doi.org/10.1029/2001WR900007>
- Goswami, U., Sarma, J.N., Patgiri, A.D., 1999. River channel changes of the Subansiri in Assam, India. *Geomorphology* 30, 227–244. [https://doi.org/10.1016/S0169-555X\(99\)00032-X](https://doi.org/10.1016/S0169-555X(99)00032-X)

- Goudie, A.S., 2006a. Global warming and fluvial geomorphology. *Geomorphology*, 37<sup>th</sup> Binghamton Geomorphology Symposium 79, 384–394.  
<https://doi.org/10.1016/j.geomorph.2006.06.023>
- Goudie, A.S., 2006b. Global warming and fluvial geomorphology. *Geomorphology*, 37<sup>th</sup> Binghamton Geomorphology Symposium 79, 384–394.  
<https://doi.org/10.1016/j.geomorph.2006.06.023>
- Grabowski, J., Wohl, E., 2021. Logjam attenuation of annual sediment waves in eolian-fluvial environments, North Park, Colorado, USA. *Geomorphology* 375, 107494.  
<https://doi.org/10.1016/j.geomorph.2020.107494>
- Grabowski, R.C., Gurnell, A.M., 2016. Diagnosing problems of fine sediment delivery and transfer in a lowland catchment. *Aquat Sci* 78, 95–106. <https://doi.org/10.1007/s00027-015-0426-3>
- Grabowski, R.C., Surian, N., Gurnell, A.M., 2014. Characterizing geomorphological change to support sustainable river restoration and management. *WIREs Water* 1, 483–512.  
<https://doi.org/10.1002/wat2.1037>
- Gran, K.B., Czuba, J.A., 2017. Sediment pulse evolution and the role of network structure. *Geomorphology, Connectivity in Geomorphology from Binghamton 2016* 277, 17–30.  
<https://doi.org/10.1016/j.geomorph.2015.12.015>
- Grant, G.E., Lewis, S.L., 2015. The Remains of the Dam: What Have We Learned from 15 Years of US Dam Removals?, in: Lollino, G., Arattano, M., Rinaldi, M., Giustolisi, O., Marechal, J.-C., Grant, G.E. (Eds.), *Engineering Geology for Society and Territory – Volume 3*. Springer International Publishing, Cham, pp. 31–35.  
[https://doi.org/10.1007/978-3-319-09054-2\\_7](https://doi.org/10.1007/978-3-319-09054-2_7)

- Grant, G.E., Schmidt, J.C., Lewis, S.L., 2003. A Geological Framework for Interpreting Downstream Effects of Dams on Rivers, in: O'Connor, J.E., Grant, G.E. (Eds.), *Water Science and Application*. American Geophysical Union, Washington, D. C., pp. 203–219. <https://doi.org/10.1029/007WS13>
- Gregory, K.J., 2006. The human role in changing river channels. *Geomorphology*, 37<sup>th</sup> Binghamton Geomorphology Symposium 79, 172–191. <https://doi.org/10.1016/j.geomorph.2006.06.018>
- Griffiths, G.A., 1981. Stable-channel design in gravel-bed rivers. *Journal of Hydrology* 52, 291–305. [https://doi.org/10.1016/0022-1694\(81\)90176-1](https://doi.org/10.1016/0022-1694(81)90176-1)
- Griffiths, G.A., 1979. Recent sedimentation history of the Waimakariri River, New Zealand. *Journal of Hydrology (New Zealand)* 18, 6–28.
- Gurnell, A., 1997. The Hydrological and Geomorphological Significance of Forested Floodplains. *Global Ecology and Biogeography Letters* 6, 219–229. <https://doi.org/10.2307/2997735>
- Harris, N., Evans, J.E., 2014. Channel Evolution of Sandy Reservoir Sediments Following Low-Head Dam Removal, Ottawa River, Northwestern Ohio, U.S.A. *Open Journal of Modern Hydrology* 2014. <https://doi.org/10.4236/ojmh.2014.42004>
- Harrison, L.R., East, A.E., Smith, D.P., Logan, J.B., Bond, R.M., Nicol, C.L., Williams, T.H., Boughton, D.A., Chow, K., Luna, L., 2018. River response to large-dam removal in a Mediterranean hydroclimatic setting: Carmel River, California, USA. *Earth Surface Processes and Landforms* 43, 3009–3021. <https://doi.org/10.1002/esp.4464>

- Harvey, A.M., 2002. Effective timescales of coupling within fluvial systems. *Geomorphology, Geomorphology on Large Rivers* 44, 175–201. [https://doi.org/10.1016/S0169-555X\(01\)00174-X](https://doi.org/10.1016/S0169-555X(01)00174-X)
- Hassan, M.A., Zimmermann, A.E., 2012. Channel Response and Recovery to Changes in Sediment Supply, in: Church, M., Biron, P.M., Roy, A.G. (Eds.), *Gravel-Bed Rivers*. John Wiley & Sons, Ltd, pp. 464–473. <https://doi.org/10.1002/9781119952497.ch33>
- Heitmuller, F.T., 2014. Channel adjustments to historical disturbances along the lower Brazos and Sabine Rivers, south-central USA. *Geomorphology* 204, 382–398. <https://doi.org/10.1016/j.geomorph.2013.08.020>
- Hey, R.D., 1988. Mathematical models of channel morphology, in: *Modelling Geomorphological Systems*. John Wiley & Sons, New York, pp. 99–125.
- Hey, R.D., Thorne, C.R., 1986. Stable Channels with Mobile Gravel Beds. *Journal of Hydraulic Engineering* 112, 671–689. [https://doi.org/10.1061/\(ASCE\)0733-9429\(1986\)112:8\(671\)](https://doi.org/10.1061/(ASCE)0733-9429(1986)112:8(671))
- Hickin, E.J., 1983. River Channel Changes: Retrospect and Prospect, in: *Modern and Ancient Fluvial Systems*. John Wiley & Sons, Ltd, pp. 59–83. <https://doi.org/10.1002/9781444303773.ch5>
- Hinshaw, S., Wohl, E., Davis, D., 2020. The effects of longitudinal variations in valley geometry and wood load on flood response. *Earth Surface Processes and Landforms* 45, 2927–2939. <https://doi.org/10.1002/esp.4940>
- Hoffman, D.F., Gabet, E.J., 2007. Effects of sediment pulses on channel morphology in a gravel-bed river. *GSA Bulletin* 119, 116–125. <https://doi.org/10.1130/B25982.1>

- Hoffmann, T., Erkens, G., Gerlach, R., Klostermann, J., Lang, A., 2009. Trends and controls of Holocene floodplain sedimentation in the Rhine catchment. *CATENA, Sediment Dynamics* 77, 96–106. <https://doi.org/10.1016/j.catena.2008.09.002>
- Hooke, J., 2003. Coarse sediment connectivity in river channel systems: a conceptual framework and methodology. *Geomorphology* 56, 79–94. [https://doi.org/10.1016/S0169-555X\(03\)00047-3](https://doi.org/10.1016/S0169-555X(03)00047-3)
- Hooke, J.M., 2015. Variations in flood magnitude–effect relations and the implications for flood risk assessment and river management. *Geomorphology, Emerging geomorphic approaches to guide river management practices* 251, 91–107. <https://doi.org/10.1016/j.geomorph.2015.05.014>
- Hooke, J.M., Harvey, A.M., Miller, S.Y., Redmond, C.E., 1990. The chronology and stratigraphy of the alluvial terraces of the river Dane Valley, Cheshire, N.W. England. *Earth Surface Processes and Landforms* 15, 717–737. <https://doi.org/10.1002/esp.3290150806>
- Hooke, R.LeB., 2000. On the history of humans as geomorphic agents. *Geology* 28, 843–846. [https://doi.org/10.1130/0091-7613\(2000\)28<843:OTHOHA>2.0.CO;2](https://doi.org/10.1130/0091-7613(2000)28<843:OTHOHA>2.0.CO;2)
- Hoyle, J., Brooks, A., Brierley, G., Fryirs, K., Lander, J., 2008. Spatial variability in the timing, nature and extent of channel response to typical human disturbance along the Upper Hunter River, New South Wales, Australia. *Earth Surface Processes and Landforms* 33, 868–889. <https://doi.org/10.1002/esp.1580>
- Huang, H.Q., Liu, X., Nanson, G.C., 2014. Commentary on a “Conceptual model for complex river responses using an expanded Lane diagram by David Dust and Ellen Wohl”,

- Geomorphology, Volume 139–140, March 2012, Pages 109–121. Geomorphology 209, 140–142. <https://doi.org/10.1016/j.geomorph.2013.07.008>
- Huang, H.Q., Nanson, G.C., 2000. Hydraulic geometry and maximum flow efficiency as products of the principle of least action. *Earth Surface Processes and Landforms* 25, 1–16. [https://doi.org/10.1002/\(SICI\)1096-9837\(200001\)25:1<1::AID-ESP68>3.0.CO;2-2](https://doi.org/10.1002/(SICI)1096-9837(200001)25:1<1::AID-ESP68>3.0.CO;2-2)
- Jacobson, R.B., 1995. Spatial Controls on Patterns of Land-Use Induced Stream Disturbance at the Drainage-Basin Scale—An Example from Gravel-Bed Streams of the Ozark Plateaus, Missouri, in: *Natural and Anthropogenic Influences in Fluvial Geomorphology*. American Geophysical Union (AGU), pp. 219–239. <https://doi.org/10.1029/GM089p0219>
- Jacobson, R.B., Coleman, D.J., 1986. Stratigraphy and Recent evolution of Maryland Piedmont flood plains. *American Journal of Science* 286, 617–637. <https://doi.org/10.2475/ajs.286.8.617>
- Jacobson, R.B., Gran, K.B., 1999. Gravel sediment routing from widespread, low- intensity landscape disturbance, Current River Basin, Missouri. *Earth Surface Processes and Landforms* 24, 897–917. [https://doi.org/10.1002/\(SICI\)1096-9837\(199909\)24:10<897::AID-ESP18>3.0.CO;2-6](https://doi.org/10.1002/(SICI)1096-9837(199909)24:10<897::AID-ESP18>3.0.CO;2-6)
- James, L.A., 2015. Designing forward with an eye to the past: Morphogenesis of the lower Yuba River. *Geomorphology, Emerging geomorphic approaches to guide river management practices* 251, 31–49. <https://doi.org/10.1016/j.geomorph.2015.07.009>
- James, L.A., 2010. Secular Sediment Waves, Channel Bed Waves, and Legacy Sediment. *Geography Compass* 4, 576–598. <https://doi.org/10.1111/j.1749-8198.2010.00324.x>

- James, L.A., 1991. Incision and morphologic evolution of an alluvial channel recovering from hydraulic mining sediment. *GSA Bulletin* 103, 723–736. [https://doi.org/10.1130/0016-7606\(1991\)103<0723:IAMEOA>2.3.CO;2](https://doi.org/10.1130/0016-7606(1991)103<0723:IAMEOA>2.3.CO;2)
- James, L.A., Lecce, S.A., 2013. Impacts of Land-Use and Land-Cover Change on River Systems, in: Shroder, J.F. (Ed.), *Treatise on Geomorphology*. Academic Press, San Diego, pp. 768–793. <https://doi.org/10.1016/B978-0-12-374739-6.00264-5>
- Jones, L.S., Schumm, S.A., 1999. Causes of Avulsion: An Overview, in: *Fluvial Sedimentology VI*. John Wiley & Sons, Ltd, pp. 169–178. <https://doi.org/10.1002/9781444304213.ch13>
- Kemper, J.T., Miller, A.J., Welty, C., 2019. Spatial and temporal patterns of suspended sediment transport in nested urban watersheds. *Geomorphology* 336, 95–106. <https://doi.org/10.1016/j.geomorph.2019.03.018>
- Kemper, J.T., Rathburn, S.L., Friedman, J.M., Nelson, J.M., Mueller, E.R., Vincent, K.R., 2022a. Fingerprinting historical tributary contributions to floodplain sediment using bulk geochemistry. *CATENA* 214, 106231. <https://doi.org/10.1016/j.catena.2022.106231>
- Kemper, J.T., Thaxton, R.D., Rathburn, S.L., Friedman, J.M., Mueller, E.R., Scott, M.L., 2022b. Sediment-ecological connectivity in a large river network. *Earth Surface Processes and Landforms* 47, 639–657. <https://doi.org/10.1002/esp.5277>
- Khan, S., Fryirs, K., 2020a. An approach for assessing geomorphic river sensitivity across a catchment based on analysis of historical capacity for adjustment. *Geomorphology* 359, 107135. <https://doi.org/10.1016/j.geomorph.2020.107135>
- Khan, S., Fryirs, K., 2020b. An approach for assessing geomorphic river sensitivity across a catchment based on analysis of historical capacity for adjustment. *Geomorphology* 359, 107135. <https://doi.org/10.1016/j.geomorph.2020.107135>

- Khan, S., Fryirs, K., Bizzi, S., 2021. Modelling sediment (dis)connectivity across a river network to understand locational-transmission-filter sensitivity for identifying hotspots of potential geomorphic adjustment. *Earth Surface Processes and Landforms* 46, 2856–2869. <https://doi.org/10.1002/esp.5213>
- Kibler, K., Tullos, D., Kondolf, M., 2011. Evolving Expectations of Dam Removal Outcomes: Downstream Geomorphic Effects Following Removal of a Small, Gravel-Filled Dam1. *JAWRA Journal of the American Water Resources Association* 47, 408–423. <https://doi.org/10.1111/j.1752-1688.2011.00523.x>
- Kleinhans, M.G., van den Berg, J.H., 2011. River channel and bar patterns explained and predicted by an empirical and a physics-based method. *Earth Surface Processes and Landforms* 36, 721–738. <https://doi.org/10.1002/esp.2090>
- Knighton, A.D., 1989. River adjustment to changes in sediment load: The effects of tin mining on the Ringarooma River, Tasmania, 1875–1984. *Earth Surface Processes and Landforms* 14, 333–359. <https://doi.org/10.1002/esp.3290140408>
- Knighton, A.D., 1980. Longitudinal changes in size and sorting of stream-bed material in four English rivers. *GSA Bulletin* 91, 55–62. [https://doi.org/10.1130/0016-7606\(1980\)91<55:LCISAS>2.0.CO;2](https://doi.org/10.1130/0016-7606(1980)91<55:LCISAS>2.0.CO;2)
- Knighton, D., 1998. *Fluvial Forms and Processes: A New Perspective*, 2 edition. Ed. Routledge, London ; New York.
- Knox, J.C., 2006. Floodplain sedimentation in the Upper Mississippi Valley: Natural versus human accelerated. *Geomorphology*, 37<sup>th</sup> Binghamton Geomorphology Symposium 79, 286–310. <https://doi.org/10.1016/j.geomorph.2006.06.031>

- Knox, J.C., 1977. Human Impacts on Wisconsin Stream Channels. *Annals of the Association of American Geographers* 67, 323–342. <https://doi.org/10.1111/j.1467-8306.1977.tb01145.x>
- Kondolf, G.M., Piégay, H., Landon, N., 2002. Channel response to increased and decreased bedload supply from land use change: contrasts between two catchments. *Geomorphology, Drainage Basin Dynamics and Morphology* 45, 35–51. [https://doi.org/10.1016/S0169-555X\(01\)00188-X](https://doi.org/10.1016/S0169-555X(01)00188-X)
- Lane, E.W., 1955. The Importance of Fluvial Morphology in Hydraulic Engineering. *Proceedings of the American Society of Civil Engineers* 81, 1–17.
- Lane, S.N., 2013. 21<sup>st</sup> century climate change: where has all the geomorphology gone? *Earth Surface Processes and Landforms* 38, 106–110. <https://doi.org/10.1002/esp.3362>
- Larsen, E.W., Girvetz, E.H., Fremier, A.K., 2007. Landscape level planning in alluvial riparian floodplain ecosystems: Using geomorphic modeling to avoid conflicts between human infrastructure and habitat conservation. *Landscape and Urban Planning* 79, 338–346. <https://doi.org/10.1016/j.landurbplan.2006.04.003>
- Lecce, S.A., 1997. Spatial patterns of historical overbank sedimentation and floodplain evolution, Blue river, Wisconsin. *Geomorphology* 18, 265–277. [https://doi.org/10.1016/S0169-555X\(96\)00030-X](https://doi.org/10.1016/S0169-555X(96)00030-X)
- Lecce, S.A., Pavlowsky, R.T., 2001. Use of mining-contaminated sediment tracers to investigate the timing and rates of historical flood plain sedimentation. *Geomorphology* 38, 85–108. [https://doi.org/10.1016/S0169-555X\(00\)00071-4](https://doi.org/10.1016/S0169-555X(00)00071-4)
- Leddy, J.O., Ashworth, P.J., Best, J.L., 1993. Mechanisms of anabranch avulsion within gravel-bed braided rivers: observations from a scaled physical model. *Geological Society,*

London, Special Publications 75, 119–127.

<https://doi.org/10.1144/GSL.SP.1993.075.01.07>

Leopold, L.B., 1973. River Channel Change with Time: An Example: Address as Retiring President of The Geological Society of America, Minneapolis, Minnesota, November 1972. GSA Bulletin 84, 1845–1860. [https://doi.org/10.1130/0016-7606\(1973\)84<1845:RCCWTA>2.0.CO;2](https://doi.org/10.1130/0016-7606(1973)84<1845:RCCWTA>2.0.CO;2)

Leopold, L.B., Huppman, R., Miller, A., 2005. Geomorphic Effects of Urbanization in Forty-One Years of Observation. Proceedings of the American Philosophical Society 149, 349–371.

Leopold, L.B., Maddock Jr., T., 1953. The hydraulic geometry of stream channels and some physiographic implications (USGS Numbered Series No. 252), The hydraulic geometry of stream channels and some physiographic implications, Professional Paper. U.S. Government Printing Office, Washington, D.C. <https://doi.org/10.3133/pp252>

Leopold, L.B., Wolman, M.G., 1957. River channel patterns: Braided, meandering, and straight (No. 282- B), Professional Paper. U.S. Government Printing Office. <https://doi.org/10.3133/pp282B>

Li, L., Lu, X., Chen, Z., 2007. River channel change during the last 50 years in the middle Yangtze River, the Jianli reach. Geomorphology, Monsoon Rivers of Asia 85, 185–196. <https://doi.org/10.1016/j.geomorph.2006.03.035>

Lisenby, P.E., Croke, J., Fryirs, K.A., 2018. Geomorphic effectiveness: a linear concept in a non-linear world. Earth Surface Processes and Landforms 43, 4–20. <https://doi.org/10.1002/esp.4096>

- Lisenby, P.E., Fryirs, K.A., Thompson, C.J., 2020. River sensitivity and sediment connectivity as tools for assessing future geomorphic channel behavior. *International Journal of River Basin Management* 18, 279–293. <https://doi.org/10.1080/15715124.2019.1672705>
- Lisle, T.E., 2007. 17 The evolution of sediment waves influenced by varying transport capacity in heterogeneous rivers, in: Habersack, H., Piégay, H., Rinaldi, M. (Eds.), *Developments in Earth Surface Processes, Gravel-Bed Rivers VI: From Process Understanding to River Restoration*. Elsevier, pp. 443–469. [https://doi.org/10.1016/S0928-2025\(07\)11136-6](https://doi.org/10.1016/S0928-2025(07)11136-6)
- Lisle, T.E., 1982. Effects of aggradation and degradation on riffle-pool morphology in natural gravel channels, northwestern California. *Water Resources Research* 18, 1643–1651. <https://doi.org/10.1029/WR018i006p01643>
- Lisle, T.E., Hilton, S., 1992. The Volume of Fine Sediment in Pools: An Index of Sediment Supply in Gravel-Bed Streams I. *JAWRA Journal of the American Water Resources Association* 28, 371–383. <https://doi.org/10.1111/j.1752-1688.1992.tb04003.x>
- Lisle, T.E., Pizzuto, J.E., Ikeda, H., Iseya, F., Kodama, Y., 1997. Evolution of a sediment wave in an experimental channel. *Water Resources Research* 33, 1971–1981. <https://doi.org/10.1029/97WR01180>
- Mackin, J., 1948. Concept of the Graded River. *GSA Bulletin* 59, 463–512. [https://doi.org/10.1130/0016-7606\(1948\)59\[463:COTGR\]2.0.CO;2](https://doi.org/10.1130/0016-7606(1948)59[463:COTGR]2.0.CO;2)
- Macklin, M.G., Lewin, J., Jones, A.F., 2014. Anthropogenic alluvium: An evidence-based meta-analysis for the UK Holocene. *Anthropocene, Landscapes in the Anthropocene* 6, 26–38. <https://doi.org/10.1016/j.ancene.2014.03.003>
- Madej, M.A., Ozaki, V., 1996. Channel Response to Sediment Wave Propagation and Movement, Redwood Creek, California, Usa. *Earth Surface Processes and Landforms* 21,

911–927. [https://doi.org/10.1002/\(SICI\)1096-9837\(199610\)21:10<911::AID-ESP621>3.0.CO;2-1](https://doi.org/10.1002/(SICI)1096-9837(199610)21:10<911::AID-ESP621>3.0.CO;2-1)

Magilligan, F.J., 1985. Historical Floodplain Sedimentation in the Galena River Basin, Wisconsin and Illinois. *Annals of the Association of American Geographers* 75, 583–594. <https://doi.org/10.1111/j.1467-8306.1985.tb00095.x>

Magilligan, F.J., Phillips, J.D., James, L.A., Gomez, B., 1998. Geomorphic and Sedimentological Controls on the Effectiveness of an Extreme Flood. *The Journal of Geology* 106, 87–96. <https://doi.org/10.1086/516009>

Major, J., East, A.E., O'Connor, J.E., Grant, G.E., Wilcox, A.C., Magirl, C.S., Collins, M.J., Tullos, D.D., 2017. Geomorphic responses to dam removal in the United States—a two-decade perspective, in: *Gravel-Bed Rivers: Processes and Disasters*. John Wiley & Sons, Chichester, Sussex, UK, pp. 355–383.

Major, J.J., O'Connor, J.E., Podolak, C.J., Keith, M.K., Grant, G.E., Spicer, K.R., Pittman, S., Bragg, Wallick, J.R., Tanner, D.Q., Rhode, A., 2012. Geomorphic response of the Sandy River, Oregon, to removal of Marmot Dam (No. 1792), U.S. Geological Survey Professional Paper. U.S. Geological Survey.

Marsh, G.P., 1864. *Man and Nature; Or Physical Geography as Modified by Human Action*. Charles Scribner, New York, NY.

Métivier, F., Barrier, L., 2012. Alluvial Landscape Evolution: What Do We Know About Metamorphosis of Gravel-Bed Meandering and Braided Streams?, in: *Gravel-Bed Rivers*. John Wiley & Sons, Ltd, pp. 474–501. <https://doi.org/10.1002/9781119952497.ch34>

- Meyer, G.A., Wells, S.G., Balling, R.C., Jull, A.J.T., 1992. Response of alluvial systems to fire and climate change in Yellowstone National Park. *Nature* 357, 147–150.  
<https://doi.org/10.1038/357147a0>
- Miller, D.J., Benda, L.E., 2000. Effects of punctuated sediment supply on valley-floor landforms and sediment transport. *GSA Bulletin* 112, 1814–1824. [https://doi.org/10.1130/0016-7606\(2000\)112<1814:EOPSSO>2.0.CO;2](https://doi.org/10.1130/0016-7606(2000)112<1814:EOPSSO>2.0.CO;2)
- Miller, S.O., Ritter, D.F., Kochel, R.C., Miller, J.R., 1993. Fluvial responses to land-use changes and climatic variations within the Drury Creek watershed, southern Illinois. *Geomorphology* 6, 309–329. [https://doi.org/10.1016/0169-555X\(93\)90053-5](https://doi.org/10.1016/0169-555X(93)90053-5)
- Montgomery, D.R., Buffington, J.M., 1998. Channel processes, classification, and response, in: *River Ecology and Management*. Pp. 1250–1263.
- Morais, E.S., Rocha, P.C., Hooke, J., 2016a. Spatiotemporal variations in channel changes caused by cumulative factors in a meandering river: The lower Peixe River, Brazil. *Geomorphology* 273, 348–360. <https://doi.org/10.1016/j.geomorph.2016.07.026>
- Morais, E.S., Rocha, P.C., Hooke, J., 2016b. Spatiotemporal variations in channel changes caused by cumulative factors in a meandering river: The lower Peixe River, Brazil. *Geomorphology* 273, 348–360. <https://doi.org/10.1016/j.geomorph.2016.07.026>
- Morgan, J.A., Nelson, P.A., 2021. Experimental investigation of the morphodynamic response of riffles and pools to unsteady flow and increased sediment supply. *Earth Surface Processes and Landforms* 46, 869–886. <https://doi.org/10.1002/esp.5072>
- Morgan, J.A., Nelson, P.A., 2019. Morphodynamic Modeling of Sediment Pulse Dynamics. *Water Resources Research* 55, 8691–8707. <https://doi.org/10.1029/2019WR025407>

- Mount, N.J., Sambrook Smith, G.H., Stott, T.A., 2005. An assessment of the impact of upland afforestation on lowland river reaches: the Afon Trannon, mid-Wales. *Geomorphology* 64, 255–269. <https://doi.org/10.1016/j.geomorph.2004.07.003>
- Mueller, E.R., Pitlick, J., 2014. Sediment supply and channel morphology in mountain river systems: 2. Single thread to braided transitions. *Journal of Geophysical Research: Earth Surface* 119, 1516–1541. <https://doi.org/10.1002/2013JF003045>
- Mueller, E.R., Pitlick, J., 2013. Sediment supply and channel morphology in mountain river systems: 1. Relative importance of lithology, topography, and climate. *Journal of Geophysical Research: Earth Surface* 118, 2325–2342. <https://doi.org/10.1002/2013JF002843>
- Murphy, B.P., Czuba, J.A., Belmont, P., 2019. Post-wildfire sediment cascades: A modeling framework linking debris flow generation and network-scale sediment routing. *Earth Surface Processes and Landforms* 44, 2126–2140. <https://doi.org/10.1002/esp.4635>
- Najafi, S., Dragovich, D., Heckmann, T., Sadeghi, S.H., 2021. Sediment connectivity concepts and approaches. *CATENA* 196, 104880. <https://doi.org/10.1016/j.catena.2020.104880>
- Nanson, G.C., Hickin, E.J., 1983. Channel Migration and Incision on the Beatton River. *Journal of Hydraulic Engineering* 109, 327–337. [https://doi.org/10.1061/\(ASCE\)0733-9429\(1983\)109:3\(327\)](https://doi.org/10.1061/(ASCE)0733-9429(1983)109:3(327))
- Nelson, A., Dubé, K., 2016. Channel response to an extreme flood and sediment pulse in a mixed bedrock and gravel-bed river. *Earth Surface Processes and Landforms* 41, 178–195. <https://doi.org/10.1002/esp.3843>
- Nelson, A.D., Church, M., 2012. Placer mining along the Fraser River, British Columbia: The geomorphic impact. *GSA Bulletin* 124, 1212–1228. <https://doi.org/10.1130/B30575.1>

- Nelson, P.A., Brew, A.K., Morgan, J.A., 2015. Morphodynamic response of a variable-width channel to changes in sediment supply. *Water Resources Research* 51, 5717–5734.  
<https://doi.org/10.1002/2014WR016806>
- Nicholas, A.P., Ashworth, P.J., Kirkby, M.J., Macklin, M.G., Murray, T., 1995. Sediment slugs: large-scale fluctuations in fluvial sediment transport rates and storage volumes. *Progress in Physical Geography: Earth and Environment* 19, 500–519.  
<https://doi.org/10.1177/030913339501900404>
- Olley, J.M., Wasson, R.J., 2003. Changes in the flux of sediment in the Upper Murrumbidgee catchment, Southeastern Australia, since European settlement. *Hydrological Processes* 17, 3307–3320. <https://doi.org/10.1002/hyp.1388>
- Osman, A.M., Thorne, C.R., 1988. Riverbank Stability Analysis. I: Theory. *Journal of Hydraulic Engineering* 114, 134–150. [https://doi.org/10.1061/\(ASCE\)0733-9429\(1988\)114:2\(134\)](https://doi.org/10.1061/(ASCE)0733-9429(1988)114:2(134))
- Paola, C., Voller, V.R., 2005. A generalized Exner equation for sediment mass balance. *Journal of Geophysical Research: Earth Surface* 110. <https://doi.org/10.1029/2004JF000274>
- Park, C.C., 1977. World-wide variations in hydraulic geometry exponents of stream channels: An analysis and some observations. *Journal of Hydrology* 33, 133–146.  
[https://doi.org/10.1016/0022-1694\(77\)90103-2](https://doi.org/10.1016/0022-1694(77)90103-2)
- Parker, G., 2008. Transport of Gravel and Sediment Mixtures, in: *Sedimentation Engineering: Processes, Measurements, Modeling, and Practice*, American Society of Civil Engineers Manuals and Reports on Engineering Practice. American Society of Civil Engineers, Reston, VA, pp. 165–251.
- Parker, G., 1979. Hydraulic Geometry of Active Gravel Rivers. *Journal of the Hydraulics Division* 105, 1185–1201. <https://doi.org/10.1061/JYCEAJ.0005275>

Parker, G., 1976. On the cause and characteristic scales of meandering and braiding in rivers.

Journal of Fluid Mechanics 76, 457–480. <https://doi.org/10.1017/S0022112076000748>

Parker, G., Shimizu, Y., Wilkerson, G.V., Eke, E.C., Abad, J.D., Lauer, J.W., Paola, C., Dietrich,

W.E., Voller, V.R., 2011. A new framework for modeling the migration of meandering rivers. Earth Surface Processes and Landforms 36, 70–86.

<https://doi.org/10.1002/esp.2113>

Passmore, D.G., Macklin, M.G., Brewer, P.A., Lewin, J., Rumsby, B.T., Newson, M.D., 1993.

Variability of late Holocene braiding in Britain. Geological Society, London, Special Publications 75, 205–229. <https://doi.org/10.1144/GSL.SP.1993.075.01.13>

Passmore, D.G., Macklin, M.G., Stevenson, A.C., O'Brien, C.F., Davis, B.A.S., 1992. A

Holocene Alluvial Sequence in the lower Tyne Valley, Northern Britain: A Record of River Response to Environmental Change. The Holocene 2, 138–147.

<https://doi.org/10.1177/095968369200200205>

Pearson, A.J., Snyder, N.P., Collins, M.J., 2011. Rates and processes of channel response to dam removal with a sand-filled impoundment. Water Resources Research 47.

<https://doi.org/10.1029/2010WR009733>

Pelletier, J.D., Brad Murray, A., Pierce, J.L., Bierman, P.R., Breshears, D.D., Crosby, B.T., Ellis,

M., Foufoula-Georgiou, E., Heimsath, A.M., Houser, C., Lancaster, N., Marani, M.,

Merritts, D.J., Moore, L.J., Pederson, J.L., Poulos, M.J., Rittenour, T.M., Rowland, J.C.,

Ruggiero, P., Ward, D.J., Wickert, A.D., Yager, E.M., 2015. Forecasting the response of

Earth's surface to future climatic and land use changes: A review of methods and

research needs. Earth's Future 3, 220–251. <https://doi.org/10.1002/2014EF000290>

- Pfeiffer, A.M., Finnegan, N.J., Willenbring, J.K., 2017. Sediment supply controls equilibrium channel geometry in gravel rivers. *Proceedings of the National Academy of Sciences* 114, 3346–3351. <https://doi.org/10.1073/pnas.1612907114>
- Phillips, J.D., 2011. Universal and local controls of avulsions in southeast Texas Rivers. *Geomorphology, Scale Issues in Geomorphology* 130, 17–28. <https://doi.org/10.1016/j.geomorph.2010.10.001>
- Phillips, J.D., 2009. Changes, perturbations, and responses in geomorphic systems. *Progress in Physical Geography: Earth and Environment* 33, 17–30. <https://doi.org/10.1177/0309133309103889>
- Phillips, J.D., 2006. Evolutionary geomorphology: thresholds and nonlinearity in landform response to environmental change. *Hydrology and Earth System Sciences* 10, 731–742. <https://doi.org/10.5194/hess-10-731-2006>
- Phillips, J.D., Slattery, M.C., Musselman, Z.A., 2005. Channel adjustments of the lower Trinity River, Texas, downstream of Livingston Dam. *Earth Surface Processes and Landforms* 30, 1419–1439. <https://doi.org/10.1002/esp.1203>
- Pierson, T.C., Pringle, P.T., Cameron, K.A., 2011. Magnitude and timing of downstream channel aggradation and degradation in response to a dome-building eruption at Mount Hood, Oregon. *GSA Bulletin* 123, 3–20. <https://doi.org/10.1130/B30127.1>
- Pitlick, J., Mueller, E.R., Segura, C., 2012a. Differences in Sediment Supply to Braided and Single-Thread River Channels: What Do the Data Tell Us?, in: *Gravel-Bed Rivers*. John Wiley & Sons, Ltd, pp. 502–511. <https://doi.org/10.1002/9781119952497.ch35>

- Pitlick, J., Mueller, E.R., Segura, C., 2012b. Differences in Sediment Supply to Braided and Single-Thread River Channels: What Do the Data Tell Us?, in: Gravel-Bed Rivers. John Wiley & Sons, Ltd, pp. 502–511. <https://doi.org/10.1002/9781119952497.ch35>
- Pizzuto, J., 2002. Effects of Dam Removal on River Form and Process: Although many well-established concepts of fluvial geomorphology are relevant for evaluating the effects of dam removal, geomorphologists remain unable to forecast stream channel changes caused by the removal of specific dams. *BioScience* 52, 683–691. [https://doi.org/10.1641/0006-3568\(2002\)052\[0683:EODROR\]2.0.CO;2](https://doi.org/10.1641/0006-3568(2002)052[0683:EODROR]2.0.CO;2)
- Pizzuto, J.E., 1990. Numerical simulation of gravel river widening. *Water Resources Research* 26, 1971–1980. <https://doi.org/10.1029/WR026i009p01971>
- Poeppl, R.E., Keesstra, S.D., Maroulis, J., 2017. A conceptual connectivity framework for understanding geomorphic change in human-impacted fluvial systems. *Geomorphology, Connectivity in Geomorphology from Binghamton 2016* 277, 237–250. <https://doi.org/10.1016/j.geomorph.2016.07.033>
- Prosser, I.P., Rutherford, I.D., Olley, J.M., Young, W.J., Wallbrink, P.J., Moran, C.J., 2001. Large-scale patterns of erosion and sediment transport in river networks, with examples from Australia. *Mar. Freshwater Res.* 52, 81–99. <https://doi.org/10.1071/mf00033>
- Rathburn, S., Wohl, E., 2003. Predicting fine sediment dynamics along a pool-riffle mountain channel. *Geomorphology, Mountain Geomorphology – Integrating Earth Systems, Proceedings of the 32<sup>nd</sup> Annual Binghamton Geomorphology Symposium* 55, 111–124. [https://doi.org/10.1016/S0169-555X\(03\)00135-1](https://doi.org/10.1016/S0169-555X(03)00135-1)

- Rathburn, S.L., Bennett, G.L., Wohl, E.E., Briles, C., McElroy, B., Sutfin, N., 2017. The fate of sediment, wood, and organic carbon eroded during an extreme flood, Colorado Front Range, USA. *Geology* 45, 499–502. <https://doi.org/10.1130/G38935.1>
- Rathburn, S.L., Rubin, Z.K., Wohl, E.E., 2013. Evaluating channel response to an extreme sedimentation event in the context of historical range of variability: Upper Colorado River, USA. *Earth Surface Processes and Landforms* 38, 391–406. <https://doi.org/10.1002/esp.3329>
- Rathburn, S.L., Shahverdian, S.M., Ryan, S.E., 2018. Post-disturbance sediment recovery: Implications for watershed resilience. *Geomorphology, Resilience and Bio-Geomorphic Systems – Proceedings of the 48<sup>th</sup> Binghamton Geomorphology Symposium* 305, 61–75. <https://doi.org/10.1016/j.geomorph.2017.08.039>
- Recking, A., 2012. Influence of sediment supply on mountain streams bedload transport. *Geomorphology* 175–176, 139–150. <https://doi.org/10.1016/j.geomorph.2012.07.005>
- Reid, H.E., Brierley, G.J., 2015. Assessing geomorphic sensitivity in relation to river capacity for adjustment. *Geomorphology, Emerging geomorphic approaches to guide river management practices* 251, 108–121. <https://doi.org/10.1016/j.geomorph.2015.09.009>
- Rice, S., 1998. Which tributaries disrupt downstream fining along gravel-bed rivers? *Geomorphology* 22, 39–56. [https://doi.org/10.1016/S0169-555X\(97\)00052-4](https://doi.org/10.1016/S0169-555X(97)00052-4)
- Rinaldi, M., 2003. Recent channel adjustments in alluvial rivers of Tuscany, central Italy. *Earth Surface Processes and Landforms* 28, 587–608. <https://doi.org/10.1002/esp.464>
- Rumsby, B.T., Macklin, M.G., 1994. Channel and floodplain response to recent abrupt climate change: The tyne basin, Northern England. *Earth Surface Processes and Landforms* 19, 499–515. <https://doi.org/10.1002/esp.3290190603>

- Rumschlag, J.H., Peck, J.A., 2007. Short-term Sediment and Morphologic Response of the Middle Cuyahoga River to the Removal of the Munroe Falls Dam, Summit County, Ohio. *Journal of Great Lakes Research*, Great Lakes Sea Lamprey Research Themes. Dam Removals and River Channel Changes 33, 142–153. [https://doi.org/10.3394/0380-1330\(2007\)33\[142:SSAMRO\]2.0.CO;2](https://doi.org/10.3394/0380-1330(2007)33[142:SSAMRO]2.0.CO;2)
- Salant, N.L., Renshaw, C.E., Magilligan, F.J., 2006. Short and long-term changes to bed mobility and bed composition under altered sediment regimes. *Geomorphology* 76, 43–53. <https://doi.org/10.1016/j.geomorph.2005.09.003>
- Sankey, J.B., Kreitler, J., Hawbaker, T.J., McVay, J.L., Miller, M.E., Mueller, E.R., Vaillant, N.M., Lowe, S.E., Sankey, T.T., 2017. Climate, wildfire, and erosion ensemble foretells more sediment in western USA watersheds. *Geophysical Research Letters* 44, 8884–8892. <https://doi.org/10.1002/2017GL073979>
- Sarker, M.H., Thorne, C.R., 2006. Morphological Response of the Brahmaputra–Padma–Lower Meghna River System to the Assam Earthquake of 1950, in: Sambrook Smith, G.H., Best, J.L., Bristow, C.S., Petts, G.E. (Eds.), *Braided Rivers*. John Wiley & Sons, Ltd, pp. 289–310. <https://doi.org/10.1002/9781444304374.ch14>
- Schumm, S.A., 1985. Patterns of Alluvial Rivers. *Annual Review of Earth and Planetary Sciences* 13, 5–27.
- Schumm, S.A., 1979. Geomorphic Thresholds: The Concept and Its Applications. *Transactions of the Institute of British Geographers* 4, 485–515. <https://doi.org/10.2307/622211>
- Schumm, S.A., 1977. *The Fluvial System*. Blackburn Press. 338 pp.
- Schumm, S.A., 1969. River Metamorphosis. *Journal of the Hydraulics Division* 95, 255–274. <https://doi.org/10.1061/JYCEAJ.0001938>

- Schumm, S.A., 1963. Sinuosity of Alluvial Rivers on the Great Plains. GSA Bulletin 74, 1089–1100. [https://doi.org/10.1130/0016-7606\(1963\)74\[1089:SOAROT\]2.0.CO;2](https://doi.org/10.1130/0016-7606(1963)74[1089:SOAROT]2.0.CO;2)
- Schumm, S.A., Parker, R.S., 1973. Implications of Complex Response of Drainage Systems for Quaternary Alluvial Stratigraphy. Nature Physical Science 243, 99–100. <https://doi.org/10.1038/physci243099a0>
- Sear, D.A., 1996. Sediment Transport Processes in Pool–Riffle Sequences. Earth Surface Processes and Landforms 21, 241–262. [https://doi.org/10.1002/\(SICI\)1096-9837\(199603\)21:3<241::AID-ESP623>3.0.CO;2-1](https://doi.org/10.1002/(SICI)1096-9837(199603)21:3<241::AID-ESP623>3.0.CO;2-1)
- Shen, H.W., Schumm, S.A., Nelson, J.D., Doehring, D. O., Skinner, M.M., Smith, G.L., Colorado State University. Engineering Research Center, 1981. Methods for assessment of stream-related hazards to highways and bridges. (No. FHWA/RD-80/160). Federal Highway Administration.
- Short, L.E., Gabet, E.J., Hoffman, D.F., 2015a. The role of large woody debris in modulating the dispersal of a post-fire sediment pulse. Geomorphology 246, 351–358. <https://doi.org/10.1016/j.geomorph.2015.06.031>
- Short, L.E., Gabet, E.J., Hoffman, D.F., 2015b. The role of large woody debris in modulating the dispersal of a post-fire sediment pulse. Geomorphology 246, 351–358. <https://doi.org/10.1016/j.geomorph.2015.06.031>
- Simon, A., 1995. Adjustment and recovery of unstable alluvial channels: Identification and approaches for engineering management. Earth Surface Processes and Landforms 20, 611–628. <https://doi.org/10.1002/esp.3290200705>
- Simon, A., 1989. A model of channel response in disturbed alluvial channels. Earth Surface Processes and Landforms 14, 11–26. <https://doi.org/10.1002/esp.3290140103>

- Simon, A., Rinaldi, M., 2000. Channel Instability in the Loess Area of the Midwestern United States. *JAWRA Journal of the American Water Resources Association* 36, 133–150.  
<https://doi.org/10.1111/j.1752-1688.2000.tb04255.x>
- Simon, A., Thorne, C.R., 1996. Channel Adjustment of an Unstable Coarse-Grained Stream: Opposing Trends of Boundary and Critical Shear Stress, and the Applicability of Extremal Hypotheses. *Earth Surface Processes and Landforms* 21, 155–180.  
[https://doi.org/10.1002/\(SICI\)1096-9837\(199602\)21:2<155::AID-ESP610>3.0.CO;2-5](https://doi.org/10.1002/(SICI)1096-9837(199602)21:2<155::AID-ESP610>3.0.CO;2-5)
- Sims, A.J., Rutherford, I.D., 2021. Local scale interventions dominate over catchment scale controls to accelerate the recovery of a degraded stream. *PLOS ONE* 16, e0252983.  
<https://doi.org/10.1371/journal.pone.0252983>
- Sims, A.J., Rutherford, I.D., 2017. Management responses to pulses of bedload sediment in rivers. *Geomorphology, Anthropogenic Sedimentation* 294, 70–86.  
<https://doi.org/10.1016/j.geomorph.2017.04.010>
- Sinha, R., Sripriyanka, K., Jain, V., Mukul, M., 2014. Avulsion threshold and planform dynamics of the Kosi River in north Bihar (India) and Nepal: A GIS framework. *Geomorphology* 216, 157–170. <https://doi.org/10.1016/j.geomorph.2014.03.035>
- Sklar, L., Dietrich, W.E., 1998. River longitudinal profiles and bedrock incision models: Stream power and the influence of sediment supply, in: Tinkler, J., Wohl, E. (Eds.), *Geophysical Monograph Series*. American Geophysical Union, Washington, D. C., pp. 237–260.  
<https://doi.org/10.1029/GM107p0237>
- Sklar, L.S., Fadde, J., Venditti, J.G., Nelson, P., Wydzga, M.A., Cui, Y., Dietrich, W.E., 2009. Translation and dispersion of sediment pulses in flume experiments simulating gravel

augmentation below dams. *Water Resources Research* 45.

<https://doi.org/10.1029/2008WR007346>

Slingerland, R., Smith, N.D., 1998. Necessary conditions for a meandering-river avulsion.

*Geology* 26, 435–438. [https://doi.org/10.1130/0091-](https://doi.org/10.1130/0091-7613(1998)026<0435:NCFAMR>2.3.CO;2)

[7613\(1998\)026<0435:NCFAMR>2.3.CO;2](https://doi.org/10.1130/0091-7613(1998)026<0435:NCFAMR>2.3.CO;2)

Smith, N.D., Smith, D.G., 1984. William River: An outstanding example of channel widening and braiding caused by bed-load addition. *Geology* 12, 78–82.

[https://doi.org/10.1130/0091-7613\(1984\)12<78:WRAOEO>2.0.CO;2](https://doi.org/10.1130/0091-7613(1984)12<78:WRAOEO>2.0.CO;2)

Soar, P.J., Thorne, C.R., 2001. Channel Restoration Design for Meandering Rivers. Report

ERDC/CHL CR-01-1. U.S. Army Corps of Engineers, Coastal and Hydraulics

Laboratory, U.S. Army Engineer Research and Development Center, Vicksburg, MS. 454

pp.

Surian, N., Ziliani, L., Comiti, F., Lenzi, M.A., Mao, L., 2009. Channel adjustments and

alteration of sediment fluxes in gravel-bed rivers of North-Eastern Italy: potentials and

limitations for channel recovery. *River Research and Applications* 25, 551–567.

<https://doi.org/10.1002/rra.1231>

Sutherland, D.G., Ball, M.H., Hilton, S.J., Lisle, T.E., 2002. Evolution of a landslide-induced

sediment wave in the Navarro River, California. *GSA Bulletin* 114, 1036–1048.

[https://doi.org/10.1130/0016-7606\(2002\)114<1036:EOALIS>2.0.CO;2](https://doi.org/10.1130/0016-7606(2002)114<1036:EOALIS>2.0.CO;2)

Swanson, B.J., Meyer, G.A., Coonrod, J.E., 2011. Historical channel narrowing along the Rio

Grande near Albuquerque, New Mexico in response to peak discharge reductions and

engineering: magnitude and uncertainty of change from air photo measurements. *Earth*

*Surface Processes and Landforms* 36, 885–900. <https://doi.org/10.1002/esp.2119>

- Takagi, T., Oguchi, T., Matsumoto, J., Grossman, M.J., Sarker, M.H., Matin, M.A., 2007. Channel braiding and stability of the Brahmaputra River, Bangladesh, since 1967: GIS and remote sensing analyses. *Geomorphology, Monsoon Rivers of Asia* 85, 294–305. <https://doi.org/10.1016/j.geomorph.2006.03.028>
- Taylor, M.P., Macklin, M.G., Hudson-Edwards, K., 2000. River sedimentation and fluvial response to Holocene environmental change in the Yorkshire Ouse Basin, northern England. *The Holocene* 10, 201–212. <https://doi.org/10.1191/095968300673746737>
- Taylor Perron, J., Fagherazzi, S., 2012. The legacy of initial conditions in landscape evolution. *Earth Surface Processes and Landforms* 37, 52–63. <https://doi.org/10.1002/esp.2205>
- Topping, D.J., Mueller, E.R., Schmidt, J.C., Griffiths, R.E., Dean, D.J., Grams, P.E., 2018. Long-Term Evolution of Sand Transport Through a River Network: Relative Influences of a Dam Versus Natural Changes in Grain Size From Sand Waves. *Journal of Geophysical Research: Earth Surface* 123, 1879–1909. <https://doi.org/10.1029/2017JF004534>
- Topping, D.J., Rubin, D.M., Nelson, J.M., Kinzel III, P.J., Corson, I.C., 2000a. Colorado River sediment transport: 2. Systematic Bed-elevation and grain-size effects of sand supply limitation. *Water Resources Research* 36, 543–570. <https://doi.org/10.1029/1999WR900286>
- Topping, D.J., Rubin, D.M., Vierra Jr., L.E., 2000b. Colorado River sediment transport: 1. Natural sediment supply limitation and the influence of Glen Canyon Dam. *Water Resources Research* 36, 515–542. <https://doi.org/10.1029/1999WR900285>
- Trimble, S.W., 2009. Fluvial processes, morphology and sediment budgets in the Coon Creek Basin, WI, USA, 1975–1993. *Geomorphology, Climate and long-term human impact on*

- sediment fluxes in watershed systems 108, 8–23.  
<https://doi.org/10.1016/j.geomorph.2006.11.015>
- Trimble, S.W., 1999. Decreased Rates of Alluvial Sediment Storage in the Coon Creek Basin, Wisconsin, 1975-93. *Science* 285, 1244–1246.  
<https://doi.org/10.1126/science.285.5431.1244>
- Trimble, S.W., 1983. A sediment budget for Coon Creek basin in the Driftless Area, Wisconsin, 1853-1977. *Am J Sci* 283, 454–474. <https://doi.org/10.2475/ajs.283.5.454>
- Trimble, S.W., 1981. Changes in Sediment Storage in the Coon Creek Basin, Driftless Area, Wisconsin, 1853 to 1975. *Science* 214, 181–183.
- Tunncliffe, J., Brierley, G., Fuller, I.C., Leenman, A., Marden, M., Peacock, D., 2018. Reaction and relaxation in a coarse-grained fluvial system following catchment-wide disturbance. *Geomorphology, New Zealand's Landscape: A Memorial Tribute to Noel A. Trustrum* 307, 50–64. <https://doi.org/10.1016/j.geomorph.2017.11.006>
- United Nations, Department of Economic and Social Affairs, Population Division, 2019. World urbanization prospects: the 2018 revision.
- Van De Wiel, M.J., Coulthard, T.J., 2010. Self-organized criticality in river basins: Challenging sedimentary records of environmental change. *Geology* 38, 87–90.  
<https://doi.org/10.1130/G30490.1>
- Venditti, J.G., Dietrich, W.E., Nelson, P.A., Wydzga, M.A., Fadde, J., Sklar, L., 2010. Effect of sediment pulse grain size on sediment transport rates and bed mobility in gravel bed rivers. *Journal of Geophysical Research: Earth Surface* 115.  
<https://doi.org/10.1029/2009JF001418>

- Venditti, J.G., Nelson, P.A., Bradley, R.W., Haught, D., Gitto, A.B., 2017. Bedforms, Structures, Patches, and Sediment Supply in Gravel-Bed Rivers, in: Gravel-Bed Rivers. John Wiley & Sons, Ltd, pp. 439–466. <https://doi.org/10.1002/9781118971437.ch16>
- Walker, A.E., Moore, J.N., Grams, P.E., Dean, D.J., Schmidt, J.C., 2020. Channel narrowing by inset floodplain formation of the lower Green River in the Canyonlands region, Utah. GSA Bulletin 132, 2333–2352. <https://doi.org/10.1130/B35233.1>
- Ward, A.S., Morgan, J.A., White, J.R., Royer, T.V., 2018. Streambed restoration to remove fine sediment alters reach-scale transient storage in a low-gradient fifth-order river, Indiana, USA. Hydrological Processes 32, 1786–1800. <https://doi.org/10.1002/hyp.11518>
- Warner, R.F., 1984. Man’s impacts on Australian drainage systems. Australian Geographer 16, 133–141. <https://doi.org/10.1080/00049188408702865>
- Wathen, S.J., Hoey, T.B., 1998. Morphological controls on the downstream passage of a sediment wave in a gravel-bed stream. Earth Surface Processes and Landforms 23, 715–730. [https://doi.org/10.1002/\(SICI\)1096-9837\(199808\)23:8<715::AID-ESP877>3.0.CO;2-0](https://doi.org/10.1002/(SICI)1096-9837(199808)23:8<715::AID-ESP877>3.0.CO;2-0)
- Wilcock, P.R., Crowe, J.C., 2003. Surface-based Transport Model for Mixed-Size Sediment. Journal of Hydraulic Engineering 129, 120–128. [https://doi.org/10.1061/\(ASCE\)0733-9429\(2003\)129:2\(120\)](https://doi.org/10.1061/(ASCE)0733-9429(2003)129:2(120))
- Williams, G.P., Wolman, M.G., 1984. Downstream Effects of Dams on Alluvial Rivers (No. 1286), Geological Survey Professional Paper. U.S. Geological Survey, Washington, D. C.
- Wohl, E., 2020. Rivers in the Anthropocene: The U.S. perspective. Geomorphology, The Binghamton Geomorphology Symposium: 50 years of Enhancing Geomorphology 366, 106600. <https://doi.org/10.1016/j.geomorph.2018.12.001>

- Wohl, E., 2018. Geomorphic context in rivers. *Progress in Physical Geography: Earth and Environment* 42, 841–857. <https://doi.org/10.1177/0309133318776488>
- Wohl, E., 2017. Connectivity in rivers. *Progress in Physical Geography: Earth and Environment* 41, 345–362. <https://doi.org/10.1177/0309133317714972>
- Wohl, E., 2016. Spatial heterogeneity as a component of river geomorphic complexity. *Progress in Physical Geography: Earth and Environment* 40, 598–615. <https://doi.org/10.1177/0309133316658615>
- Wohl, E., 2015. Legacy effects on sediments in river corridors. *Earth-Science Reviews* 147, 30–53. <https://doi.org/10.1016/j.earscirev.2015.05.001>
- Wohl, E., 2014. *Rivers in the Landscape*. John Wiley & Sons.
- Wohl, E., 2004. Limits of downstream hydraulic geometry. *Geology* 32, 897–900. <https://doi.org/10.1130/G20738.1>
- Wohl, E., Bledsoe, B.P., Jacobson, R.B., Poff, N.L., Rathburn, S.L., Walters, D.M., Wilcox, A.C., 2015. The Natural Sediment Regime in Rivers: Broadening the Foundation for Ecosystem Management. *BioScience* 65, 358–371. <https://doi.org/10.1093/biosci/biv002>
- Wohl, E., Brierley, G., Cadol, D., Coulthard, T.J., Covino, T., Fryirs, K.A., Grant, G., Hilton, R.G., Lane, S.N., Magilligan, F.J., Meitzen, K.M., Passalacqua, P., Poepl, R.E., Rathburn, S.L., Sklar, L.S., 2019a. Connectivity as an emergent property of geomorphic systems. *Earth Surface Processes and Landforms* 44, 4–26. <https://doi.org/10.1002/esp.4434>
- Wohl, E., Brierley, G., Cadol, D., Coulthard, T.J., Covino, T., Fryirs, K.A., Grant, G., Hilton, R.G., Lane, S.N., Magilligan, F.J., Meitzen, K.M., Passalacqua, P., Poepl, R.E., Rathburn, S.L., Sklar, L.S., 2019b. Connectivity as an emergent property of geomorphic

- systems. *Earth Surface Processes and Landforms* 44, 4–26.  
<https://doi.org/10.1002/esp.4434>
- Wohl, E., Marshall, A.E., Scamardo, J., White, D., Morrison, R.R., 2022. Biogeomorphic influences on river corridor resilience to wildfire disturbances in a mountain stream of the Southern Rockies, USA. *Science of The Total Environment* 820, 153321.  
<https://doi.org/10.1016/j.scitotenv.2022.153321>
- Wohl, E., Rathburn, S., 2003. Mitigation of Sedimentation Hazards Downstream from Reservoirs. *International Journal of Sediment Research* 18, 97–106.
- Wohl, E., Scott, D.N., 2017. Wood and sediment storage and dynamics in river corridors. *Earth Surface Processes and Landforms* 42, 5–23. <https://doi.org/10.1002/esp.3909>
- Wolman, M.G., 1967. A Cycle of Sedimentation and Erosion in Urban River Channels. *Geografiska Annaler. Series A, Physical Geography* 49, 385–395.  
<https://doi.org/10.2307/520904>
- Wolman, M.G., 1955. The natural channel of Brandywine Creek, Pennsylvania (No. 271), Professional Paper. U.S. Government Printing Office. <https://doi.org/10.3133/pp271>
- Womack, W.R., Schumm, S.A., 1977. Terraces of Douglas Creek, northwestern Colorado: An example of episodic erosion. *Geology* 5, 72–76. [https://doi.org/10.1130/0091-7613\(1977\)5<72:TODCNC>2.0.CO;2](https://doi.org/10.1130/0091-7613(1977)5<72:TODCNC>2.0.CO;2)
- Zinger, J.A., Rhoads, B.L., Best, J.L., 2011. Extreme sediment pulses generated by bend cutoffs along a large meandering river. *Nature Geosci* 4, 675–678.  
<https://doi.org/10.1038/ngeo1260>

Zunka, J.P.P., Tullos, D.D., Lancaster, S.T., 2015. Effects of sediment pulses on bed relief in bar-pool channels. *Earth Surface Processes and Landforms* 40, 1017–1028.

<https://doi.org/10.1002/esp.3697>

## CHAPTER 5: CONCLUSIONS

The fluvial system is an interconnected network of components, linked together by connections that vary in magnitude across time and space and regulate the flow of water, sediment, and nutrients through the landscape (Fryirs, 2013; Wohl et al., 2019). Though such understanding has a long and rich history (Schumm, 1977), it has only recently become clear that these tendrils of connection bind more than just the physical compartments of the system to one another: they also govern the biological and ecological functioning of the system, and those aspects depend considerably on the dynamics of the linkages (Poff et al., 1997; Wohl et al., 2015). What has thus begun to crystallize is the idea of the fluvial system as not only a web of tangible elements, but also one of intrinsically connected processes – geomorphic, ecologic, biologic, hydrologic – that operate in conjunction and together influence one another over ample spatial and temporal scales. This dissertation has sought to explicitly emphasize and expand these ideas of process linkages. To that end, in the work delineated and discussed prior, I have established that historical erosion and distal downstream forest regeneration are intrinsically linked processes.

In the Little Snake, Yampa and Green River Basins of Colorado, Wyoming, and Utah, evidence suggests that key tributaries of the Little Snake River – Sand Wash, Sand Creek, and Muddy Creek – underwent historical erosion that together spanned the period of 1880-1940 and substantially increased the sediment loads of the mainstem Yampa and Green Rivers. Moving downstream, substantial portions of cottonwood forest in Deerlodge Park and Tuxedo Bottom date to this period of extensive erosion, as do rates of elevated channel change. Together, it is thus clear that arroyo incision in tributary basins and channel change and concomitant cottonwood forest establishment in distal downstream locations are inextricably linked processes

governed by the idea of sediment-ecological connectivity. This conceptual framework, which relates and establishes geomorphic and ecologic process as connected across ample space and time, further emphasizes process linkages in large watersheds and posits that similar relations should be observed across river basins with similar histories.

Fingerprinting of the sediment that comprises the rooting surface of the Deerlodge Park forest on the Yampa River further strengthens the sediment-ecological connection: results indicate that the large majority of sediment on which Deerlodge Park cottonwoods grow was sourced from the Sand Wash and Muddy Creek tributaries that were undergoing arroyo incision in this historical period. These results further emphasize that ecologic and geomorphic processes are highly linked across ample space ( $10^5$  km<sup>2</sup>) and time ( $10^2$  yrs). Moreover, management of large-watersheds that is concerned with maintaining valuable floodplain forests into the ever-uncertain future must be holistic, undertaken at the full watershed scale, and built-upon strong communication with managers, stakeholders, and scientists in all parts of the basin.

Together, results from the Yampa and Green indicate that sediment is an essential resource that must be valued similar to flow and managed accordingly. A review of the extant literature concerning the geomorphic impact of sediment supply increases reveals a similar idea: management of low-gradient rivers in response to a sediment influx must be based upon thresholds of influx effectiveness that, when exceeded, precipitate a change in the observed scales of geomorphic adjustments. In short, the processes of sediment production in distal basins are intrinsically linked to the processes of channel change and forest establishment far downstream. Large watersheds thus function and can be conceived as networks of process connections, with rates and magnitudes of one process (e.g., cottonwood regeneration) in a given area the result of the same aspects of another process (e.g., arroyo incision) elsewhere.

Of course, this work is not without several limitations. For one, downstream travel times remain relatively poorly constrained. Prior work suggests that the fine fraction of sand, which comprises the rooting surface of downstream cottonwoods, can traverse the Yampa and Green network in as little time as a few months (Topping et al., 2018). However, further work is needed to better quantify sediment travel times on the Yampa and Green and further strengthen the temporal linkage between arroyo incision and downstream forest establishment. A possibly fruitful potential pathway would be to attempt to quantify downstream travel times via a connectivity modeling framework (*sensu* Czuba and Foufoula-Georgia, 2015). Secondly, the influence of grain size related dynamics on the limits of conclusions drawn from the sediment fingerprinting results remains unclear – for instance, the sediment sourced from additional tributaries could have played a major role in the bed dynamics of the river but simply never made it up onto the floodplain. Despite these caveats, the work conducted within this dissertation and summarized here provides important insight into the functioning of watersheds as connected systems and emphasizes geomorphological and ecological processes as intrinsically linked across time and space at the full-watershed scale.

In addition to the future needs just mentioned, there are a myriad of additional concepts and ideas that remain to be explored, both within the Yampa-Little Snake Basin and with regards to a more general application of the ideas developed here. First, related specifically to the Little Snake, there is an opportunity to explore questions of tributary influence by examining the longitudinal distribution of sediment via a geochemically-based fingerprinting approach of both channel and floodplain sediment, wherein regularly spaced samples are used to analyze downstream patterns of sediment geochemistry and examine that pattern is altered at and around tributary junctions (*sensu* Hardy et al., 2010). Such an undertaking would help to improve

understanding of how lateral tributary inputs influence the dynamics of sand-bed rivers (*sensu* Rice, 1998) and how the importance of a given tributary scales with various watershed parameters (such as perennial vs ephemeral flow or management practices). Such an investigation would help to further our understanding of process linkages in large watersheds and expand conceptualizations of how to target management to be most effective in large watersheds.

Second, also within the Yampa-Little Snake system, there is a possibility to use our collected data to test the role of sampling frequency and spatial extent on sediment fingerprinting results. Utilizing artificial mixtures (Batista et al., 2022) and the geologic map of the region, we can begin to explore, for example, how failing to sample the upper reaches of Muddy Creek or leaving out five samples from an extensively sampled geologic unit might impact results. In this manner, evaluation of various sampling scenarios can be performed. Such an undertaking would help to improve sampling approaches for future fingerprinting studies that may be constrained by time or budget.

Finally, beyond the Yampa basin, the general applicability of the sediment-ecological connectivity framework can be explored. As asserted here and within Chapter 2, the framework should apply to any basin with a similar history of upstream historical erosion and downstream riparian pioneer species. Establishing and examining the applicability of the framework in additional basins, such as the Bega or the Ringamaroo rivers in Australia, would assist in further emphasizing the connections between geomorphic and ecologic processes in large river basins; this would, in turn, increasingly accentuate the need for holistic management if vital riverine landscapes are to persist. As demonstrated by the work contained within this dissertation, such future research is essential to continue to increase our understanding of the inextricably intertwined fluvial system.

## 5.1. References

- Batista, P.V.G., Laceby, J.P., Evrard, O., 2022. How to evaluate sediment fingerprinting source apportionments. *J Soils Sediments* 22, 1315–1328. <https://doi.org/10.1007/s11368-022-03157-4>
- Czuba, J.A., Foufoula-Georgiou, E., 2015. Dynamic connectivity in a fluvial network for identifying hotspots of geomorphic change. *Water Resources Research* 51, 1401–1421. <https://doi.org/10.1002/2014WR016139>
- Fryirs, K., 2013. (Dis)Connectivity in catchment sediment cascades: a fresh look at the sediment delivery problem. *Earth Surface Processes and Landforms* 38, 30–46. <https://doi.org/10.1002/esp.3242>
- Hardy, F., Bariteau, L., Lorrain, S., Thériault, I., Gagnon, G., Messier, D., Rougerie, J.-F., 2010. Geochemical tracing and spatial evolution of the sediment bed load of the Romaine River, Québec, Canada. *CATENA* 81, 66–76. <https://doi.org/10.1016/j.catena.2010.01.005>
- Poff, N.L., Allan, J.D., Bain, M.B., Karr, J.R., Prestegard, K.L., Richter, B.D., Sparks, R.E., Stromberg, J.C., 1997. The Natural Flow Regime. *BioScience* 47, 769–784. <https://doi.org/10.2307/1313099>
- Rice, S., 1998. Which tributaries disrupt downstream fining along gravel-bed rivers? *Geomorphology* 22, 39–56. [https://doi.org/10.1016/S0169-555X\(97\)00052-4](https://doi.org/10.1016/S0169-555X(97)00052-4)
- Schumm, S.A., 1977. *The Fluvial System*. Blackburn Press.
- Topping, D.J., Mueller, E.R., Schmidt, J.C., Griffiths, R.E., Dean, D.J., Grams, P.E., 2018. Long-Term Evolution of Sand Transport Through a River Network: Relative Influences of a Dam Versus Natural Changes in Grain Size From Sand Waves. *Journal of Geophysical Research: Earth Surface* 123, 1879–1909. <https://doi.org/10.1029/2017JF004534>

Wohl, E., 2015. Legacy effects on sediments in river corridors. *Earth-Science Reviews* 147, 30–53. <https://doi.org/10.1016/j.earscirev.2015.05.001>

Wohl, E., Brierley, G., Cadol, D., Coulthard, T.J., Covino, T., Fryirs, K.A., Grant, G., Hilton, R.G., Lane, S.N., Magilligan, F.J., Meitzen, K.M., Passalacqua, P., Poepl, R.E., Rathburn, S.L., Sklar, L.S., 2019. Connectivity as an emergent property of geomorphic systems. *Earth Surface Processes and Landforms* 44, 4–26. <https://doi.org/10.1002/esp.4434>

## APPENDIX A: ARROYO ASSUMPTIONS, VOLUME CALCULATIONS, AND CHANNEL MIGRATION DETERMINATION

Volume estimations in Muddy Creek and Sand Wash – the two tributary basins with ample evidence of arroyo incision – began with field investigation to determine and constrain the vertical position of the pre-arroyo creek.

### **A.1. Muddy Creek Assumptions**

In Muddy Creek, field observation reveals a distinct sequencing of three terraces present at many locations (Figure 3 in text and Figure A6) – QT3: a high terrace covered in greasewood and other small vegetation demarcated creek-ward by a graded slope down to a lower surface; QT2: a middle terrace, covered by large sagebrush and notably more heavily vegetated than the higher terrace in nearly all locations where vegetation has not been removed by land managers, which abruptly terminates at a vertical scarp 2-5 m down to QT1: a lower terrace, vegetated by smaller (likely younger) sagebrush and less aerially extensive than the higher terraces, which abruptly terminates at a vertical scarp 1-2 m down to the active floodplain. The active floodplain varies in width throughout the basin but is often vegetated by willow or grasses, located above the modern channel, which is inset within the larger arroyo consistently from the mouth of Muddy Creek to at least 40 km upstream.

Evidence for QT2 as the level of the pre-arroyo Muddy Creek floodplain abounds. First, remnants of the pre-arroyo channel mapped in the 1881 GLO when no arroyo was present (Figure A.1) were noted as “old channels” on the 1915 GLO resurvey and, in some cases, can still be found today, always on T2. Second, relict channels observed on T2 either in the field or in aerial photographs are confirmed to align with channel locations of Muddy Creek as mapped

in the 1881 initial survey or 1915 resurvey (Figure A.2). The T2 surface is additionally readily observable in historical aerial images; 1938 aerial photographs depict a relatively heavily

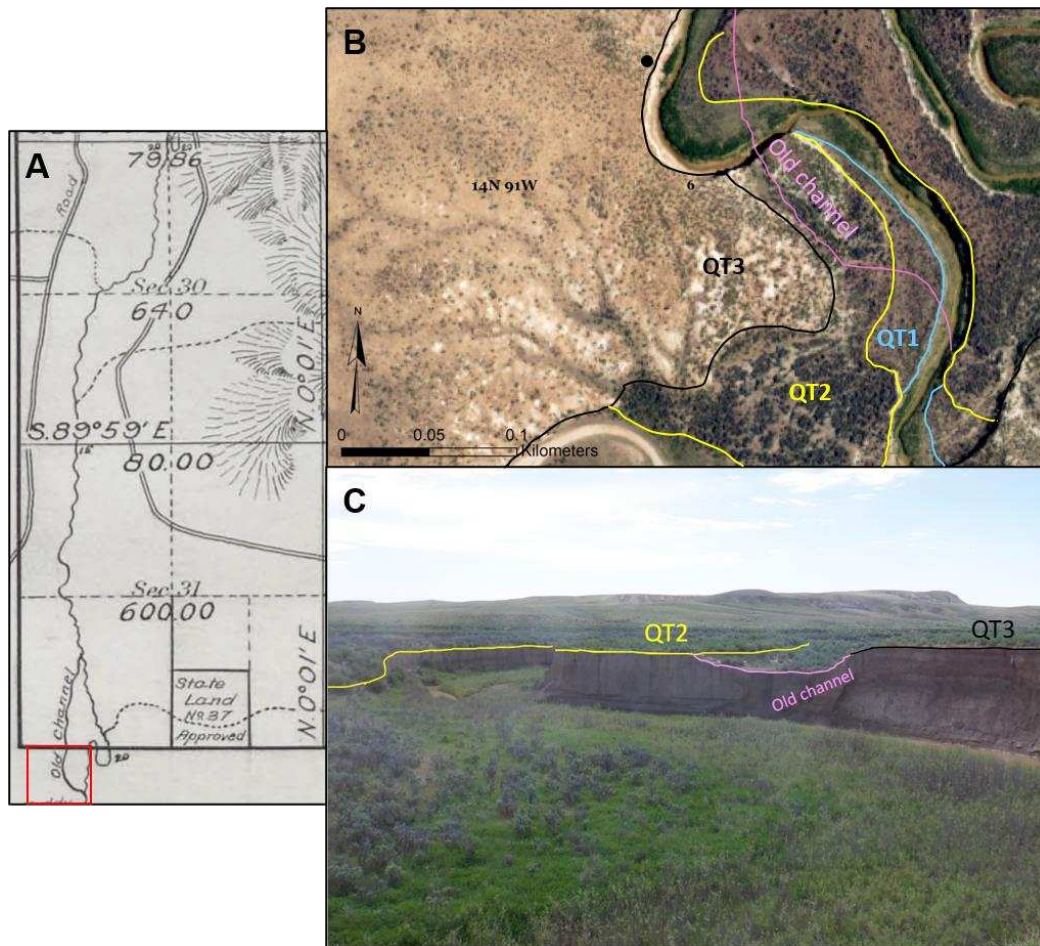


**Figure A.1.** (A) Pre-arroyo Muddy Creek channel in location observed by the GLO surveyors in 1915. Red box indicates the field of view presented in the next panel. (B) Plan view of the delineated old channel from the 1915 map on 2017 NAIP imagery of Muddy Creek and associated terraces. The black dot denotes the approximate location of the photograph in the next panel. Terrace labels are as follows: QT3-high terrace; QT2- middle terrace; QT1-low terrace. (C) Oblique view of the old Muddy Creek channel as identified on the 1881 map and by field investigation. Terraces visible in the field of view are delineated.

Vegetated, extensive surface below which the channel had incised at all locations. Taken at a time likely relatively soon after incision, these photographs suggest that the T2 level was the floodplain of Muddy Creek prior to arroyo entrenchment. The QT1 surface also appears to be an erosional, rather than aggradational, surface, essentially representing a pause in arroyo incision

for a period, wherein the creek meandered before subsequently incising. There is no field evidence of vegetation burial or discontinuities in sedimentary layers at locations where the QT1 wall meets the QT2 wall (Figure A.3), further suggesting the QT1 surface is an erosional terrace. Surfaces identified as QT1 in the field appear were already observably above creek level in the 1938 photos, indicating that incision had progressed past the QT1 level by that time. Therefore, the volume of eroded sediment removed during the period of arroyo development is the “empty space” in field measured cross sections below the T2 level.

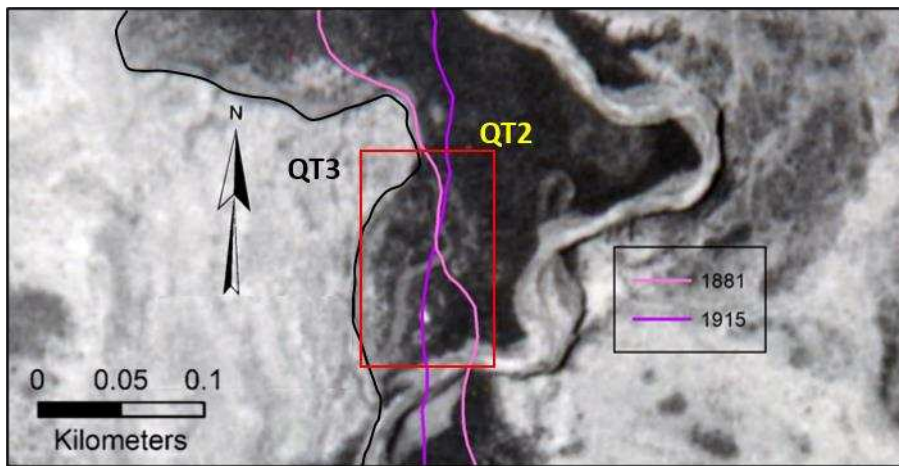


**Figure A.2.** Pre-arroyo channel of Muddy Creek (red box) as observed and identified in 1938 aerial photographs in T14NR91W S18. Digitized channels from 1881 GLO map and 1915 GLO map in pink and purple, as well as identified terraces. Note the proximity of the old channel to the mapped channel location in 1915 and that the old channel is restricted to the surface of QT2.

### **A.2. Sand Wash Assumptions**

In Sand Wash, in contrast to the multiple terraces observed in Muddy Creek, field investigation revealed a single terrace below which the current inset channel and floodplain of Sand Wash now lie. The terrace, dubbed simply as “terrace”, is sparsely vegetated with greasewood and other small xeric shrubs, and is separated from the present-day active floodplain of Sand Wash by vertical arroyo walls. Within the arroyo is an inset floodplain surface vegetated by sagebrush, tamarisk, and occasional Russian olive. This surface is potentially depositional;

buried tamarisk occur in several locations throughout and surfaces that appear as active channel or relatively “young” floodplain in 1938 photographs are now heavily vegetated floodplains (Figure A.4). It is likely that this surface formed subsequent to arroyo incision due to sediment storage that formed an inset floodplain within the arroyo walls, a progression that is consistent with arroyo evolution models for the area (Womack and Schumm, 1977; Schumm et al., 1984; Gellis et al., 1991).

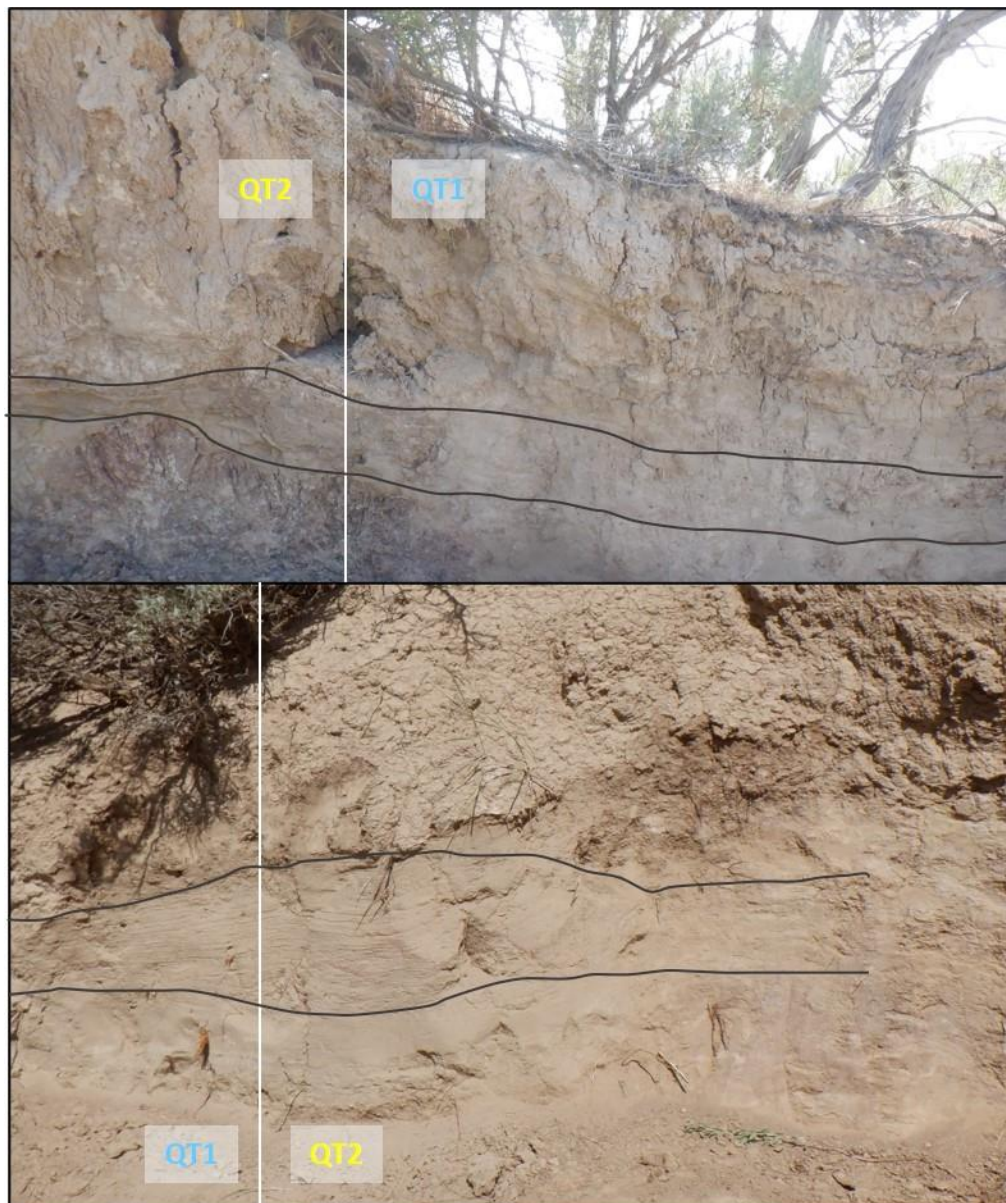


**Figure A.3.** Contact in two separate locations between the scarps of QT1(lower) and QT2 (middle) terraces in Muddy Creek. Continuity in sedimentary structures in the subsurface (separated by the white line) suggests that the QT1 surface was formed by additional incision subsequent to the formation of QT2.

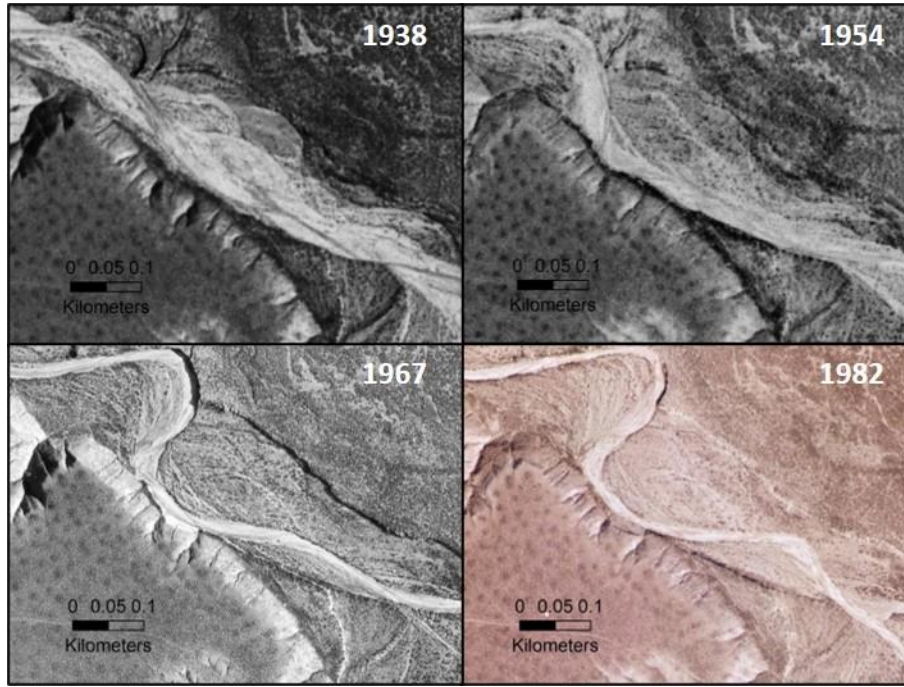


**Figure A.4.** Narrowing of the Sand Wash channel and formation of an inset floodplain from 1938-1982. The channel goes from a wide braided active channel within the walls of the arroyo to an inset meandering channel and floodplain with little retreat of the arroyo walls, suggesting decreases in flow and sediment transport.

Because incision in Sand Wash likely predates that of Muddy Creek by several decades, and because the drainage of Sand Wash is richer in non-cohesive sand, evidence of the level of the old channel (i.e. the level from which the arroyo incised) is lacking. There are no “old channels” mapped on the 1906 GLO resurvey and we found none on the terrace. However, as argued in the body of the text, given the directions in the *Manual of Surveyor Instructions* (1881) to note “the distances measured on the true line to the bank first arrived at, the course downstream at points of intersection, and their widths on line” (White, 1991) it is unlikely that the GLO surveyors would have described a large arroyo as simply a “gulch” in the initial 1881 survey and failed to note its width. It is additionally unlikely that original surveyors would have

mapped a large arroyo with a single line, given the official instructions to illustrate “the distance on line at the crossings of streams, so far as such can be noted on the paper” (White, 1991). This suggests that the large arroyo that was present by the 1906 survey had not yet entrenched in 1881. Extensive unstable vertical sandy arroyo walls and absence of old woody plants or soil development within the arroyo are consistent with the hypothesis that it was incised after 1881. Given field observations of a single terrace, it thus follows that the channel incised from the level of that terrace.

Monuments placed by the 1906 re-survey on the terrace surface proximal to Sand Wash were found by a resurvey crew in 1984. The persistence of the 1906 corner monuments on the former floodplain further suggests that the channel was unable to access this surface, i.e. Sand Wash was incised below the terrace by this time (Figure A.5). The volume of eroded sediment due to arroyo incision in Sand Wash was thus calculated, similarly to Muddy Creek, as the empty space between terrace walls as surveyed in 2019.



**Figure A.5.** Monumented  $\frac{1}{4}$  section corner between S26 and S25 in T8NR98W. The monument stone to mark the corner placed by surveyors during the 1906 survey was located by surveyors during a subsequent resurvey in 1984. Given the proximity to the Sand Wash channel, the monuments persistence suggests that the 1906 channel was incised below the terrace surface on which the  $\frac{1}{4}$  section corner monument sits at the time it was placed.

### A.3. Volume estimations in Sand Wash and Muddy Creek

As discussed previously, Sand Wash and Muddy Creek both exhibit ample field evidence of historic arroyo incision. To calculate eroded volume from these tributary watersheds, cross section measurements were made at section lines in both catchments in 2019. Corresponding terrace surfaces were identified by both field observation of vegetation, stratigraphy, and valley position and by measurement of relative elevation in cross section; a cross section representing the “eroded” portion was thus created at each section line (Figure A.6). We calculated the volume of sediment eroded from the channel segment between two adjacent cross-sections by multiplying their mean “eroded” area by the intervening channel length. This volume was then multiplied by the density of loose sand ( $1442 \text{ kg/m}^3$ ) to determine the estimated mass of sand derived from tributary erosion.

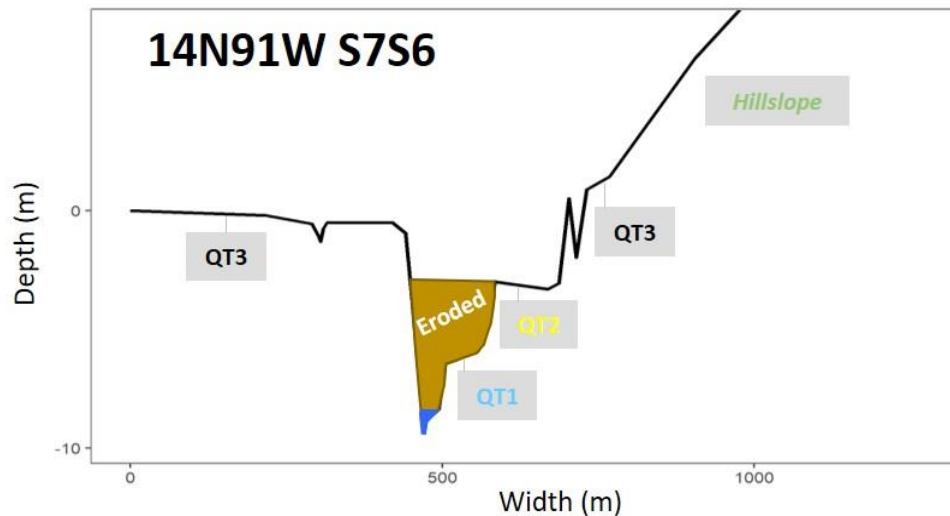


**Figure A.6.** Measurement of modern cross section of Muddy Creek at Township 14 N Range 91 W subdivision line S7S6 and various identified surfaces. The eroded volume is the volume in cross section below the level of the T2 terrace (outlined in brown).

### A.4. Sand Creek assumptions and volumes estimations

1882 and 1937 GLO survey notes indicate the channel widened, on average, by roughly 100 m by 1937. Calculations of width using subsequent aerial photography and modern day

measured cross sections suggest that Sand Creek subsequently narrowed from 1937 to present. However, as addressed in the main text, Sand Creek lacks the observable evidence of historical erosion via arroyo incision that can be found in Muddy Creek and Sand Wash; this is likely a result of the scarcity of cohesive silt- and clay-sized sediment necessary for preserving the characteristic high vertical walls of an arroyo. Though volume contributed directly from channel widening can be calculated, this is likely only a small portion of the sediment evacuated during this period and estimations of historical throughput of sediment are relatively unfeasible. This limitation renders even a first-order estimation of exported sediment totals impractical with the current dataset. Total contributing sediment volume from Sand Creek during the period of historical erosion were thus not estimated.

#### **A.5. Conservative nature of the estimates**

Volume estimates obtained by the above discussed methods are conservative. In Muddy Creek, estimates were calculated using field measurements made in what appears to be the most active portion of the historical arroyo; there is likely additional unaccounted-for volume from the downstream portions of the creek where land access was restricted. In Sand Wash, estimates again were made using what field evidence indicates was the most heavily eroded portions of the arroyo; similar to Muddy Creek, there is likely additional eroded volume downstream from a small portion of the channel where land access was limited. Additional volume likely not captured in these estimates came from areas where the channels of Muddy Creek and Sand Wash eroded into alluvial fans of small tributary watersheds. Finally, sediment contributions from tributary channels and upland sources are also not included. In terms of overall sediment exported to the Little Snake River, the total figure obtained by summing the estimated exported volume of Muddy Creek and Sand Wash represents a conservative, minimum estimate. In

addition to the exported volumes themselves being conservative estimates for the reasons delineated above, the total figure reported does not include sediment exported from any tributaries not included in this analysis (namely Sand Creek), as well as upland areas and tributary fans along the Little Snake themselves. For these reasons, the  $30 \pm 8$  million metric tons added to the background sediment load of the Yampa due to arroyo incision in Muddy Creek and Sand Wash represents a minimum estimate of the total sediment exported to the mainstem rivers during the historical period of tributary erosion.

#### **A.6. Estimating temporal change in channel migration rate at forest sites**

Historical maps and aerial photographs were obtained and georeferenced as described in the main text. Root-mean square error of the referencing error ranged from 3 to 8 meters. Maps and photographs were referenced using a first-order polynomial (affline) transformation (Zanoni et al., 2008; Affek, 2013; Grabowski and Gurnell, 2016; Quik and Wallinga, 2018). No historical map was able to be referenced for the Tuxedo Bottom reach due to a lack of quality ground control points.

Channel migration between years was then quantified by delineating the channel on each historical map, historical aerial photo, and modern imagery corresponding to a specific year (Figure A.7 and A.8), calculating channel area, and calculating the area of overlap between the channel in a given year and the channel in the prior image or document. Overlap was quantified as:

$$\%_{overlap} = \frac{A_{overlap}}{A_{current} + A_{prior} - A_{overlap}}$$

where  $A_{current}$  represents the area of the channel in a given year of interest (e.g., 2019),  $A_{prior}$  represents the area of the channel in prior document or photograph (e.g., 1938), and  $A_{overlap}$  is the area of the overlap between those two channels. In this manner, we determined a percent overlap

for the channel in the years when active arroyo incision and erosion was widespread in tributary basins, and percent overlap between the channel around the cessation of that erosion and the channel at present. This yields an estimate of relative channel dynamism for the period of arroyo incision as compared to the period since.

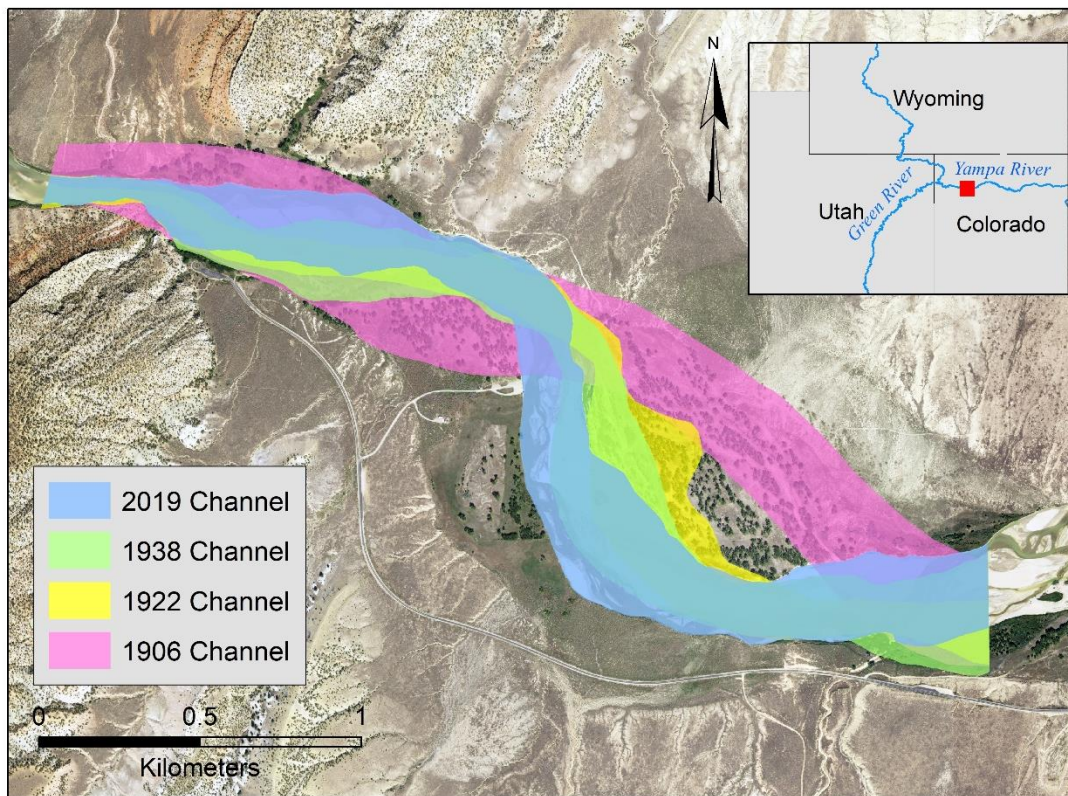


**Figure A.7.** Delineated channels in the Deerlodge Park forest reach from a 1906 GLO map, a 1922 USGS plan survey, 1938 aerial photographs, and 2019 National Agricultural Imagery Program aerial imagery.

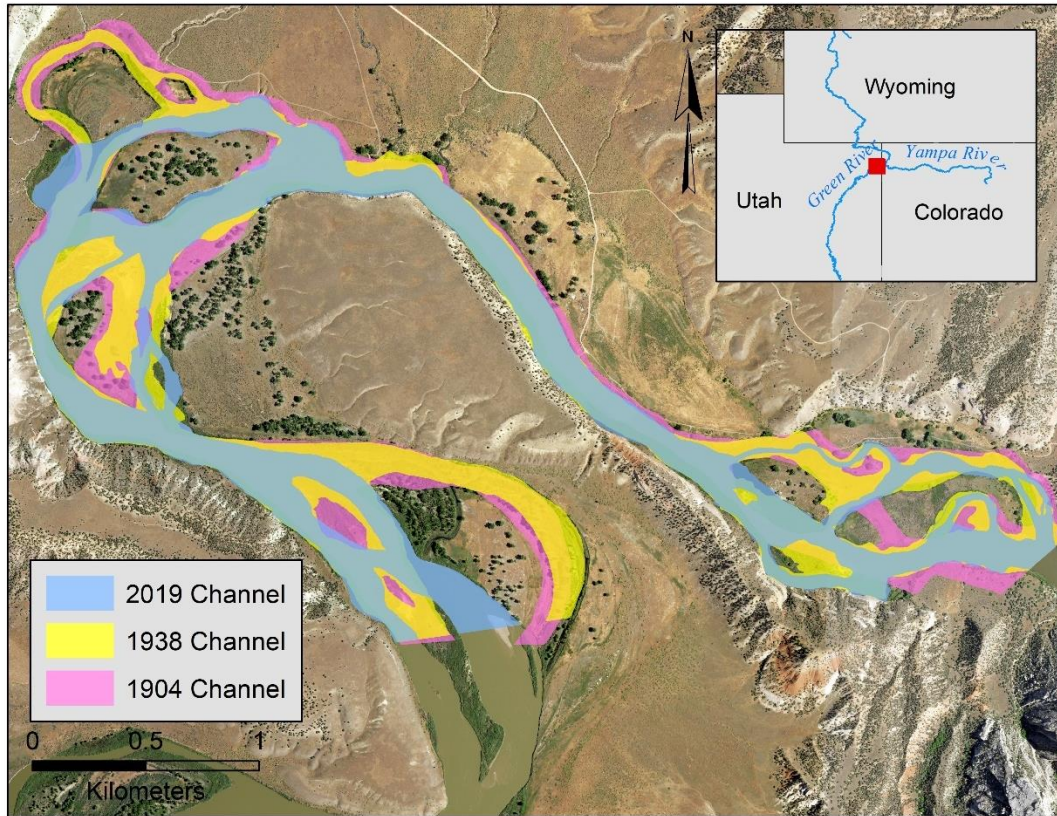


**Figure A.8.** Delineated channels in the Island Park forest reach from a 1904 GLO map, 1938 aerial photographs, and 2019 National Agricultural Imagery Program aerial imagery.

APPENDIX B: TREE CORES SURROUNDING TRENCH AND PXRF ELEMENTAL DATA FOR CONSERVATIVE TRACERS

**Table B.1.** Center years and other metadata for cored trees in the immediate vicinity of the trench in Deerlodge Park on the Yampa River, Colorado, USA (Figure 1c). DBH: diameter at breast height; Height: height of tree in m; Vigor: % of the canopy infilled with leaves; Center Year: determined center year from dendrochronologic analysis of core; dir\_a, dir\_b, dir\_c, dir\_d: cardinal direction of each core for each tree. At least two cores were taken from each tree.

date	tree_id	dbh	height	vigor	species	gender	Center Year	dir_a	dir_b	dir_c	dir_d
2020-08-10	DLX26	84.10	22.20	90	Hybrid	unk	1918	n	e		
2020-08-10	DLX27	95.20	20.20	90	Hybrid	unk					
2020-08-10	DLX28	85.80	21.00	95	Hybrid	unk	1921	n	se		
2020-08-10	DLX29	108.10	17.40	85	Hybrid	unk		n	e		
2020-08-10	DLX30	97.80	19.20	95	Hybrid	unk	1919	ne	nw	nw	
2020-08-10	DLX31	81.50	20.80	90	Hybrid	unk	1914	n	sw		
2020-08-10	DLX32	124.80	25.00	95	Hybrid	unk	1938	s	e		
2020-08-10	DLX33	112.10	25.80	95	Hybrid	unk	1915	n	w		
2020-08-10	DLX34	86.00	19.40	70	Populus fremontii	unk	1920	e	n		
2020-08-10	DLX35	101.90	18.20	80	Populus fremontii	unk		sw	e	n	
2020-08-10	DLX36	223.00	26.40	75	Populus fremontii	unk	1872	w	s	e	n
2020-08-12	DLX37	89.20	13.00	50	Populus fremontii	unk	1863	s	w		
2020-08-12	DLX38	24.20	14.60	100	Populus fremontii	unk	1922	w	e		
2020-08-12	DLX39	85.50	21.60	95	Hybrid	unk	1920	nw	se		
2020-08-12	DLX40	78.80	0.00	5	Hybrid	unk	1918	w	n	e	e
2020-08-12	DLX41	81.70	0.00	0		unk		sw			
2020-08-13	DLX42	22.80	11.80	95	Populus fremontii	unk		ne	sw		
2020-08-13	DLX43	24.50	11.40	95	Populus fremontii	unk	1994	w	e		

**Table B.2.** Standard-corrected concentrations (ppm) of conservative tracers for every sample from both the floodplain sink sediment and from each tributary source area.

Sampling Area	Sample Number	Mg	Al	Ca	Ti	Fe	Sr	Y	Nb
Deerlodge Park Floodplain Trench	1	3580.1	48457	23346	1270	11053	344	9.8	6.8
Deerlodge Park Floodplain Trench	2	4519.1	46245	22290	1451	10838	322	11	6.9
Deerlodge Park Floodplain Trench	3	4460.4	45821	23837	1405	10271	315	13	8.2
Deerlodge Park Floodplain Trench	4	2963.9	47939	24110	1478	11688	396	11	7.3
Deerlodge Park Floodplain Trench	5	4519.1	44692	21838	1514	10230	306	11	8
Deerlodge Park Floodplain Trench	6	5370	54481	25931	1738	16749	366	15	11
Deerlodge Park Floodplain Trench	7	6074.2	48127	35838	1525	12709	379	14	9
Deerlodge Park Floodplain Trench	8	4255	47092	21658	1603	10989	334	11	7.6
Deerlodge Park Floodplain Trench	9	4401.7	44268	18816	2368	11645	317	13	7.6
Deerlodge Park Floodplain Trench	10	4636.5	47209	23294	1655	11433	329	11	7
Deerlodge Park Floodplain Trench	11	4401.7	49727	25330	1370	12149	356	11	7.6

Deerlodge Park Floodplain Trench	12	3638.8	46621	20062	1691	10446	322	9.8	6.9
Deerlodge Park Floodplain Trench	13	5047.2	50057	23446	1617	11238	341	10	7.6
Deerlodge Park Floodplain Trench	14	5458	50951	25033	1439	12939	364	11	8.2
Deerlodge Park Floodplain Trench	15	6074.2	52786	26090	1698	16111	397	14	8.8
Deerlodge Park Floodplain Trench	16	2905.2	46715	20093	1500	10967	314	11	6.9
Deerlodge Park Floodplain Trench	17	5927.5	54669	28649	1620	17330	428	12	8.7
Deerlodge Park Floodplain Trench	18	4548.4	53445	26106	1360	14423	401	11	8.7
Deerlodge Park Floodplain Trench	19	4049.6	50763	24549	1331	13945	394	11	8.4
Deerlodge Park Floodplain Trench	20	5458	50998	31767	1733	12832	403	12	8
Deerlodge Park Floodplain Trench	21	5017.9	49068	20439	1462	11033	355	9.8	6.9
Deerlodge Park Floodplain Trench	22	4812.5	48645	24175	1281	10814	343	9.8	6.9
Deerlodge Park Floodplain Trench	23	3814.9	45445	22706	1623	11386	324	12	7.3
Deerlodge Park Floodplain Trench	24	3022.6	44315	21443	1956	10694	321	11	6.8
Deerlodge Park Floodplain Trench	25	3521.4	43844	20181	2032	10499	324	12	7.1

Deerlodge Park Floodplain Trench	26	3814.9	46856	21341	1381	10368	334	10	7.1
Deerlodge Park Floodplain Trench	27	5927.5	47609	31735	1759	12534	354	13	7.4
Deerlodge Park Floodplain Trench	28	5428.7	46198	24453	2023	11281	337	13	7.6
Deerlodge Park Floodplain Trench	29	4548.4	49304	23977	1423	11210	344	11	7.1
Deerlodge Park Floodplain Trench	30	4416.4	47480	21813	1714	11207	324	14	7.3
Deerlodge Park Floodplain Trench	31	4959.2	45774	23455	1785	11334	330	12	7.3
Deerlodge Park Floodplain Trench	32	5340.7	47186	24776	2387	13304	337	16	8.5
Deerlodge Park Floodplain Trench	33	4724.5	48174	26817	1708	11714	345	12	7.1
Deerlodge Park Floodplain Trench	34	3902.9	47986	21857	1506	10884	351	9.4	7.6
Little Snake River above Muddy Creek	1	4526.4	49421	14183	4467	21524	320	19	9.6
Little Snake River above Muddy Creek	2	3785.5	50998	12502	2604	15512	325	13	7.1
Little Snake River above Muddy Creek	3	4583.6	49944	12852	3933	22150	293	17	9.4
Little Snake River above Muddy Creek	4	4401.7	48551	11967	4222	21443	277	19	9
Little Snake River above Muddy Creek	5	4563.1	49586	12222	2871	19875	300	15	7.9

Little Snake River above Muddy Creek	6	4665.8	44550	12061	3151	16351	260	16	7.4
Little Snake River above Muddy Creek	7	4929.9	45586	12353	2615	16097	264	15	8
Little Snake River above Muddy Creek	8	3668.1	44108	10447	3239	15139	241	15	7.4
Little Snake River above Muddy Creek	9	3756.2	44080	10530	4096	17694	265	16	9
Little Snake River above Muddy Creek	10	3345.4	44503	10247	3529	14023	220	15	7.9
Little Snake River above Muddy Creek	11	4548.4	44127	9850	3526	15881	265	16	8.5
Little Snake River above Muddy Creek	12	2729.2	40427	9004.5	3056	16134	248	15	11
Little Snake River above Muddy Creek	13	3902.9	41277	14315	4424	20233	268	20	12
Little Snake River above Muddy Creek	14	3022.6	40959	9718.5	2761	13589	239	15	8.4
Little Snake River above Muddy Creek	15	3712.2	43562	12159	2606	13787	255	10	9
Little Snake River above Muddy Creek	16	2670.5	39132	11725	2254	13507	245	15	6.9
Little Snake River above Muddy Creek	17	3378.9	38767	10867	3348	14373	232	15	8.7
Little Snake River above Muddy Creek	18	2993.3	41868	12281	2962	15575	260	15	8.4
Little Snake River above Muddy Creek	19	3316	39468	9093.8	3923	14849	218	19	9

Little Snake River above Muddy Creek	20	2377.1	40250	10987	1782	11267	255	11	7.6
Little Snake River above Muddy Creek	21	3550.8	39915	10036	2879	13679	236	12	7.6
Little Snake River above Muddy Creek	22	2039.6	31362	6492.2	1095	8047.9	176	7.9	6.7
Little Snake River above Muddy Creek	23	4871.2	43374	12777	2123	13688	248	13	6.9
Little Snake River above Muddy Creek	24	2054.3	34262	7992.7	3202	13054	206	18	9.8
Little Snake River above Muddy Creek	25	3374.7	44315	11641	2148	14158	257	13	7.9
Little Snake River above Muddy Creek	26	4489.7	43233	10612	2091	13495	249	12	7.4
Little Snake River above Muddy Creek	27	5047.2	49398	11830	2738	18829	288	15	8.5
Little Snake River above Muddy Creek	28	3668.1	47421	11915	2640	16516	284	13	7.6
Little Snake River above Muddy Creek	29	4416.4	48927	11460	2568	17916	285	15	8
Little Snake River above Muddy Creek	30	3844.2	45445	11555	2749	16289	292	14	7.7
Little Snake River above Muddy Creek	31	4284.3	50245	13833	3402	20155	304	16	7.6
Little Snake River above Muddy Creek	32	4665.8	46856	11576	3549	19792	279	15	8.2
Little Snake River above Muddy Creek	33	4614.4	49739	11895	2965	19714	294	14	8.3

Little Snake River above Muddy Creek	34	3961.6	48786	13227	2606	18025	312	14	8.4
Little Snake River above Muddy Creek	35	4020.3	48833	25342	2070	12934	372	12	6.6
Little Snake River above Muddy Creek	36	5164.6	49539	12401	3673	22285	292	18	8.2
Little Snake River above Muddy Creek	37	6191.6	52739	11969	2194	18454	289	15	7.9
Little Snake River above Muddy Creek	38	3580.1	42762	12241	2460	13912	247	13	7.7
Little Snake River above Muddy Creek	39	3668.1	45680	12043	2978	15747	266	15	8
Upper Yampa River	1	4255	45162	9267.7	6126	25907	205	37	12
Upper Yampa River	2	3785.5	47468	10418	2257	16378	212	15	7.7
Upper Yampa River	3	4020.3	46904	7325.4	2125	15338	209	15	8.4
Upper Yampa River	4	3433.4	46292	7203.8	2318	15374	210	17	8.5
Upper Yampa River	5	3902.9	43468	12829	1912	15119	199	15	8.4
Upper Yampa River	6	4841.8	41959	14774	1716	13564	195	13	8.4
Upper Yampa River	7	3873.5	39938	16742	1598	12228	172	14	6.9
Upper Yampa River	8	4372.4	39449	18601	1833	13063	208	13	7.3
Upper Yampa River	9	3286.7	36605	17825	2002	12352	164	12	7.1
Upper Yampa River	10	4548.4	39898	14520	1712	13640	198	13	8
Upper Yampa River	11	3492.1	36393	16602	1825	11449	155	14	7.9
Upper Yampa River	12	5017.9	45915	9315.7	2707	17165	213	17	9
Upper Yampa River	13	5017.9	46621	9443.4	3411	18553	208	22	9.6
Upper Yampa River	14	4343	48457	8644.6	2505	16355	215	21	8.5
Upper Yampa River	15	3433.4	48362	8674.2	3030	17932	228	25	10
Upper Yampa River	16	4665.8	49680	8716.9	2940	19705	221	18	9.1
Upper Yampa River	17	4401.7	46151	9790.2	5687	26606	214	32	12

Upper Yampa River	18	4695.1	49257	11482	3530	24147	230	35	13
Upper Yampa River	19	2699.8	41679	13939	1944	14239	212	16	8.4
Upper Yampa River	20	4167	43374	13209	3554	19795	205	20	9.5
Upper Yampa River	21	4343	36911	18953	1618	11357	179	11	7.9
Upper Yampa River	22	4401.7	43421	13198	2216	15432	208	14	8.4
Upper Yampa River	23	3609.5	38667	10843	4534	18773	205	23	10
Upper Yampa River	24	3932.2	43951	14731	3804	22046	199	24	9.8
Upper Yampa River	25	4137.6	44127	13797	2242	16241	201	14	7.9
Upper Yampa River	26	5047.2	43969	14588	2342	16203	208	15	7.9
Upper Yampa River	27	5076.6	42668	16253	2473	17062	208	16	8.4
Upper Yampa River	28	4548.4	43656	15925	3624	22603	205	25	12
Upper Yampa River	29	4460.4	41021	12425	7580	42905	198	36	17
Upper Yampa River	30	3697.5	41700	12633	3332	19890	195	16	9.8
Upper Yampa River	31	4049.6	44597	13193	7707	40899	211	39	16
Upper Yampa River	32	3726.8	46904	10912	2653	18024	204	19	8.8
Upper Yampa River	33	4196.3	49492	8188.4	2255	16799	195	17	8.4
Upper Yampa River	34	5604.8	52881	8352.4	2048	18149	215	16	9
Upper Yampa River	35	4959.2	51516	7923.4	2021	17582	203	17	9.8
Upper Yampa River	36	5648.8	51186	8865.1	2590	18496	218	18	9.2
Upper Yampa River	37	3257.3	48739	7813.3	2590	17275	211	18	8.5
Upper Yampa River	38	4783.2	52692	9508.2	3486	24712	205	29	11
Upper Yampa River	39	3316	47609	7158.5	2953	16601	204	17	9.1
Upper Yampa River	40	3433.4	42338	6470.4	3811	17645	200	23	10
Upper Yampa River	41	4489.7	46103	7522.2	2410	16052	202	20	8.7
Upper Yampa River	42	4255	47092	9053.3	2394	16400	204	21	9.9
Upper Yampa River	43	3609.5	45774	7443.5	4237	21524	195	32	11
Upper Yampa River	44	2846.5	38315	20620	1233	8267.1	163	8.1	7.1
Upper Yampa River	45	2905.2	36267	17860	3019	12745	154	17	9.3
Upper Yampa River	46	5692.8	47562	9347.9	2840	17248	203	20	9.5

Upper Yampa River	47	2523.8	42809	23940	1855	14521	228	17	7.9
Upper Yampa River	48	2465.1	42515	14352	1772	13864	209	13	8.4
Upper Yampa River	49	5546.1	53163	9632.9	2694	20412	219	21	9.8
Upper Yampa River	50	4665.8	48315	8220.4	2048	15859	218	20	8.7
Upper Yampa River	51	4812.5	48221	8440.1	2789	18407	207	17	9.1
Upper Yampa River	52	4460.4	47704	8504.4	3069	18974	211	20	9.1
Upper Yampa River	53	4607.1	48833	10479	2431	18972	230	21	9.3
Upper Yampa River	54	4284.3	47939	8259.3	2018	16502	212	15	8.7
Upper Yampa River	55	3844.2	50151	8525.2	2392	17779	216	19	9
Muddy Creek	1	3697.5	38812	16133	1101	9996	150	10	6.5
Muddy Creek	2	1555.5	29273	10698	1239	7248	121	9.4	6.2
Muddy Creek	3	2523.8	32585	13228	976.2	7165.6	128	8.1	5.5
Muddy Creek	4	2259.7	30159	11940	1143	7631.4	118	9.4	6.5
Muddy Creek	5	3374.7	31198	16261	1215	6965.1	143	6.5	5.7
Muddy Creek	6	2875.9	31153	15799	1128	6964.2	139	7.3	5.4
Muddy Creek	7	2318.4	34536	11540	998	8253.9	189	11	3.3
Muddy Creek	8	1467.4	31830	13500	894.5	6530.6	181	9.8	9.2
Muddy Creek	9	2670.5	32452	13757	1053	8071.5	132	8.6	5.7
Muddy Creek	10	3140	31663	16700	676.5	6438.4	142	8.1	5.7
Muddy Creek	11	2083.6	35255	14113	953.8	9567	171	9.4	8.8
Muddy Creek	12	1584.8	29684	12174	740.8	7548.7	135	8.6	3.3
Muddy Creek	13	3433.4	32486	13666	1468	8716.2	142	14	3.3
Muddy Creek	14	2919.9	28284	12049	1239	7264.7	128	10	6.2
Muddy Creek	15	1291.4	30317	11911	1038	7629.1	131	9	6.3
Muddy Creek	16	3286.7	32883	14645	1271	10489	143	12	6
Muddy Creek	17	1643.5	22725	38917	772.5	6047.4	244	9	8.8
Muddy Creek	18	1115.3	20962	21373	632.2	5142.7	140	6.5	5.7
Muddy Creek	19	1760.9	26752	13398	734.8	9013	131	8.1	3.3
Muddy Creek	20	3022.6	29409	11606	1085	10338	118	9.4	3.3

Muddy Creek	21	5956.9	50857	40745	1780	20904	275	20	3.3
Muddy Creek	22	1790.2	24137	7784.5	1065	7896.4	111	6.5	3.3
Muddy Creek	23	1496.8	21886	10222	963.5	9093.6	99.8	8.3	3.3
Muddy Creek	24	3022.6	32876	15503	1458	11324	138	13	3.3
Muddy Creek	25	1995.6	22707	6973.5	1059	5640.2	116	13	13
Muddy Creek	26	4401.7	36962	17752	826.3	6795.6	166	7.3	3.3
Muddy Creek	27	3286.7	32825	11627	1241	7939.7	129	10	6.8
Muddy Creek	28	4343	36878	22565	961.2	7935.3	163	7.7	3.3
Muddy Creek	29	2025	28944	14446	894.2	6996.4	132	9	3.3
Muddy Creek	30	2289	34263	15267	1062	10064	159	9.8	5.7
Muddy Creek	31	2171.7	31174	11521	961.2	7229.7	145	9	5.7
Muddy Creek	32	1702.2	28742	11453	783.8	5940.9	125	6.9	7.1
Muddy Creek	33	3316	31700	12250	1737	10080	113	15	3.3
Muddy Creek	34	-58.4	27379	17626	689.6	6285.2	183	10	9.6
Muddy Creek	35	1672.8	34046	11595	1181	10916	126	12	3.3
Muddy Creek	36	1848.9	37576	15447	1265	10597	173	10	6.3
Muddy Creek	37	880.6	29044	11520	1230	9148.4	141	9	3.3
Muddy Creek	38	3051.9	33558	15525	1549	10346	150	11	6.3
Sand Creek	1	7336	73494	25877	2198	17644	389	18	12
Sand Creek	2	7130.6	74106	23454	1904	16931	345	17	14
Sand Creek	3	9155.2	73965	21007	2545	16941	363	17	12
Sand Creek	4	6279.6	78954	9591.3	2023	16514	217	20	10
Sand Creek	5	9859.4	69918	31745	2195	20220	518	16	12
Sand Creek	6	6661.1	33393	89196	2092	15663	571	18	7.9
Sand Creek	7	8509.7	59658	31652	2429	17744	614	15	10
Sand Creek	8	9096.5	46574	57568	7524	34991	612	30	15
Sand Creek	9	8274.9	62717	31126	2455	18360	642	17	11
Sand Creek	10	7042.5	63564	29794	2095	14475	682	13	9.1
Sand Creek	11	7600.1	60364	31348	4592	24513	648	23	11

Sand Creek	12	7101.2	61964	30810	2598	17574	667	17	8.8
Sand Creek	13	6397	62670	32506	3346	19801	682	20	9.3
Sand Creek	14	7776.1	63423	30686	2340	16524	667	15	9.1
Sand Creek	15	7541.4	63705	32439	3921	22322	680	20	12
Sand Creek	16	7805.5	64129	30444	1654	14097	685	14	8.4
Sand Creek	17	6837.2	58858	30906	3708	19847	619	21	11
Sand Creek	18	6455.7	61823	31037	2486	16206	668	17	8.8
Sand Creek	19	5282	51657	21452	1290	9997.1	417	11	7.7
Sand Creek	20	4049.6	68694	24001	1118	9299.4	594	9.8	8.5
Sand Creek	21	6397	62011	29632	1875	12558	599	15	12
Sand Creek	22	7130.6	61164	30360	4113	23174	556	29	12
Sand Creek	23	6426.4	62340	30584	2445	16413	659	16	9.3
Sand Creek	24	6954.5	62293	30146	3557	20447	662	21	8.7
Sand Creek	25	6617.1	60611	29828	1915	15312	642	15	8.5
Sand Creek	26	7277.3	62952	31575	3603	20271	671	20	9.8
Sand Creek	27	8392.3	62387	31605	3536	21184	654	18	10
Sand Creek	28	6925.2	59705	32472	5142	26438	635	25	11
Sand Creek	29	6807.8	58575	32724	6847	34578	629	39	16
Sand Creek	30	5047.2	61023	31905	1671	12429	618	13	7.9
Sand Creek	31	5663.4	58858	26695	2753	16442	647	21	12
Sand Creek	32	7981.5	61776	28886	7569	33349	654	32	16
Sand Creek	33	6602.4	62811	27534	2831	17494	674	19	10
Sand Creek	34	6250.3	58105	26415	4582	24539	605	26	16
Sand Creek	35	9712.7	60034	27116	5076	27540	585	30	13
Sand Creek	36	5927.5	65494	28423	1990	14563	713	15	8.2
Sand Creek	37	6485	64788	27395	2213	14735	708	15	7.7
Sand Creek	38	8509.7	62999	28387	2226	16812	647	17	11
Sand Creek	39	7629.4	64505	26358	2190	16556	646	18	10
Sand Creek	40	5839.5	65352	26618	1677	12303	714	13	9.1

Sand Creek	41	7482.7	62152	28553	3726	20053	690	23	9.5
Sand Creek	42	5311.3	65258	28559	2164	14529	761	14	8.2
Sand Creek	43	6881.2	60011	33632	3588	22066	656	24	13
Sand Wash	1	10476	57022	35578	1703	17607	539	12	8.5
Sand Wash	2	10388	57869	44507	2238	25393	508	20	16
Sand Wash	3	9213.9	61352	38312	1841	19236	607	14	11
Sand Wash	4	9976.8	59987	41786	2100	22344	555	16	12
Sand Wash	5	7453.3	57540	32388	1573	14774	508	13	8.8
Sand Wash	6	11151	56928	43309	2580	28632	480	20	15
Sand Wash	7	8509.7	56269	40732	2140	20137	412	17	12
Sand Wash	8	10886	58575	39883	2119	19263	553	15	10
Sand Wash	9	6543.7	59328	39447	1742	15841	767	13	7.9
Sand Wash	10	7570.7	58434	30901	2367	15421	591	13	8.4
Sand Wash	11	7776.1	60740	33712	1684	13437	630	12	8
Sand Wash	12	6455.7	64129	28803	1656	13813	775	13	9.1
Sand Wash	13	6103.6	62529	35172	1674	14207	599	12	8.2
Sand Wash	14	5663.4	58481	34059	3077	20323	617	17	11
Sand Wash	15	7306.6	59893	41087	2308	17842	657	15	9.5
Sand Wash	16	7071.9	61164	36176	1959	16104	617	15	9.1
Sand Wash	17	8685.7	62199	36988	1701	15991	645	13	8.7
Sand Wash	18	6558.4	57540	42411	1541	13874	600	13	7.7
Sand Wash	19	7013.2	59046	38607	1391	13570	633	11	8.8
Sand Wash	20	4695.1	55516	34904	1430	12457	592	12	8.7
Sand Wash	21	9155.2	62199	33381	1405	14213	630	11	9.6
Sand Wash	22	5956.9	56975	30502	2234	14929	523	13	9.1
Sand Wash	23	6646.4	60128	32268	1614	14036	589	12	8.6
Sand Wash	24	6573.1	58293	36009	1780	15392	597	12	8.8
Sand Wash	25	6602.4	65870	53273	1519	14140	806	22	23
Sand Wash	26	8157.6	59281	36774	2729	17975	614	14	9.3

Sand Wash	27	7805.5	59470	38033	2031	17366	627	15	9.1
Sand Wash	28	8715.1	63329	35399	1513	14673	633	13	11
Sand Wash	29	6485	54481	33662	1721	12238	458	12	7.4
Sand Wash	30	8304.3	60011	35341	1877	15670	607	13	9.6
Sand Wash	31	6866.5	47421	50550	1860	16045	529	11	8
Sand Wash	32	8228	59997	36694	1923	17627	699	15	11
Sand Wash	33	8920.5	62058	36675	1652	15207	689	11	8.5
Sand Wash	34	7658.7	61023	37693	1653	15103	621	13	9.5
Sand Wash	35	5722.1	47468	16371	2260	11401	287	11	7.7
Sand Wash	36	6631.8	58152	35329	1466	14739	592	13	9.9
Sand Wash	37	7864.1	58858	33826	4482	23926	612	19	11
Sand Wash	38	6132.9	61917	39871	1923	16127	656	15	9
Sand Wash	39	6954.5	62340	33910	1962	16385	644	13	9.6
Sand Wash	40	7424	59281	35979	3525	21954	642	14	8.8
Sand Wash	41	9507.3	62905	38279	2929	20653	706	15	8.7
Sand Wash	42	7101.2	59093	33209	3102	19263	596	13	9.8
Sand Wash	43	4812.5	62905	35920	2344	15939	715	13	9.3

---

**Table B.3.** Standard-corrected mean concentrations and standard errors ( $\sigma_M$ ) (ppm) of conservative tracers in each sampling area

Sampling Area	Al	Al $\sigma_M$	Ca	Ca $\sigma_M$	Fe	Fe $\sigma_M$	Mg	Mg $\sigma_M$	Nb	Nb $\sigma_M$	Sr	Sr $\sigma_M$	Ti	Ti $\sigma_M$	Y	Y $\sigma_M$
Deerlodge Park Floodplain Trench	48204.3	480.8	24154.4	618.9	12007.3	310.9	4574.7	149.8	7.7	0.1	348.5	5.2	1629.5	46.6	11.7	0.3
Little Snake River above Muddy Creek	44717.8	755.4	11800.0	437.6	16299.7	514.3	3907.3	142.1	8.2	0.2	267.3	5.7	2961.4	119.6	14.7	0.4
Upper Yampa River	45124.3	585.9	11695.5	540.1	18093.2	794.2	4172.6	104.2	9.3	0.3	203.8	2.2	2869.2	179.2	19.5	0.9
Muddy Creek	31262.4	872.5	15084.9	1083.6	8477.7	427.8	2453.1	181.3	5.5	0.4	146.5	5.6	1080.7	44.5	9.8	0.4
Sand Creek	62298.4	1081.3	30745.0	1671.7	18917.4	891.7	7080.1	185.2	10.6	0.3	611.7	16.7	3065.1	234.6	19.1	0.9
Sand Wash	59255.7	542.6	36690.9	870.6	16866.7	551.6	7621.5	236.8	9.9	0.4	603.6	14.2	2054.1	95.3	13.9	0.4